M.Sc. Graduation Project:

Soil-structure interaction modelling in performance-based seismic jetty design

Final report

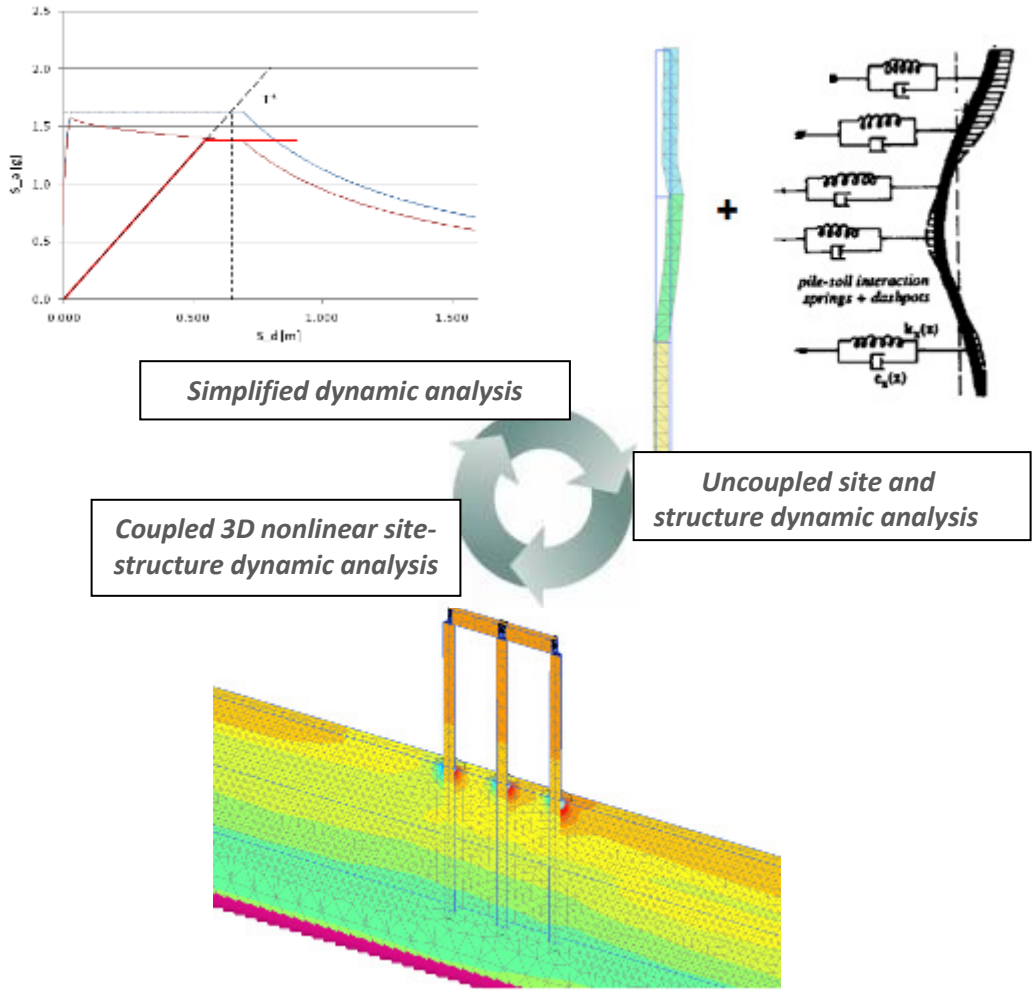

Editor: ***Besseling, F. (Floris)***

Graduation Committee: ***Prof. ir. A.W.C.M. Vrouwenvelder***
(Chairman of the Committee, TU Delft, section Structural mechanics)
Prof. dr. A.V. Metrikine (TU Delft, section Structural Mechanics)
Dr. ir. R.B.J. Brinkgreve (TU Delft, section Geo-engineering & Plaxis)
Ir. H.J. Lengkeek (Internship supervisor, Witteveen+Bos)
Ir. L.J.M. Houben (TU Delft)

Delivery date: ***19th of June 2012***

M.Sc. Graduation Project:

Soil-structure interaction modelling in performance-based seismic jetty design

Editor:	*Besseling, F. (Floris)*
Student number:	*4025768*
Email:	*f.besseling@student.tudelft.nl*
Graduation Committee:	*Prof. ir. A.W.C.M. Vrouwenvelder* *(Chairman of the Committee, TU Delft, section Structural Mechanics)* *Prof. dr. A.V. Metrikine (TU Delft, section Structural Mechanics)* *Dr. ir. R.B.J. Brinkgreve (TU Delft, section Geo-engineering & Plaxis)* *Ir. H.J. Lengkeek (Internship supervisor, Witteveen+Bos)* *Ir. L.J.M. Houben(TU Delft)*
Delivery date:	*19th of June 2012*
Status:	*Final*
Number of pages:	*108*

Summary

The importance of soil structure interaction in seismic design of structures is a recognized by the modern seismic design community, that is very much moving towards performance based design principles. Particularly for structures with deep foundations in soft soil conditions, soil-structure interaction is recognized to be an important factor that has to be considered in design. Jetty structures obviously are such structures. On the contrary seismic design standards do hardly provide any straight forward tools for engineers to account for soil-structure interaction in design. It is clear that a problem exists, which has initiated this study.

In the first phase of the study a literature review is conducted, where important developments relating to performance based seismic jetty design and soil-structure interaction are collected. Based on this literature review three suitable design approaches are found for jetty structure design, being simplified dynamic analysis (push-over + response spectrum), uncoupled dynamic analysis and coupled dynamic analysis.

Then the second phase of the study is geared towards static pile-soil interaction and pushover analysis of single piles and jetty structures by modelling the soil as a conventional Winkler foundation or by performing more advanced hardening soil finite element analysis. Proper selection of clay parameters for the hardening soil model hereby is a critical step in order to be able to verify p-y expressions. After calibration of Winkler foundations for single piles, related issues like pile group effects are studied by means of finite element pushover analysis and subsequently p-multipliers for these effects can be defined for dynamic jetty analysis.

Subsequently the focus is shifted towards free field dynamic analysis of soil deposit for vertically propagating shear waves, because of its importance for seismic analysis of deep foundations. Both linear and nonlinear finite element modelling are performed and compared to equivalent linear frequency domain analysis solutions for layered soils. The conclusions drawn from this phase are important input for the jetty dynamic analysis.

Then the seismic jetty response was calculated along the different methods. First by means of simplified dynamic analysis and then by both uncoupled and coupled dynamic analysis. Based on the results recommendations are proposed regarding the importance of soil-structure interaction for future jetty projects and how it should be accounted for, where both performance as well practical issues are taken into consideration..

Table of contents

1 Preface

This master thesis finalizes my master study Structural Engineering, specialization Structural Mechanics at Delft University of Technology. The project as part of the master track covers 40 ECTS and was executed in the period ranging from September 2011 to June 2012.

Over this period I have almost continuously enjoyed the interesting project. Now the master thesis scope has finished, but still interesting questions relating the soil-structure interaction problem arise. I definitely will try to address some of these during the remainder of my career in structural/geotechnical engineering.

The study, titled "Soil structure interaction modelling in seismic jetty design" is commissioned by Witteveen+Bos Consulting Engineers and was executed at Witteveen+Bos Deventer under the supervision of Ir. H.J. (Arny) Lengkeek. I would like to express my gratitude to Witteveen+Bos for offering me this position and a special gratitude to Arny for his dedicated support.

The graduation committee for this project consist of the following members:

Prof. ir. A.W.C.M. Vrouwenvelder	(Chairman of the Committee, TU Delft, section Structural Mechanics)
Prof. dr. A.V. Metrikine	(TU Delft, section Structural Mechanics)
Dr. ir. R.B.J. Brinkgreve	(TU Delft, section Geo-engineering & Plaxis)
Ir. H.J. Lengkeek	(Internship supervisor, Witteveen+Bos)
Ir. L.J.M. Houben	(TU Delft)

I would like to thank the committee for their guidance and support, and additionally the Plaxis technical support team for solving many problems together.

Special thanks to Lotte for her great support and to my parents providing me the opportunity to finish my master study in Delft.

Deventer, 19th of June 2012

Floris Besseling

2 Introduction

Earthquakes are among the most devastating natural disasters humans have faced over history. Since civilisation has developed, and demand for all kind of buildings and other type of structures has increased, the risk related has increased inherently. Even over the past few years direct and indirect effects by earthquake result thousands of fatalities when affecting densely populated areas like in Southern Sumatra - Indonesia (2009), Haiti Region (2010), Southern Qinghai - China (2010) and Japan (2011), with 1,117, 316,000, 2,968 and 20,352 fatalities respectively.

With the development of civilisation during the last century, buildings and, infrastructure have increased exponentially in number and size, which inherently has increased the risks related to earthquakes. In this perspective ports are of special importance because of their major significance for earthquake recovery and the large amount of hazardous materials that are transferred and stored in these areas. Hence, earthquake resistance and safety of port structure needs special attention from this perspective.
Port structures may be subdivided in several categories like gravity quay walls, sheet pile quay walls, pile supported wharves and piers/jetties, cellular quay walls, quay walls with cranes and breakwaters. This thesis focuses primarily on pile supported piers, often referred to as jetties, piers or pile-deck systems. Typically, these jetty structures consist of a concrete deck on top of series of long reinforced or prestressed concrete piles or tubular steel piles. Over the past decades vessel sizes have increased resulting an increase in jetty size as well. This results a global trend switch to the use of tubular steel piles, as was already common in offshore engineering practice and hence is taken as a starting point in this study.

Traditionally, soil-structure interaction effects were ignored in seismic design of structures, since they were believed to only have favourable effects. The lengthening of the period shifts the structure response to the spectral branch of lower accelerations which implies a reduction of inertia forces in the structure. However along modern performance based design principles soil-structure interaction effects are recognized to not necessarily have beneficial but even may have very detrimental effects for the response of the superstructure (Priestley & Park, 1987) (Mylonakis, Nikolaou, & Gazetas, 1997), (Mylonakis & Gazetas, 2000). The global trend shift towards performance based design in the seismic engineering branch implies an increasing focus on displacements rather than on inertia forces, which makes proper consideration of soil structure interaction a critical factor. Additionally the failure of foundations their selves and possible effects of soil failure have become a more important issue in seismic design. The effects of soil structure interaction have been subjective to research for about half a century, but are still under discussion.

Code provisions relating to soil-structure interaction nowadays are still very limited and straight forward procedures to account for soil structure interaction in design are not included in most codes. Simplified dynamic analysis methods are commonly used as a starting point, where the role and possible effects of soil-structure interaction in the response often remain unclear. On the contrary research activities at universities all over the world already are far ahead, providing a variety of knowledge in this field. The connection with engineering practice however appears to be somehow lost, which forms a problem for practicing engineers dealing with design of structures in seismically active areas. This study focuses on the performance of available and usable design methods for practicing engineers that need to account for soil structure interaction in seismic jetty design.

The present study is concentrated at a case jetty project, that typically meets the conditions regarding deep piled end-bearing foundations in soft soil, for which according to standards and literature, soil-structure interaction effects are considered most important. Although the case project typically represents the common situation of deep end-bearing jetty foundations in a soft soil deposit, it should be noted that differently situated jetty structures may result different critical design issues. However, since master's thesis research requirements limits the scope of the research, it is chosen to focus primarily on this typical situation, not performing a complete parametric study on varying local conditions. This latter study is recommended for further study by a future graduating student or may be attended as part of future Witteveen+Bos jetty projects in seismic areas.

3 Project Description

This study exists of four main phases:

The first part is a literature study of seismic engineering principles and related geotechnical as well structural aspects, with a focus on soil structure interaction and analysis of structures with deep foundations in soft soil conditions. The literature study is based on research papers, seismic design codes and seismic engineering text books. First, seismic design principles in general are studied. Recommendations regarding how to design structures for seismic loading will be summarized and conclusions will be drawn regarding the most suitable seismic design methods for jetty structures. Subsequently the focus is shifted more towards typical jetty structure related analysis issues, where soil structure interaction under seismic loading is in various literature and seismic standards recognized to be a significant factor to be included in design.

The second part focuses on the static analysis of pile-soil interaction and laterally loaded piles A comparative study is performed, in which the widely used beam on nonlinear Winkler foundation technique for laterally loaded piles is verified by pushover analysis with geotechnical engineering finite element software Plaxis 3D, making use of advanced soil constitutive models. Proper selection of hardening soil parameters herein was a critical step in order to reasonably use the numerical modelling as a tool for p-y curve validation. Possibilities for defining equivalent 2D models that properly represent the horizontal jetty response are investigated. Based on finite element analysis of pile groups p-multipliers are established that correctly reduce Winkler foundation capacity for pile group effects.

Then the third phase of the study addresses free field site response analysis for a soil deposit overlying the stiffer bedrock, subjected to vertically propagating shear waves. This common step in earthquake geotechnical engineering provided soil deposit and soil surface motions for selected bedrock input signals. Subsequently in simplified dynamic analysis procedures usually the soil surface acceleration amplitude is applied in a response spectrum procedure. However when soil-structure interaction by the pile shafts is to be accounted for, the soil deposit motion along the entire shaft has to be calculated. The free field responses are obtained by equivalent linear frequency domain analysis and Plaxis 2D analysis, where ultimately the performance of the very new Plaxis 3D dynamic module was verified. Typical performances of different available Plaxis soil constitutive models in dynamics are studied and recommendations regarding their application are formulated.

Subsequently in the fourth phase of the study simplified dynamic analysis and uncoupled and coupled dynamic analysis are performed for the site and structure. Based on the jetty lateral load-deformation characteristics obtained from pushover analysis, simplified dynamic analysis will be performed. The calibrated green field soil models resulting from the previous stage are used as a basis for constructing coupled dynamic models and the free field responses are applied to the structural model in uncoupled dynamic jetty analysis. The goal of this stage is to compare and assess structure responses obtain along the different approaches and investigated how soil structure interaction effects may affect the response

Finally, concluding remarks relating recommended seismic design procedures for jetty structures will be postulated, where the importance of coupling of soil and structure response is considered as well.

4 Theoretical Background

4.1 Earthquakes

4.1.1 Earthquake origin

Earthquakes are caused by vibrations of the Earth's surface due to a sudden release of energy somewhere in the Earth's crust. This energy is generated by a gradually build up of stresses along plate boundaries, induced by continental drift of the tectonic plates, as can be described by the elastic rebound theory. The continental drift is nowadays believed to be driven by convection currents within the Earth's mantle forming a continuous cycle of heating and cooling of the material it consists of.
Earthquakes can be characterized by various criteria. First of all they can be subdivided into two main categories, the inter-plate and intra-plate earthquakes. Intra-plate earthquakes are generate by faults in the plate interior where inter-plate earthquakes are generated by faults along the plate boundaries. Generally the strongest earthquakes are generated by inter-plate faults, since build-up stresses are typically higher at these locations.
Plate boundaries are categorized as divergent, convergent or transcurrent, depending on the relative movement of the adjacent plates. Additionally, three types of fault movements can be identified, i.e. the normal fault, the reverse of thrust fault and the strike-slip fault as indicated in Figure 4.1.

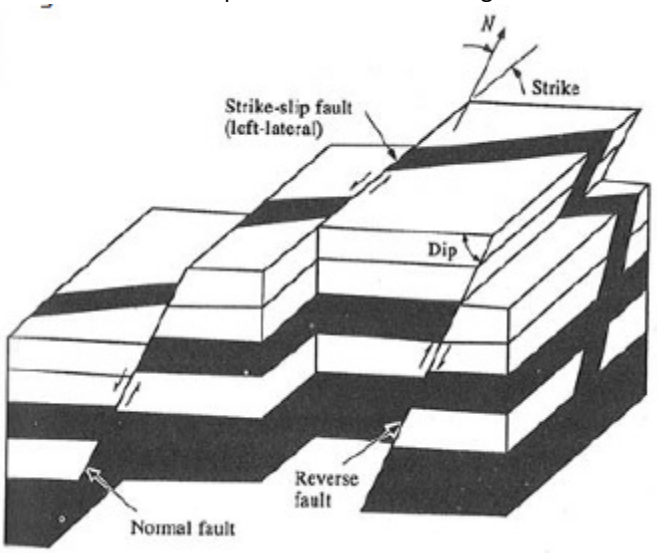

Figure 4.1: Interplate boundary types (after Clough and Penzien (1993))

The nature of faults and their activity is accounted for in probabilistic seismic hazard assessments and therefore is of interest in earthquake engineering. Additionally the distance of the site considered to the fault is of importance, where for near-fault projects vertical ground motions, directivity effects and high frequency content of the seismic signal are important issues to consider in design.

4.1.2 Magnitude, intensity and seismic moment

Earthquake levels can be described along different types of measuring scales. Important measures in earthquake engineering that sometimes are mixed up are magnitude, intensity and moment. Magnitude is the amount of energy released from the earthquake source. Intensity represents the impact of an earthquake on a specific site and so depends on distance from the epicentre and local soil conditions. Seismic moment is a measure for the overall deformation at the fault and can be interpreted simply in terms of ground deformation. Seismic moment is considered to be rather accurate in calculating the earthquakes source strength.
The most common magnitude scale applied in earthquake engineering practice is the Richter Scale, ranging from 0 to 10. An intensity scale often used is the Modified Mercalli Intensity Scale (MMI) ranging form I to XII.

Seismic moment scales also have been proposed by researchers, e.g. (Hanks & Kanamori, 1979) and (Kanamori, 1983). More information regarding this earthquake measuring scales can be found in most earthquake engineering textbooks.

4.1.3 Soil waves and attenuation

Once a tremor has been generated by a sudden release of energy, stress waves start propagating through the Earth's crust, causing soil deformations, which can be described along the wave propagation through solids theory, for which one is referred to (Kramer, 1996; Verruijt, 2005).

Considering the soil to react to local disturbances as an elastic solid, a variety of wave types are allowed which makes the resulting ground motion quite complex to determine.
First of all the waves can be subdivided into body waves and surface waves. Body waves again can be subdivided into primary waves (also denoted as pressure waves or P-waves) and secondary waves (also denoted as shear waves or S-waves). Shear waves can again be subdivided into S_h-waves and S_v-waves, indicating the direction of ground movement to be respectively horizontal or vertical. Elastic wave theory provides that P-waves travel faster than S-waves and therefore will be the first waves to arrive. P-waves can travel through solids as well liquids, where S-waves can travel through solids only. This implies that S-waves cannot travel through the Earth's liquid core where P-waves can.

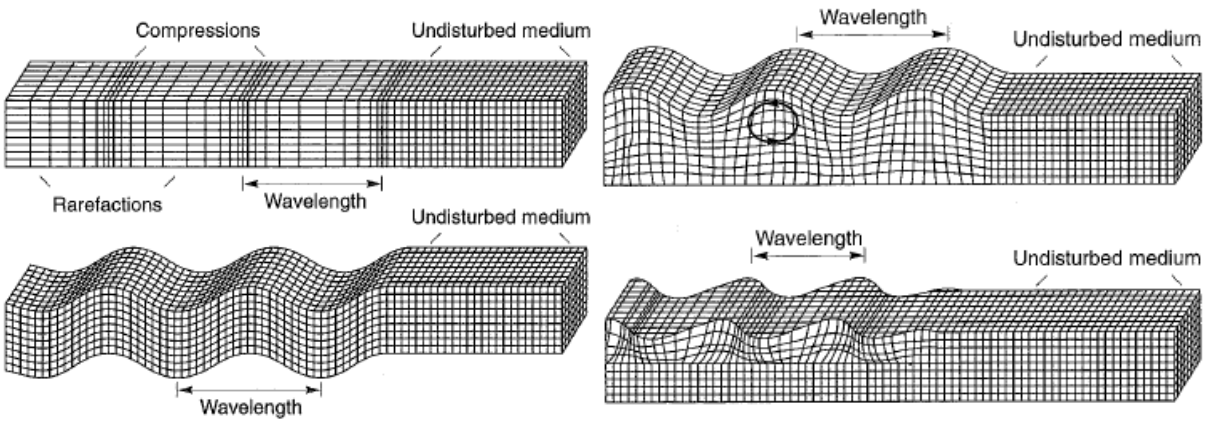

Figure 4.2: Top left: Compression body wave, Bottom left: Shear body wave, Top right: Surface Rayleigh wave, Bottom right: Surface Love wave (From S.L. Kramer, Geotechnical Earthquake Engineering (1996))

Surface waves also can be split up in two important sub-categories, i.e. Rayleigh waves and Love Waves. Rayleigh waves are the result of interaction between P and S_v waves and their existence was first demonstrated by the English physicist John William Strutt (Lord Rayleigh) in 1885. Rayleigh waves are analogous to water waves and can be shown to exist in a homogeneous elastic half-space. Love waves are the result of interaction between P and S_h waves and where deduced by the Britisch mathematician A.E.H. Love. Love waves require a surficial layer of lower S-wave velocity compared to the underlying half-space. Other types of surface waves exist, but are considered to be much less relevant from an earthquake engineering point of view.

Wave propagation affect seismic signal while it travels away from its source. Thereby understanding and using the principles of wave propagation make seismologist able to predict site soil response based on ground conditions along the travel path of the wave. Principles of dispersion, refraction, diffraction and filtering of wave signals are of importance in this sense. Traditionally, seismologists accounted for wave propagation by empirical local attenuation laws, which are averages found from recorded accelerograms. With increasing experience in this field specialist become able to define local seismic signals more accurately, by making use of advanced models. Nevertheless it should be noted that it is always to be recommended to check results by advanced models against these local empirical attenuation laws and simple site response analysis techniques.

4.1.4 Site amplification effects

Fault characteristics together with wave propagation effects determine the local bedrock ground motion intensity, frequency content and duration. Then to determine design ground level ground motions is to account for site amplification effects. It is noted that in this study the effects of surface waves are not considered, where it is restricted to the common engineering approach representing the seismic load by vertically propagating shear waves only.

The site amplification effects are characterized by the natural frequencies of the soil deposit, which can be estimated (Kramer, 1996) based on the averaged present soil shear wave velocity and soil deposit height as:

$$f_n = \frac{v_s}{4H}\left(1+\frac{n}{2}\right), n = 0,1,2,.... \quad (4.1)$$

Often the soil deposit parameters are taken over the top 30 meters of the deposit, but whether this common depth is appropriate is very much project dependent. Generally the top 30 meter approach is most appropriate for rather short period content of the bedrock signal, as for longer periods seismic wave lengths are much longer than 30 meters and response is likely to be affected by soil characteristics at much greater depths. From equation (4.1) the fundamental frequency and fundamental period of the soil deposit are easily derived to be:

$$f_0 = \frac{1}{T_0} = \frac{v_s}{4H} \quad (4.2)$$

It is noted that averaging the soil deposit characteristics over depth may result in inaccurate predictions of actual site amplification. A better estimate generally is obtained by performing site response analysis including the layering of the deposit, for which one is referred 4.4.1.

4.2 Seismic hazard assessment, probabilistic or deterministic approach

In the preceding paragraphs, factors affecting a seismic site input signal were discussed. Ground motions can be estimated on the basis of these factors, which is called site seismic hazard analysis. Two seismic hazard analysis approaches are distinguished; i.e. deterministic seismic hazard assessment and probabilistic seismic hazard assessment. In the first approach a particular governing earthquake scenario is deterministically assumed to be governing based on the available information on seismic sources in the surrounding area. In the second approach uncertainties in fault location and activity, earthquake magnitude, wave attenuation and return period are taken into account in a probabilistic calculation resulting in a local ground shaking level related to a certain probability of exceedance. Generally for a specific construction site, different bedrock shaking levels with related return period or probability of occurrence in a certain time interval are provided.
Modern seismic standards define ground motion levels mostly in the probabilistic setting. A remarkable exception in this sense is the new approach adopted in the U.S. NEHRP 2012 seismic design regulations, that for very high seismicity areas shift from probabilistic-based ground motion levels to maximum-to-be-expected ground motion levels for near active fault areas in order to obtain more economic designs.

Probabilistic seismic hazard assessment procedures are subdivided by many standards in a simplified code based approach and a detailed site specific probabilistic seismic hazard assessment. The simplified code based method defines design peak accelerations based on topographic location and local soil conditions only, where in the site specific detailed assessment procedure all possible influencing factors may be accounted for. For sites where strong ground motions are to be expected or soil conditions are very much varying or weak, a detailed site specific seismic hazard assessment is recommended by most standards. Estimating ground motion levels and its reliance on incomplete or uncertain information makes the seismic hazard analysis process dependent on unavoidable subjective decisions by the engineer. Hence it is noted that an additional check of the resulting ground motions by simplified assessment procedures is recommended as well.

4.3 Performance based design

In traditional structural engineering and earthquake engineering practice most structures were designed primarily based on static, or equivalent static loads (derived from inertia forces). However, the conventional force based approach has proved to suffer from several shortcomings when used in seismic design, which are related to the extreme load levels for high intensity earthquakes. These shortcomings are mostly related to:

- Interdependency of strength and stiffness;
- Uncertainties related to appropriate force reduction factors and ductility capacity
- Redistribution possibilities in irregular structures when properly designed for.

Generally too heavy designed structures result from purely force based design, for which it seems hard to ensure sufficient ductility under earthquakes exceeding the design level earthquake. Furthermore also redistribution of forces over structural elements is more difficult to appropriately account for in structural design and a clearer view on possible failure modes may result more effective and consequently more economic designs. Since lessons learned after strong earthquakes in the 1990s a trend switch has taken place in which performance based design has become an increasingly popular methodology in earthquake engineering practice.

The key concept in performance/deformation based design is the inclusion of design damage or deformation criteria rather than design forces as a starting point in seismic design. Post-elastic structural behaviour is preferably directly incorporated in design were coupling with ductility and damping can be achieved. Generally, the design deformation objectives are related to a structural importance class, combined with a multi-level (usually a dual-level) intensity approach. Important details relating to this two-way approach are presented in the next sections for the following seismic regulations:

- Eurocode Regulations for Earthquake Resistant Design (NEN-EN 1998, 2004)
- Turkish Technical Seismic Regulations for Port and Harbour Structures (Turkish Technical Seismic Regulations, 2008)
- ISO Seismic Design Regulations (ISO 19901-2, 2004; ISO 19902:2006, 2006; ISO 19903, 2006)
- U.S. NEHRP and MOTEMS Seismic Design Regulations (NEHRP Fema-450, 2012; MOTEMS, 2010)
- PIANC Seismic Design Guidelines for Port Structures (PIANC, 2001)

Simplified performance based seismic design techniques for buildings have been under discussion already for many years and are therefore widely available. However, for port structures accuracy of simplified methods is less clear. Goel has proposed performance based design methods for pile-deck systems (Goel, 2010), however it is noted that accuracy of the analytically derived expressions is not verified by experiments which will be done in the near future.

4.3.1 Structural importance classes

Seismic standards generally specify performance objectives based on a structure importance class and an earthquake motion level. The former is presented herein as it is described in Eurocode (importance classes I, II, III or IV). Other seismic codes have somewhat different nomenclature, MOTEMS defines a Risk Classification (High, Medium or Low), the Turkish Seismic Design Regulations define a structure category (Special, Normal, Simple, Unimportant), NEHRP defines a Seismic Use Groups (SUG I, II and III) and PIANC follows the Japanese Standard that defines structure classes (Special, A, B or C) Main properties of port structures that are decisive for the related importance class are:

- If the structure is open to the public
- To which extended is the structure of importance for earthquake recovery
- If hazardous materials will be treated at the structure (Eurocode, Turkish Reg., NEHRP, PIANC)
- Maximum vessel size and annual amount of cargo transferred at the structure (MOTEMS)

In the following paragraph earthquake motion levels as defined in various seismic standards are summarized, based on structure importance class IV or equivalent.

4.3.2 Earthquake motion levels

In the common dual-level design approach, two design earthquake motion levels are defined and related performance objectives based on structure importance class are established.

Table 4.1: Dual level Earthquake motions for High Importance Class structures (including LNG/Oil Jetties) summarizes earthquake motion levels provide by different seismic standards.

Table 4.1: Dual level Earthquake motions for High Importance Class structures (including LNG/Oil Jetties)

Standard	*Structure class*	*Earthquake motion level*	*Probability Of Exceedance over period T (POE) and mean return period (MRP)*
Eurocode 8	Importance class IV *	Damage limitation requirement earthquake	POE = 17% in 50 years MRP = 261 years
		No collapse requirement earthquake	POE = 4% in 50 years MRP = 1303 years
Turkish Seismic Regulations 2008	Special Structures	E1 earthquake	POE = 50% in 50 years MRP = 72 years
		E2 earthquake	POE = 10% in 50 years MRP = 475 years
		E3 earthquake	POE = 2% in 50 years MRP = 2475 years
NEHRP - Fema 450	Seismic Use Group III ***	Maximum probable event (MPE)	POE = 50% in 50 years MRP = 72 years
		Maximum reasonable to be expected earthquake level	POE = 2% in 50 years MRP = 2500 years or deterministically determined **
MOTEMS 2010 California Building Code	High Risk Classification	Level 1 earthquake	POE = 50% in 50 years MRP = 72 years
		Level 2 earthquake	POE = 10% in 50 years MRP = 475 years ****
ISO 19901-2 (simplified procedure)	Exposure level L1, Seismic risk category 4	Extreme level earthquake	Undefined, because ELE level related to ALE level by reserve capacity coefficient C_r. Back-calculation by EC8 annual P_{exc} expressions and C_r = 2 results: POE = 22% in 50 years, MRP = 312 years
		Abnormal level earthquake	POE = 2% in 50 years MRP = 2500 years
Pianc	Special Class	Level 1 earthquake likely to occur during structure life span	POE = 50% in approximately 50 years, MRP = 72 years
		Level 2 rare infrequent high intensity earthquake	POE = 10% in approximately 50 years, MRP = 475 years

* According to Eurocode 8 ground peak accelerations are multiplied by an importance factor. In order to then obtain equivalent motion levels a formula is suggested to calculated annual rate of exceedance probabilities corresponding to different motion levels: $H(a_g) = k_0(a_{g,ref}\gamma_1)^{-k}$, where k_0 is a site specific constant, γ_1 is the importance factor and k is a constant approximately equal to 3.

* In FEMA-450 Commentary 1.2 the related earthquake level is termed the reasonably representative of the most severe ground motion for moderate seismic zones. Subsequently one design structures for this maximum considered earthquake multiplied with factor 2/3 to the performance criteria applicable to the damage control limit state. Additionally it is stated that for zones of high seismicity a PSHA may give too high structural demands, which are much higher than structural demands for characteristic magnitudes of earthquakes gener-

ated every few hundred years by these faults. Therefore a deterministic procedure is proposed for calculation near fault high seismicity ground motion levels.
** NEHRP couples SUG to response quantities and performance objectives, not directly to ground motion intensity.
*** In the new ASCE standard currently under development, which probably will also affect future MOTEMS standards, level 2 earthquakes will be related to 2% in 50 years earthquakes.

As shown in Table 4.1, design earthquake levels vary considerably with the different seismic design standards. Interestingly, the seismic port design standards MOTEMS (U.S.) and Pianc (a lot of input from the U.S.) provide significantly lower return periods for the highest level design earthquake, compared to the Eurocode seismic regulations and Turkish seismic regulations for Construction of Coastal and Harbour Structures.

4.3.3 Performance objectives, ductility and damage criteria

Seismic design standards generally provide performance objectives related to predefined safety targets, based on structural classes and design earthquake levels. Additionally these objectives may be modified by the client in consultation with regulators, or to meet regional requirements where they exist. The level to which performance objectives are specified in different seismic standards differs considerably. Some codes exactly quantify allowable material strains and structure displacements for different earthquake levels (Turkish Seismic regulations, MOTEMS, Pianc), where others only generally specify a state of allowable damage (Eurocode 8, ISO Seismic regulations).

In this research on seismic jetty design, the focus will be on performance objectives for these type of port structures. It has to be noted that performance objectives for these type of structures are less common than the detailed requirements formulated for building structures.

4.3.3.1 Eurocode 8

Eurocode 8 seismic regulations (NEN-EN 1998, 2004) do not provide specific performance objectives for jetties or other type of pile supported port structures. General deformation requirements given in Eurocode 8 primarily focus on verification of rotation in potential plastic hinges in general for any type of structue. These requirements are provided in Eurocode 8 -1 and are referred to in other parts of the standard, including the part on foundation design.

In order to be allowed to benefit of plastic hinging in seismic design, according to Eurocode 3, steel circular hollow sections need to be of section class 1 or 2, which is guaranteed if:

$$\frac{D}{t} < 70\frac{235}{f_y} \tag{4.3}$$

Where D and t are the tube diameter and thickness respectively and f_y [MPa] is the material yield strength.

With respect to the two typical limit states (Damage Limitation Requirement and No Collapse Requirement), Eurocode 8 requires no or very minor damage due to ground motions associated with the first limit state, however no typical limit rotations for piles are presented. With respect to the second limit state the code allows rotations up to the real ultimate rotation capacity, divided by structural safety factor depending on kind of material considered. It is stated that material related partial factors should account for strength degradation due to cyclic loading. If not available, partial factor γ_M for persistent or transient loading may be applied.

According to Eurocode 8, piles should be designed to remain elastic, but may under certain conditions (that are not further defined) be allowed to develop plastic hinge at their heads.

4.3.3.2 Turkish Technical Seismic Regulations (2008)

This paragraph on Turkish Technical Seismic Regulations performance objectives is based on the chapter on seismic design of pile quays and jetties (Turkish Technical Seismic Regulations, 2008). The modern Turkish Seismic Regulations are already strongly adapted to deformation based design principles, significantly further than many other seismic design standards. The displacement based design is in these regulations fully integrated and also appointed as such. Furthermore typically a complete chapter is related to seismic design of

port structures, where other seismic standards often lack specific regulations for this group of structures. Performance objectives for jetty structures presented in these regulations are:

- Conform these seismic regulations, plastic hinges are not allowed to develop in decks of pile quays and jetties. Plastic hinges may only develop in piles or monolithic pile-deck connections.
- For both the resistance-based design approach and the deformation-based design approach limit relative deformations at jetty deck level are presented:
- Limit strains for different earthquake levels are presented as shown in Table 4.2

Table 4.2: Limit strains for structural steel according to Turkish Seismic Regulations (2008)

	Minimum Damage	Controlled Damage
Resistance-based design	0.008	0.015
Deformation-based design	0.008	0.025

It is worth noting that the allowed material strains for the minimum damage performance objectives are considerably beyond initial yielding, which seems to be a general trend in different seismic regulations. Apparently much higher strains can be accepted according to this standard, even for the minimum damage requirements.

The pile curvatures corresponding to the limit strains shown in Table 4.2 may be calculated according to:

$$\varphi_{ls} = \frac{\alpha \varepsilon_{ls}}{D} \tag{4.4}$$

Where $\alpha = 2.25$ and $\alpha = 2.10$ are dimensionless factors for circular concrete piles and rectangular concrete piles respectively. For steel pipe piles no limit curvature expressions are given. To prevent for plate buckling under these high stress/strain levels, the regulations require minimum t/D ratio's for tubular steel piles to be:

$$\frac{D}{t} \le c\frac{E}{f_y} \le 80 \tag{4.5}$$

Where c is a dimensionless factor ranging from 0.08 to 0.14, depending on the pile installation procedure and eventual pile fill.

4.3.3.3 MOTEMS/NEHRP Fema 450

MOTEMS is the Californian seismic design guideline for marine oil terminals (MOTEMS, 2010). MOTEMS is part of the California Building Code, is to a far extent adopted to the concept of performance-based design. Californian oil terminals that are subjective to high near fault seismicity are being designed according to these standards. The MOTEMS guidelines therefore partly overrule NEHRP Fema-450 when it comes to seismic resistant of port structures in the U.S. Besides, NEHRP is primarily focussed on earthquake resistant design of buildings. Hence in the present study performance objectives according to MOTEMS are treated, and performance objectives according to NEHRP Fema-450 are not.

According to MOTEMS, plastic deformation mechanisms are not allowed in decks. Strain limits for steel pipe piles as specified in MOTEMS are presented in Table 4.3.

Table 4.3Limit strains for structural steel according to MOTEMS (2010)

	Level 1	Level 2
Limit strain ε_{ls} at pile-deck connections	0.008	0.025
Limit strain ε_{ls} at in ground plastic hinges	0.004	0.008

Additionally it is stated that each structural component expected to undergo inelastic deformation shall be defined by its moment-curvature relation. These moment curvature relations may be developed based on the Level 1 and Level 2 limit strains as shown above, which can be translated into typical limit curvatures for steel piles as:

- Steel section first yield curvature:

$$\varphi_y = \frac{2\varepsilon_y}{D} \tag{4.6}$$

- Steel section effective yield curvature:

$$\varphi_{y,eff} = \frac{(2.1 \sim 2.2)\varepsilon_{y,eff}}{D} \tag{4.7}$$

- Steel section limit strain curvature:

$$\varphi_{ls} = \frac{2\varepsilon_{ls}}{D} \tag{4.8}$$

Based on these limit strains, global structural displacement capacity may be determined by a nonlinear static procedure. Yield curvatures and estimated plastic hinge length may subsequently be used to calculated rotations and displacements at yield.

4.3.3.4 ISO Standards

ISO guidelines (ISO 19901-2, 2004) provide general descriptive performance requirements for both ELE (Extreme Level Earthquake) and ALE (Abnormal Level Earthquake) design levels. However, no clear numerical limit values for deformation parameters are provided.

Among the most important requirements for ELE design are:

- Limited nonlinear behaviour is permitted, brittle degradation shall be avoided
- Secondary structural components shall follow the same ELE design rigour as that of primary components
- Joints strengths shall exceed calculated elastic joint forces and moments
- At foundation component element level an adequate margin shall exist with respect to axial and lateral failure of piles. At the foundation system level an adequate margin shall exist with respect to large-deflection mechanisms which would damage or degrade and require repairs to the structure or its ancillary systems
- Not any loss of functionality in safety, escape or evacuation systems is allowed due to the ELE

With respect to ALE events the requirements are:

- Structural elements are allowed to exhibit plastic degrading behaviour, but catastrophic failures should be avoided
- Stable plastic mechanisms in foundations are allowed, but catastrophic failure modes such as instability or collapse should be avoided.
- Joints are allowed to exhibit limited plastic behaviour within their ultimate strengths, but shall be designed to demonstrate sufficient ductility and residual strength at these deformation levels
- Safety, escape and evacuation systems shall remain functional during and after an ALE event

It may be clear that ISO performance objectives are very generally formulated, giving quite some freedom to the engineer, while on the other hand covering all most important performance requirements for the dual level approach.

4.3.3.5 Pianc

Assuming the jetty structure to be a Special Class structure, PIANC design guidelines for port structures (PIANC, 2001) require the structure to remain serviceable for a Level 1 and serviceable/repairable for a Level 2 earthquake event.

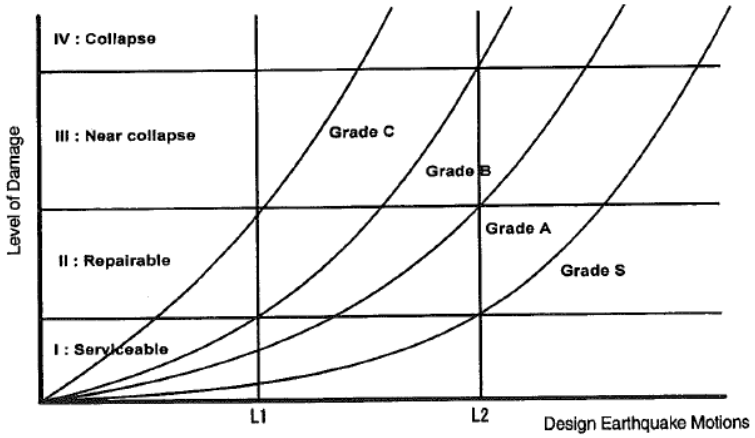

Figure 4.3: Schematic figure of performance grades (From Pianc (2006))

Limit residual displacements for pile supported wharves, related to the Degree II damage level as provided by PIANC are presented in Table 4.4. It should be noted that performance objectives as indicated in PIANC strictly apply to wharves. It is reasonable that similar values apply to jetties, where it might be expected that performance objectives in transverse direction are less strict for jetties, but this will depend very much on use of the jetty (chemicals, spill risks, etc.)

Table 4.4: Limit residual displacements according to Pianc (2006)

	Degree II damage level
Differential settlement between deck and land behind it	0.1~0.3 m
Residual tilting towards the sea	2° = π/90 rad

For piles and other structural components it is required that flexural failure should precede shear failure. PIANC follows MOTEMS in the definition of allowable deformations related to the dual limit state approach and moment curvature relations. Again it may be noted that again the limit strain for the low level L1 earthquake (0.008) exceeds the steel strain at yield by a factor 4 - 6, depending on the steel quality. This implies that experiences from the past have shown that only minor damage will result for this relatively high limit strain level that exceeds the strain at initial yielding by far. Limit strains subsequently can by linked to limit curvatures, which then determine plastic rotation capacity as:

$$\theta_p = \varphi_p L_p = (\varphi_{ls} - \varphi_y) L_p \tag{4.9}$$

Where the plastic hinge length (L_p) depends on the section shape and the slope of the moment diagram in the vicinity of the plastic hinge. Plastic hinge lengths in piles located below ground level are consequently also affected by subgrade reaction stiffness of the soil, but since they are not repairable after a seismic event they are generally not accepted.

PIANC provides that for structural analysis it will often be adequate to represent the response by a bi-linear approximation as shown in Figure 4.4. It is noted that the representative yielding bending moment is taken typically higher than the bending moment corresponding to the onset of first yielding (consequent with equations (4.4) and (4.7)).

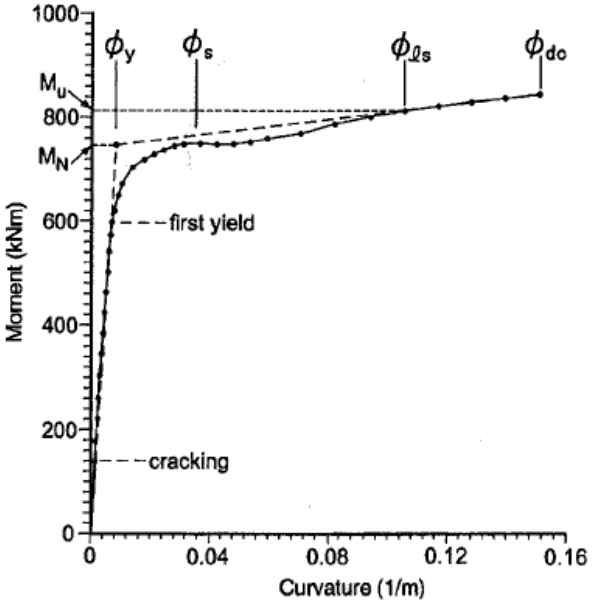

Figure 4.4 Pile cap moment-curvature (From Pianc (2006))

The simplified bi-linear moment-curvature relations for the plastic hinges accordingly are defined as:

$$(EI)_i = \frac{M_n}{\varphi_y} \; for \; \varphi < \varphi_y \; and \; (EI)_p = \frac{M_u - M_n}{\varphi_{ls} - \varphi_y} \; for \; \varphi_y < \varphi < \varphi_{ls} \qquad (4.10)$$

4.3.3.6 Conclusions on performance objectives

According to the considered seismic design standards, the most important concluding remarks regarding performance objectives for pile-deck port structures are:

- All performance objectives seem to overlap for a quite substantial part and all are defined according to the generally adopted dual level design approach;
- Pure elastic response is not a limit state to be considered, even for the low level earthquake
  Therefore, using elastic stiffness as a starting point in design is not the best choice. Hence, start with designing for high level earthquake and then checking for low level seems the best approach;
- Limit material strains are provided by most seismic design standards. Starting from these limit strains and plastic hinge lengths, maximum allowable rotations in structural nodes can be determined. Defining appropriate plastic hinge lengths may be quite difficult, estimations may be based on the theory of plasticity, (Hartsuijker, 2004);
- Maximum allowable deck displacements for jetties seem to be governed by the jetty use and installations on top of it. Limit displacements therefore seem to partly be supplied by the owner of the structure, based on a risk assessment.
- PIANC guidelines define not only performance objectives during a seismic event, but also limit residual displacements. Past earthquakes have shown that these residual displacements for port structures are greatly affected by soil failure and foundations-soil interaction, for which performance objectives are limited since these topics are less significant for buildings. Simplified techniques do not include such soil failure related problems. Hence, nowadays finite element dynamic analysis of the entire soil-structure system by making use of advanced soil models is getting more common. These modern techniques generally provide better insight on deformations and stresses along the structure and eventually result more economic designs and a clearer view on possible failure modes, among other advantages.
- Past earthquakes have resulted many cases of jetty pile failure due to unacceptable bending moments in the piles induced by combined kinematic and inertial action, resulting unacceptable permanent deformations. For typical jetty structure configuration with the deck having a much higher bending stiffness compared to the piles, extreme bending moments in piles will be located first at the pile-deck connection and subsequently a in-ground plastic will be formed. With respect to reparability, most

seismic design standards do not allow for the in-ground plastic hinge to form, where at the pile-deck connection a considerable degree of pile plastic deformations is allowed.

Although MOTEMS specifies performance objectives in a quite detailed way, it is relatively limited in describing how to implement these performance objectives. A valuable complementary document in this sense is the book Displacement-Based Seismic Design of Structures ((Priestley, Calvi, & Kowalski, 2007). The book is not an legally established design standard, but does completely comply with the MOTEMS standard. It provides performance objectives identical to the performance objectives as presented in MOTEMS and besides also extensively describes how to practically implement these requirements in seismic design.
Additional recommendations for determination of ductility capacity levels for pile deck systems are provided by Goel (Goel, 2010). A simplified procedure is proposed in which the embedment of the pile in the soil is simplified by assuming an equivalent fixity depth. Subsequently ductility capacity expressions are developed based for different boundary conditions for the pile-deck connection. It should be noted that assumptions underlying this simplified procedure should be well verified. Additionally one should realize that the procedure is very new, and additional research and verification against test results is recommended to establish its accuracy.

4.4 Available seismic design methods

Seismic design of port structures is a discipline where geotechnical and structural earthquake engineering are involved. Consequently for these projects structural and geotechnical design procedures need to be combined. The two groups of design procedures are considered in this paragraph in succession.

4.4.1 Geotechnical soil site response analysis

Seismic excitation levels at bedrock level are provided from global seismic hazard maps or preferably from a site specific probabilistic seismic hazard assessment. In this study the common engineering approach considering only vertically propagating shear waves is followed, where surface waves are not considered. Then surface motion levels are calculated based on local soil conditions that determine the transfer function for surface motion due to bedrock motion. Often for computational convenience a 1D problem is considered which then is considered to behave as an (equivalent) linear Kelvin-Voigt solid, for which the 1D shear wave equation can be written as:

$$\rho \frac{\partial^2 u}{\partial t^2} = G \frac{\partial^2 u}{\partial z^2} + \eta \frac{\partial^3 u}{\partial z^2 \partial t} \tag{4.11}$$

Which has the a general solution of the form:

$$u(z,t) = Ae^{i(\omega t + k^* z)} + Be^{i(\omega t - k^* z)} \tag{4.12}$$

Where k^* is a complex wave number and the two terms relate to upward and downward propagating waves respectively. The constants A and B are determined based on interface and boundary conditions at the soil layer interfaces and the surface and bedrock boundaries of the soil deposit.

4.4.1.1 Roesset's site response amplification function approximation

Roesset's site response amplification function (Roesset, 1970) for motion amplitudes at surface level due to excitation at bedrock level is a solution of the problem of vertically propagating shear waves through a homogeneous soil deposit as presented above, and is defined as:

$$A(f) = \frac{2}{\left|(1+\alpha)e^{ikH} + (1-\alpha)e^{-ikH}\right|} \tag{4.13}$$

Where $\alpha = \dfrac{\rho_{soil} v_{soil} (1+\xi_{soil})}{\rho_{bedrock} v_{bedrock} (1+\xi_{bedrock})}$ is the soil-rock impedance as a function of soil and rock density, shear wave velocity and damping ratio respectively, $k = \dfrac{\omega}{v_{soil}(1+\xi_{soil})}$ is the wavelength as a function of frequency and H is the soil deposit height.

When one then assumes the bedrock to be rigid, and the damping ratio to be relatively small, the Roesset amplification function can be simplified to:

$$A(f) \approx \frac{1}{\sqrt{\cos^2\left(2\pi f \frac{H}{v_s}\right) + \left(2\pi f \frac{H \cdot \xi}{v_s}\right)^2}} \tag{4.14}$$

Where this amplification function is a simplification of the complex Roesset solution of a single soil layer problem where analogies of complex power functions and goniometric functions are utilized.
If a soil profile is homogeneous or close to homogeneous and ground motion levels are not very high, Roessets approximation may be considered to provide reasonable estimates of actual site response. However, often these conditions are not met in practice and the soil layering is preferred to be included in the site response transfer function.

4.4.1.2 1D equivalent linear multi-layered soil site response analysis

Nonlinear multi-layered analysis conceptually provides the most accurate transfer function for surface motion due to bedrock motion, but computational effort is often relatively high and validation of results by a more simple methods is to be preferred in order to eliminate numerical errors.
For this purpose a 1D equivalent linear multi-layered soil site response analysis in the frequency domain is often used. It is noted that this analysis type does not account for boundary disturbances and 2D or 3D wave propagation. However, when a continuous soil profile reasonably may be assumed, the 1D solution may be expected to be close to the finite element analysis results, provided that finite element model boundary effects are limited. The 1D multilayered linear analysis configuration is depicted in Figure 4.5, where for equivalent linear analysis soil parameters are iteratively determined based on average strain levels.

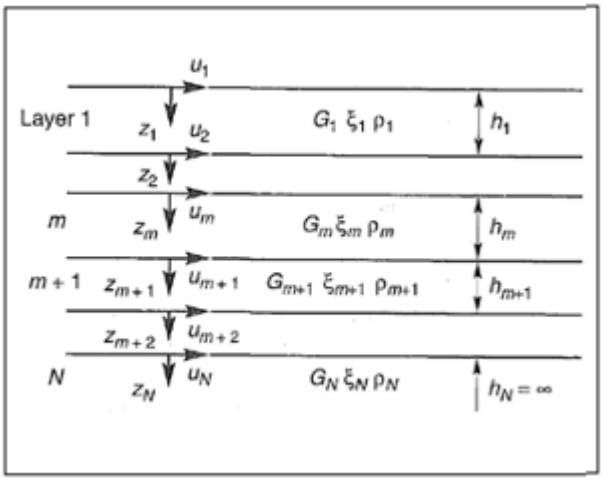

Figure 4.5: Multi-layered linear analysis configuration (after Kramer, 1996)

For a multi-layered soil deposit, transfer functions are derived based on boundary conditions at surface level and interface conditions related to compatibility requirements at the layer interfaces, for which one is referred to (Kramer, 1996).

The multi-layered linear approach is extended to an equivalent linear approach by including an iterative procedure for convergence of strain level and related shear modulus and critical damping percentage as is observed for soils. The representative effective strain level according to (Idriss and Sun, 1992) is determined to be approximately

$$\gamma_{eff,layer} = R_\gamma \gamma_{\max,layer} \tag{4.15}$$

Where $\gamma_{\max,layer}$ [-] is the maximum shear strain observed in a soil layer during the considered time history and $R_\gamma = (M-1)/10$ a dimensionless reduction factor, with M being the earthquake magnitude measured according to the Richter scale.

4.4.1.3 Finite element free field site response analysis

2D or 3D finite element models for free field site response analysis account for different types of waves to develop in the continuum, which by definition will give a more accurate representation of actual surface motions due to bedrock excitation compared to the 1D approximation. Besides, in such analysis 2D/3D site geometric properties (e.g. slopes, basins, discontinuous soil profiles) affecting the wave field can be included. By using a nonlinear advanced soil model it additionally is possible to account for a nonlinear soil constitutive behaviour, which is not included in a simplified (equivalent) linear approximation. Drawbacks of the potentially more accurate nonlinear analysis are the higher accuracy and the difficulties in modelling nonlinear behaviour accurately.

Finite element free field site response analysis is in practice performed to validate the finite element models with respect to disturbances by model boundaries and sensitivity to mesh coarseness. It is a preliminary step towards coupled dynamic analysis of site and structure. When a proper dynamic free field model is obtained, the structure can be included and the response of the coupled soil-structure system can be calculated.

4.4.2 Structural seismic design methods

Seismic standards and guidelines allow structural engineers to use many different structural analysis methods, with varying complexities. It is often preferable to apply analysis methods with increasing levels of complexity levels in succession, in order to optimize the design procedure in terms of efficiency and final accuracy. Relative simple methods are then used in preliminary design stages, followed by more advanced methods for final design. Generally the complexity of the recommended analysis procedure increases with increasing ground motion level and increasing structure importance. Roughly the structural analysis methods as included in different seismic codes can be subdivided in three main categories, according to PIANC:

- Simplified analysis
- Simplified dynamic analysis
- Dynamic analysis

Furthermore, along performance based design principles, design methods can be divided in methods to be used to determine structural deformation capacity and methods to be used to determine structural deformation demand.

4.4.2.1 Simplified analysis

Different types of simplified analysis procedures may be distinguished. However almost all are based on elastic pseudo-static loads, combined with code specified factors accounting for structural nonlinear response.
In resistance based design, simplified analysis the order of magnitude of the elastic response. Subsequently the response beyond the elastic range is estimated based on the obtained elastic response and code-specified multiplication factors.
In performance based design, the simplified analysis procedures are used to estimate structural geometry based on allowed limit performance objectives (e.g. strains, displacements or drifts) by an iterative procedure optimizing the stiffness/ductility properties of the structure.

Traditional methods estimate pseudo-static loads based on the soil characteristics of the upper 30 meters of the soil profile, resulting in a response spectrum representing the response of a SDOF oscillator at the soil surface due to an excitation at bedrock level. Most seismic standards provide design response accelerations in such a spectral format. Based on local soil conditions an elastic design spectrum for a single degree of freedom system with damping ratio 0.05 is provided, from which the design structural acceleration can be read based on the structure's eigen-frequency. Although seismic elastic design spectra seem to differ considerably over different standards, the key features are similar for all of them. Stiff soil conditions transfer energy to the higher frequency range, where less stiff soils shift spectral energy to the lower frequencies

Design elastic response spectra provided in most seismic standards are based on 5% critical damping. Some standards specify how to account for other structural %-critical damping values, which can be very beneficial since higher damping values lower the design response spectrum.
Additionally most seismic design codes allow the design elastic response spectra to be reduced for behaviour beyond the elastic range. For example Eurocode 8 includes a behaviour factor q to account for this, while ISO

standards make use of seismic reserve capacity factor C_r to distinguish nearly elastic response level earthquakes from very rare infrequent high-intensity earthquakes.

Figure 4.6 shows the Eurocode 8 response spectra, indicating the spectral dependence on local soil conditions. The period at the horizontal axis is related to the SDOF natural period, and S_a at the vertical axis is the SDOF maximum absolute acceleration for the governing ground acceleration amplitude.

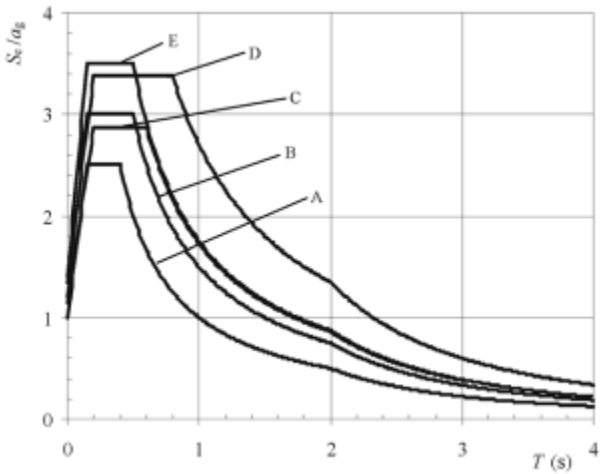

Figure 4.6: NEN-EN-1998:2005 Elastic horizontal response spectra

According to PIANC, simplified analysis is of limited value for jetty structure design in high seismicity areas. Most seismic design standards (PIANC, MOTEMS, Turkish Technical Seismic Regulations) do not recommend or even not allow these most simplified methods to be used for port structures in high importance/risk classes or structures in high seismicity areas. Important factors herein are the effects of soil nonlinearity and coupling of structure-foundation-soil which is of particular importance for pile-deck systems in soft soil conditions.

4.4.2.2 Simplified dynamic analysis

In simplified dynamic analysis the structural behaviour beyond the elastic range is analyzed by means of a pushover analysis. In this type of analysis the structure is loaded incrementally up to values beyond its elastic response range. By this means the elastic and post-elastic behaviour is determined, which subsequently is accounted for in the response spectrum procedure. More specifically, the elastic response spectrum is reduced based on ductile structural behaviour and additionally, secant structural dynamic properties are determined from the secant stiffness of the structure which provided the secant structure fundamental period. The accuracy of these simplified dynamic type of analyses is relatively well established for multi-story buildings, but less extensive research has been dedicated to its performance for port structures including pile-deck systems.

Various simplified dynamic procedures with different levels of complexity have been proposed by various researchers over the past decades, among the most important contributions are summarized below:

- Capacity spectrum method (CSM) (Freeman, 1998; Freeman, 2000)

This method was the first such type method. Freeman in this sense is considered the pioneer in this field. The method uses pushover, combined with response spectra including various damping values. The capacity spectrum method was the first method to use the acceleration-displacement-response-spectrum (ADRS) format. However, there is no clear link provided between ductility from pushover to spectra reduction by damping.

- N2 method (Fajfar, 1999)

The N2-method as proposed by Fajfar, is very similar to the CSM method. Fundamental difference is that in the N2 method, ductility obtained from push-over analysis is linked to spectra reduction by means of the equal displacement rule. Fajfar has included in his paper several limitations of the N2-method, which are partly related to this equal-displacement rule assumption. Generally is has been proven that the method seems to provide relatively accurate results in the medium to long period range, but performs significantly worse in the low period range. Additionally the method seems to underestimate responses for very soft local soil conditions. The

static nonlinear method as proposed by Fajfar and others, relies on the coupling of demand and capacity via the discussed relation between force reduction by R_μ and displacement increase beyond the elastic range by μ. MOTEMS chapter 3104F.2.3.2.5 provides additional relationships dealing with the correct estimate of ductility and spectral damping ratios.

- Multi-mode (adaptive) methods (Chopra & Goel, 2002; Chopra & Goel, 2004; Chopra, Goel, & Chintanapakdee, 2004; Aydinoglu & Fahjan, 2003; Kalkan & Kunnath, 2006)

The two methods describe previously estimate seismic demand based on the first natural frequency only. Past research has shown that this single-mode approach may introduce errors when higher modes contribute significantly to structural response. The cumulative participating modal mass to be included is set to 90% in most seismic design standards, requiring so called multi-mode push-over response spectrum methods. Among the most important contributions is the research done by Chopra and Goel (2002, 2004), who proposed a modal pushover response spectrum procedure and showed that this would increase accuracy of predicted response for reinforced concrete multi-story buildings. Later on Kalkan & Kunnath (2006) proposed an adaptive variant of this modal procedure, taking into account changing structural properties during an seismic event. It is noted that despite this adaptive character seems to make the method more accurate, it also complicates the nonlinear static method and increases it's computational demand. This makes it less attractive for practical engineering purposes.

The nonlinear modelling tools used for pushover analysis in simplified dynamic analyses are most often structural engineering finite element software packages (e.g. Scia Engineer, USFOS or Seismostruct), that are capable of accurately modelling all important nonlinearities in the structure. However, for jetty structures it also seems reasonable to use geotechnical engineering software like Plaxis in order to better model soil-structure interaction and allow for interaction of site and structure response.

4.4.2.3 Dynamic analysis

The method to be used for dynamic analysis of structures depends on the level of (non)linearity in structural behaviour. Assuming a structure to behave as a linear system is generally reasonable in the range of relatively low load levels, where nonlinear behaviour of the system is limited.
For dynamic analysis of linear systems the following two techniques are commonly used:

- Modal analysis, when damping is assumed to have the Rayleigh damping format
- Fourier analysis, when damping does not fit to the Rayleigh damping format.

The assumption of Rayleigh damping will generally not be appropriate if the system to be analysed exist out more parts with significantly different stiffness and damping characteristics. Coupled soil-structure systems are typically such systems where for the soil a much higher damping ratio will be realistic than for the structure.

The techniques available for analysis of linear systems are computationally much more convenient compared to the analysis of nonlinear systems. For this reason it is often attempted to define an equivalent linear system that approximates the response characteristics of the true nonlinear system. Major drawbacks of the equivalent linear approximation are the difficulties in obtaining accurate equivalent stiffness and damping characteristics, since these are depending on the varying load level. High intensity earthquakes generally result in structural responses beyond the elastic range, and consequently the assumption of equivalent linearity has limited applicability.

In dynamic analysis of nonlinear systems, the structural response is calculated by nonlinear numerical time integration. A powerful tool available is the finite element formulation of the problem. Accuracy and stability of the time integration process depend on the formulation of the time integration. Explicit and implicit schemes are available. For stability reasons generally an implicit scheme is preferred. A commonly used family of implicit time integration schemes is the Newmark (1959) type family, that is based on the following equations:

$$u^{t+\Delta t} = u^t + \dot{u}^t \Delta t + \left(\left(\frac{1}{2} - \alpha_N \right) \ddot{u}^t + \alpha_N \ddot{u}^{t+\Delta t} \right) \Delta t^2$$
$$\dot{u}^{t+\Delta t} = \dot{u}^t + \left((1 - \beta_N) \ddot{u}^t + \beta_N \ddot{u}^{t+\Delta t} \right) \Delta t \qquad (4.16)$$

Where α_N and β_N are the Newmark coefficients that determine the accuracy and stability of numerical time integration. Combined with the dynamic equilibrium equation at the end of the considered time step:

$$m \cdot \ddot{u}^{t+\Delta t} + c \cdot \dot{u}^{t+\Delta t} + k \cdot u = F \tag{4.17}$$

These equations provide the basis for computing $\ddot{u}^{t+\Delta t}$, $\dot{u}^{t+\Delta t}$ and $u^{t+\Delta t}$ from the known acceleration, velocity and displacement at the end of the previous time step.

Providing the input of the finite element model to be accurate, dynamic time integration analysis conceptually is the most accurate tool available to analyse the response of a nonlinear system. However, as recognized in most seismic design standards, the sensitivity of structural response to the input seismic motion is high. Hence, it is always to be required to perform the analysis for a number of different seismic input signals.

4.4.2.4 Structural analysis method selection

Along the principles of performance based seismic design, the following statements regarding the preferred design methods to be used can be made.
Regarding the deformation capacity of structures:

- Deformation capacity of structures can best be demonstrated by a static nonlinear pushover analysis. When advanced models are used, the actual structural response can be very well approximated by nonlinear pushover analysis.

Regarding the deformation demand of structures:

- The degree and importance of nonlinearity in the system are decisive factors for the type of deformation demand analysis method to be applied.
- For linear (or almost linear) systems, seismic deformation demand may be calculated by using modal analysis or Fourier frequency domain analysis of the (equivalent) linear system, for Rayleigh or non-Rayleigh damping respectively.
- For nonlinear systems of which the response is governed by the fundamental mode, simplified dynamic single mode response spectrum methods will provide reasonable results. A related minimum participating modal mass of the first mode is set to 90% by most seismic standards.
- For nonlinear systems of which higher modes contribute significantly to the response, multi-mode simplified dynamic response spectrum methods are generally more appropriate compared to a single mode approximation. However, the modal combination rule to be used is very much structure dependent (Chopra, 2001), which introduces a significant uncertainty in the results
- Using an adaptive variant of the multi-mode simplified dynamic response spectrum methods may increase accuracy of calculated demand. However, it also significantly increases computational demand. Consequently one may doubt whether this extended simplified dynamic analysis method is preferable instead of the nonlinear dynamic analysis.
- Nonlinear dynamic analysis is a powerful tool for calculation structural deformation demand. Load deformation characteristics can be implemented varying with load level, as is for actual structures. Using advanced material models allows for inherently including hysteretic damping in the system. Two drawbacks are the high computational costs and its sensitivity to the selected seismic input signal. The former drawback is becoming less critical with increasing computational capacity. The latter is overcome by selecting a number of seismic input signals and use an envelope as seismic design demand.

4.5 Jetty structural dynamics (under earthquake excitation)

4.5.1 Mathematical representation of systems under seismic loading

Dynamic characteristics of a structure are determined by its geometry and the distribution of mass, stiffness and damping over the structure. In order to analyse the structure, a representative mathematical model needs to be defined. The structure geometry is discretised and the structure boundaries have to be defined. Mass, stiffness and damping are assigned to the structure degrees of freedom, which then results the multi-degree of freedom equation of motion in matrix notation:

$$[M]\underline{\ddot{u}} + [C]\underline{\dot{u}} + [K]\underline{u} = F(t) \tag{4.18}$$

Where:

$[M]$ = The mass matrix

$[C]$ = The damping matrix

$[K]$ = The stiffness matrix

$\ddot{\underline{u}}, \dot{\underline{u}}, \underline{u}$ = The acceleration, velocity and displacement vectors

$F(t)$ = The external force vector

In case of earthquake loading, the structure response to imposed ground motions is to be computed. Elastic and damping forces are then related to relative motion levels of the structure to the ground, however internal forces are linear with the absolute accelerations. From these observations equation of motion (4.18) can be transformed into equation of motion (4.19):

$$[M]\ddot{\underline{u}}(t)+[C]\dot{\underline{u}}(t)+[K]\underline{u}(t)=-[M]\underline{\iota}\ddot{u}_g(t) \quad (4.19)$$

Where $\ddot{\underline{u}}(t)$ and $\ddot{u}_g(t)$ are the structure acceleration vector and ground acceleration varying in time, $\dot{\underline{u}}(t)$ and $\underline{u}(t)$ are the structure relative velocity and displacement vectors and $\underline{\iota}$ is the influence vector having entries equal to 1 for al degrees of freedom in the direction on ground motion and 0 otherwise.

4.5.2 Coupling of superstructure, foundation and soil

For building structures the traditional approach was to define the system boundary at foundation level, so foundations and structure-soil interaction are not included in the dynamic mathematical models. Where this was believed to give proper results, nowadays according to performance based design principles it is believed that nonlinear soil foundation structure interaction may be very significant, beneficial or detrimental and hence should be taken into consideration (Gazetas, 2012).

For jetties and other geotechnical structures with heavy deep piled foundations forming a very prominent part of the entire structure, the need for inclusion of foundation and soil in design is much more obvious. For jetty structures where piles are monolithically forming both an important part of the superstructure and the foundation it is clear that one needs to consider the pile in jetty dynamic analysis.
Analysing the response of the piles themselves during earthquakes is traditionally done by following a two-way approach that is based on superposition of kinematic and inertial effects in order to obtain the governing maximum bending moments in the piles. However, since for jetties the piles are such a prominent structural part, coupled analysis seems to be preferred for these type of structures, in order to obtain reliable global jetty responses. The coupled analysis directly will provide pile bending moments that are resulting from combined kinematic and inertial loading at the piles and hence will be the governing design bending moments resulting from the seismic load case.

Including the structure-soil interaction effects in the seismic analysis means that the boundaries of the mathematical model will be extended to include soil constitutive behaviour in the analysis. The traditional approach is to represent the soil by a Winkler bedding supporting the piles. Then along an uncoupled approach, the support nodes of the Winkler bedding excited by motions based on a free field response analysis. The alternative is to construct a coupled finite element model both the soil overlying bedrock and the jetty structure, for which the coupled response to a bedrock excitation is calculated. Both options are schematically shown in Figure 4.7

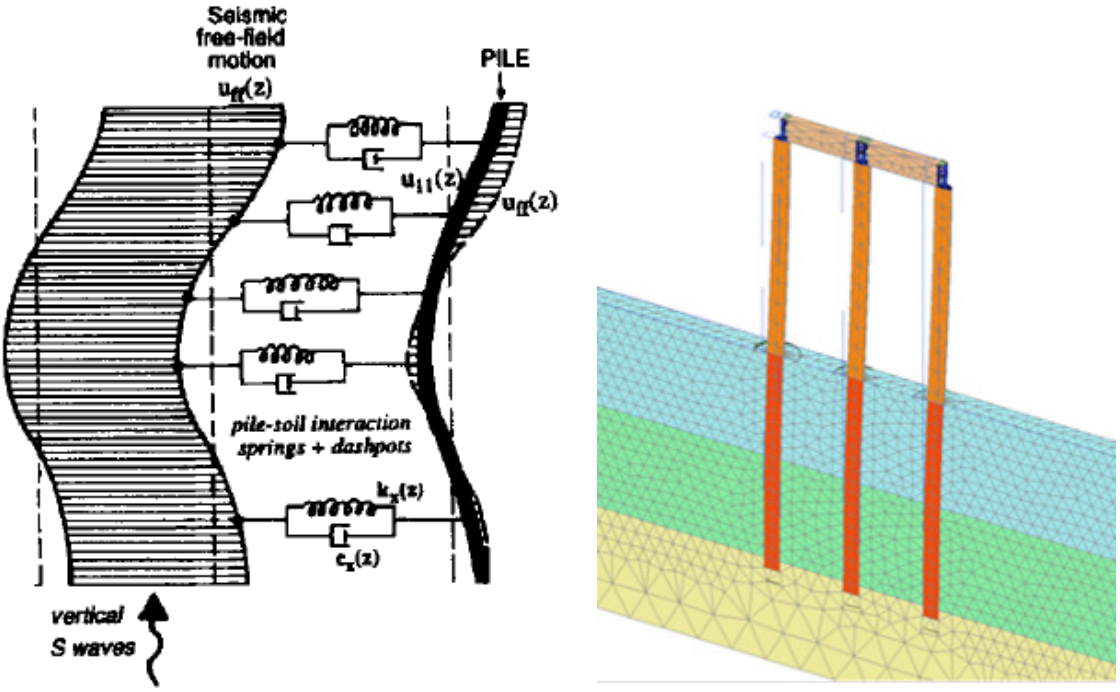

Figure 4.7: Pile as a Beam on Winkler Foundation model approach (left) and Coupled soil deposit + jetty structure finite element model analysis (right)

4.5.3 Higher mode contributions in response

When a structure is excited by an earthquake motion signal, the total vibration of the structure can be described as a superposition of vibrations in the structure its eigen-modes for linear structures. The contribution of a mode to the total structure response is represented by the modal participation factor or effective modal mass for a certain direction, corresponding to the mode considered. Modal participation factors are defined as:

$$\Gamma_n = \frac{\underline{\phi}_n^T \underline{\underline{M}}\, \underline{I}}{\underline{\phi}_n^T \underline{\underline{M}}\, \underline{\phi}_n} \tag{4.20}$$

Where $\underline{\phi}_n$ is the mode vector of the nth mode considered, $\underline{\underline{M}}$ is the system mass matrix and $\underline{\underline{I}}$ is the identity matrix. Modal participating factors absolute values are dependent of the mode shape normalisation scheme, for which reason the absolute value of the modal participation factor has not reason. To overcome this problem effective modal mass may be defined as:

$$m_n = \frac{\left(\underline{\phi}_n^T \underline{\underline{M}}\, \underline{I}\right)^2}{\underline{\phi}_n^T \underline{\underline{M}}\, \underline{\phi}_n} \tag{4.21}$$

The higher this effective modal mass, the more prominent the mode will be present in the total response. The presence of a specific modal response in the total response is determined by the frequency content of the ground surface response signal and the sharpness of the input seismic signal. The sharper the input signal is, the more the response will be like a pure pulse-response, for which higher modes are more prominent in the response.

Simplified dynamic techniques in earthquake engineering rely on a number of presumed failure modes, which often is assumed to be represented by the structures' fundamental mode only. However, restricting the response to the fundamental mode only, may introduce quite substantial errors when modal participating masses of higher modes have substantial values, the input signal is very much pulse-like or a large static component is present. Most seismic design standards recommend to take into account sufficient number of modes up to 90% cumulative participating modal mass.

Modern standards restrict the use of these single mode simplified dynamic methods to structures being symmetric in their two main horizontal direction, which is related to the recognized severe effects of torsional effects in structure responses.
This study focuses on soil-pile interaction aspects for jetty structures and rotational effects due to asymmetry and excitation phase differences for great jetty lengths are not considered. However, the distribution of participation modal mass in the transverse jetty direction will be identified for the typical jetty structure with soft soil conditions, which may be linked to the performance of a fundamental mode simplified dynamic analysis.

Modal analysis for linear systems results a structure dynamic response on its natural modes, where modal amplitudes depend on the dynamic excitation. However, the maximum total motion amplitude for transient dynamic problems is not determined, since modal responses extremes not necessarily do occur at the same moment in time. Various approximations are available. Summing all modal maxima gives an upper bound, which is usually too conservative for design. More accurate estimates of total response based on random vibrations theory are available. The simplest one sums the squares of the modal maxima and subsequently takes the square root to determine the extreme total response (SRSS). This procedure seems to give good results if natural periods are sufficiently separated (by a factor 1.5 according to Kramer, (1996) page 582). As an alternative, also procedures that account for correlation between modes are available, for cases of closely spaced modes. A method of this type is the complete quadratic combination (CQC) rule, in combination with the Der Kiureghian correlation coefficient ((Chopra, 2001) page 557)

It should be noted that both modal combination rules (based on random vibrations theory) and the response spectra provided in codes, originally related to wide band seismic input signals with relatively long phases of strong ground motion. Hence, results provided by these methods might be less accurate when these conditions are not met for a design case. This problem is recognized in various earthquake engineering research papers and textbooks. Dynamic time history analysis is generally considered to be preferred for these cases (Chopra & Chintanapakdee, 2001) , see Chopra 2001 page 559)

4.5.4 Damping

4.5.4.1 Actual damping in structures

The structures' mass and stiffness to be included in the mathematical model (Equation (4.19)) are in general relatively easy to estimate. In contrast, defining proper damping values is much more difficult. Various frequency dependent and frequency independent sources of damping that are believed to be important for seismic jetty design are:

Frequency dependent:
- Structural material damping
- Damping resulting locally from strongly nonlinear soil behaviour adjacent to a pile
- Soil material damping for saturated permeable soils (from pore fluid moving relative to the soil skeleton)
- Soil radiation damping (energy transport through the soil to the far field)
- Hydrodynamic damping (velocity dependent drag forces acting on the pile)

Frequency independent:
- Structural friction damping (frictional damping in e.g. bolted connections)
- Soil material damping for dry and impermeable soils (friction of soil grains moving with respect to each other)

Including all different damping contributions in a mathematical model for earthquake response analysis should conceptually result the most accurate estimate of actual response of the structure. However, this approach is uncommon in engineering practice for the following reasons:
- Correct damping with proper physical background still unknown
- It is a laborious task to properly include all different damping contributions
- Conditioning of damping matrix may become computationally inconvenient
- Common FEA software does not provide the option to define damping such a specific way.

Instead, an equivalent Rayleigh critical viscous damping percentage is often defined to approximate the effects of various damping mechanisms present in the real structure. However, the following related problems can be defined:

- Actual damping resulting from hysteretic behaviour often is a nonlinear function of motion amplitude, as a result it is difficult to properly include damping in the Rayleigh format for dynamic problems with strongly varying motion amplitudes.
- Rayleigh viscous damping by definition is frequency dependent, where actual damping sources not necessarily are frequency dependent, e.g. hysteresis loops due to nonlinearities is known to be frequency independent.

Computational advantages of using linear equivalent viscous Rayleigh damping traditionally where considered to outweigh whatever compromises are necessary in the viscous damping approximation. However nowadays it is believed that in nonlinear dynamic analysis a better approximation of actual damping is obtained when hysteresis behaviour (by nonlinearities) and some additional Rayleigh damping are combined. The Rayleigh damping part then is governing the total damping for low level responses, where it becomes negligible compared to the hysteretic energy dissipation for high level responses.

4.5.4.2 Rayleigh damping and Extended Rayleigh damping formulation

The Rayleigh (proportional, classical) damping format, as presented in equation (4.22), is computationally convenient as it meets orthogonality properties of the damping matrix.

$$[C] = \alpha[M] + \beta[K] \tag{4.22}$$

Where,

$[C]$ = the material damping matrix for the system

$[M]$ = the mass matrix for the system

$[K]$ = the mass matrix for the system

$\alpha \; and \; \beta$ = damping constants

As represented in Figure 4.8, the damping ratio for the n[th] mode of the system is:

$$\xi_n = \frac{\alpha}{2 \cdot \omega_n} + \frac{\beta \cdot \omega_n}{2} \tag{4.23}$$

Where,

ω_n = the n[th] mode natural circular frequency

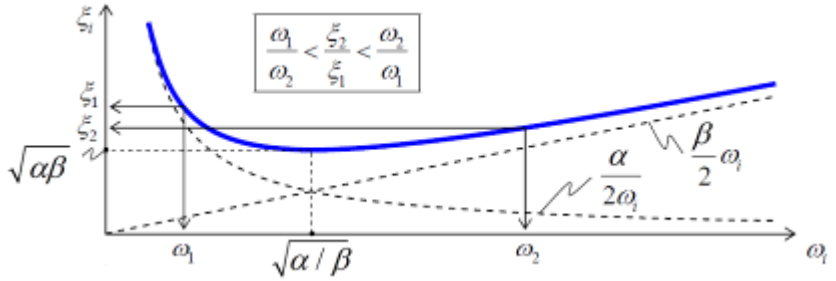

Figure 4.8: Rayleigh damping over a certain range of frequencies

The damping coefficients α and β are usually determined from specific system damping ratio's of the i[th] and j[th] modes of vibration according to:

$$\alpha = \xi \frac{2\omega_i \omega_j}{\omega_i + \omega_j}$$
$$\beta = \frac{2}{\omega_i + \omega_j} \tag{4.24}$$

Where,

$\omega_i \text{ and } \omega_j$ = the i[th] and j[th] mode natural circular frequency respectively

ξ = the assumed material damping ratio for all the structures' vibrations modes necessary to ensure reasonable values for all modal damping ratios prominent in structural response.

Applying Rayleigh damping will result a diagonal modal damping matrix, so an uncoupled system for which modal analysis can be applied. The resulting natural modes are similar to the undamped ones. On the contrary, non-Rayleigh damping results a non-diagonal modal damping matrix, and natural modes may differ from undamped ones.

A variant of Rayleigh damping is the stiffness proportional damping, which is obtained by setting Rayleigh parameters $\alpha = 0; \beta \neq 0$. This variant is characterized by increasing linear with frequency, and therefore is often considered a useful measure for damping out high frequency content in numerical response that is not prevented from oscillating by time integration solution procedure.

Since viscous damping conceptually introduces frequency dependent damping in the system, one should be very careful with defining the Rayleigh damping parameters. A proper damping value over the entire frequency range of interest should be obtained. An alternatives is available known as Extended Rayleigh Damping or Caughey damping (Clough & Penzien, 1993), where more than two basis modes/frequencies can be specified and so the damping matrix is constructed in a different way, aiming at having a more constant damping value over the frequency range of interest.

$$[C] = [M] \sum_{b=0}^{N-1} a_b \left(\left[M^{-1} \right] [K] \right)^b \tag{4.25}$$

Where:

N = the number of frequencies/modes incorporated

a_b = a scalar facto defined by $\xi_n = \frac{1}{4\pi f_n} \sum_{b=0}^{N-1} a_b \left(2\pi f_n\right)^{2b}$

Although this damping formulation may provide widening of the frequency range with proper damping values, its drawback is the higher computational demands that will result. (Hashash & Park, 2002)

The Rayleigh damping approach may be very attractive, it physical background is lacking. Furthermore the effective critical damping percentages are often arbitrarily defined, where instead careful selection is required. Defining a certain Rayleigh viscous damping factor, results essentially frequency dependent effective damping over the varying range of frequencies. One should make sure that the effective damping values obtained have reasonable values, at least within the frequency range of interest.

4.5.4.3 Structural material and friction damping

Structural damping results from micro-scale material straining (material damping) and friction between surfaces moving relative with respect to each other (friction damping). The former is related to heat production in materials due to vibrations which is a phenomena still poorly understood, but clearly a material dependence can be found. The latter is e.g. provided by work done by friction in e.g. bolted connections or other structural slipping surfaces.

Generally structural material and friction damping are combined into only one equivalent viscous damping parameter. The value of the damping parameter may be found based on literature, or be calculated from the structures global nonlinear pushover curve / global hysteresis loop as proposed by (Priestley et al., 2007) and (PIANC, 2001) page 229). The area within a hysteresis loop represents the energy dissipated in a cycle by the viscous damper. Hence it can easily be related to an equivalent viscous damping percentage by relating it to the maximum potential energy present in the system (the spring) during a cycle.

Eurocode 8 recommendations (NEN-EN 1998, 2004) provide an equivalent viscous damping ratio of 5% critical to be included in seismic analysis, where different values have to be specified. ISO 19902 recommendations (ISO 19902, 2006) provide maximum modal damping ratios up to 5% for fixed steel offshore structures during ELE events, where additional damping, e.g. hydrodynamic or soil induced, shall be substantiated by special studies. For fixed steel offshore structures under ALE events where inelastic behaviour of both structure and damping is likely, damping values varying up to 10% critical may be applicable. ISO19903 recommendations (ISO 19903, 2006) provide maximum damping values of 5% critical to simulate damping originating from structural joint and hydrodynamic energy dissipation for seismic analysis of fixed concrete offshore structures. Again, higher values according to these regulations shall be justified by special studies

4.5.4.4 Soil radiation damping

Radiation damping is the transport structural vibration energy to the far field, and often referred to in literature as geometric damping/attenuation. Transport of energy providing the radiation damping effect is only possible for waves at frequencies beyond the cut-off frequency of the soil which for soil columns can be shown to be equal to the fundamental frequency of the soil profile (Wolf & Deeks, 2004)

Radiation damping is much stronger for 3D spreading body waves than for 2D spreading surface waves (decay rates are respectively $1/\sqrt{r}$ and $1/r$). As a result surface waves generally are more prominent for structural response on relative big distances from the fault rupture ((Kramer, 1996), page 179).

In 2D axi-symmetric or 3D geotechnical finite element analysis radiation damping is automatically included, where in 2D plane strain analysis radiation damping is hardly present. In reality radiation waves may travel towards 'infinity' where in geotechnical finite element models model suffer from for computational limitations. In order to prevent radiating soil waves generated by structure motions to reflect at the boundaries and simulate radiation damping effects, finite element model boundaries should be set such that radiating waves are damped by material damping while travelling towards the boundary, or including absorbent boundaries to prevent wave reflection. In finite element models, boundaries cannot be defined too far away for computational convenience, therefore artificial Rayleigh material damping in combination with absorbing boundaries are often used to provide the actual attenuation of stress waves to the far field by radiation damping.
In beam on Winkler foundation models, radiation damping may be accounted for by adding a radiation damping contribution to the total viscous damper parallel to the Winkler spring, as is treated in paragraph 4.6.3.6.

4.5.4.5 Soil material damping

For dry soils soil material damping resulting from heat energy loss due to friction forces between soil grains when the soil is vibrating. This friction induced type of damping is generally believed to be frequency-independent (Hardin, 1965), and is characterized by hysteresis soil behaviour. For saturated permeable soils the damping however is characterized better as viscous frequency dependent damping (Michaels, 1998; Michaels, 2008) , since it is governed by pore fluid motion through the soil skeleton generating heat energy. For very large pore spaces the friction between water and soil particles then again drops, decreasing actual frequency dependence of material damping (Stoll, 1985).
Traditionally soil damping was assumed frequency independent because this was convenient in relation to the Kelvin-Voigt description of soils, as it easily fits into the definition of a constant complex shear modulus. Essentially a equivalent non-viscous viscosity is defined as equivalent viscosity $\eta = 2G\xi/\omega$ resulting a constant damping ratio. More recently an alternative representation to the Kelvin-Voigt solid (termed the Kelvin-Voigt-Maxwell-Biot model) was published for the specific case of shear strain (Michaels, 2006a; Michaels, 2006b) For practical purposes however mostly an equivalent viscous (frequency dependent) damping or a fixed damping ratio resulting a constant complex shear modulus is defined.

Critical damping percentages can be estimated based on soil shear strain levels, plasticity index and confining pressure according to (Vucetic & Dobry, 1991; Ishibashi & Zhang, 1993). A similar but more simple hyperbolic relationship was proposed by proposed by (Hardin & Drnevich, 1972), that also has proven to give accurate estimates of real soil behaviour. In Eurocode 8 an approximation of strain dependent soil stiffness and damping parameters based on ground accelerations as in Table 4.5 is given, from which may be concluded that for high level earthquakes damping ratios exceeding 0.10 are found.

Table 4.5: Ground acceleration related shear wave velocity, shear modulus and damping characteristics

Ground acceleration ratio $a_g S / g$ [-]	damping ratio [-]	$v_s / v_{s,\max}$ [-]	G / G_0 [-]
0.10	0.03	0.90 ($\pm$ 0.07)	0.80 ($\pm$ 0.10)
0.20	0.06	0.70 ($\pm$ 0.15)	0.50 ($\pm$ 0.20)
0.30	0.10	0.60 ($\pm$ 0.15)	0.36 ($\pm$ 0.20)

Where the $\pm$ SD values can be used to introduce a certain level of conservatism, or to account for soil type, where the higher values are more appropriate for stiffer soil conditions and the lower values are more appropriate for softer soil condition, S is the Eurocode 8 soil factor, g the gravity constant, and $v_{s,\max}$ and G_0 the small strain soil parameters.

For soils, damping is considered to be frequency independent, since it is considered to be produced by irreversible plastic deformations of the material. Therefore often a equivalent viscosity $\eta = 2G\xi / \omega$ is defined, which makes the damping in the soil profile frequency independent. The definition of the equivalent viscosity is advantageous to analyse rate independent damping by frequency domain analysis. However, with transformation back to the time domain problems arise when using an equivalent viscosity.

4.5.4.6 Damping at the soil-structure interface

Increased soil material damping in the region surrounding the pile is observed. Due to the relatively high deformation levels extreme hysteresis behaviour is locally present, resulting from high local soil strain levels and plastic shearing at the soil-pile interface. Other effects related to e.g. scour for clays may contribute to increased damping values as well.
Within the nonlinear Winkler concept hysteretic loops dissipating energy are included in load displacement characteristics due to nonlinear stiffness development for cyclic loading-unloading-reloading. The representative damping value strongly varies with displacement amplitude. In addition a material damping term for the adjacent soil may be defined, which is often estimated by expressions as are presented in paragraph 4.6.3.6. As a consequence of highly plastic local soil behaviour adjacent to a pile, radiation damping is reduced by this zone. Therefore radiation damping is sometimes considered to be present in the far field only. (El Naggar & Bentley, 2000)

4.5.4.7 Hydrodynamic damping

The unsupported part of jetty piles are surrounded by free water or air. When during an earthquake the relative velocities of the pile and the water are nonzero, drag and inertia forces will result according to Morrison's equation (explained in Dynamics of Offshore Structures (Wilson, 2003), page 25). The drag force varies linearly with the relative velocity of the pile and the surrounding water. Thereby, it forms an additional viscous damping. The dependence on relative velocity of the pile and the water makes the amount of damping difficult to determine during seismic events, since the motion of the water itself is an uncertain input parameter. Hence is it uncertain whether the hydrodynamic forces continuously damp structure response, or on the contrary at some moments amplify it.

In this study the focus is on soil structure interaction during earthquake and for simplicity the pile interaction with water by hydrodynamic excitation or damping are assumed to be zero. Based on literature this appears a conservative assumption with respect to the total amount of damping included in the model.

4.5.4.8 Numerical damping

Numerical damping has no relation with any physical process in structural/soil dynamics, and may result from a certain numerical time integration scheme applied in time domain analysis. The time integration scheme applied affects the stability of results and energy dissipation for certain frequency ranges. Various time integration schemes are available, a frequently used family of time integration methods is the Newmark family of which three schemes are presented in table Table 4.6: Time integration schemes. The properties of an integration method of this family are determined by two parameters, β_N and γ_N, which affect the stability and the

accuracy of the method. Independent of the integration method used, it is in terms of accuracy always wise to limit dt to $0.1T_n$, T_n being the highest mode with significant response contribution. However, for conditionally stable methods, stability requirements may require much smaller time stepping, making the method less convenient for practical purposes. Hence, unconditionally stable methods generally are to be preferred. A generalization of the Newmark-β methods is the Hilber, Hughes and Taylor (HHT)-α method where parameter α is introduced and the condition that the acceleration is constant during the time stepping interval is added. The parameter α modifies the equation of motion as it is solved in the numerical time integration and adds numerical energy dissipation, however it cannot be predicted as a damping ratio. An unconditionally stable 2nd order accurate method is obtained if $0 \le \alpha \le 0.33; \beta = (1+\alpha)^2 / 4; \gamma = 1/2 + \alpha$. For dissipation parameter $\alpha > 0$, frequencies above $1/2\Delta t$ are damped out with this integration scheme. The performance of the method appears to be very similar to the use of stiffness proportional damping

Table 4.6: Time integration schemes

Integration scheme	Parameters	Stability	Numerical damping
Linear acceleration method	β_N =1/6, γ_N =1/2	Conditionally stable	No numerical damping
Constant average acceleration method (By default adopted in Plaxis)	β_N =1/4, γ_N =1/2	Unconditionally stable	No numerical damping
Newmark, HHT-α modification	α =0.1 → β_N =0.3025, γ_N =0.60	Unconditionally stable	Numerical damping by numerical dissipation parameter α

By default Plaxis numerical time integration adopts the average acceleration method, which does not introduce numerical damping. No numerical damping has a disadvantage that response contributions of high frequencies that are resulting from the numerical process are not filtered out. Hence in the present study, seismic bedrock signals were filtered by a band-pass 0.1 - 15 Hz Butterworth filter. Though, (Sigaran Loria & Jaspers-Focks D.J, 2011) reported in their study the insensitivity of site responses to inclusion of numerical damping. Consequently when numerical instability problems are obtained it seems reasonable to change the numerical integration scheme to the HHT-α method with numerical dissipation parameter α = 0.1.

4.6 Soil representation in pile-soil interaction modelling

4.6.1 General comments on soil representation in seismic modelling

In this chapter, soil material models are discussed. Material models are described by a set of equations representing the constitutive behaviour of the material. Strictly, a material model in this sense should describe material mechanical properties in terms of stress and strain, as indeed is the case for soil continua models. However, in relation to laterally loaded piles also a simplified approach is available, in which soil response is described in relation to only one kinematic parameter, being the lateral pile deflection.

Response of soil to laterally loaded piles is not only depending on soil mechanical properties, but also by nature of loading. Where static loading is the simplest and often well be described, long duration cyclic loading generally may result strong degrading of soil mechanical properties, where for dynamic loading impedance is also partly determined by a kind of damping part related to loading rate. Seismic loading is somewhat different in this sense, since it is a short duration, cyclic, high-rate loading. Predicting actual soil response is therefore quite complicated and therefore often poorly presented in too simple models.

4.6.2 Linearization of soil response

Dynamics of linear systems can be analysed in the frequency domain, which is very beneficial form an computational point of view. Basically, the constitutive relationship is assumed to be (equivalent) linear corresponding to a certain load level, where stiffness is adapted to account for nonlinear behaviour and a corresponding damping percentage is derived, as depicted in Figure 4.9. Equivalent linear techniques have been developed for

both soil site response analysis (Schnabel, Seed, & Lysmer, 1972) and pile structure interaction analysis (Novak, 1974; Gazetas & Dobry, 1984a). For both subcategories holds that an iterative procedure is required in order to include the proper equivalent stiffness and estimated damping in the analysis.

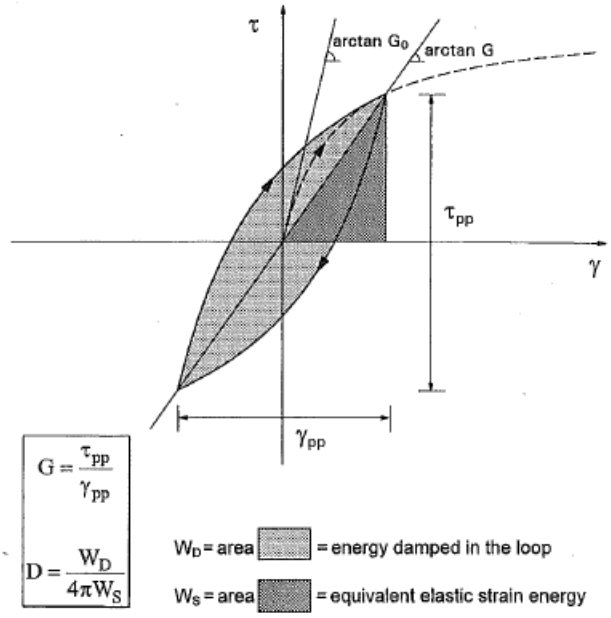

Figure 4.9: Equivalent linear stiffness and damping

4.6.3 The beam on Winkler-foundation concept and nonlinear p-y curves

4.6.3.1 The Winkler concept and p-y curves, an introduction

Interaction of piles and surrounding soil may in its most simple form be represented by the beam on Winkler foundation model. Fundamental assumption underlying this model is that adjacent soil layers are reacting independent when subjected to differential loading. Obviously this Winkler hypothesis does not represent reality, but is very convenient from a computational perspective. Probably for this reason it has become very popular in engineering practice. The nonlinear impedance relation of lateral pile displacement to soil reaction force in these Winkler models is traditionally done by defining so called p-y curves. The extensive development of conventional p-y based approaches seems very much supported by limited computational capacity in the past. Moreover, it is remarkable that the simple static p-y curves are based on only a relatively limited amount of field and lab experiments, where they are often used beyond the range they were validated for.

Different soil types have different physical properties, resulting different typical soil type related p-y curves. Expression for p-y curves as a function of representative soil parameters were proposed for some generalized soil type categories, based on testing projects mostly including full scale tests for some typical pile diameters and soil conditions. The most widely used p-y curve expressions for soft clay, stiff clay and sand will be presented in the next sections and used a starting point in the present study.

Ultimate resistance in p-y curves is generally related to the lowest value of two failure mechanisms. A wedge failure mechanism governing at shallow depths and flow failure around the pile at greater depths. This dual approach is implemented in most proposed p-y curve expressions.
It is observed that cyclic loading significantly degrades soil mechanical properties, which makes it necessary to distinguish between monotonic backbone p-y curves and the degraded cyclic p-y curves. As also indicated in the introduction of this paragraph, cyclic degrading effects are based on long-duration cyclic loading, which makes it very doubtful if these degradation effects will be present during the typically transient earthquake excitation. Additionally, some researchers proposed to adapt the static p-y expressions for dynamic loading as a function of loading frequency, as discussed in section 4.6.3.5.

4.6.3.2 P-y curves for soft clay

P-y curve expressions for soft clay have been proposed by Matlock (Matlock, 1970) and are adopted in the ISO recommendations. A summary of the proposed procedure is presented Figure 4.10 and Table 4.7.

The main input soil parameters for soft clay p-y curves are undrained shear strength c_u, effective unit weight γ' and strain parameter ε_{50}, defined as the strain related to half the ultimate soil resistance. Typical ε_{50} values for soft clays range about 0,01-0,02 (Matlock, 1970), where Reese and van Ympe (2001) suggests somewhat lower values. Ultimate resistance is given as a function of depth, and limited by $p_f = 9*c_u$ to $p_f = 12*c_u$, which is still under discussion. The former expression for p_f (Broms, 1964b) is adopted in ISO recommendations, where more recent research (Randolph & Houlsby, 1984; Murff & Hamilton, 1993; Martin & Randolph, 2006; Jeanjean, 2009) consider this value to be too conservative.

Cyclic loading of soft clays might result a significant ultimate strength reduction for shallow depths, as recognized by Matlock (1970). The procedure for post-cyclic loading beyond onset of softening is characterized by a value of p is equal to zero up to the previous maximum deflection, followed by a second branch parallel to the secant initial stiffness up to intersection with the curve for cyclic loading. More recent studies have shown that lateral load transfer in clay can degrade significantly more than adopted in ISO guidelines, particularly if the loading is two-way. At shallow depths remoulding and gapping may occur, where at greater depths overburden will prevent gapping but remoulding still may cause softening. Some relatively simple mechanical analogues have been developed (Boulanger, Curras, Kutter, Wilson, & Abghari, 1999), which approximate the complex cyclic behaviour of soft soil by a series of nonlinear springs, sliders and dashpots. Matlock (1970) p-y curves have infinite initial stiffness, which is recognized to result numerical problems in dynamic analysis. This problem may be solved by the use of an adjusted stiffness k_e for the initial portion (e.g. as developed along elastic theory (Vesic, 1961) or as presented in (DNV OS-J101, 2012) until the point where both curves intersect. The adjustment for the first portion of the p-y curve is included in Figure 4.10: P-y curves for soft clay according to Matlock (1970)

Table 4.7. The intersection typically corresponds to $0.23 < p/p_u < 0.35$. Another possible approach is to just approximate the smooth Matlock p-y curve by a multi-linear fit, having an non-infinite initial stiffness.

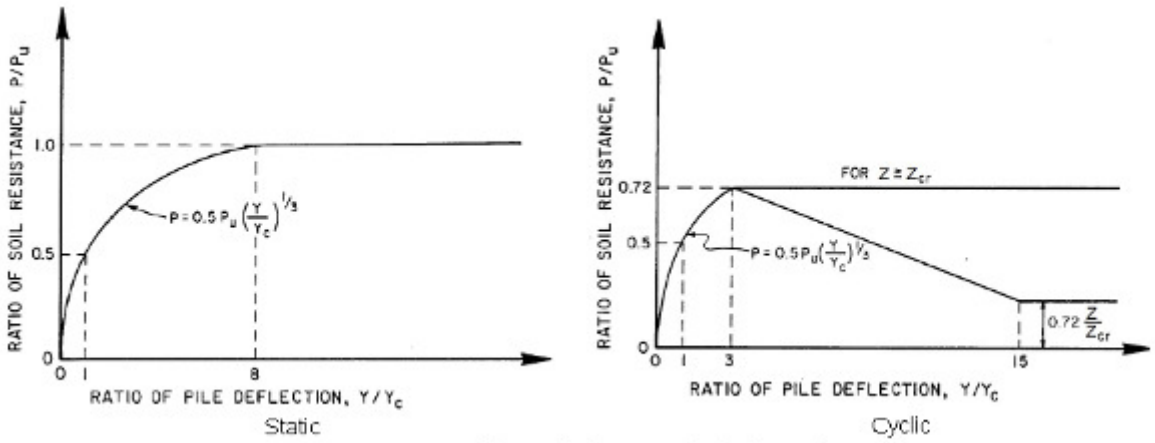

Figure 4.10: P-y curves for soft clay according to Matlock (1970)

Table 4.7 P-y curves for soft clay under monotonic (static) and cyclic loading

Monotonic (static) loading	
Compute Ultimate soil resistance	$p_u = \min \begin{Bmatrix} \left(3 \cdot c_{u,avg} \cdot D + \gamma' \cdot z \cdot D + J \cdot z \cdot c_{u,avg}\right) \cdot \\ 9 \cdot c_u \cdot D \end{Bmatrix}$
Determine deflection at one-half the ultimate soil resistance y_{50}	$y_{50} = 2.5 \cdot \varepsilon_{50} \cdot D$

Develop p-y curve expression	$p = p_u \cdot 0.5 \cdot \left(\frac{y}{y_{50}} \right)^{1/3}$

Cyclic loading	
Develop p-y curves for p<0,72p_u as for static loading	See table static loading
Calculate transition depth z_r	$z_r = \frac{6 c_u D}{\gamma' D + J c_u}$
Adjustment initial stiffness according to Vesic (1961)	$k_e = 2 \cdot 0.65 \left(\frac{E_s D^4}{E I_{pile}} \right)^{1/12} \frac{E_s}{1-\nu^2}$ up to intersection with conventional Matlock p-y curve
For depths beyond z_r	$p = 0.72 p_u$
For depths less than z_r	$p = 0.72 p_u$ at $y = 3 y_{50}$ $p = 0.72 p_u \frac{z}{z_r}$ at $y = 15 y_{50}$

Where:

c_u	=	Undrained shear strength
D	=	Pile diameter
J	=	Soil related constant (Matlock (1970): 0.5 for soft clay to 0.25 for medium clay)
N	=	Lateral bearing capacity factor Broms (1965): N = 9, Randolph and Housbly (1984), Martin and Randolph (2006), Murff and Hamilton (1993): 9.14 < N < 11.92, depending on roughness of the pile-soil interface.
p_u	=	Ultimate soil resistance
y_{50}	=	Deflection at one-half the ultimate soil resistance
z	=	Depth
z_r	=	Transition depth (depth where limit value by flow failure mechanism is reached)
γ’	=	Effective soil unit weight
ε_{50}	=	Strain at one-half the ultimate soil resistance Matlock (1970): 0.020 for soft remoulded clay, 0.010 for medium clay, 0.005 for stiff or brittle sensitive clay Peck et al. 1974 relates ε_{50} values directly to values for undrained shear strength c_u
k_e	=	Initial stiffness adjustment dynamic analysis

4.6.3.3 P-y curves for stiff clay

Common p-y curves for stiff clay are according Reese and Welsh (Reese, 1975). The procedure is summarized in Table 4.8. It should be noted that these expressions were based on full scale testing of steel pipe piles in stiff clay which was probably expansive and therefore continued to imbibe water as cycling progressed. Therefore the use of Reese and Welsh (1975) p-y expressions for cyclic loading may lead to conservative results for many other clays.

Similar to soft clays, stiff clay ultimate resistance is related to the lowest of wedge failure or flow failure. Stiff clays typically show a rapid deterioration of ultimate strength when loaded cyclically up to large deflections. Besides, cyclic loading of stiff clays may induce gapping which in presence of free water may result scouring by hydraulic action, resulting in further loss of resistance. Cyclic p-y curves for stiff clays without free water being present generally will not show these typical softening effects, which also was included by Reese and Welsh (1975). However, this will be of no relevance in this research regarding seismic jetty response since free water will always be present and therefore will not be discussed in more detail.

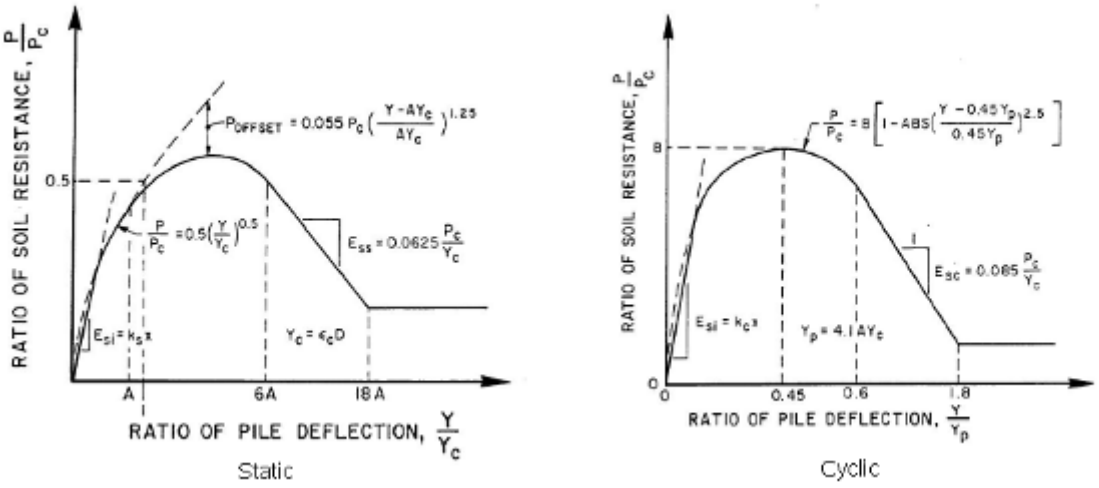

Figure 4.11: P-y curves for stiff clay according to Reese and Welsh (1975)

Table 4.8 P-y curves for stiff clay in presence of free water under monotonic (static) and cyclic loading

Monotonic (static) loading	
1. Compute ultimate soil resistance	$p_u = \min\begin{Bmatrix} 2c_{u,avg}D + \gamma' Dz + 2.83c_{u,avg}z \\ 11c_u D \end{Bmatrix}$
2. Establish initial straight line portion	$p = k_s zy$ for static or $p = k_c zy$ for cyclic
3. Develop p-y curve using the following expression	$p = 0.5p_u\left(\frac{y}{y_{50}}\right)^{1/2}$, $y_{50} = \varepsilon_{50}D$
4. Develop the second parabolic branch of the p-y curve (from A_s*y_{50} to 6*A_s*y_{50})	$p = 0.5p_u\left(\frac{y}{y_{50}}\right)^{0.5} - 0.055p_u\left(\frac{y - A_s y_{50}}{A_s y_{50}}\right)^{1,25}$
5. Develop the straight line branch (from 6*A_s*y_{50} to 18*A_s*y_{50})	$p = 0.5p_u(6A_s)^{0.5} - 0.411p_u - \frac{0.0625}{y_{50}}p_u(y - 6A_s y_{50})$
6. Develop final straight line branch (beyond 18*A_s*y_{50})	$p = 0.5p_u(6A_s)^{0.5} - 0.411p_u - 0.75p_u A_s$

Cyclic loading	
Execute step 1 to 3 from the static case	Follow step 1 to 3 of static curve as presented above
Develop parabolic branch (up to 0,6*y_p)	$p = A_c p_u\left(1 - \left(\frac{y - 0.45y_p}{0.45y_p}\right)^{2.5}\right)$, $y_p = 4.1A_c y_{50}$
Develop straight line branch (from 0,6*y_p to 1,8*y_p)	$p = 0.936p_u A_c - \frac{0.085}{y_{50}}p_u(y - 0.6y_p)$
Develop final straight line branch (beyond 1,8*A_s*y_{50})	$p = 0.936p_u A_c - \frac{0.102}{y_{50}}p_u y_p$

Where:

A_s = Constant for static case, as a function of non-dimensional depth

A_c = Constant for cyclic case, as a function of non-dimensional depth

c_u = Undrained shear strength

c_a	=	Average undrained shear strength over depth z
D	=	Pile diameter
k_s	=	Initial subgrade reaction constant for static loading
k_c	=	Initial subgrade reaction constant for cyclic loading (Matlock (1970): 0.5 for soft clay to 0.25 for medium clay)
y_{50}	=	Deflection at one-half the ultimate soil resistance
z	=	Depth
γ'	=	Effective soil unit weight
ε_{50}	=	Strain at one-half the ultimate soil resistance (Preferably to be derived from laboratory tests, if not available Reese and van Ympe (2001) provide values from 0.004 to 0.007 related to average undrained shear strength)

Matlock also proposed p-y curves for stiff clays (Matlock, 1979) by adapting his original p-y curves for soft clays to account for more brittle behaviour, especially when cyclically loaded. However, his proposal was not tested against field measurements.

Typically seismic design standards, including ISO recommendations and former API RP2A only give some comments on p-y curves for stiff clay, but do not provide closed form expressions as are presented for soft clay and sand. This indicates the scattering that is obtained for various stiff clay response characterizations, apparently making it difficult to establish generalized p-y expressions. .

Care should be taken when dealing with sensitive brittle soft clays, initial stiffness may be relatively high (ε_{50} ~ 0.005) but subsequently an extreme softening behaviour is obtained for these types of clays (Randolph & Gouvernic, 2011)

It should be noted that the p-y relationships as presented above do relate force per unit length p to deformation y, by a relation linearly depending on pile diameter D. (O'Neill & Dunnavant, 1984; Dunnavant & O'Neill, 1985; Juirnarongrit & Ashford, 2001) however have shown that this linear relation may not be most appropriate for clays, where y_{50} was found to decrease for increasing D, resulting a conservative initial stiffness by adopting conventional p-y expressions for greater pile diameters.

4.6.3.4 P-y curves for sand

The simple plasticity mechanisms that govern the ultimate resistance for clays, cannot be constructed for sand. Simple lower bounds cannot be constructed because of combined stress field, and upper bound solutions cannot be defined because normality rule requires dilation to occurs, which is not allowed at great depths where the constant volume boundary condition applies. As a result it is more difficult to determine the limiting lateral resistance in sand and ultimate resistance for sand at varying depths is therefore primarily based on empirical formulations. Lateral bearing factors are then defined as $N = P_f / (D * \sigma'_v)$. Different simple straight forward expressions for N have been proposed by various researchers over the past, e.g. (Brinch Hansen J., 1961; Broms, 1964a; Barton, 1982; Meyerhof, 1995). (Reese, Cox, & Koop, 1974) did explicitly distinguish between the two possible failure mechanism mentioned before (i.e. wedge failure or horizontal flow failure) and came up with some theoretical expressions for ultimate soil resistance extended with empirical adjustment factors. The expressions for ultimate resistance proposed by Reese et al. (1974). Reese et al. (1974) describe the p-y relationship by three straight line portions and a parabolic curve. A different p-y expression related to p_{ult} after Reese et al (1974), was proposed by O'Neill and Murchison and included in API and ISO recommendations (O'Neill & Murchison, 1983). The combined procedure (Reese, Cox & Koop. (1974) and O'Neill and Murchison (1983) is outlined in Table 4.9.

Both Reese et al. (1974) and O'Neill and Murchison (1983) account for deterioration of soil resistance due to cyclic loading by scaling factors (A_s, A_c). However, this limited degradation (no softening) of soil properties does not include possible severe effects of liquefaction in sand, which may additionally be accounted for. Besides, cyclic loading predominantly in one direction of piles in cohesionless soil typically induces permanent deformations because soil particles cave in the gapping space at the back of the pile, preventing the pile from moving back in its initial position. This effect is also not included in the standard p-y curves but may be taken into account when constructing p-y loops for dynamic analysis (see paragraph 4.6.3.7).

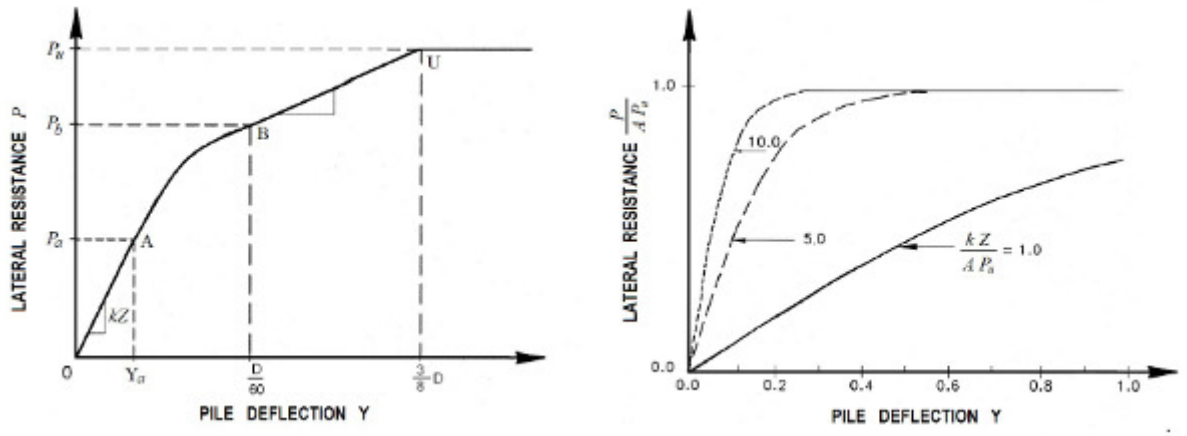

Figure 4.12: Sand p-y curves after Reese et al.(1974) (left) and O'Neill and Murchison (1983) (right)

Table 4.9 P-y curves for sand under monotonic (static) and cyclic loading

Monotonic (static) and (low rate) cyclic loading	
1.Theoretical ultimate soil resistance due to wedge failure (p_{us})	$p_{u,s} = \left(C_1 z + C_2 D\right)\gamma' z$
2. Theoretical ultimate soil resistance due to horizontal flow failure (p_{ud})	$p_{u,d} = C_3 D \gamma' z$
3. Governing theoretical ultimate soil resistance (p_u)	$p_u = \min\left\{p_{u,s}; p_{u,d}\right\}$
4. Adjustment coefficient for static or cyclic loading	$A_s = \left(3.0 - 0.8\frac{z}{D}\right) \geq 0.9$ $A_c = 0.9$
5. Develop p-y curve	$p = A p_u \tanh\left(\frac{kz}{A p_u} y\right)$

Where:

A_s	=	Adjustment coefficient for static p-y curves
A_c	=	Adjustment coefficient for cyclic p-y curves
C_1, C_2, C_3	=	Coefficients from figure 17.8.1 ISO19902:2006
k	=	Initial subgrade reaction constant from table 17.8.3 ISO19902:2006
D	=	Pile diameter
p_{us}	=	Theoretical ultimate soil resistance due to wedge failure (Reese et al. (1974))
p_{ud}	=	Theoretical ultimate soil resistance due to horizontal flow failure (Reese et al. (1974))
p_u	=	Theoretical ultimate soil resistance
z	=	Depth
ϕ	=	Soil friction angle
γ'	=	Effective soil unit weight

The Reese et al/O'Neill and Murchison p-y curve expressions for sand are adopted in ISO 19902:2006 seismic design recommendations. However, analysing the lateral bearing capacities for sand conform ISO, one may conclude that extremely high equivalent K_p-factors may result for greater depths. This is shown in Figure 4.13, where ISO lateral bearing factors are plotted with lateral bearing factors as proposed by Broms ($N = 3 \cdot K_p$) or Barton ($N = K_p{}^2$)

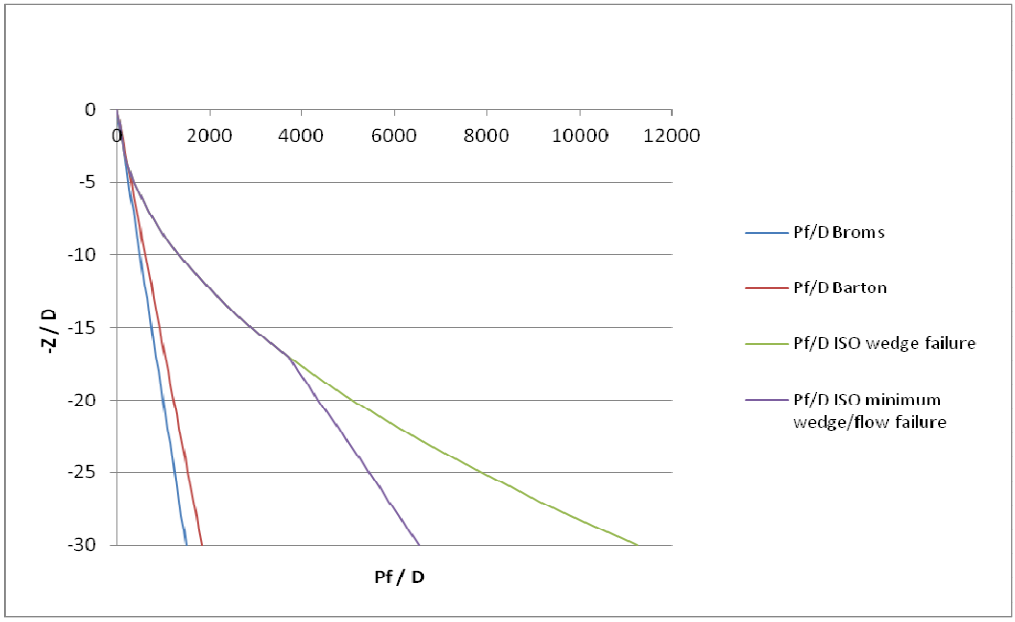

Figure 4.13: Dimensionless ultimate lateral resistance (P_u/D) for piles in sand

From Figure 4.13 one may conclude that for shallow depths up to 7*D, lateral bearing factors conform Broms, Barton and ISO do match quite well. However at greater depths ISO appears unrealistic, since allowable limit stress provided exceeds reasonable values based on the Mohr-Coulomb yield criterion by far. It therefore was decided in the present study to adapt ISO lateral bearing factors for sand layers at greater depths to Barton bearing factors. On the other hand it may be noted that greater depth soil response is less prominent in pile head response, especially for relatively small displacements. This implies only a minor influence from the too stiff adopted deeper sand layers.

Liquefaction is the phenomena of soils (partly) losing their strength temporarily, due to a set up of pore pressure, caused by high rate cyclic loading of the soil. The rise of pore pressure induces a decrease of effective stress causing the soil to lose its strength and transform into a viscous substance. In general loose and relatively fine sands are most prone to liquefaction. The simplest approach for lateral pile analysis in the presence of liquefiable layers is to neglect contribution of these layers to pile capacity, or even evaluate which additional loading effects liquefaction of these layers may result. Typically buckling instability of axially loaded piles due to temporary loss of lateral resistance in liquefied layers may become a problem. Correctly adapting soil response characteristics for liquefaction effects and implementing these in analyses has proven to be very difficult. Very recently Bouckovalas has proposed how to possibly implement liquefaction phenomena in the p-y curve format (Bouckovalas, 2012). These proposed expressions are not evaluated or adopted in this study because they were proposed when this study was almost finished. However for future projects comparison of responses along these expressions, advanced soil models allowing for liquefaction and test results of pile in liquefiable soils is recommended.

4.6.3.5 Dynamic p-y curves

As mentioned before, response to lateral pile movement is depending on the load nature. Generally the response for dynamic (high rate) loading is stiffer than the response to a gradually increasing static load. These effects have been recognized in many studies and resulted in different attempts to develop dynamic stiffness relations to be used for pseudo-static analysis. El Naggar and Bentley (2000) proposed a closed form empirical formulation for dynamic single pile p-y curves as a function of a static single pile nonlinear p-y curve, soil type and loading frequency as:

$$p_{dynamic} = p_{static}\left(\alpha + \beta a_0{}^2 + \kappa a_0\left(\frac{\omega y}{D}\right)^n\right) \quad (4.26)$$

Where:

$p_{dynamic}$ = dynamic value of p on the p-y curve at depth z

p_{static} = static value of p on the p-y curve at depth z according to ISO recommendations
y = pile lateral deflection
a_0 = dimensionless frequency of loading, defined as $a_0 = \omega D / (2v_s)$
ω = circular frequency of loading equal to $\omega = 2\pi f$
D = pile diameter
α, β, κ, n = empirical constants related to soil type as presented in Table 4.10Dynamic p-y curve parameter constants for a range of soil types*, after NCHRP report 461 page 18Table 4.10

$p_{dynamic}$ resulting from equation (4.26) for increasing displacements and high loading frequencies is limited by the ultimate lateral bearing capacity of the soil.

Table 4.10Dynamic p-y curve parameter constants for a range of soil types*, after NCHRP report 461 page 18

Soil type	Typical parameters	α	β		κ	n
			$a_0 < 0.025$	$a_0 > 0.025$		
Soft clay	$c_u < 50kPa, v_s < 125m/s$	1	-180	-200	80	0.18
Medium clay	$50 < c_u < 100\,kPa$ $125 < v_s < 175\,m/s$	1	-120	-360	84	0.19
Stiff clay	$c_u > 100\,kPa,\ v_s > 175\,m/s$	1	-2900	-828	100	0.19
Medium dense sand (saturated)	$50 < D_r < 85\,\%$ $125 < v_s < 175\,m/s$	1	3320	1640	-100	0.1
Medium dense sand (un-saturated)	$50 < D_r < 85\,\%$ $125 < v_s < 175\,m/s$	1	1960	960	-20	0.1
Dense sand (saturated)	$D_r > 85\,\%, v_s > 175\,m/s$	1	6000	1876	-100	0.15

* $D = 0.25, L/D = 40, 0.015 < a_0 < 0.225$

Note that α is always unity, since it has to be ensured that for $\omega = 0$ the static stiffness is returned from the expression. El Naggar and Bentley based the empirical parameter constants on tests on a pile with diameter equal to 0.25 m, and no test results on typical much greater diameter offshore piles are performed. El Naggar and Bentley considered the stiffness relations for a frequency range 0 – 10 Hz, which they consider to be typical for earthquakes. They concluded that the proposed dynamic p-y curves resulted responses in good agreement with predictions based on a two-dimensional analysis. However, it was noted that accuracy is less for very stiff soil conditions. Accuracy increases for frequencies greater than 4 Hz, since plane strain dynamic stiffness model assumptions tend to become less accurate when a situation approaches the static limit case. Later on, as reported in NCHRP 2001 report 461, the dynamic p-y curve expressions where verified along test results, again a good accuracy of the method proposed by El Naggar and Bentley in 2000 for the given range of application was found.

The dynamic multiplier is a function of frequency, which can easily be established for frequency domain analysis or loading types fixed at a certain frequency. However, since seismic excitation spans a range of frequencies, it is not suitable for analysis in the time domain. An approximation may be found by establishing the dynamic multiplier based on the most prominent frequency in the spectrum. A reasonable approximation may be found in fixing the dynamic stiffness multiplier to the structure fundamental-frequency, the power spectrum mean frequency defined as:

$$\Omega = \frac{m_1}{m_0} \tag{4.27}$$

or to the power spectrum response central frequency, which is defined as:

$$\Omega = \sqrt{\frac{m_2}{m_0}} \tag{4.28}$$

Where

$m_i = \int_0^{\omega_N} \omega^i G(\omega)\, d\omega$ is the i[th] order moment of the power response spectrum and

$\omega_N = \pi / \Delta t$ is the Nyquist frequency, being the highest frequency in the Fourier series.

It was investigated how the dynamic multiplication factors according to El Naggar and Bentley develop with frequency and displacement amplitude. Significant dynamic multipliers where found. As an indication for f equal to 5 Hz and y ranging from 0.01 to 0.1 m, the multipliers are approximately 2-8, 3-6 and 1-3 for soft clay, stiff clay and dense sand respectively.

4.6.3.6 Viscous dampers parallel to the p-y springs

In dynamic analysis of seismic pile-soil interaction, damping is included in the soil interaction models. Since damping tends to increase for increasing loading rates, various researchers (Gazetas & Dobry, 1984b; Nogami, Otani, Konagai, & Chen, 1992; Makris & Gazetas, 1992; Kavvadas & Gazetas, 1993) proposed to include a viscous damper parallel to the p-y spring element. Others (El Naggar, 1996; El Naggar & Bentley, 2000) have proposed to define separately the near- and far-field contributions for both linear springs and dashpots. Both methods have resulted relatively accurate predictions of dynamic pile response. However, the amount of damping in very much simplified models is often quire arbitrarily chosen, because of its dependence on both displacement amplitude and loading frequency.

Because of the increasing contribution to total stiffness of the frequency dependent imaginary part, El Naggar and Bentley (see previous paragraph) also attempted to fit expression for dynamic nonlinear stiffness in the more conventional complex valued stiffness. This results equation (4.29):

$$p_{dynamic} = (k_1 + ik_2)\, y = (k + i\omega c(\omega))\, y \tag{4.29}$$

where $k = \frac{p_{static}}{y}$ and $c(\omega) = \frac{p_{static}\left(\beta a_0^{\,2} + \kappa a_0 \left(\frac{\omega y}{D}\right)^n\right)}{\omega y}$

The real part $k_x(\omega)$ represents dynamic stiffness and the imaginary part $c_x(\omega)$ is related to the out-of-phase frequency dependent damping, which is generally considered a sum of energy dissipation by material hysteretic damping in the near field and radiation damping in the far field. However, this approach resulted too high damping contribution to overall dynamic stiffness for the higher frequencies.

Alternative expressions for dashpot coefficient accounting for the energy dissipation by the soil are proposed by different researchers. Common practice is to add separate contributions for both hysteretic material damping and radiation damping as:

$$c_{dashpot} = c_r + c_m \tag{4.30}$$

According to Kagawa and Kraft, the expression for material damping can be related to average shear strain amplitude in the soil which they related to local lateral pile displacement by:

$$\gamma_{avg} = \left(\frac{1+\upsilon}{2.5D}\right) y_{pile}(z) \tag{4.31}$$

For which $y_{pile}(z)$ is often obtained from simplified dynamic analysis or can be found by a iterative procedure.

Subsequently, a damping ratio corresponding to the average shear strain amplitude may be defined, and the dashpot coefficient then can be determined as:

$$c_m = 2k_{\sec ant}(y)\frac{\xi}{\omega} \tag{4.32}$$

Among the first to present expressions for the radiation damping were Berger et al (Berger, 1977). The Berger 1D model utilizes the analogy with 1D wave radiation in a rod and accounts for radiation of energy in both the direction of shaking (compression waves) and in the transverse direction (shear waves). Berger proposed as dashpot parallel to the soil spring (dynamic stiffness), with a dashpot coefficient equal to:

$$c_r = 2D\rho v_s\left(1+\frac{v_p}{v_s}\right) \tag{4.33}$$

Where v_p and v_s are related through the soil Poisson's ratio υ when linear elastic material behaviour is assumed:

$$v_p = v_s\sqrt{\frac{2(1-\upsilon)}{1-2\upsilon}} \tag{4.34}$$

Consequently, v_p tends to infinity if Poisson's ratio approaches 0.5 (undrained soil material behaviour), which is not realistic. According to Gazetas and Doby (1984) v_p may be better estimated as:

$$v_p = \frac{3.4v_s}{\pi(1-\upsilon)} \approx 2v_s \tag{4.35}$$

Where they used the Lysmer's analog wave velocity, derived for surface foundations subjected to vertical oscillations. In their study Gazetas and Dobry also proposed an alternative expression, that is based on assuming radiating waves in four quarter-planes (shear waves for two quarter-planes and compression waves for two quarter-planes) and assume a horizontal plane-strain situation. Adding up energy that is radiated away in total will then provide the following expression for the dashpot coefficient:

$$c_r = 2D\rho_s v_s\left(1+\left(\frac{3.4}{\pi(1-\upsilon)}\right)^{5/4}\right)\left(\frac{\pi}{4}\right)^{3/4} a_0^{-1/4} \tag{4.36}$$

Where $a_0 = \pi fD / v_s$

4.6.3.7 P-y loops for dynamic analysis

The p-y curve expressions as discussed in the previous sections have primarily been developed for static loading, where cyclic variants are just models to be used for again static analysis with reduced stiffness representing the cyclic nature of loading. These nonlinear curves in fact are hypo-elastic models because unloading occurs along the loading path. When applied in dynamics, these extended conventional static models do not include hysterese behaviour and possible residual displacements as is observed for real soils and of which the former is inherently is providing damping.

The damping artificially often is added to the model by introducing equivalent viscous dampers as proposed by many researchers and discussed before. With respect to peak displacements and peak stresses during seismic loading this simplifications have proven to result reasonably estimates of actual pile response. However, not allowing for plastic deformations results the ignorance of possible residual displacements, which is problematic from a performance based design perspective. In order to allow for residual displacements in time domain analysis using p-y curves, they need to be transformed into p-y loops, properly accounting for hypo-elastic, plastic and unload/reload behaviour of the soil. Several researchers have attempted to develop proper p-y loop models by empirical fitting to experiments. A mathematical model allowing for p-y loop definition was developed (Allotey & El Naggar, 2005) and is schematically presented in Figure 4.14. From the figure it becomes evident how many input parameters the model is based on, which makes it impractical for design purposes and very prone to errors.

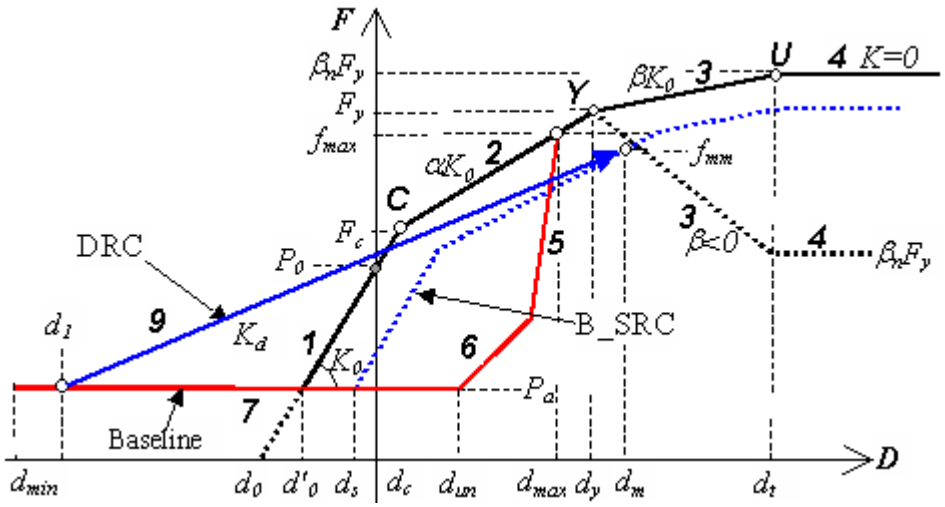

Figure 4.14: P-y loop mathematical model after Allotey and El Naggar (2005)

Instead, when using pile-soil interaction with advanced well established soil continua models, the loading-unloading-reloading loops are much more straight forward included based on a lower number and more common soil input parameters.

4.6.3.8 Additional comments on p-y curves

The p-y curve expressions as defined by ISO recommendations are strictly only valid for homogeneous soil. In practice, this obviously will not be the case for deep foundations. To deal with this problem, one needs to adopt the expressions for layering of the soil. This can be done by changing the way in which vertical effective stress and average cohesion over depth are included in the expressions. In this research the curves adopted for soil layering will be used for the comparative studies.

The initial stiffness as present in p-y curves always has been under discussion. Various papers and codes recognize this problem and its related sensitivity of results. Additionally, soil degradation and loading history dependence are poorly accounted for in the conventional p-y based approach. It seems always to be advised to perform a sensitivity analysis of the results obtained in order to ensure proper and safe designs based on the very much simplified p-y based approach.

4.6.3.9 Pile group effects

Piles installed in groups to form a foundation might interact when loaded, because of overlapping stress field is the surrounding soil. Interaction effects may reduce lateral stiffness as well lateral ultimate capacity. In general reductions are related to spacing in the loading direction to pile diameter ratio and pile group geometry. When analysis piles in groups by means of Winkler models, these efficiency reduction due to piles interacting might become significant, especially when piles are closely spaced.

Studies have been performed in the past decades, resulting different empirical efficiency factors for leading and trailing pile rows under lateral loading. Reductions up to 60% for ultimate capacity and 75% for lateral stiffness and have been suggested by Poulos and Davis (1980) as indicated. NCHRP Report 461 (Transportation Research Board, 2001) provides even more extreme reductions for subgrade modulus of pile positioned in groups, decreasing to approximately 0.30 for second or third trailing pile rows. Reese and van Ympe provide empirical reduction factors for lateral bearing capacity of pile groups as a function of pile spacing (Reese & an Ympe, 2001).
An Excel sheet was constructed for finding the reduction factors by Reese and van Ympe, related to pile group geometry. Efficiency reduction factors for two closely positioned piles are shown in Figure 4.15. Based on these factors the total efficiency for a pile in a group can be found by multiplication of efficiency reduction factors due to all adjacent piles:

$$e_{pile} = \prod_{i=1..n} e_{adjacent\,pile\,i} \tag{4.37}$$

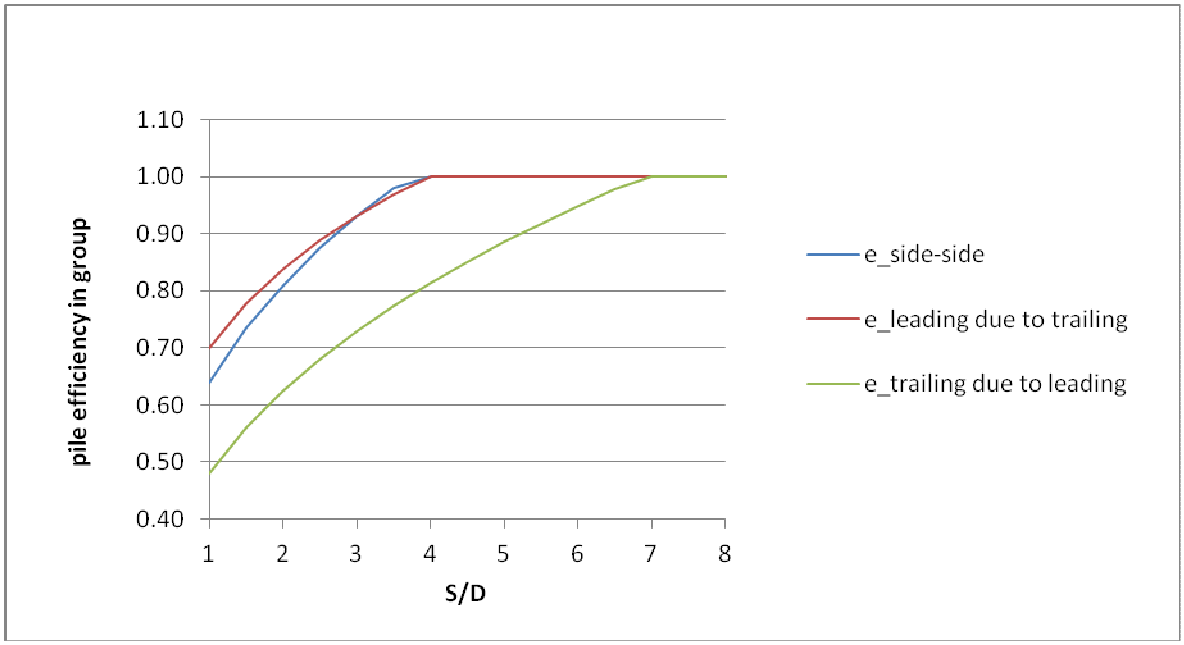

Figure 4.15: Efficiency reduction factors according to Reese and van Ympe (2001)

4.6.3.10 T-z and Q-z curves for axial pile behaviour

Although this study focuses on lateral behaviour of piles, also the axial response needs to be considered in order to be able to obtain reasonable Winkler foundations for the jetty, where rocking effects introduce axial pile movements. Axial pile response in the Winkler foundation concept is described by the Q_{shaft}-z and Q_{tip}-z curves. Q_{shaft}-z curves describe the relation between axial displacement and soil reaction acting at the pile shaft per unit pile length. Q_{tip}-z curves represent the relation between pile tip displacement and the related soil reaction force acting at the pile tip. In this study for simplicity linear relationships are assumed for these axial pile impedances, where it is realized that in reality nonlinear characteristics are obtained. A distinction generally is made between axial response for cohesive and cohesionless soils. For cohesive soils the axial impedance is often described as a function of stress level and undrained shear strength, where for cohesionless soils axial response is found as a function of stress level and empirical bearing factors related to relative density. The linear impedances adopted in this study are according to ISO-19902 chapter 17.4, to which one is referred for more details (ISO 19902, 2006).

4.6.4 Continuum material models for soil

4.6.4.1 General comments on continua material models for soil

Mechanical properties of a continua are described by a set of constitutive equations relating stress to strain tensors, or stress rate tensors to strain rate tensors as is often implemented in numerical procedures. Traditionally, soil constitutive behaviour was often simplified to just linear elastic perfectly plastic models. Over the past decades more advanced soil constitutive models have been developed. In this research the Hardening Soil model (Schanz, Vermeer, & Bonnier, 1999) and Hardening Soil small strain model (Benz, 2006) as implemented in the finite element code Plaxis are considered. Basic features of these models will be discussed in this paragraph.

4.6.4.2 Hooke's law of linear elasticity and the Mohr-Coulomb failure criterion

Hooke's law of linear elasticity for continua probably is the simplest constitutive model available is to describe the continuum deformations. However, when deformations increase the assumption of perfect linearity gives a very poor description of actual soil behaviour. Among the most used theory to account for material nonlinear-

ity is the theory of plasticity. Perfectly plastic material behaviour is represented by the Mohr-Coulomb yield criterion, which can be schematically represented in the principal stress space as shown in Figure 4.16. An alternative representation of the yield surface for perfect plasticity without the Mohr-Coulomb corner points was proposed by Drucker and Prager, but is not adopted in this study.

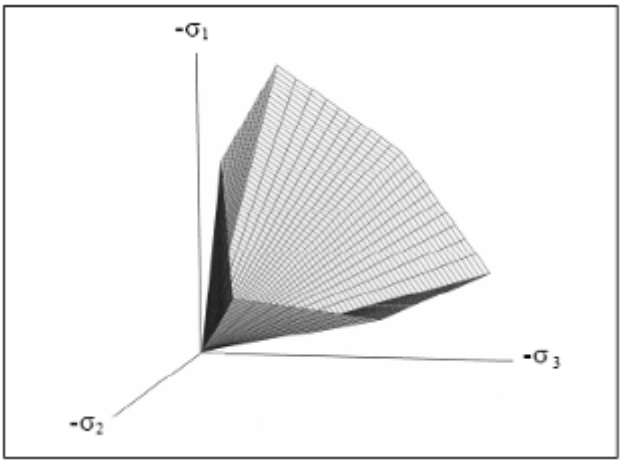

Figure 4.16 The Mohr-Coulomb yield criterion in the 3D principal stress space

Inside the cone representing the yield criterion, material behaviour is essentially elastic. At the cone the material behaviour is dominated by plastic straining. Stress configurations outside the cone cannot exist within the Mohr-Coulomb concept. For more information regarding computational Mohr-Coulomb material modelling one is referred to (Plaxis Material Models Manual, 2011; Sluys & Borst de, 2010)

4.6.4.3 The Hardening-Soil model

In the Mohr-Coulomb model, material yielding only is a function of the stress tensor. However, for many materials this actually will not be the case. As a result of plastic straining history, the yield function may develop, instead of being fixed in the principal stress space. This phenomena is called hardening, for which generally two types are distinguished, being strain hardening and kinematic hardening. Strain hardening is included in the HS model and can be subdivided in compression hardening and shear hardening. Material models including hardening/softening conceptually better represent actual soil behaviour when implemented in soil finite element calculations. It is however noted that real soil hardening behaviour is very complex and most models account for this in a very simplified way. The soil constitutive model including hardening adopted in this study has been developed (Schanz et al., 1999) and it has been implemented in the Plaxis finite element code. Provided a proper parameter selection, the HS-model is known to represent soil constitutive behaviour reasonably accurate for both soft and stiffer soil types, which is related to its features of stress dependent stiffness, different for both virgin loading and unloading/reloading as is also observed for real soils.

In fact the HS model allows for hardening related to material effective stresses, but on top of it a Mohr Coulomb model is applied based on ultimate strength parameters (c' and φ') governing the ultimate failure state of the material. This is schematically represented in Figure 4.17. Plaxis offers the possibility to input effective strength/stiffness parameters for both drained and undrained analysis, where undrained material behaviour then is governed by effective parameters and excess pore pressure generation based on the pore water bulk modulus (Plaxis Undrained calculation method A). Alternatively one may input effective stiffness parameters with undrained shear strength (Undrained calculation method B), .which however removes the stress dependent stiffness feature from the constitutive model.

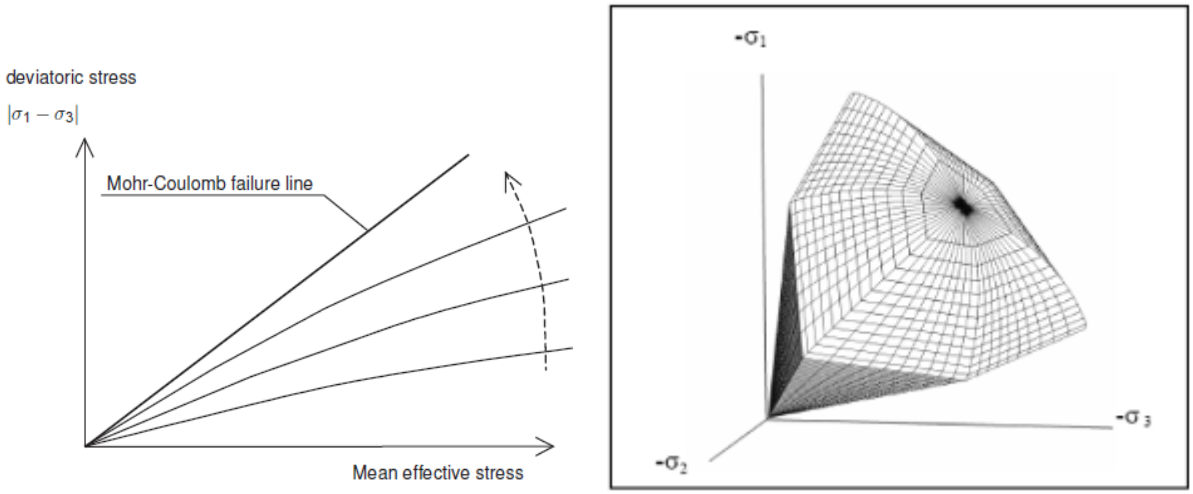

Figure 4.17: (left) Expansion of the Mohr-Coulomb yield surface in the HS model for increasing effective stresses
Figure 4.18: (right) The closed HS model yield surface including the yield cap

In the hardening soil model, stiffness develops as a function of the stress/strain state. Three types of soil stiffness (E_{50}, E_{oed} and E_{ur}) can be inputted independently for three typical loading conditions being triaxial loading, oedemeter loading and unloading/reloading respectively.

Expansion of the yield surface cone is related to shear strains and stiffness parameter E_{50} where on the other hand the expansion of the yield cap (see Figure 4.18) is governed by E_{oed} and the isotropic stress/strain state. The shape of the cap closing the elastic region is determined indirectly by K_0^{nc} and E_{oed}. E_{ur} governs elastic behaviour within the yield contour resulting from previous ultimate stress/strain states.
Stiffness parameters as mentioned before depend on stress conditions, which would imply that a specific stiffness needs to be inputted based on local assumed stress state.

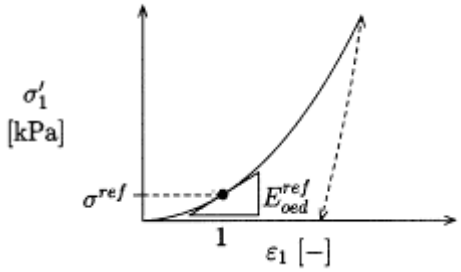

Figure 4.19: Development of E_{oed} with stress level

Within the Plaxis hardening soil model this cumbersome selection of input parameters is not required. Instead, the user has to input a reference soil stiffness for a fixed stress level of p_{ref} = 100 kPa, and the program automatically adapts stiffness as a function of local stress conditions, the soil ultimate strength properties and a factor representing the level of stiffness stress dependence.

More details and background regarding the Plaxis Hardening soil model can be found in the Plaxis 2D materials manual.

4.6.4.4 The hardening soil model with small strain stiffness overlay model

As explained in the previous section, unloading/reloading within the yield surface is assumed to be linear elastic in the original Hardening Soil model. However, truly elastic unloading/reloading behaviour for soils is only observed in the very small strain range, where stiffness is high. When strains grow, the unloading/reloading stiffness has a nonlinear dependency on strain amplitude, as indicated in Figure 4.20

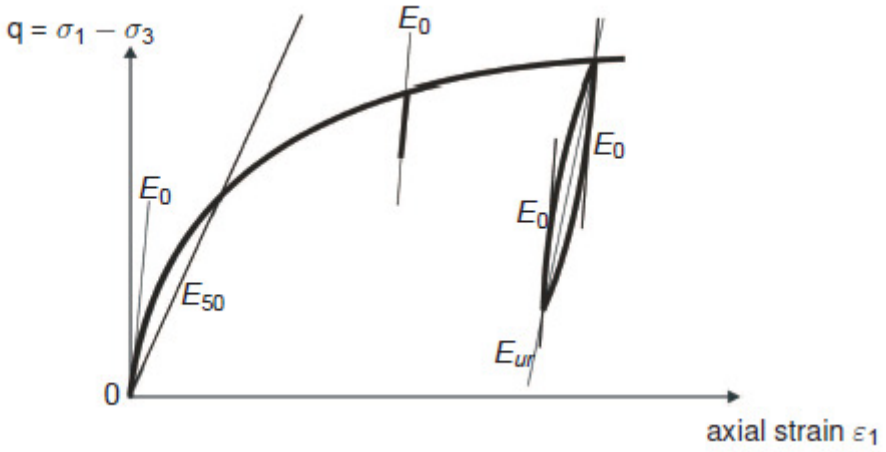

Figure 4.20: HSsmall stress dependent stiffness for triaxial loading conditions

A small strain overlay model including this phenomena, has been developed for the HS model (Benz, 2006). Since the HSsmall model in Plaxis is only an extension of the conventional HS model, it needs only two additional parameters to be defined, i.e. the very small-strain shear modulus G_0 and the shear strain level $\gamma_{0,7}$ at which the secant shear modulus G_s is reduced to 72.2% of G_0. From various test data, it is found that the stress-strain curve for small strains can approximately be described by a simple hyperbolic law. The basic characteristic of this hyperbolic relation (Hardin & Drnevich, 1972) is a decrease of stiffness, with increasing strains due to loss of intermolecular and surface forces within the soil skeleton. As a result, actual soil stiffness also for unloading/reloading depends on the small strain loading history, which in the HSsmall model is in accordance to Figure 4.21 taken into account by:

$$\frac{G_s}{G_0} = \frac{1}{1 + a\left|\frac{\gamma}{\gamma_{0.7}}\right|} \tag{4.38}$$

Where a =0.385, $\gamma_{0.7}$ is the reference strain input parameter as discussed before and γ is a function of the strain history, determined to be a scalar quantity by Benz (2006). Subsequently the HSsmall model constitutive soil relation in the small strain range is easily found from the secant shear modulus G_s as determined by equation (4.38) above, differentiation with respect to strain then results a tangent expression which can be used in time integration procedures.

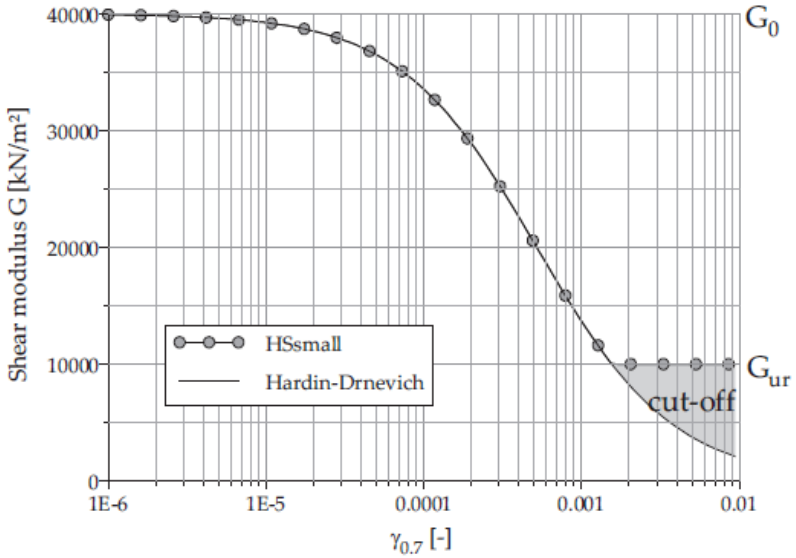

Figure 4.21: Small strain stiffness reduction according to the HSsmall model

As indicated, only two additional parameters G_0^{ref} and $\gamma_{0.7}$ need to be defined for the HSsmall model compared to the HS model. The former parameter may (just as for the HS model) be inputted related to a reference stress level and many correlations are presented in literature. A good correlation to void ratio for many soils was presented (Hardin & Black, 1969) or to unload/reload stiffness as empirically defined by Alpan (Alpan, 1970). The latter reference strain level may be related to the soil plasticity index, or can be defined by using the original Hardin-Drnevich relationship and the Mohr-Coulomb failure criterion.

Under the dynamic loading, unloading/reloading loops as included in the HSsmall model introduce a hysteretic damping component. According to the Hardin-Drnevich relationship for G/G_o as a function of shear strain, this damping will be negligibly small for small motion amplitudes, which appears to be unrealistic compared to actual soil behaviour. Therefore it is recommended (Brinkgreve, Kappert, & Bonnier, 2007) to introduce additionally a small amount of Rayleigh damping in the model. For this Rayleigh damping 1-2% of critical damping may be assumed to be reasonable. On the contrary, the same study shows the hysteretic damping at higher shear strain levels resulting from the HSsmall model to be overestimating actual clay material damping, which can be solved by setting G_0 closer to G_{ur}.

More detailed description of the HSsmall model formulation, its background and comments on the input parameters can be found in the Plaxis Material Models Manual or in the dissertation report by Benz (Benz, 2006).

5 Case study project

This Master's thesis project focuses on a pile soil interaction problem for a case jetty project. In this chapter a brief description of this case project is presented. For more information one may contact Witteveen+Bos.

5.1 Jetty location and geometry

The new terminal that is intended to be developed is located in the Eastern part of the Sea of Marmara
The jetty will consist of tubular steel piles, supporting a reinforced concrete deck. At the connection pile-deck, the piles are fixed in the deck which is considered to have a much higher bending stiffness. For the soil-structure interaction analyses a critical jetty cross-section is selected, as presented in Figure 5.1. The critical cross-section selected is in deep-water, since displacements are expected to reach highest levels at this location and thus will be critical in the displacement based design approach. Extension of the study to shallower water depths is recommended for future studies.

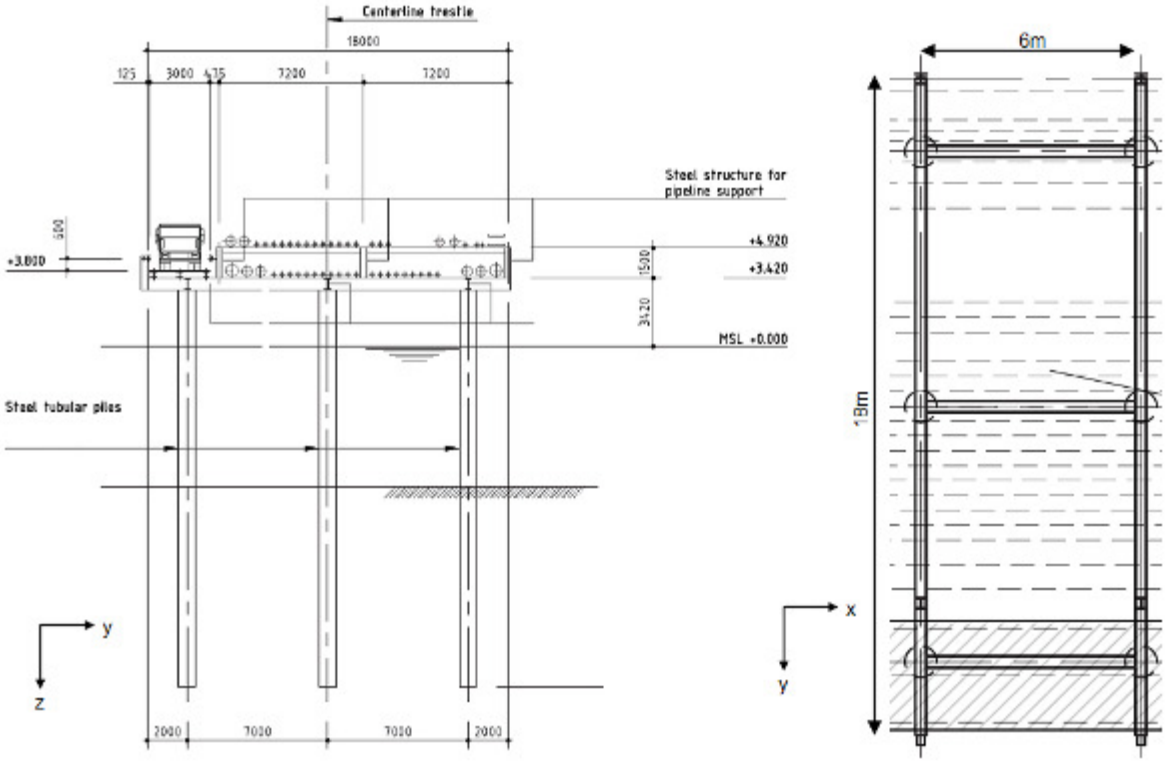

Figure 5.1: Characteristic jetty cross-section

5.2 Seismic activity at the project location

Seismicity near the intended jetty is governed by a series of tectonically active faults and basins that are located at the western end of the North Anatolian Fault. The North Anatolian Fault (NAF) is separating the Anatolian micro plate from the Eurasian plate. To the east of the Marmara Sea, the NAF is a single strand with a narrow deformation zone. Then NAF splits in western direction into north, middle and south branches distributed over a 120 km broad zone around the Marmara Sea. This situation is indicated by Figure 5.2. Fault movements can be characterized as large scale right lateral strike slip movements extending between Eastern Anatolia and the Aegean Sea. Furthermore, there are some pull-apart depression basins through NAF, one of which is crossing the Izmit Gulf and Marmara Sea.

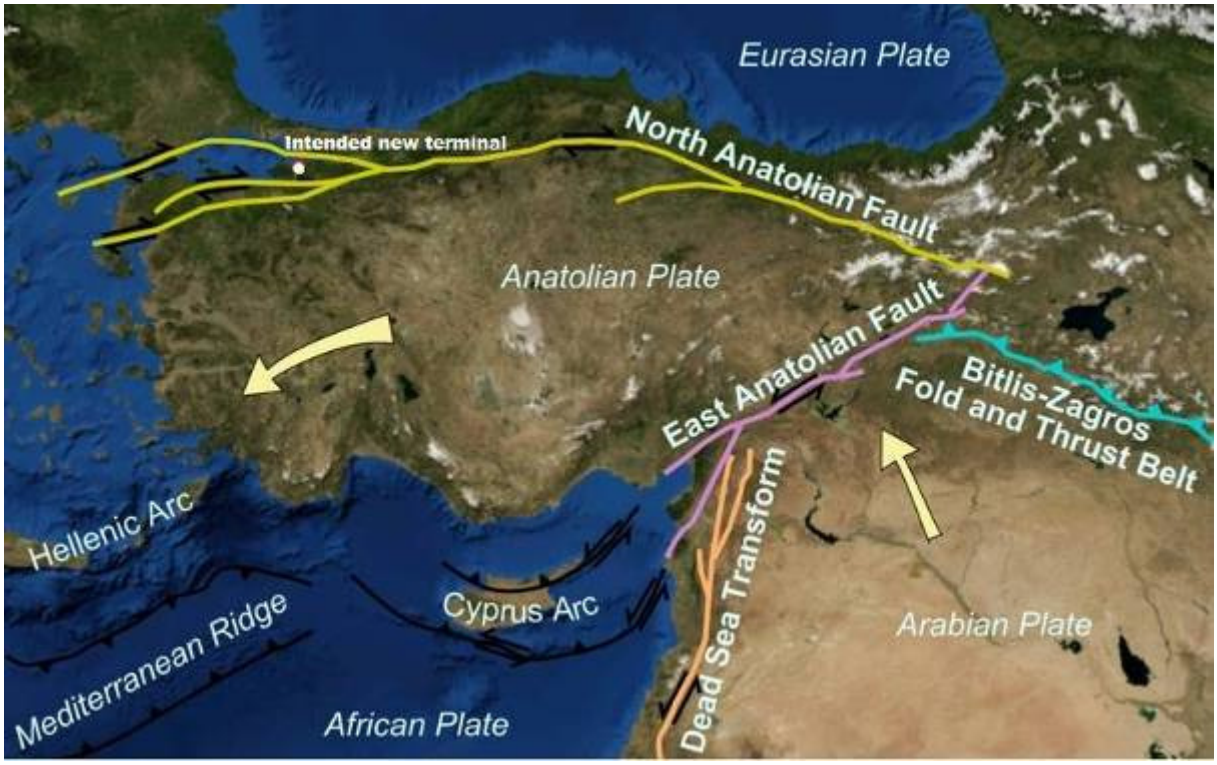

Figure 5.2: Tectonic plates and faults

- Different seismic hazard studies performed over the past decade, where for this project, according to Erdik . (Erdik, 2004). the following design bedrock acceleration levels are to be considered:
- $a_{g,bedrock}$ = 0.70 g for a Mean Return Period of 475 years which is equivalent to a probability of exceedance of 10% in 50 years
- $a_{g,bedrock}$ = 1.02 g for a Mean Return Period of 2475 years which is equivalent to a probability of exceedance of 2% in 50 years

These numbers show the extremely high seismic activity of the region, requiring the new build structure to have significant seismic resistance in order to reach acceptable failure probabilities and ensure a proper performance of the structure even for very high earthquake levels.

5.3 Geotechnical characterisation

Geotechnical parameters used in this study are based on soil survey executed. Some of the available soil survey and laboratory results are doubtful. These difficulties are often obtained for projects, and consequently a parameter selection sheet (Appendix I) was constructed to enhance proper parameter selection. Several empirical correlations are included, for which references are presented in the parameter selection sheet as well. Important contributions were found from (Lengkeek, 2003) for sand parameters, textbooks of (Schonfield & Wroth, 1968; Kulhawy & Mayne, 1990; Muir Wood, 1990) for clay parameters and (Benz, 2006) regarding small strain soil behaviour.
For verification of the obtained soil model parameters, the Plaxis Soil Test Module for triaxial conditions was used. It is noted that verification by the Plaxis Soil Test module not necessarily provides correct soil parameters for practical application,. Though with inclusion of the correct stress levels, correlations between undrained and drained stiffness and effective undrained shear strength levels are verified.

The soil characteristic parameters following from the available soil survey and the parameter selection sheet are summarized in Table 5.1

Table 5.1 Soil profile description

Soil profile for GEOSAN Borehole06, UTM35 E: 704396 N:4507802, Seabed level: 18,00 m-MSL				
Soil layer	C1, clay, soft	C2, clay, medium-stiff	S3, sand, very dense	C3, clay hard (Engineering bed-rock level)
Top level layer [m+MSL]	-18.00	-28.00	-38.00	-48.00
γ_{eff} [kN/m^3]	10.9	12.2	18.0	
γ_{sat} [kN/m^3]	16.6	17.4	20.2	
w_n [%]	52.6	43.1	-	
PI [%]	45	44	0	
ϕ' [°]	23	26	35	
c' [kN/m^2]	2.5	5	0	
c_u [kN/m^2]	4 – 21	31 – 50	0	>200
OCR [-]	1.5	1.5	1	

Which has resulted the following material input parameters for the Plaxis Hardening Soil materials.

Table 5.2: Plaxis Hardening Soil input parameters

Soil profile for GEOSAN Borehole06, UTM35 E: 704396 N:4507802, Seabed level: 18,00 m-MSL			
Soil layer	C1, clay, soft	C2, clay, medium-stiff	S3, sand, very dense
γ_{eff} [kN/m^3]	10.9	12.2	18.0
γ_{sat} [kN/m^3]	16.6	17.4	20.2
ϕ' [°]	23	26	35
c' [kN/m^2]	2.5	5	0.5
OCR [-]	1.5	1.5	1
$K_{0,oc}$	0.80	0.75	0.50
m [-]	0.9	0.9	0.5
E'^{ref}_{50} [kN/m^2]	2900	3800	50000
E^{ref}_{oed} [kN/m^2]	1440	1680	58000
E^{ref}_{ur} [kN/m^2]	10000	12500	200000
G^{ref}_o [MN/m^2]	28000	36000	150000
$\Upsilon_{0.7}$ [-]	5.3 10^{-4}	5.0e-4	1.5e-4
v_{s0}^{ref} [m/s^2]	129	142	269
$v_{s0}^{midlayer}$ [m/s^2]	82	144	317
K_h [m/s]	7.5e-10	3.0e-10	1.0e-3
K_v [m/s]	5.0e-10	2.0e-10	1.0e-3

5.4 Seismic site characterization

Ground characterization affects frequency dependent amplification of a site and structures built at this site, which is represented in a seismic response spectrum. In order to establish the site specific spectral shape, average soil characteristics over the top 30 m are generally determined. The top 30 m. of the soil profile (-18,0 + MSL to -48,0 + MSL) is characterized by $v_{s,avg30}$ = 161 m/s^2, where $v_{s,avg30}$ is based on the shear modulus. It is noted that the shear wave velocity presented in Table 5.2 is related to reference small strain stiffness G_0, where lower values will be found for increasing strain levels. Based on the upper bound shear wave velocities corresponding to shear stiffness at mid-layer stress levels, the estimated upper bound site fundamental frequency would be:

$$f_0 = \frac{v_{s,avg}}{4H} = \frac{(82 \cdot 10 + 144 \cdot 10 + 317 \cdot 10)/30}{4 \cdot 30} = 1.5Hz \qquad (5.1)$$

The ground profile corresponds to the site classes according to seismic design standards as presented in Table 5.3.

Table 5.3 Ground profile characterization according to seismic standards

Standard	Site class
Eurocode	D
Turkish code, ISO 19901-2 and NEHRP-FEMA450	E
PIANC	indicates that various codes provide characteristic profiles

Earthquake design procedures according to various standards have been compared in the preliminary study. The way in which design peak ground accelerations and design spectra are computed appear to be somewhat different in the various standards, however generally all provide a similar response spectrum approach. Response spectra according to the Turkish Seismic Regulations, The U.S. Fema450 and the international ISO standards are identical, provided that the same input parameters are used, where Eurocode 8 gives somewhat different response spectra. Hence, in this section the response spectra provided by Turkish seismic regulations (representing also U.S and ISO standards) and Eurocode 8 are presented. The input peak ground accelerations and site specific spectral input parameters for different earthquake levels are based on a site specific probabilistic seismic hazard assessment (Erdik, 2004)

5.4.1 Turkish/ISO seismic regulations response spectra

According to the Turkish seismic regulations, a jetty where hazardous materials or chemicals are handled is a special class structure, resulting in the following performance objectives:
- No damage for E1 level earthquake
- Minor repairable damage for E2 level earthquake (structural response up to elastic-plastic limit)
- No collapse requirement for E3 level earthquake

The response spectra characteristics related to the three earthquake levels are presented in the tables below. Bedrock acceleration a_g and spectral parameters S_s and S_1 are after (Erdik, 2004). The spectra is derived based on ground acceleration values and local soil classification. The response spectra is then constructed by simple formula for which one is referred to the related seismic design standard.

The response spectra given by the U.S. Fema450 /MOTEMS and the ISO recommendations are identical to the spectra conform the Turkish Seismic Regulations, provided that identical input parameters are used. According to ISO global seismic hazard maps, the governing peak ground acceleration for the site considered should be less, but the PSHA by Erdik (2004) overrules these lower seismic levels.

Table 5.4: Elastic Design Response Spectrum (5% damping) parameters, site class E

Earthquake level	E1 (50% probability of exceedance in 50 years, MRP = 72 years)	E2 (10% probability of exceedance in 50 years, MRP = 475 years)	E3 (2% probability of exceedance in 50 years, MRP = 2475 years)
Peak ground acceleration bedrock a_g [g]	0.30	0.70	1.02
Spectral value S_s [g]	0.65	1.54	2.32
Spectral value S_1 [g]	0.26	0.70	1.14
F_a [g]	1.4	0.9	0.9
F_v [g]	2.96	2.40	2.40
S_{ms} [g]	0.91	1.39	2.09
S_{m1} [g]	0.77	1.68	2.74
S_{ae} [g]	0.91	1.40	2.10
T_o [s]	0.17	0.24	0.26
T_s [s]	0.85	1.21	1.31

5.4.2 Eurocode EN-1998 (2005) response spectra

EN-1998 defines seismic intensity based on two separate performance requirements:
- The Damage Limitation Requirement (DLR)
- The No Collapse Requirement (NCR)

These two limit states are related to seismic return periods and exceedance probabilities. Subsequently these quantities can be scaled according to a structural importance class.
According to EN-1998 a jetty where potentially hazardous materials or chemicals are handled, should be in structural importance class III or IV:

- Importance class III: high risk to life and large economic and social consequences of failure
- Importance class IV: exceptional risk to life and extreme economic and social consequences of failure

This classification appears to be subjective to the engineers interpretation. For this case the jetty is assumed to be a class IV structure, resulting an importance factor $\gamma_1 = 1.4$.
Erdik et al. provides the governing peak ground acceleration based on a site specific probabilistic seismic hazard assessment to be $a_{gR,NCR} = 0.7$ g with a probability of exceedance of 10% in 50 years, which is the reference situation for the EN-1998 "No Collapse Requirement". This can be transformed into $a_{gR,DLR} = 0.41$ g for the "Damage Limitation Requirement" Subsequently both acceleration values need to be scale in order to include the seismic importance class, resulting:
- $a_{g,DLR} = 0.57$ g, related to exceedance probability of 17.4 % in 50 years, MRP = 261 years
- $a_{g,NCR} = 0.98$ g, related to exceedance probability of 3.6% in 50 years, MRP = 1303 years

According to the soil investigation as described in paragraph 5.3, the local conditions are comparable to site class C of D according to EN-1998.

Table 5.5Elastic Design Response Spectrum (5% damping) parameters, site class D

Earthquake level / spectrum type	DLR, spectrum type 1	DLR, spectrum type 2	NCR, spectrum type 1	NCR, spectrum type 2
Peak ground acceleration bedrock a_g [g]	0.57	0.57	0.98	0.98
Soil factor S	1.35	1.8	1.35	1.8
S_{ae} [g]	1.92	2.56	3.30	4.41
T_B [s]	0.2	0.1	0.2	0.1
T_C [s]	0.8	0.3	0.8	0.3
T_D [s]	2.0	1.2	2.0	1.2

It is noted that peak response spectral values conform Eurocode 8 reach higher values than the peak spectral values resulting from Turkish, U.S. or ISO seismic recommendations. For the case project considered Turkish and ISO seismic recommendations are valid and accordingly the response spectra provided by these codes will be adopted in design.

5.5 Jetty structural characteristics

This study focuses primarily on the dynamic soil-structure interaction effects typical for jetty structures. The structural geometry therefore is taken as a starting point, and based on the Witteveen+Bos design report. The geometrical properties of the deep water tubular steel piles are presented in Table 5.6.

Table 5.6 Pile Geometry

Pile geometry		Design value
Sea bottom level	[m + MSL]	-18.00
Pile top level	[m + MSL]	3.80
Pile tip level	[m + MSL]	-39.00
Pile	[-]	Ø1372/26
Pile moment of inertia	[mm^4]	$\pi/64 \times (1372^4 - 1320^4) = 2.49*10^{10}$

Pile material parameters used in design are shown in Table 5.7. The material properties shown are representative values as used for seismic design considerations.

Table 5.7 Material parameters

Pile material parameters		Design value
Steel quality	[-]	S275J0H according to EC-10219;2006
Steel mass density	[kg/m^3]	7860
Steel representative yield strength $f_{y,rep}$	[N/mm^2]	275
Steel ultimate tensile strength f_u	[N/mm^2]	500
Steel Young's modulus E_s	[N/mm^2]	210,000

Combining pile geometry and material parameters, the jetty masses to be included in dynamic analysis are defined as presented in Table 5.8.

Table 5.8 Jetty masses for dynamic analysis

Pile dynamic characteristics		Design value
Pile mass	[kg/m^1]	$7860 \times \pi \times 1{,}372 * 0.026 = 880.8$
Added mass water enclosed in the pile	[kg/m^1]	$1000 \times 0.25 \times \pi \times 1.372^2 = 1478.4$
Total mass pile + water	[kg/m^1]	880.8 + 1478.4 = 2359
Added mass soil enclosed in the pile	[kg/m^1]	$1670 \times 0.25 \times \pi \times 1.372^2 = 2469.0$
Total mass pile + soil	[kg/m^1]	880.8 + 2469.0 = 3350
Representative deck mass	[kN/6m jetty]	791.8
Pile bending stiffness EI_{pile}	[kNm^2]	$5.23*10^6$

At the pile-deck connections, the piles are typically embedded in the concrete deck beams that are integrated with the deck slab. The effective stiffness of this concrete section (beams + effective part of the deck) can be assumed to be much more stiff than the single pile bending stiffness. Therefore, the piles can be considered fixed for rotations by the deck. The connection pile-deck will be a plugged dowel type connection, built up by a concrete plug fixed in the steel hollow section, connected to the deck concrete by reinforcement dowels. To enhance ductile capacity of the structure, it is possible to design the connection to provide additional rotational capacity and a certain amount of hardening beyond the onset of plastic hinging of the pile. Alternatively the rotational capacity may be provided by plastic hinging of the pile section, for which the highest bending moment will occur at the connection with the deck. Damage will then be concentrated to this region which can be repaired relatively well after a strong earthquake.

In the present study, the design of the ductile connection will not be treated in detail. The post-yield hardening of the pile at the deck connection is determined based on ultimate acceptable strain levels for the dual level earthquakes provided by design standards. Based on these strain levels the post-yield hardening capacity and the related ductility are determined according to the theory of elasticity/plasticity for circular hollow sections, where a simplified bilinear moment-curvature relations is assumed. Results are presented in Table 5.9.

Table 5.9: Bilinear approximation rotational fixity stiffness deck-pile

Parameter	Unit	Value
Initial fixity stiffness		
$M_{y,initial\ yield} = I_y f_y / (D/2)$	[kNm]	9984
$M_{y,eff} = 1.1 M_{y,initial\ yield}$	[kNm]	10980
$\varphi_{y,eff} = 1.1 \varepsilon_y D / 2$	[rad/m]	0.002
$\theta_{y,eff} = 0.5 \varphi_{y,eff} L_{fixation length}$ Where the effective fixation length of the pile in the concrete is assumed at 1.00 m	[rad]	0.001
$K_{initial} = M_{y,eff} / EI_{pile}$	[kNm/rad]	10^7
Post-yield hardening fixity stiffness		
$\Delta\varepsilon_p = \varepsilon_u - \varepsilon_{y,eff}$	[-]	0.024
$\Delta\varphi_p = \Delta\varepsilon_p D / 2$	[rad/m]	0.017
$\Delta\theta_p = \Delta\varphi_p L_p$ Where L_p is the effective plastic hinge length, which can be estimated as $L_p \approx D$ or $L_p \approx x(\alpha - 1)/\alpha$ Where x is the distance over which bending moment decreases linearly from $M_{\max}$ to zero $\approx 15m$ and $\alpha = M_{u,eff} / M_{y,eff} \approx 1.1$, resulting $L_p \approx 1.4$	[rad]	0.025
$K_{post-yield\ hardening} = (M_u - M_{y,eff}) / \Delta\theta_p$	[kNm/rad]	$4.3*10^4$
Post-yield hardening ratio $r = K_{post-yield\ hardening} / K_{initial}$	[-]	0.004

6 Analysis method

6.1 Introduction

The goal of this study is to analyze the operation and result of available performance based seismic design approaches for jetty structures under soft soil conditions, where according to literature soil structure interaction is recognized as an important factor. Within the performance based design strategy, the acceptable seismic design procedures for jetty structures are:

- Simplified dynamic analysis by static pushover analysis combined with a response spectrum procedure
- Two step uncoupled dynamic analysis of the site and the structure
- Coupled dynamic analysis of site and structure system

All three design methodologies will be followed for a case jetty project, as a two-way approach also is recommended in most seismic design standards. Figure 6.1 summarizes the possible analysis procedures along performance based seismic design. Simplified dynamic analysis procedures are often the starting point, where dynamic analysis is known to may provide more economical designs where they give more insight in possible failure modes. Dynamic analysis traditionally is performed for first the site and then the structure separately, where increasing computational capabilities nowadays also allow for coupled response of site and structure. Both the uncoupled and the coupled approach will be part of the study. The new released Plaxis 3D dynamics module is a valuable tool for performing coupled analysis of site and structure. Verification of its operation, capabilities and limitations in dynamic jetty analysis will be part of this study.

Figure 6.1 summarizes the three possible analysis approaches towards the seismic jetty response, and accordingly are included in this study. It is investigated how the different methods account for soil-structure interaction effects in seismic jetty response analysis. Steps that subsequently will be taken within the three performance based design approaches are described in the next paragraphs.

It is noted that, as in many other studies, full scale test results for direct verification of the results from the different models are not available, where they obviously would provide very valuable verification. This problem as is often faced in seismic design is partly overcome by proper step-by-step verification in all steps, which is required in order to in the end have valuable results.

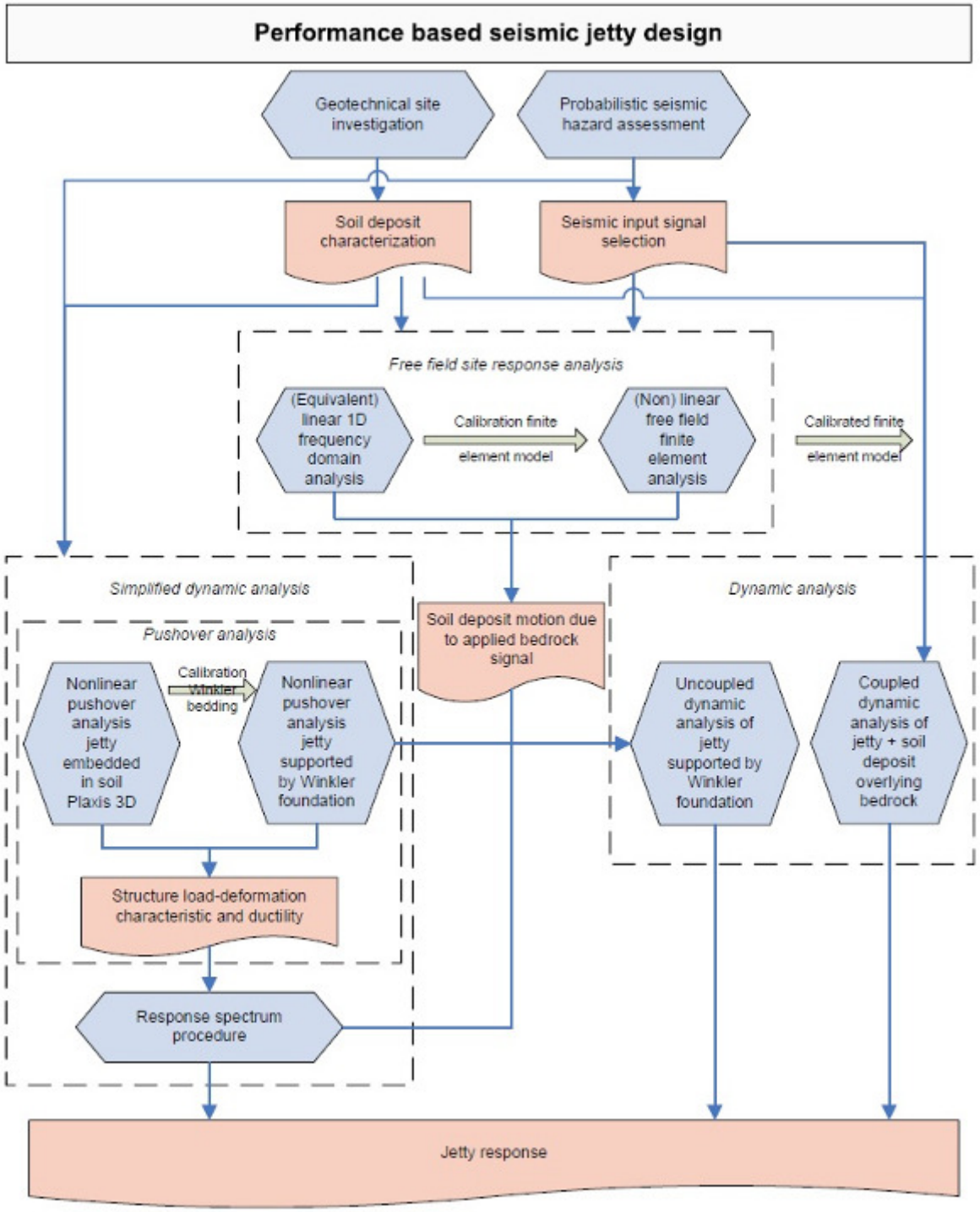

Figure 6.1: Analysis procedure flowchart

6.2 Pushover analysis

6.2.1 Static pushover analysis on conventional piles supported by Winkler foundation models

Static pushover analysis forms the basis for simplified dynamic analysis procedures which is often used for seismic design in engineering practice. In this stage pushover analysis on piles laterally supported by a nonlinear Winkler foundations will be performed. This simplified Winkler models are often used to represent the soil because of their computational convenience. Nonlinear Winkler spring characteristics corresponding to the local soil conditions will be based on common expressions as presented in paragraph 4.6.3.

Code provisions regarding the spring characteristics of the discrete Winkler foundation are initially adopted and are discretised as a function of local soil parameters, pile diameter and local depth, with a 1 m spacing. In analyses Matlock p-y curves for soft clay are used for the very soft C1 clay and the soft C2 clay layers, the O'Neill and Murchison p-y curves for sand are used for the S3 sand layer. The p-y expressions used do not include cyclic softening, since the cyclic reduction as obtain for long term unloading/reloading is not to be expected during an earthquake for the undrained conditions of the clay. Degradations is only to be expected in the very top soil layers, where resistance will contribute only very limited due to the soft soil present. For input convenience the nonlinear springs are approximated by equivalent tri-linear springs. The p-y curve characterizations of soil impedance varying with depth are presented in appendix III.

First pushover analysis are performed on single pile models, since in the continuum soil modes group effect need to be excluded in this initial phase. Subsequently pushover analysis on three-pile jetty cross-section models are performed. For the single pile models a rotational spring on top is included in the models, having an initial stiffness equal to the pile bending stiffness and a post-yield stiffness approximately equal to the pile post-yield bending stiffness, resulting in some hardening after yielding in the pile structural model.

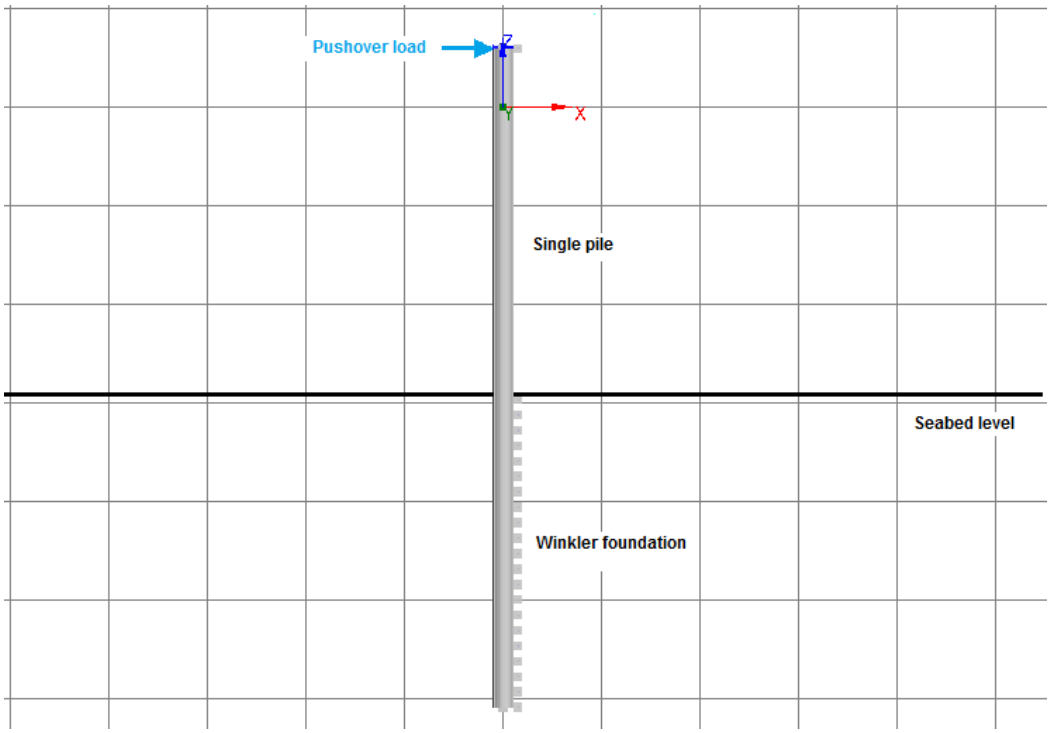

Figure 6.2 Single pile supported by nonlinear Winkler foundation model in Seismostruct

6.2.2 Static pushover analysis on a single pile embedded by a continuum with the Hardening Soil constitutive models in Plaxis

In the present study, the correspondence in lateral pile behaviour between piles supported by conventional Winkler foundation models and piles embedded in a soil continuum (Plaxis Hardening Soil model) is verified. The adopted procedure towards a proper well-established Plaxis 3D pile-soil model is explained in this paragraph.

The HS and HSsmall constitutive models as described in paragraph 4.6.4 are applied in the analyses. Soil input parameters for the hardening soil models where determined, equivalent to the input parameters for the Winkler model. The Plaxis models are build up gradually, to prevent inclusion of errors in the models and to verify its capabilities and limitations. Initially only a lateral load at pile head is included in the pushover models for computational convenience. Finally a vectorial load pattern will be applied to obtain the approximate load deformation characteristics of the system for seismic loading.

First a wall with free head is modelled with Plaxis 2D and 3D plane strain models. The wall is given a bending stiffness equal to the bending stiffness of the pile, in fact representing the typical situation of a row of piles having centre-to-centre distance of 1 pile diameter. Possible pile modelling by a combined plate+solid is investigated by checking the performance of a similarly defined wall section in Plaxis 3D. The pushover responses from the Plaxis 3D models have to be similar in order to establish proper operation of the 3D models, provided that the more simple 2D model was also built correctly.
As a next step the top rotation fixity of the pile is introduced in the model. The fixation in the single pile model represents the presence of the deck that prevents pile head rotations for the actual jetty cross-section. The top fixity included in the models will initially be given elastic characteristics with a very high dummy stiffness. Subsequently an artificial elasto-plastic fixation with hardening will be constructed by making use of elasto-plastic and elastic fixed-end anchors in Plaxis 3D. This work-around was required since elasto-plastic plates are not included in Plaxis 3D. Proper operation of the fixity is verified by comparing these models to models including rigid fixities and by studying the development of bending moments at pile head.

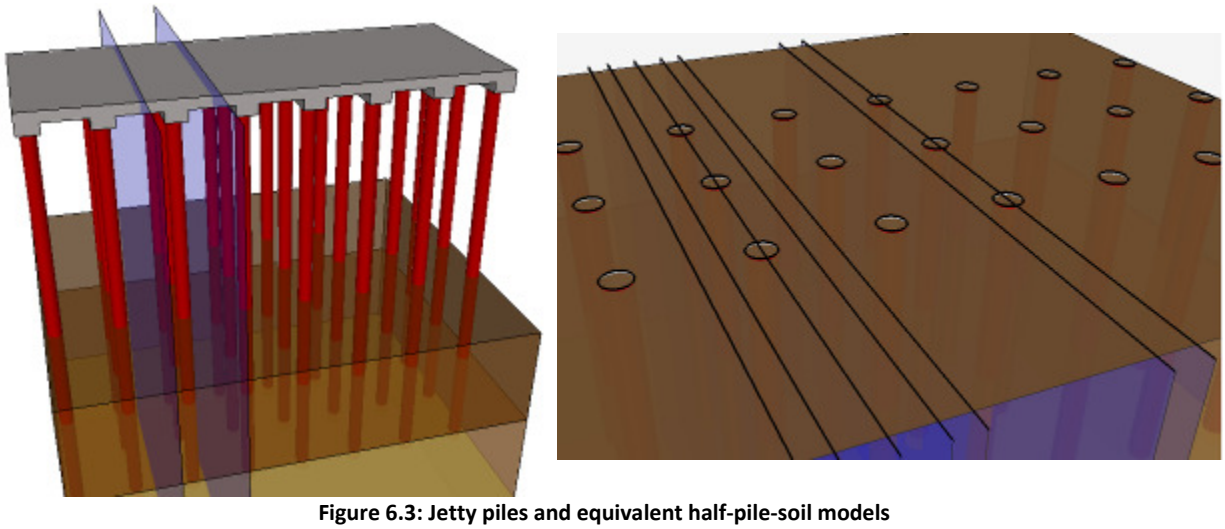

Figure 6.3: Jetty piles and equivalent half-pile-soil models

Based on the wall models one may conclude whether both the composite plate-solid modelling and the inclusion of elasto-plastic rotational fixation at the head are properly operating. Then both can applied in a 3D single pile model. For computational convenience, only half a pile is modelled. A model width of 3 m was used because this is equivalent to a side-side centre-to-centre distance of >4*D for the piles, which based on Reese and Ympe (2001) would imply that no efficiency reduction will be present. Both a circular and a rectangular pile configuration with equivalent bending stiffness have been modelled for excluding problems related to the circular shape modelling in Plaxis 3d. The results confirm proper behaviour of the circular section.

With the pile and fixity properly included in the Plaxis model, soil parameters can be varied in order to establish the sensitivity of the global structure response to variations in these parameters. Results will be compared to

the results from pushover analysis on equivalent pile with Winkler foundation models. Based on this comparative study the equivalence of the models for static loading can be studied, which is a precondition in order to compare dynamic responses of both models under seismic loading.

6.2.3 Equivalent Plaxis 2d pile model based on the Plaxis 3d and Winkler model push-over characteristics

Geometric 3D effects important for piles cannot be included in a 2D equivalent model. However, for computational convenience it would be attractive to define a plane strain Plaxis 2D (wall) model, equivalent to the Plaxis 3D (pile) model. This equivalent Plaxis 2D model then can be used to perform computationally less demanding 2D dynamic analyses instead of 3D dynamic analyses. Additionally it is noted that the Plaxis 2D modelling options are more complete (e.g. implementation of elasto-plastic structures). This forms a different reason for which development of equivalent Plaxis 2D pile-soil interaction may be attractive.

In actual pile-soil interaction arching effect in the soil result spreading of the loading over an effective width of about 2*D to 4*D, depending on the soil internal friction angle φ. Arching of stresses in the soil is related to the concept op group efficiency for pile groups, meaning the reduction of pile capacity due to intersecting load spreading fields of adjacent piles. The phenomena of group efficiency has been studied by many researchers in the past. Reese and Van Ympe (2001) have collected these test results and developed efficiency reduction formulas based on these data. In this study a pile efficiency estimate calculation sheet was built, for which one is referred to appendix III. According to Reese and van Ympe (2001), efficiency of piles will not be reduced for side-side centre-to-centre distances larger than 4*D, where D is the pile diameter. In order to study the arching/spreading effects for the soft soil conditions in Plaxis, Plaxis 3D analyses with models of different width have been performed, implying a pile having a particular side-side spacing from adjacent piles.

Based on the static pushover characteristics compared for both Plaxis 2D and 3D models, it will be judged whether it is reasonably possible to define an equivalent jetty model in Plaxis 2D.

6.2.4 Pushover analysis of the case study jetty cross-section in transverse direction

In the preceding, the focus has been on lateral response of single piles, and the effects of side-side pile spacing. For many civil engineering applications, including jetty structures, piles are also spaced in the direction of loading and consequently piles affect each other in this direction too. The side-side pile spacing considered in the pushover analyses for the jetty cross-section is the actual pile spacing of the case study jetty piles, which is equal to 6 m. In the transverse jetty direction, which is generally assumed to be the governing direction for seismic analysis, the pile spacing is 7 m, where the case jetty is supported on three rows of piles. Figure 6.4 shows the 3D and 2D Plaxis jetty cross-section models on the left and right respectively.

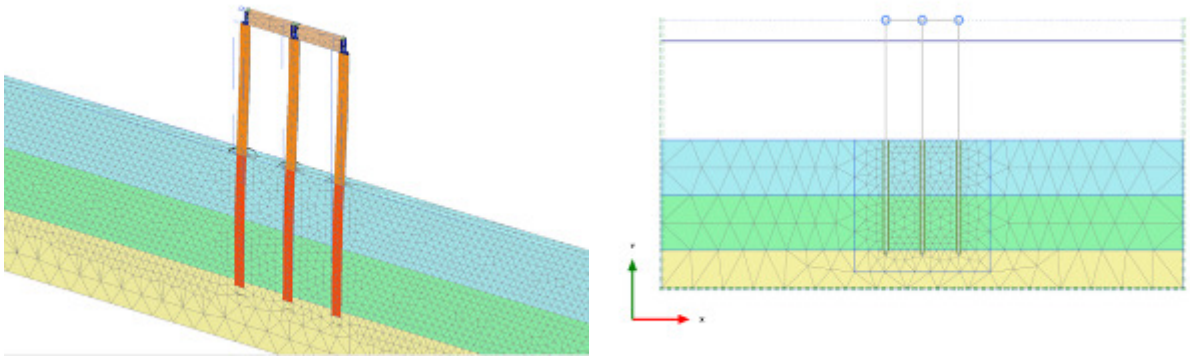

Figure 6.4: 3D and 2D Plaxis jetty cross-section models

In Plaxis 3D modelling of elastic-plastic plates is not implemented. Consequently for the jetty cross-section analysis an artificial elastic-plastic rotation fixity was modelled.

Jetty cross-section pushover analysis will provided information regarding pile group efficiency of piles spaced in the loading direction. Based on Reese and van Ympe (2001) one may expect an efficiency reduction up to 20% for the trailing piles for the considered jetty design geometry, where other literature (see 4.6.3.9) provide even higher reductions. Based on the Plaxis 3D analysis these efficiency reductions will be re-assessed for the case study soft soil conditions.

Subsequently pushover analysis of an equivalent 2D jetty cross-section model will be performed, aiming at correctly capturing the jetty load deformation characteristics with a 2D model approximation for performing the dynamic analyses.

Deviations for the 2D model approximations are expected to be caused by two conceptual errors in the 2D model:

- Load spreading around leading piles is prevented in a 2D approximation, which probably will prevent trailing piles from mobilizing lateral resistance, ultimately reducing total lateral stiffness for the jetty;
- Local failure effects may be expected to be less pronounced in the 2D approximation, which probably will increase lateral stiffness.

The simplified Winkler model will result a response identical to the response obtained for a single pile, since soil response acting the jetty piles is completely independent if p-y element support nodes are not connected (Figure 6.5). Consequently, the response obtained from a multi-pile jetty cross-section may be expected more stiff than the equivalent Plaxis 2D and 3D jetty cross-section pushover models. In order to account for group efficiency reduction of adjacent piles, the required reduction of Winkler soil spring stiffness and ultimate capacity will be determined based on comparison to the Plaxis 3D jetty pushover analysis results.

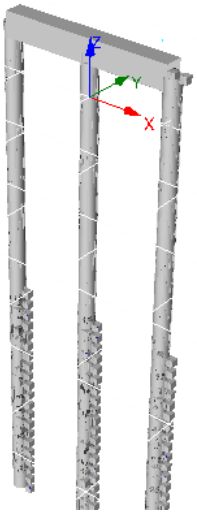

Figure 6.5: Jetty cross-section supported by Winkler foundation

6.3 Simplified dynamic analysis based on the push-over results

Recommendations according to the various seismic design standards as presented in chapter 3 of this study will be followed. The simplified dynamic analysis N2 response spectrum method as proposed by Fajfar (Fajfar, 1999) and summarized in paragraph 4.4.2.2 will be applied. This method is similar to the performance based simplified dynamic analysis procedure provided by Turkish Technical Seismic regulations for Port and Harbour structures, appendix C.

The response spectrum according to Turkish Seismic Regulations and ISO (see 5.4.1) is adopted and the governing peak ground acceleration is found from equivalent linear frequency domain free field site response analysis. The N2 method as proposed by Fajfar relies on the equal displacement assumption forming the link between damping and ductility, for which is noted that its accuracy may be less for structures on soft soil conditions. As an alternative the equal potential energy norm may be adopted, but for the structure fundamental frequency range typical in jetty design the ductility reduction of response spectra according to either the equal-

displacement or the equal-potential energy norm will be reasonably similar according to Miranda & Bertero. (Miranda & Bertero, 1994)

The number of modes to be included can be estimated by approximating the modal participation factors based on an equivalent linear system. In this study no multi-mode simplified dynamic analysis will be performed because of time limitations. The possible improvement in accuracy of the obtained jetty response by applying multi-mode techniques is recommended for future studies.

Pushover forces are distributed over the jetty transverse cross-section according to the product of the mass vector and the fundamental eigenvector, where forces related to pile and soil inertia forces below seabed level will be neglected. These approximations result the commonly used method for calculation of the seismic response of multi-story buildings. It is noted that soil-structure interaction by kinematic pile loading is neglected by this simplified approach. The fundamental mode shape of the jetty structure in transverse direction is determined by modal analysis in Seismostruct, with the soil stiffness being approximated by the initial p-y stiffness.

Better accounting for soil structure interaction in simplified dynamic analysis for the deep founded jetty structure would require determination of the coupled soil structure dynamic characteristics. In order to do so, a dynamic analysis of the coupled system is required, from which the eigenmodes of the coupled system can be found. Then according to the lowest eigenmodes, the simplified dynamic analysis may be performed. It is noted that the computational benefits of the simplified dynamic analysis method are then not longer present and hence this path is not further investigated in this study.

The displacements obtained from the simplified dynamic analysis will be compared to displacements resulting from uncoupled or coupled dynamic site and structure analyses, from which accuracy of single-mode simplified dynamic analysis for jetty structures in soft soil conditions can be estimated.

6.4 Free field site response analysis

The free field response for excitation at bedrock level is calculated along the 1D linear elastic frequency domain analysis and by finite element analysis in Plaxis 2D and 3D. In the Plaxis finite element analysis Linear Elastic (LE), Mohr-Coulomb (MC), HS and HSsmall material models are used in order to be able to first make a proper comparison to the frequency domain solution with respect to numerical modelling issues and then study the effects of the more advance soil models.

A continuous layered soil profile as is assumed to be representative in this study, reduces the free field analysis to a 1D problem. However, when performing Plaxis finite element analysis, boundary influences are known to disturb free field site response results within a region around the boundary. In order to exclude these effects to affect the site response, boundaries have to be taken far enough away and some damping has to be included in the model preventing waves reflecting at the boundaries to significantly affect the motions at the model centre. It is noted that a new type free dynamic boundary is available in Plaxis 2D, which conceptually would perfectly describe a 1D case. Since these new boundaries are not implemented in Plaxis 3D, a proper comparison of 2D and 3D models cannot be made when different boundaries are included. Hence in this study the Plaxis viscous dynamic boundaries are used in both Plaxis 2D and 3D. In a sensitivity study regarding model width, linear elastic material behaviour will be assumed in order to made a proper comparison with the 1D analytical solution and speed up analyses. A Rayleigh viscous damping ratio of 0.05 is included for the linear elastic soil, which is believed to be a conservative lower bound value for actual soil damping during moderate and high intensity earthquakes. Sensitivity of model width is studied for both harmonic bedrock signals (3 and 10 Hz) and the selected Duzce signal. The required model width will be based on analysis of both horizontal and vertical motions of the surface level from the model centre towards the lateral boundaries.

Both Plaxis 2D and Plaxis 3D finite element analysis are performed in order to assess the performance of the very new Plaxis 3D dynamic module. Responses for LE, MC, HS and HSsmall soil material models are compared to find response dependence on soil model type and possible equivalent linear elastic approximations with related viscous damping percentages.

6.4.1 Input signals

In the present study it is assumed that the input bedrock motions are horizontally polarized shear waves propagating vertically. As input motions both harmonic motions and random earthquake bedrock signals are used. Only a horizontal bedrock motion in transverse jetty direction is assumed and consequently the Plaxis 3D free field site response results should match the free field site response as obtained from Plaxis 2D. As a simplification, the vertical accelerations at bedrock level are in this study set to zero. Additionally Rayleigh surface waves are not considered too. It is realized that these traditional assumptions in seismic design may be an over-simplification for a near fault location, but including them is beyond the scope of this study.

The seismic input signals that are selected meet the following selection criteria:

- Preferably the signals should be recorded from the active fault governing the case project location or a similar type of strike-slip fault;
- Signals should be measured for stiff soil conditions in order to be applicable as a bedrock level excitation;
- Since the case project location can be considered near-fault, a near fault signal should be selected

For the case jetty project two signals from the North Anatolian Fault earthquakes (1999) are selected from the PEER strong motion database:

- DUZCE_375_N (P1551)
- KOCAELI_IZT090 (P1103)
- KOCAELI_SKR090 (P1109)

These bedrock input signals are presented in spectral format by Figure 6.6. and for representation in the time domain one is referred to appendix IV.

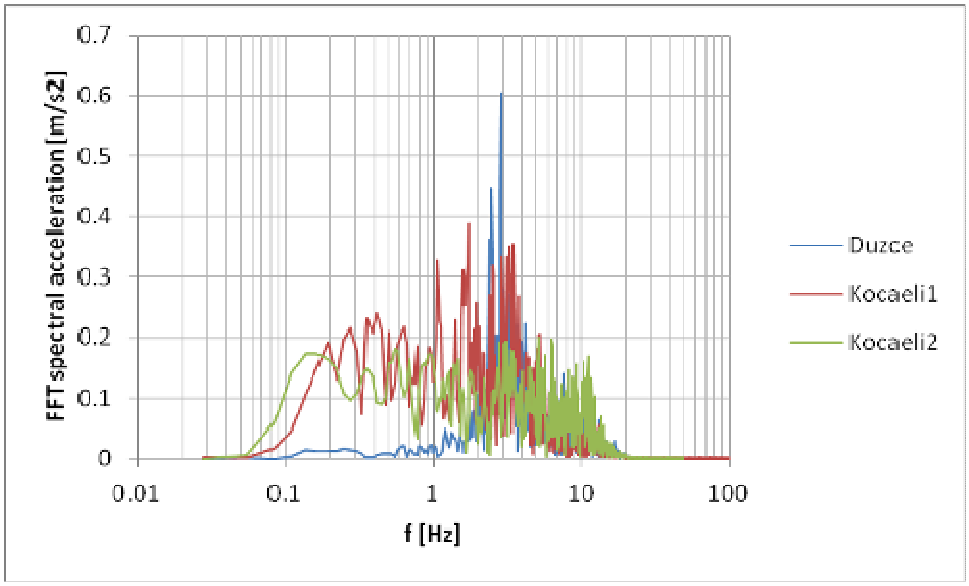

Figure 6.6: Selected North Anatolian Fault bedrock acceleration spectra Duzce, Kocaeli_IZT and Kocaeli_SKR from PEER database

As can be obtained from the spectral representations of the signals, the energy is concentrated in the band ranging from 0.1 to 15 Hz, which is of importance for the finite element mesh size. Based on the frequency domain representation of the signals (Figure 6.6) it can be concluded that the Duzce (narrow band) and Kocaeli2 (broad band) signals have very different characteristics, where Kocaeli1 can be characterized somewhere in between. Consequently dynamic analysis will for time limitations be performed for the Duzce and Kocaeli2 signal only, where it is noted that in actual design a higher minimum number of seismic input signals is required.

The harmonic acceleration time histories included have a frequency of 3 Hz and 10 Hz and an amplitude of 2 m/s^2, which is a reasonable mean amplitude for the high intensity part of the earthquake motions scaled at $a_{g,bedrock}$ for the moderate level earthquake according to paragraph 5.2. Harmonic signals are included because of their simplicity for checking the model performance with respect to mesh size and boundary effects and make an easy comparison to the analytical solution. A 3 Hz frequency signal is selected because it is a frequency very prominent in the selected real seismic signals. A 10 Hz frequency signal is chosen because it is an

upper limit high energy containing frequency of the real seismic spectra, and analysing the response of this higher harmonic signal can be used to determine allowable mesh element sizes.

6.4.2 Dynamic soil material parameters

As a part of the site response analysis study, a comparative study on results by linear elastic, Mohr-Coulomb and HSsmall material models is executed in order to analyze the performance of the different models. Actual soil behaviour in dynamic Plaxis analysis is conceptually best described by using the Hardening Soil Small Strain stiffness soil constitutive model, provided that soil parameters are properly defined. The HSsmall model includes stress dependent stiffness development and small strain stiffness features, which introduces hysteretic damping in the model. However, for verification of the HSsmall model operation, linear elastic and Mohr-Coulomb soil models are included in this study.

The HS and HSsmall soil models as implemented in Plaxis have a stress dependent stiffness, and consequently soil layers will not be homogeneous. For linear elastic and Mohr Coulomb models stiffness is assumed constant over the a soil layer, and fixed at values corresponding to the stress level present at mid-layer depth.

For over-consolidated material subjected to seismic loading the actual shear modulus will develop ranging from upper limit G_0 for small strain levels to lower limit G_{ur} for large strain level, where damping levels will develop inversely. The resulting lower and upper limit dynamic soil parameters are presented in Table 6.1. For other soil parameters, one is referred to paragraph 5.3.

Table 6.1: Dynamic soil parameters for LE/MC and HSsmall material models

Parameter		Clay C1	Clay C2	Sand S3
ρ_{sat}	[kg/m^3]	1692	1777	2059
Lower bound soil dynamic characteristics for the unload/reload range				
$E_{mid\,layer}$	[kPa]	4000	12000	275000
$G_{ur,mid\,layer}$	[kPa]	1670	5000	114000
$v_{s,ur}$	[m/s^2]	31	53	236
Upper bound soil dynamic characteristics for the unload/reload range				
$G_{0,ref}$	[kPa]	28000	36000	150000
$G_{0,mid\,layer}$	[kPa]	11367	36880	207304
$\gamma_{0.7}$	[-]	0.00053	0.00050	0.00015
$v_{s,o}$	[m/s^2]	82	144	317

Strain dependent characteristics of soils vary with soil type. Many different curves for G_s / G_0 and $\xi_{\%crit}$ based on cyclic strain levels have been proposed. In this study the (Hardin & Drnevich, 1972) relationship (extended by (Santos & Correia, 2001) and (Benz, 2006)) as adapted in the Plaxis Hardening Soil small strain stiffness model is adopted. Additionally a comparison is made to Ishibashi and Zhang (Ishibashi & Zhang, 1993) who proposed expressions for G_s / G_0 and ξ as a function of plasticity index, confining pressure and shear strain. These curves have been adopted in the present study and are shown in the next figures for the three present soils.

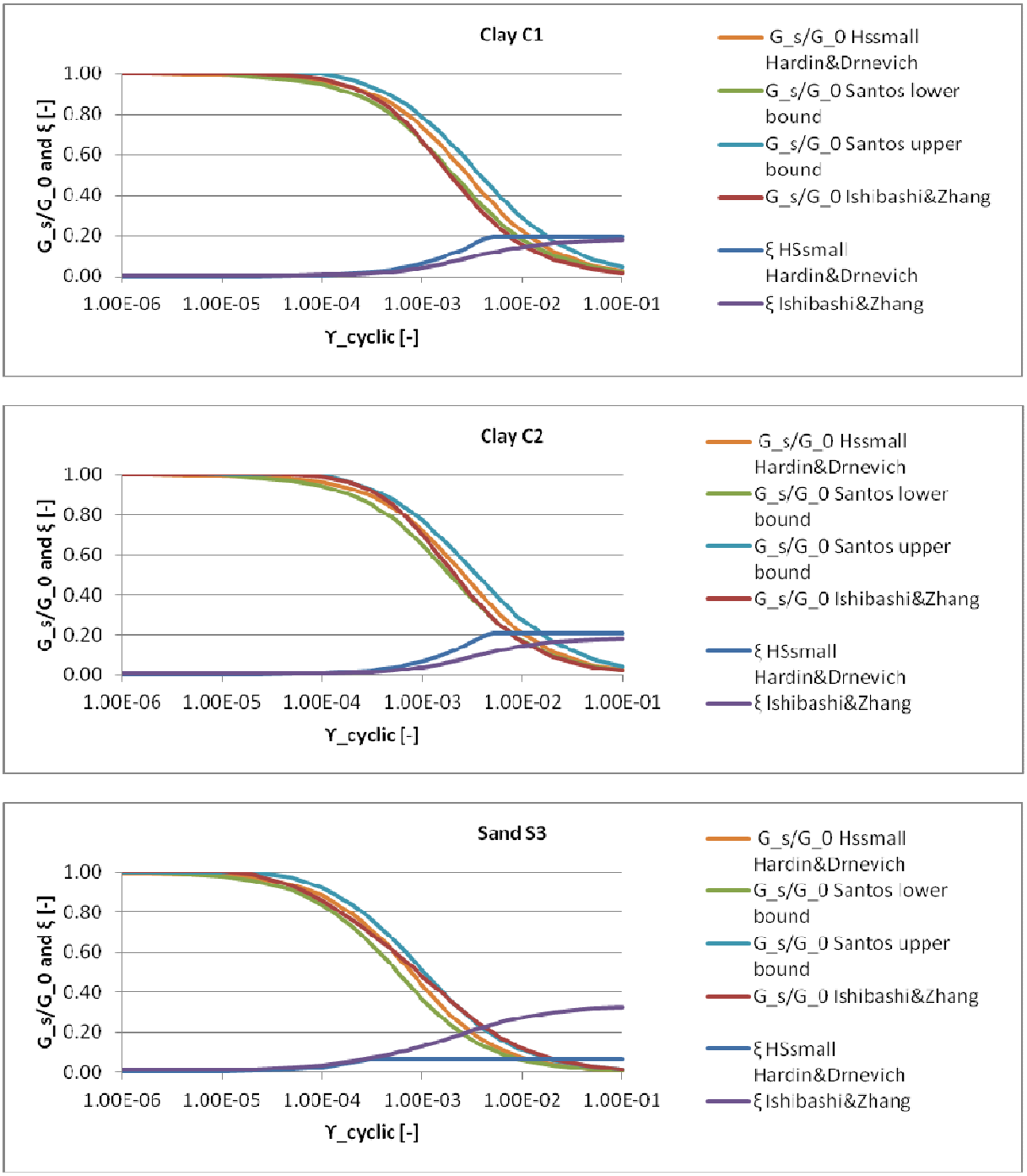

Figure 6.7: Shear strain related shear modulus reduction and damping characteristics note that cut-off $G_{t,small\ strain} > G_{ur}$ in the HSsmall model is not included in the graphs

The graphs show the good correspondence of the different modulus reduction curves. The HSsmall Hardin & Drnevich damping curves for clay seem to somewhat overestimate damping for high strain levels, as was also noted by Brinkgreve, Kappert and Bonnier (2007) (Brinkgreve et al., 2007). For qualification of the related error however actual strain levels are required, which will be point of attention in a later stage. The damping levels for the dense sand after Ishibashi and Zhang turn out to be much higher compared to the HSsmall model included damping. However, the very high damping levels based on PI=0 are not believed to be very accurate for dense sands (oral communication H.J. Lengkeek and D.J. Jaspers-Focks (2012)) and therefore will not be adopted.

6.4.3 Free field site response analysis by 1D Fourier frequency domain analysis

Fourier frequency domain analysis techniques for 1D site response are used in this study as a reference for numerical analysis. The conceptually linear frequency domain analysis for a multi-layered soil profile is enhanced with an iterative procedure to account for strain dependent stiffness and damping characteristics of the soil. Accuracy of this approximation is verified and conclusions are drawn regarding its usability for predicting site responses. As a reference for checking operation of (equivalent) linear multilayered response analysis, the Roesset approximation of the site amplification function (see paragraph 4.4.1.1) was adopted.

Equivalent linear site response analysis of a multi-layered soil profile is in this study coded in Matlab. The Matlab code for 1D analysis of vertically propagating shear waves through a multi-layered soil profile is based on theory as outlined in the book of Kramer (Kramer, 1996) and briefly summarized in paragraph 4.4.1.2. The Matlab script can be found in appendix VI

It is noted that the frequency domain analysis uses the Fast Fourier Transform algorithm, which is known to introduce errors in violating the response initial conditions because it is based on periodic responses. This effect is more pronounced for relatively short transient problems with low frequency content and short period of rest included at the end of the input signal (Chopra, 2001). The previous response period may then not be sufficiently damped out at the start of the considered response. If introduced errors are too significant, the input signal may be elongated or an improved Fourier method with corrective solution may be applied.

6.4.4 Free field site response analysis by Plaxis 2D/3D finite element analysis

Free field site response finite element analysis is in the present study performed in Plaxis 2D and 3D dynamic modules. The focus during the free field response analysis in Plaxis 2D is to determine the influence of boundary disturbances, the effects of model width, mesh size and the performance of Plaxis hardening soil models on site response. In this stage the model will be optimized with respect to these parameters. Subsequently equivalent Plaxis 3D free field analysis is performed which should conceptually give identical results. In order to have equivalent models in the 2D and 3D modules the following starting points are used:

- Standard viscous absorbent boundaries, and not the improved tied types of absorbent boundaries are used as a starting point since these are only available in Plaxis 2D and not in Plaxis 3D
- Absorbent boundaries are only applied at the x-min and x-max lateral boundaries. Along the y-min and y-max lateral boundaries in Plaxis 3D a plane strain boundary condition is assumed as it is in Plaxis 2D
- In both Plaxis 2D and 3D bedrock motions are only applied in x-direction. For the Plaxis 3D models the bedrock degrees of freedom in y-direction are fixed.

Since the Plaxis 3D dynamics module is very new, the quality of results from the 3D site response analysis is not very well established an in this study judged by comparison to the 2D equivalent model and the equivalent linear analytical solution. If based on this comparison the 3D model is believed to give proper results, it can be used to perform dynamic analysis of the coupled soil-structure system.

6.4.4.1 Mesh element size and critical time stepping

In order to allow for proper wave propagation in the FE model, the maximum element size is restricted according to Lysmer and Kuhlmeyer (Lysmer & Kuhlmeyer R.L., 1969) :

$$element\ size_{layer} \leq \frac{\lambda_{layer}}{5} = \frac{v_{s,layer}}{5 f_{\max}} \tag{6.1}$$

The stiffness dependency on stress level in the Hardening Soil material models results an actual very low stiffness level in the soil just below seabed level. As a consequence very small elements would be required in this region, which is computationally inconvenient. The maximum element sizes per layer are in this study determined based on the mid-layer stress levels as shown in Table 6.2.

The element size based on the very low shear wave velocity for clay C1 is very small and therefore will result extremely long required calculation time. Therefore it was investigated what would be the effects of a somewhat coarser mesh. The results are shown in paragraph 7.2.1.1.

Then, the maximum allowable time step is determined based on the well known Courant's condition, which restricts the time step by allowing a wave to not travel over more than one element length within a dynamic time step. The maximum time step herein is based on the compression wave velocity because wave reflections may result compression wave disturbances in the model that may not give spurious responses.

$$\frac{v_{c,layer}\Delta t}{element\ size_{layer}} \le 1 \rightarrow \Delta t_{\max} \le \frac{element\ size_{layer}}{v_{s,layer}\sqrt{\frac{2(1-\nu_{ur})}{(1-2\cdot\nu_{ur})}}} \tag{6.2}$$

Table 6.2: Finite element sizes and dynamic time steps

Parameter		Clay C1	Clay C2	Sand S3
Lower limit parameters for LE and MC soil models				
$v_{s,ur}$	[m/s^2]	31	53	236
$element\ size_{layer}$	[m]	0.41	0.71	3.14
Upper limit parameters HSsmall soil model				
$v_{s,o}$	[m/s^2]	82	144	317
$element\ size_{layer}$	[m]	1.09	1.92	4.22
$element\ size_{layer,applied}$	[m]	1.00	1.30	1.80
$\Delta t_{Courant,LE}$		0.016	0.012	0.004
$\Delta t_{Courant,HSsmall}$		0.006	0.004	0.003

Compared to the rule of thumb that $dt < 0.1T_{highest\,mode} = 0.1/\,f_{highest\,mode} = 1/15 = 0.066$, the dynamic time steps in Table 6.2 can be considered sufficiently small.

It is noted that the default number of required substeps provided by Plaxis is much higher when undrained analysis is applied for soil. This is explained by Plaxis calculating the number of steps required based on compression wave velocities that tend to infinity when Poisson's ratio approaches 0.5 as is included in Plaxis for undrained conditions.

6.4.4.2 Finite element model width

The required model width is determined based on free field analysis for both the two selected Harmonic signals and the Duzce natural seismic bedrock signal. Criteria used for determination of required model width are:

- Convergence of horizontal accelerations at the centre of the model with the 1D frequency domain solution
- Limited amplitude of vertical oscillations at seabed level in the centre area of the finite element model, which are resulting from wave reflections at boundaries.

In Plaxis analyses for validation of the required model width, linear elastic material will be adopted for computational convenience and because plasticity effects will only further limit boundary effects. An linear elastic stiffness will be estimated based on equivalent linear frequency domain analysis. 5% critical Rayleigh viscous damping will be adopted. This will give a conservative approximation of the required model width, since actual soil damping during moderate to high intensity earthquakes will generally be higher, at least for soft soil conditions.

6.5 Dynamic analysis of jetty on nonlinear Winkler foundation for support node motions resulting from free field analysis

In this stage the "structural engineering" approach for dynamic analysis of the jetty structure vibrations in transverse direction is followed. The response of the structure to motions applied to the Winkler support nodes will be calculated with finite element code Seismostruct, as indicated in Figure 6.8.

The motions applied to the Winkler support nodes are inputted as acceleration time histories, resulting from equivalent linear site response analysis in the frequency domain, which results the essentially uncoupled response analysis of site and structure. It is chosen to use site response results from frequency domain analysis because this approach is attractive for its low computational effort and reasonable results for a cases where a 1D approximation of the site is acceptable. By this means a method completely parallel to the computationally demanding Plaxis finite element analysis will be developed. Additionally, to be able to make proper comparison, also the response of the Winkler jetty model for ground motions obtained from Hardening soil finite element site analysis was performed. The performance of both methodologies will be resulting from this study.

The Winkler discrete p-y springs applied in the model are identical to the static p-y springs (see appendix III), where additional dynamic "stiffness" is provided by viscous dampers added parallel to the p-y springs (see appendix III). Jetty rocking effects introduce axial pile loads although loading will essentially be horizontal. Accordingly axial pile impedances have been defined, where they are for simplicity linearized at the initial stiffness according to ISO 19902 chapter 17 recommendations. For the resulting axial stiffness developing with depth, one is referred to appendix III.

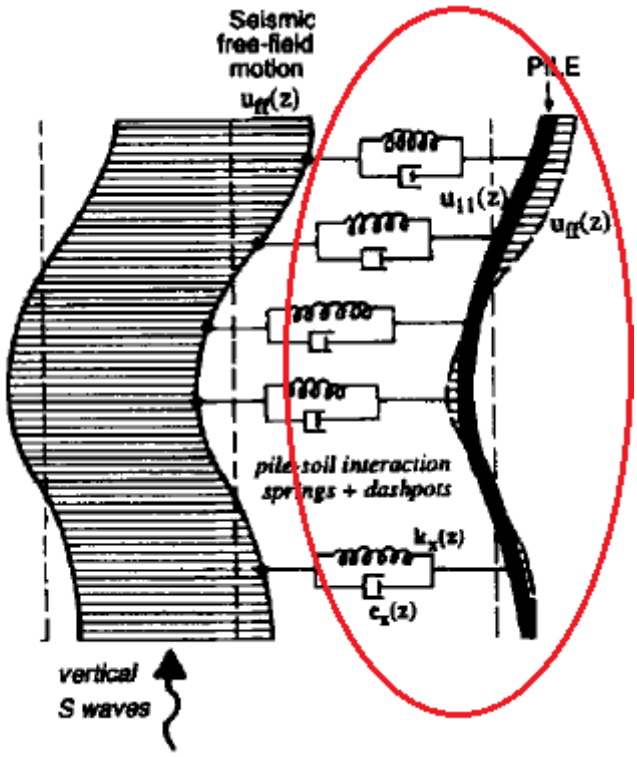

Figure 6.8: Structural model of pile/jetty supported by Winkler p-y springs + dashpots

The properties of these dashpots will be defined according to the simplified dashpot coefficients that account for both material damping at the interface and radiation damping in the far field, as obtained from literature and presented in paragraph 4.6.3.6. The viscous dampers parallel to the static p-y springs can in Seismostruct only be implemented in the stiffness proportional Rayleigh damping format, resulting essentially frequency dependent damping. This may be assumed reasonable for the radiation damping contribution, but seems unreasonable for the material damping part dominated by hysteretic behaviour. In order to have a best-estimate damping included in the mathematical dynamic model, it will be fitted at the fundamental frequency of the structure, that is determined by modal analysis of the system with initial soil stiffness springs included. The re-

sulting damping modal damping ratios consequently will be higher for the higher frequency range and lower for frequencies below the structures fundamental frequency. Structure damping is assumed to have value of 5% critical, which may be assumed conservative for strong level earthquakes. As in Plaxis dynamic analysis a Hilbert-Hughes-Taylor numerically damped time integration scheme with dissipation parameter $\alpha = 0.1$ will be adopted in dynamic Winkler analysis.

As for Plaxis analysis, geometrical nonlinearities will not be included in the Seismostruct Winkler model analysis. As a result second order effects will be neglected. According to Priestley (2007) second order effects significance may be assessed by an stability index obtained from drifts, vertical loads and maximum allowable bending moments:

$$\theta_{\Delta} = \frac{P\Delta}{M_d} \tag{6.3}$$

Where for steel structures a limit value of 0.05 is proposed. Verification of this criterion for the jetty structure considered results a maximum allowable drift based on this stability index that exceeds the drift at onset of in-ground plastic hinging. Hence the prevention of in-ground plastic pile hinging is governing and the P-Δ effects are not further considered.

The focus in jetty response analysis from the beam on Winkler foundation models will be on:

- Acceleration response in time and frequency domain
- Dynamic peak displacements and (if soil plasticity included) residual displacements
- Pile bending moments and plastic hinging
- Frequency domain representation of soil-structure interaction effects

The obtained response will be compared to the results from simplified dynamic analysis and the results from coupled 3D Plaxis dynamic soil deposit + jetty structure analysis.

6.6 Coupled transverse dynamic analysis of a slice soil deposit and jetty structure

In this final stage of the study, coupled dynamic analysis of soil deposit overlying engineering bedrock and the jetty structure is performed.

The bedrock seismic input signals applied to the coupled models are the Duzce and Kocaeli2 recorded accelerograms in accordance with paragraph 6.4.1, where bedrock peak accelerations are adopted following from the probabilistic seismic hazard assessment (see paragraph 5.2):

- $a_{g,peak\ bedrock}$ = 0.70 g with probability of exceedance 10% in 50 years
- $a_{g,peak\ bedrock}$ = 1.02 g with probability of exceedance 2% in 50 years

A plane strain 3D finite element model of a slice of the soil deposit including a section of the jetty in transverse direction is defined. The soil deposit model is defined based on the calibrated model resulting from free field site response analysis. Nonlinear time history analysis is performed with a damped HHT-Newmark time integration scheme having dissipation parameter $\alpha = 0.1$.

The jetty structure is modelled essentially elastic, where predefined plastic hinges are included at the pile-deck connection locations according to paragraph 5.5. Possible in ground plastic hinging of the piles is not included in the models, where this may be justified since from reparability and post-earthquake investigation requirements plastic hinging at these locations has to be prevented.

The focus in jetty response analysis from these coupled models will be on:

- Acceleration response in time and frequency domain
- Dynamic peak displacements and (if soil plasticity included) residual displacements
- Pile bending moments and plastic hinging
- Frequency domain representation of soil-structure interaction effects
- Soil failure

A comparison of the obtained response to responses found from simplified dynamic and uncoupled dynamic design procedures will be made with respect to these response measures.

7 Results

7.1 Nonlinear Pushover Analysis

In this paragraph the pushover analysis results of the Winkler and continuum models are presented and discussed. Initially the load deformation characteristics are determined for a pile loaded at the pile head. Subsequently the load deformation characteristics related to the vectorial inertia load pattern based on the systems eigen frequencies are determined, as is common to form the input for the simplified dynamic analysis procedure.

7.1.1 Pushover Analysis on 2D wall models compared to Winkler pile models

Figure 7.1, Figure 7.2 and Figure 7.3 show the head load-displacement characteristics of the single pile supported by discrete p-y springs and equivalent walls ($EI_{wall} = EI_{pile}$) embedded in a soil continuum, for a free head and a pile head fixed for rotations (as in a jetty structure) respectively.

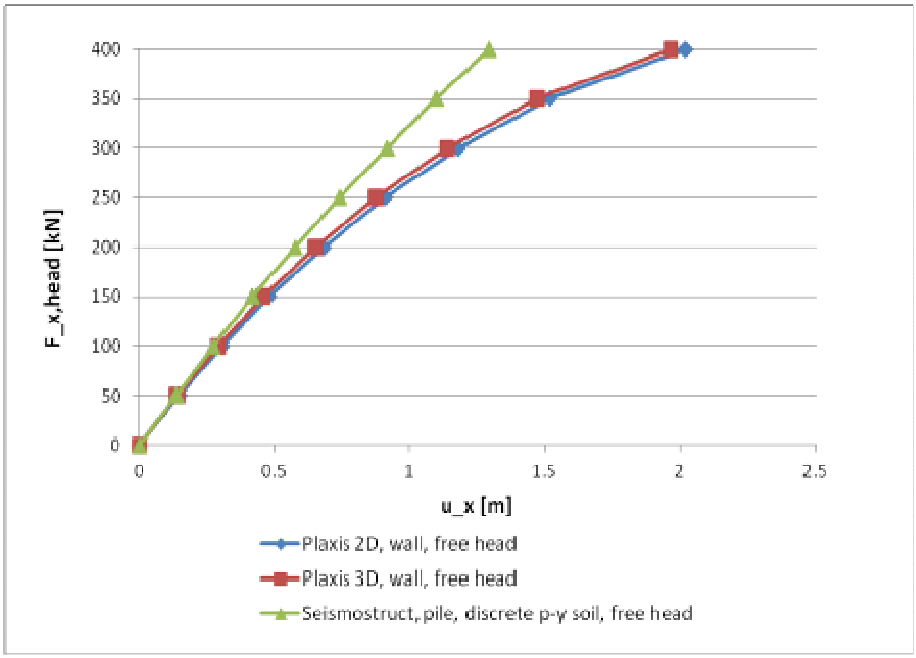

Figure 7.1: Wall/pile (free head) head displacement $u_{x,head}$

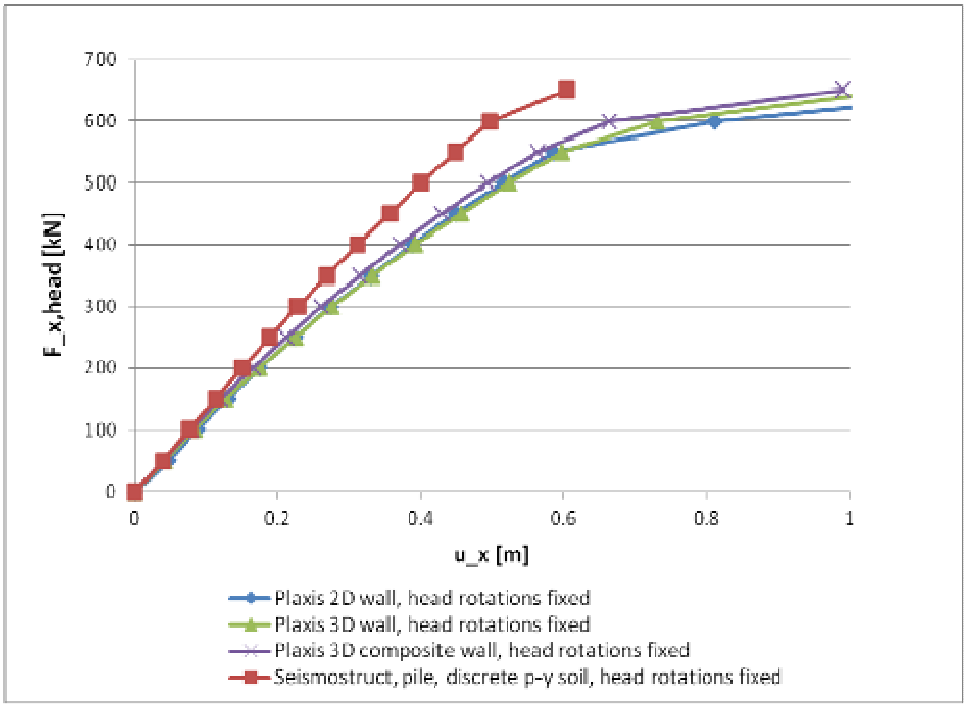

Figure 7.2: Wall/pile (head fixity) head displacements $u_{x,head}$

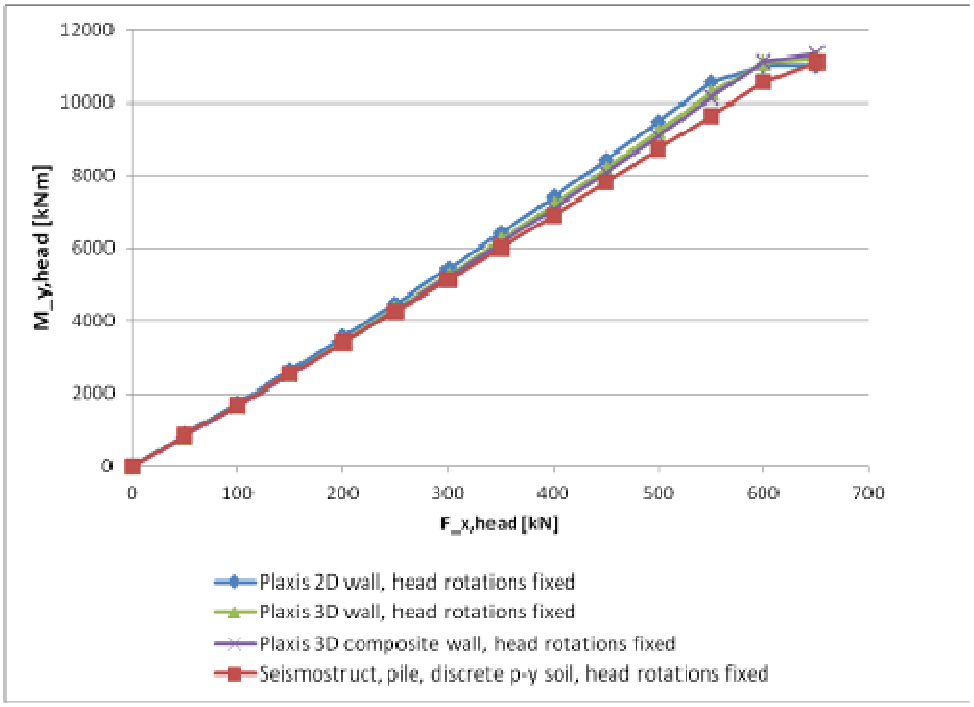

Figure 7.3: Wall/pile (head fixity) head bending moments $M_{y,head}$

The results show the initial stiffness to be in good agreement. Moreover, also the ultimate resistance seems to correspond relatively well, but the overall stiffness of the pile supported by discrete Winkler p-y springs is higher. This conclusion may be explained by the wall configuration excluding load spreading/arching effects in the soil, where for a pile arching effects in the soil decrease effective material stresses and therefore increase the system stiffness. The results show the response of the Plaxis 2D models to be slightly more flexible than the Plaxis 3D models. This can be explained by the higher order elements used in Plaxis 2D, resulting is a slightly more flexible model. Focussing on the composite wall section built from a plate surrounded by a solid, one may conclude that the behaviour is very close to the behaviour of the equivalent plate. An additional check on the proper operation of the composite pile was performed by giving the soil an extemely high stiffness, which gives

us the pile fixed for translations and rotations at seabed level, which is a case that can easily be checked by the solution known from elementary mechanics.

In Plaxis 3D, elasto-plasticity for plates is not available, hence an artificial fixation by means of elastic and elasto-plastic fixed-end anchors was constructed. The proper operation of this solution is proved by the almost identical load-deformation characteristics and head bending moment development of the Plaxis 2D and Plaxis 3D models as is shown in figures Figure 7.2 and Figure 7.3. Nevertheless for performance based seismic design purposes the lacking of elasto-plastic plates in Plaxis is a real shortcoming for desiging engineers, and is strongly recommended for future improvement of the software.

7.1.2 Pushover analysis on 3D single pile models

7.1.2.1 Pushover analysis with derived Hardening soil parameters

For the jetty geometry with pile diameter D=1.4m and a side-side pile spacing of 6m, a 3D soil model width for a half-pile model of 3m was adopted. Figure 7.4 shows the pushover characteristics (represented by top displacement and head bending moment development) of the physical 3D pile models in Plaxis 3D, compared to the discrete Matlock p-y spring models. In contradiction to the wall models discussed previously, in the 3D pile models, spreading/arching effects in the soil are included resulting a more stiff response compared to the previously treated wall models.

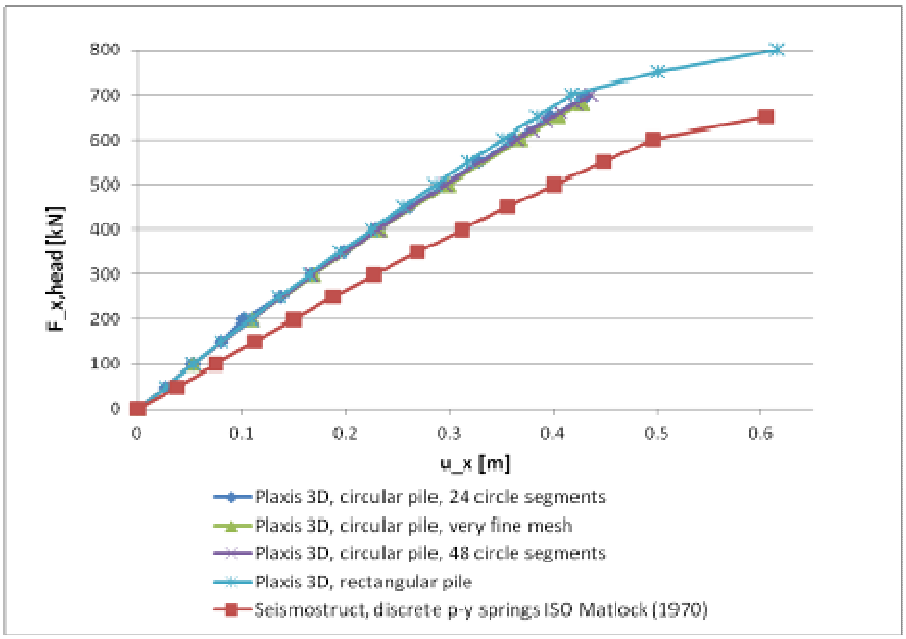

Figure 7.4: Pile head displacement $u_{x,head}$ for various pile configurations in Plaxis 3D, compared to pile on Winkler nonlinear supports

More stiff behaviour results, and ultimate lateral resistance of the pile in these 3D models is also higher. To exclude these deviations to be related the finite element mesh configuration, sensitivity of mesh coarseness and operation of the circular shaped pile are studied by enhancing mesh quality of the circular pile and calculating the response for an equivalent rectangular pile. The load-displacement results (see Figure 7.4) prove the to be almost insensitive to model refinements, although mesh quality as indicated by Plaxis was improved significantly. A similar insensitivity was found for resulting pile head bending moments.

Inclusion of the interface provided some additional flexibility in the Plaxis models, but these effects are minimized by the program, that determines an optimum between reducing flexibility and preventing ill-conditioning of het stiffness matrix. However, physical background for the additional flexibility is lacking, since the interface in the models essentially is a numerical tool. The pile soil interface in Plaxis was modelled as a rigid interface. Reducing the interface strength parameter R_{inter} would increase displacements, since more plasticity at the interface would occur. At the front of the loaded pile this would be nonsense. At the backside

of the pile it might be a tool to include gapping, but this turned out to have hardly any effect on global pile response since very similar pushover response curves resulted. Hence the interface properties are kept default in order to not converge results of the Plaxis 3D models by just adapting a model parameter without physical background.

Based on the observations presented above, one may conclude that the stiffer behaviour obtained from Plaxis 3D is a result of the actual behaviour of the Hardening Soil model. Since Matlock p-y expressions are empirically derived, one would not expect such significant deviations to be found from models in which the soil is represented by the advanced Plaxis Hardening soil model, although some deviations obviously may be expected. Hence the Plaxis 3D models need to be validated more precisely in order to be able to judge their accuracy.

Parameters included in this sensitivity analysis are:

- Plaxis undrained analysis type A (effective stiffness / effective strength parameters) or B (effective stiffness / undrained shear strength parameters)
- Undrained vs. consolidation analysis for clay
- Over-consolidation of soil layers
- Soil stiffness parameters

Results of variations in these parameters to structural response are discussed next.

7.1.2.2 The type of undrained analysis in Plaxis 3D

Initially, for het clay layers in the model, undrained analysis type A was selected because of generally better performance of this type of analysis compared to type B undrained analysis. In type A analysis the effective soil parameters have to be entered, the program subsequently determines the undrained soil behaviour based on these parameters and the pore pressure generation. Undrained shear strength for these models is a function of stress state as was already included in the Plaxis Soil Test verifications for the selected parameters.

Since results now seem to deviate significantly from the Winkler p-y curve model resuls, it is investigated whether these deviations may be introduced by the undrained analysis type in Plaxis 3D. The soil undrained type of analysis for the clays is set to B, where it should be realized that this removes the stress dependency of stiffness from the constitutive model and hence actual parameters should be applied. Undrained shear strength increasing with depth, identical as used for Matlock p-y expressions is included. The load deformation results of this model results the following conclusions:

- Stiffness is not affected, indicating no significant deviations in plasticity development for the lower loading range and therefore a proper stress-state dependent inclusion of the undrained shear strength in the undrained type A soil models.
- Model stability is worse for undrained type B analysis of the clay layers, since no equilibrium can be found starting already from relatively low load levels. Plaxis 3D indicates that the soil body collapses which may be doubted, since method A is able to find equilibrium for higher loads.

7.1.2.3 Undrained or consolidation analysis for the clay layers

Initially plastic undrained analysis of clay layers was assumed, because Matlock (1970) p-y expressions were derived for short term loading. Plastic undrained analysis however is equivalent to infinitely short time steps, which is different from the short time steps in experiments. In order to include effects of this finite time (slight consolidation possible) in the pushover models, the analysis type is set to consolidation analysis. The permeability coefficients as derived by the soil parameter selection sheet (Appendix II) are used:

Table 7.1: Clay permeability parameters

Soil layer	k_h [m/s]	k_v [m/s]
Clay C1	7.5e-10	5e-10
Clay C2	3e-10	2e-10

The intermediate time step for subsequent loading stages is taken 10 sec, which combined with low permeability for clay will hardly result any consolidation, as is the case for the short term behaviour considered.

Results of the short term consolidation pushover analysis are presented in Figure 7.5, where they are plotted together with the load-displacement characteristics of the model with undrained constitutive clay material behaviour and the discrete p-y soil model.

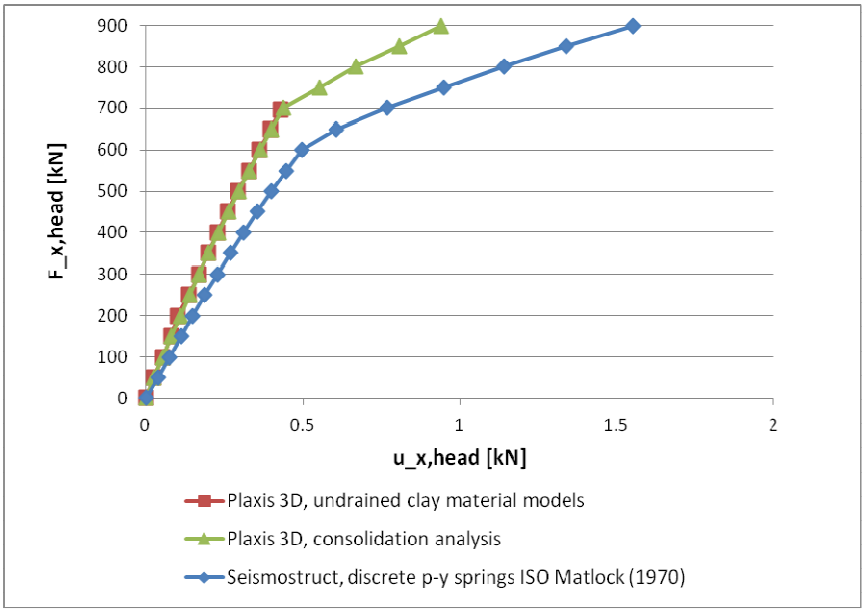

Figure 7.5: Pile head displacement $u_{x,head}$ for different Plaxis undrained analysis types

Figure 7.5 results two conclusions:

- Accepting limited consolidation for the clay material does not affect the global response characteristics of the pile-soil system
- The consolidation analysis model in Plaxis 3D is more stable for tracing the load-displacement path beyond onset of plastic hinging at the pile head, were a sudden change in soil state will result. A closed explanation for this remarkable observation has not been found, but it appears to be related to local instability resulting an unacceptable error and therefore no convergence of the finite element solution. The ability of tracing the load displacement path in the very nonlinear range is interesting from the displacement based design perspective, where ductility of the system has to be proved. It is therefore recommended to improve the stability of plastic analysis in Plaxis.

7.1.2.4 Overconsolidation of the soft soil layers

Based on correlations with unit weight, void ratio and undrained shear strength, the clay layers present appear to be slightly over-consolidated. Consequently an OCR of 1.5 was adopted in the models. However, for clay it is known that OCR values based on these correlations may actually not be observed if aging effects can also affect soil properties like water content and plasticity index. For the slightly over-consolidated parameters, the constitutive behaviour of the soil according to the Hardening Soil model, is dominated by the more stiff elastic unload/reload behaviour. The p-y expressions according to Matlock were derived for normally consolidated or slightly over-consolidated soft clays. Although an OCR equal to 1.5 is relatively low, its effects on global structural response are considered in this study. Material parameters for both clay layers were set to normally consolidated and effect is presented in Figure 7.6.

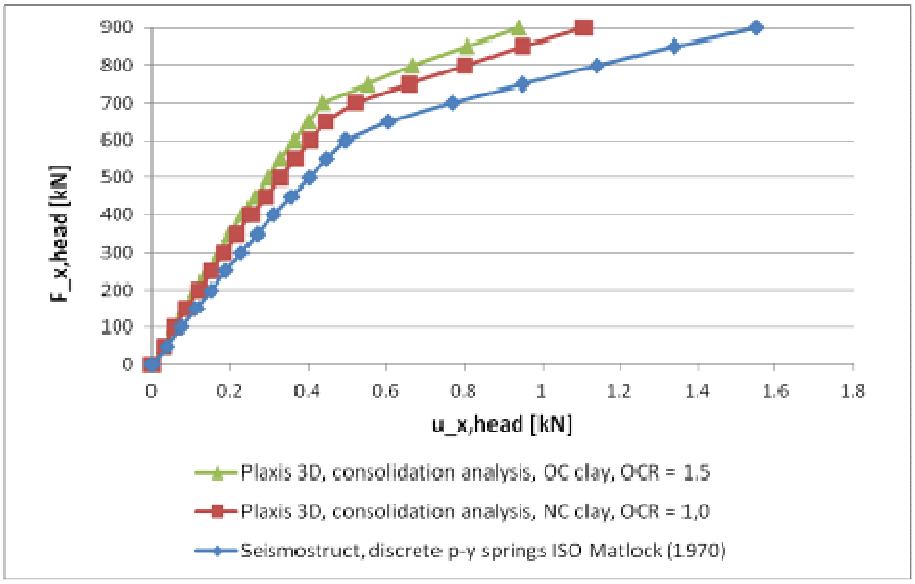

Figure 7.6: Sensitivity of pushover curve to clay over-consolidation

The figure shows the influence of the over-consolidation on global pushover response characteristics. The following conclusion can be drawn:

- The effects of over-consolidation are clear, but can be considered relatively limited. Stiffness decrease is in the order of a 10% for the normally consolidated compared to the over-consolidated (OCR = 1.5) clay material state.

This can be explained by Figure 7.7, that shows the very local concentration of stresses, that exceed the pre-consolidation pressure already for relatively low lateral loads at the pile head. Beyond the pre-consolidation pressure the soil material stiffness decreases, resulting an increasing contribution of local normally consolidated soil state to the global lateral pile response.

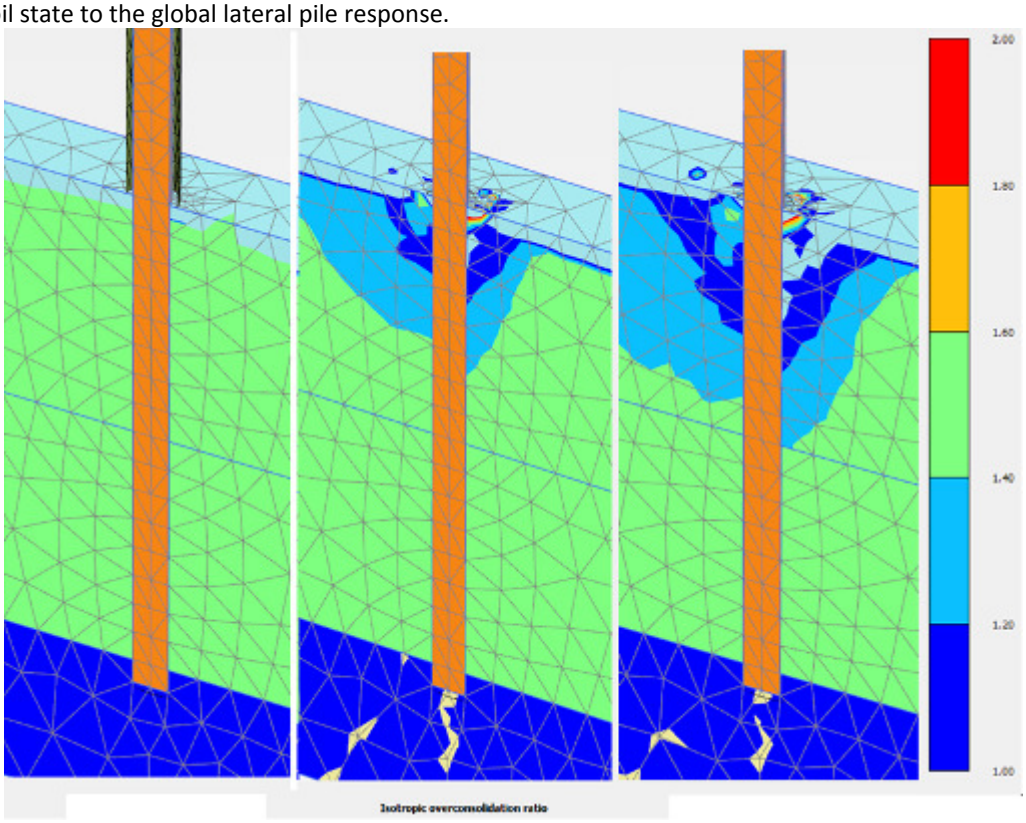

Figure 7.7: Overconsolidation ratio development for increasing lateral pile loads (0, 100, 200 kN/pile)

It is noted that the change from over-consolidated soil state to normally consolidated soil state reduces the effective undrained shear strength, which is a function of local stress state, as can be observed from tri-axial tests. In this sense it is inconsistent to compare the Plaxis 3D outcome of models with normally consolidated clay to the p-y models that are based on c_u values for the slightly over-consolidated clays.

7.1.2.5 Soil stiffness parameters

Soil stiffness parameters initially included in the models are best estimates based on available soil data and correlations from literature. Nevertheless, stiffness parameters for clay are in general very difficult to classify when limited soil survey is available. Even stiffness parameters resulting from tests always should be treated carefully, as the handling of the soil may significantly disturb local stress state and especially soil stiffness parameters. As a result, it is common in geotechnical engineering to multiply/divide soil stiffness parameters by a factor 2 in order to establish sensitivity of the analysis to variations in these stiffness parameters.

In the present study, the soil stiffness parameters are divided by a factor 2, in order to investigate whether this may reduce global stiffness towards the lower stiffness as is observed for pile models with soil represented by the Matlock p-y expressions. The results are shown in Figure 7.8

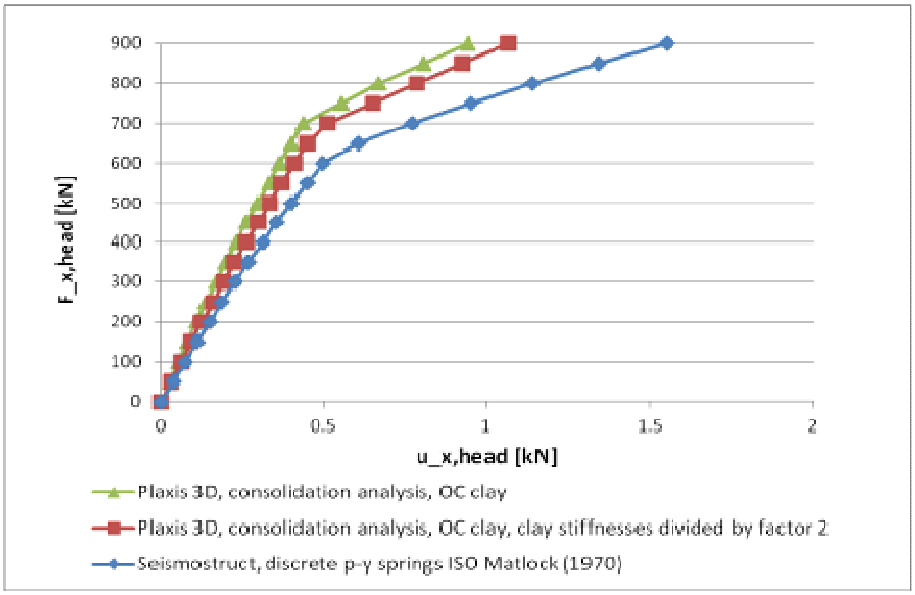

Figure 7.8: Sensitivity of pushover curve to clay stiffness variations

Based on Figure 7.8 the following may be concluded:

- The reduction of initial stiffness for the global pile-soil system is order 10%, which is much lower than the soil stiffness reduction of 50%. Hence, the soil response seems to be strongly affected by local plasticity in the soil adjacent to the pile and stiffness dependent deformations of a larger soil body seems to have a minor effect. The reduction percentage is comparable to the initial stiffness reduction resulting if the clay layers are given a normally consolidated state.
- Even when the best-estimate stiffness parameters are reduced by a factor 2, the global response is more stiff than the response obtained from the pile-Winkler p-y soil models.

7.1.2.6 P-y expressions for the discrete Winkler foundation after Jeanjean. (2009)

Based on the previous considerations, a more stiff response is obtained for the Plaxis 3D pile soil models compared to the models with discrete p-y soft clay soil after Matlock, irrespective of any reasonable variations in soil parameters in the Plaxis 3D models. Consequently it is doubted whether Matlock's p-y expressions are representative for soft clays.

Although Matlock's expressions are most commonly applied in design, several studies (Martin & Randolph, 2006; Jeanjean, 2009) have shown that they may generally be too conservative. Alternative p-y expressions with test verification have been proposed, of which the data sets from Jeanjean (2009) fit best to the case con-

sidered in this study, in which soil response is dominated by the very soft to soft clay deposits. Jeanjean (2009) proposes p-y expressions that fit in the equation of (O'Neill, Reese, & Cox, 1990):

$$p = p_u \tanh\left(\frac{G_0}{100 c_u}\left(\frac{y}{D}\right)^{0.5}\right) \tag{7.1}$$

Where:

$$p_u = N_p c_u$$

$$N_p = 12 - 4e^{\left(\frac{-\xi z}{D}\right)}$$

$$\xi = \begin{cases} 0.25 + 0.05\lambda \,(for\ \lambda < 6) \\ 0.55 \,(for\ \lambda \geq 6) \end{cases}$$

$$\lambda = \frac{c_{u,seabed}}{c_{u,incr} D}$$

Where p_u is a function of undrained shear strength, pile diameter and depth.
Jeanjean showed in his study that the Matlock p-y expressions are significantly underestimating both modulus and ultimate resistance of soft clay soil. The tests performed by Jeanjean to verified the proposed p-y expressions were performed on a 1:48 scale, which might be a source for deviations when using these expressions for big diameter piles.

As for the Matlock (1970) p-y expressions, the actual p-y curves according to Jeanjean as a function of depth and estimated soil parameters are determined in Excel (Appendix III) Again for practical convenience bilinear fittings were sought, which subsequently were adopted in the Seismostruct pushover analysis.

The global response results are presented in Figure 7.9.

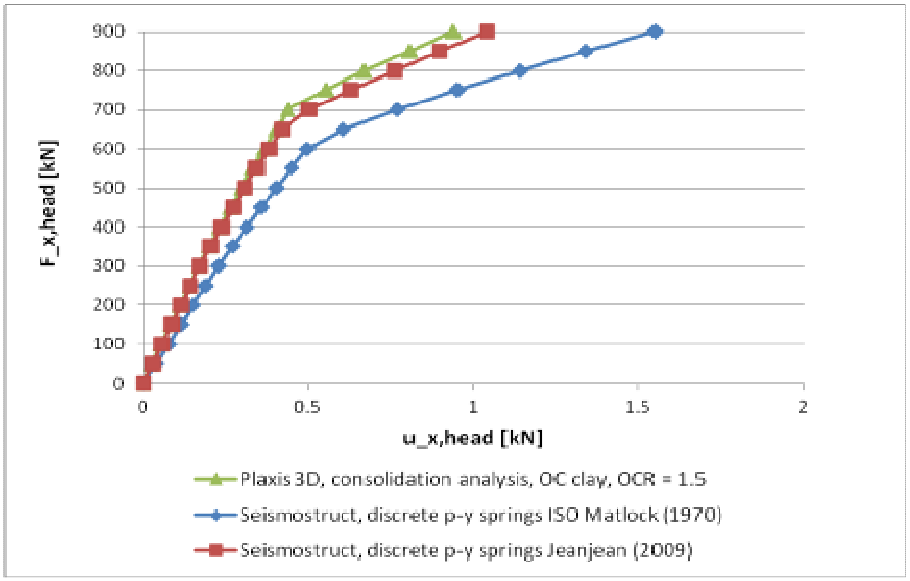

Figure 7.9: Performance of conventional Matlock (1970) p-y curves and recently developed Jeanjean (2009) p-y curves for soft clay compared to 3D Plaxis modelling

As shown in the figure, the Plaxis 3D model and Seismostruct model with Jeanjean p-y springs result global lateral pile responses that are very similar. In order to further investigate the local soil actions on the pile for both models, the development of bending moment along the pile are plotted in Figure 7.10

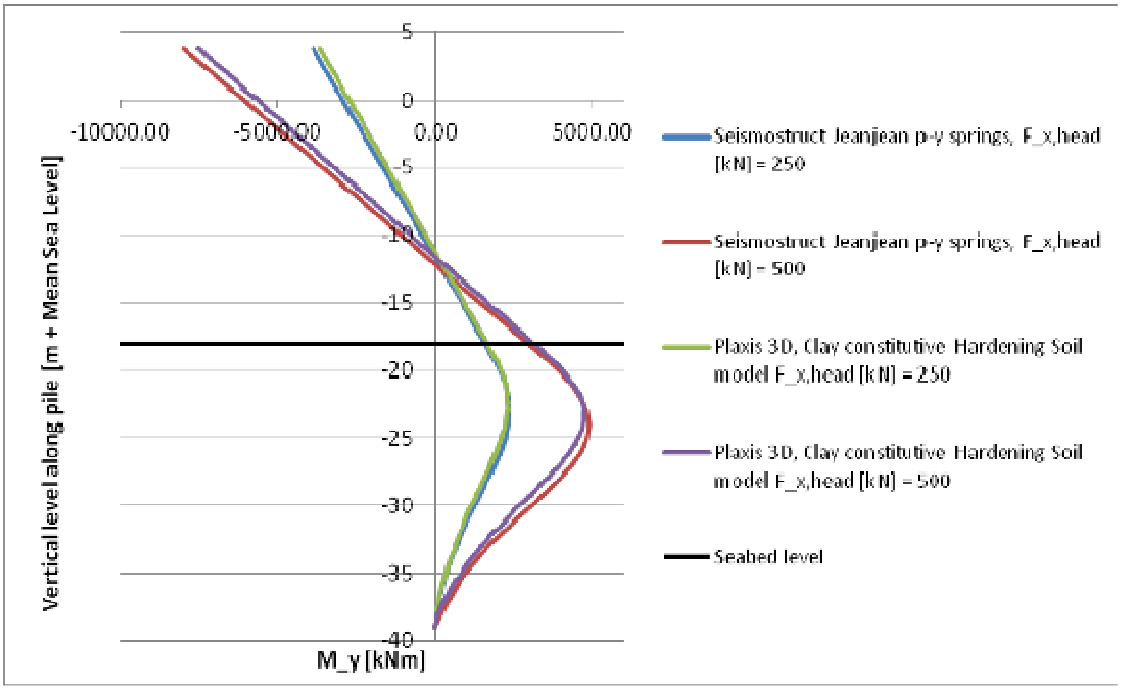

Figure 7.10: Local bending moment along pile for discrete nonlinear Winkler pile model and Plaxis 3D pile model

The conclusions that can be drawn from Figure 7.9 and Figure 7.10 are:

- The global response resulting from the model with p-y soil after Jeanjean (2009) fits well to the global pushover response obtained from the Plaxis 3D model with the soil parameters most likely based on the parameter sheet.
- The local soil actions on the pile resulting from the Plaxis 3D analysis fit to the local soil actions of the Jeanjean p-y springs, providing confidence in accuracy of both analysis. Only slight deviations in soil response are found for the deeper clay layers, that in the Plaxis 3D model behave slightly more stiff, resulting in a stronger decrease om the pile bending moment with depth in these soil layers.
- The gradient of the bending moment line near pile tip level is relatively low, especially for the lower loading. Consequenly shear force in the pile is low at this level, indicating the limited influence of the presence of the stiff sand layer on lateral pile response. This was also to be expected based on the medium-long characterisation of the pile ($\lambda = (k_{secant,soil}/EI_{pile})^{0.25}$) according to the beam on winkler foundation concept, which implies that the tip boundary condition is of limited importance for pile head response and the lateral pile behaviour to be governed by the soil response in the top soil layers.
- Although most common and adopted in API and ISO design guidelines, Matlock p-y expressions (as also reported in literature) appear to be too conservative.
- The p-y expressoins after Jeanjean give approximately similar response as the Plaxis 3D model with the advance hardening soil model. This supports the Jeanjean expressions to give reasonable results, even when extrapolated to diameters much bigger than the diameters used in the tests performed by Jeanjean that are at the basis of the proposed p-y expressions.
- Based on Jeanjean (2009) and the present study, it seems reasonable to use the Jeanjean p-y expressions for future design applications. However, despite the good fit for the current project, verification by a Plaxis 3D analysis is to be recommended because of the well known limitations of the Winkler model concept. In this study p-y expressions according to Jeanjean will be adopted. Dynamic stiffness multipliers according to El Naggar and Bentley (2000) will not be applied in dynamic analysis, since they were derived for the much more flexible Matlock static p-y springs and consequently may lead to an overestimation of dynamic stiffness.
- Despite the locally nonlinear soil response as present in the analysis, global soil response is almost linear. Consequently also structure global response is approximately linear up to the onset of plastic hinging at the pile head. Then in the second branch up to failure, again almost linear behaviour is obtained. Consequently, an equivalent linear system may be determined for calculating response of pile-soil systems for low level earthquakes, however for higher intensity earthquakes structural

nonlinearities and soil failure are expected to have a pronounced effect on the response and should be included in the analysis.

- The bilinear elastic - perfect plastic approximation of global system response as proposed in the Fajfar (1999) simplified dynamic analysis method does not account for post-yield hardening in the system, which based on the pushover results seems to give a conservative approach for the pile-soil system that shows significant increase of resistance (±40%) in the "post-yield" branch.

7.1.3 Linearization of pile-soil interaction

The approximate bilinear load deformation relationship as is obtained from Figure 7.9 for both the discrete Winkler p-y model and the finite element continuum model imply that the system behaves almost linear for lateral loads that are below the load level corresponding to onset of plastic hinging in the pile. Despite the very local nonlinear characteristics of the soil structure interaction, it must be concluded that averaging over the pile length results an approximately linear system. This important conclusion can be used for calculating pile-responses for low level earthquakes by means of linear dynamic methods which is very beneficial from computational point of view. From this conclusion the question arises which lateral pile-soil spring stiffness to apply in linear models. Lateral pile deformations (except from the very top part of the pile) remain relatively low up to onset of plastic hinging. Hence it seems reasonable to adapt the upper bound initial bilinear spring stiffness (which was used as an approximation of actual p-y curves) for linear low load level calculations. The result is shown in Figure 7.11.

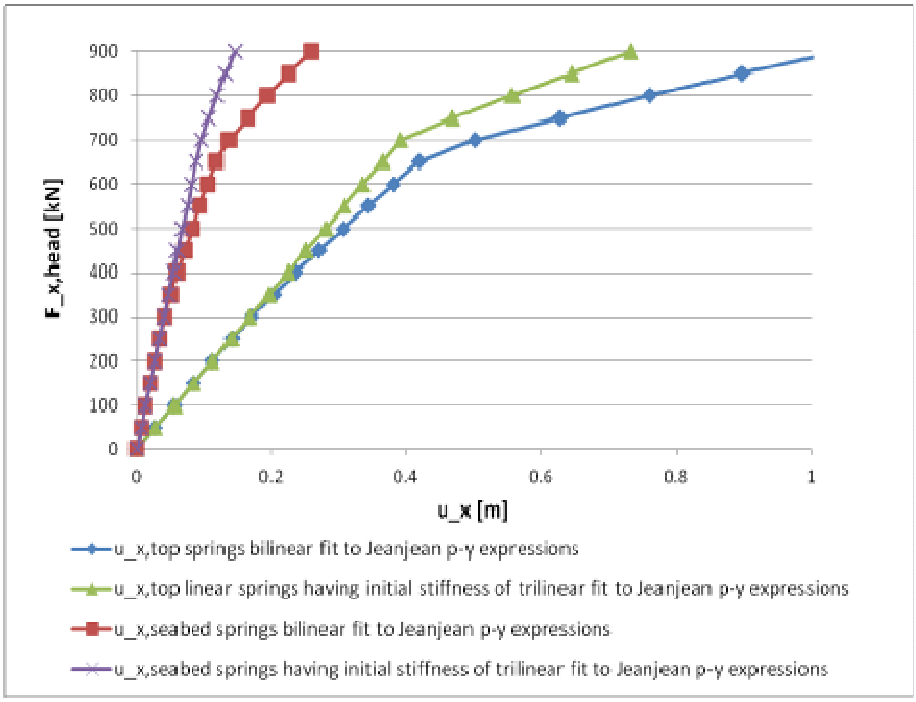

Figure 7.11: Effect of linearized soil springs on lateral pile response

A slightly stiffer response is obtained from the linear springs, but it may be concluded that a good approximation of global lateral pile response can be found by the linear approximation up to the load level corresponding to the onset of pile plastic hinging. However for high level earthquakes, according to performance based design principles, deformation capacity of the structure should be used to dissipate energy. As a consequence for high level earthquake design a nonlinear system should be considered.

7.1.4 Equivalent Plaxis 2D model to represent lateral single pile response

In order to study the arching/spreading effects in Plaxis, Plaxis 3D analyses with models of different width have been performed, implying a pile having a particular side-side spacing from adjacent piles.
The results are shown in Figure 7.12

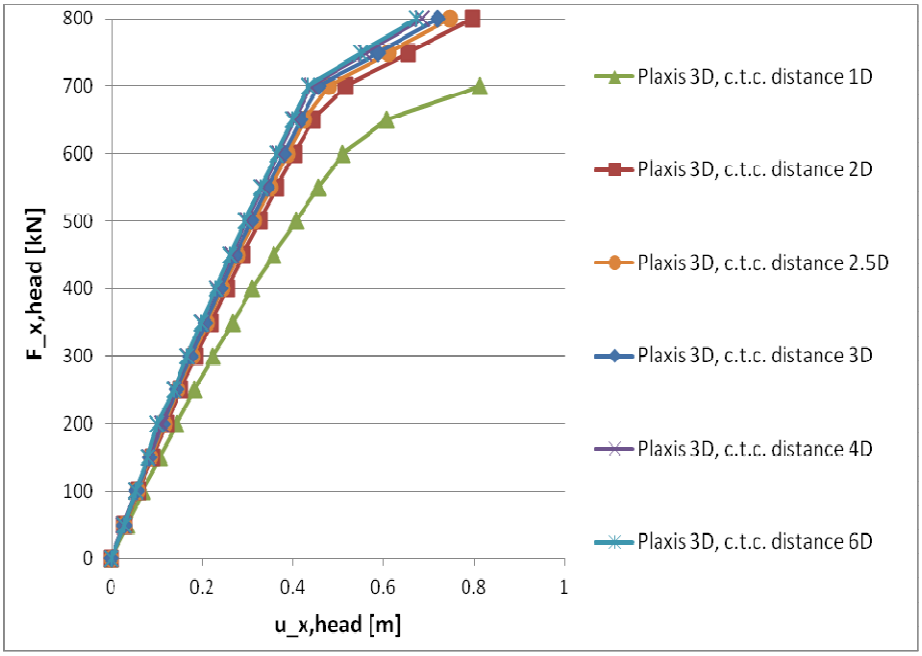

Figure 7.12: Lateral pile response sensitivity to pile side-side c.t.c. spacing

Figure 7.12 shows that based on the Plaxis 3D analyses, no efficiency reduction for side-side spaced piles has to be expected in the soft soil conditions for a pile spacing exceeding 2.5D, and hardly any reduction is observed already beyond a spacing of 2D.

According to paragraph 4.6.3.9 and the Plaxis 3D and 2D results regarding the influence of side-side pile spacing one may conclude the following:

- Performing 2D analysis on a pile (wall) model having the actual pile stiffness and a soil slice width of 1m, underestimates the stiffness and capacity of the soil when the pile spacing exceeds 1D.
- As a consequence one needs to adapt pile or soil properties in order to have a proper relative stiffness distribution in the model.
- Adapting the soil parameters is not very straight-forward, since both stiffness and strength properties of the soil in the hardening soil model will affect global strength and stiffness properties of the system in a truly non-trivial way.
- Consequently the best options available seems to reduce the pile stiffness properties and the lateral load (pushover forces as mass times acceleration), and then soil properties can remain unchanged. It is noted that this approach may be suitable for pushover analysis and dynamic analysis of head loaded piles (or inertial pile loading). It however will not be convenient for dynamic analysis of soil deposit + structure, where lateral pile load cannot be reduced since it is formed by kinematic pile loading of soil deposit responses for an applied bedrock signal.

The following figure shows the load deformation characteristic of a single pile, loaded by a lateral concentrated load at the head. From the figure one may conclude that reasonably well estimates of the actual (3D) pile behaviour are obtained from the equivalent 2D analysis when both pile capacity and load are reduced by the side-side pile spacing. Furthermore, one may conclude that reduction of the pile properties and load by a factor exceeding 2.5D is not to be advised (even when the pile spacing exceeds this spacing distance), since this would overestimate the relative soil stiffness and strength capacity in the models.

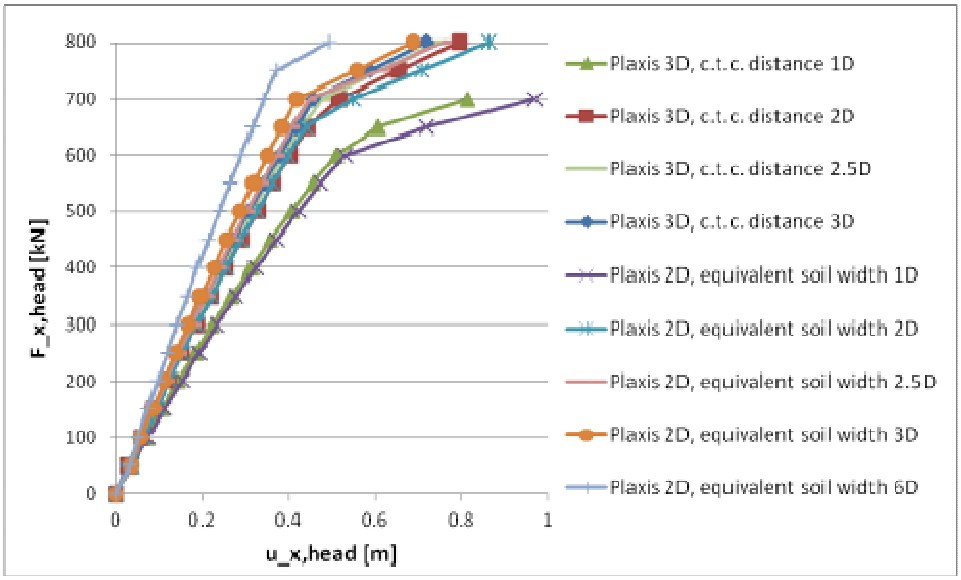

Figure 7.13: Equivalent mobilized soil width dependence on side-side pile spacing

Figure 7.14 shows the head bending moment of a single pile as a function of lateral loading for the various equivalent models related to varying pile spacing. From the figure one may conclude that the head bending moment is relatively insensitive to the pile spacing and head bending moments are reasonably well represented by the equivalent 2D models.

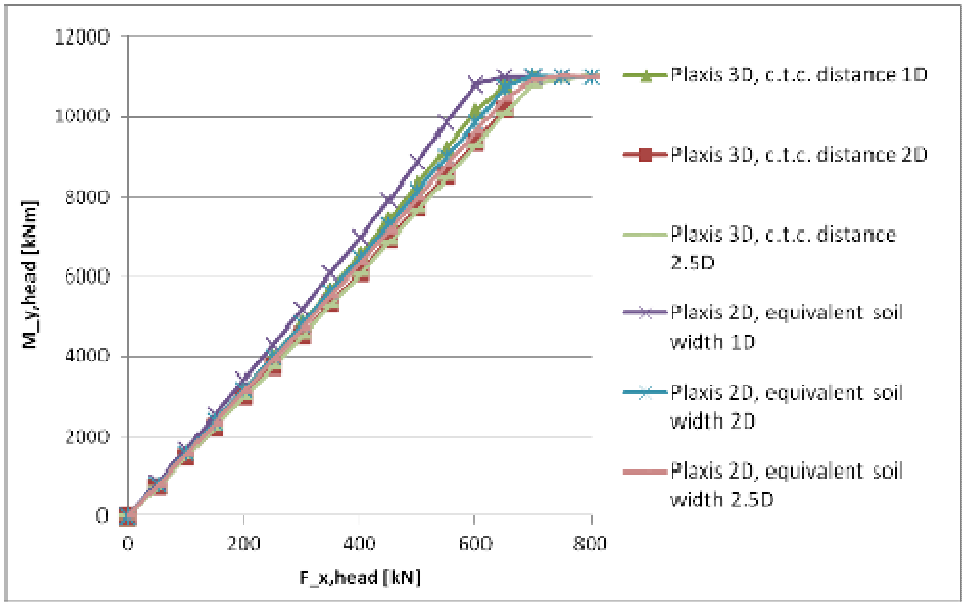

Figure 7.14: Pile head bending moment $M_{y,head}$ sensitivity to pile spacing

From the previous it may be concluded that jetty lateral pile load-deformation characteristics may reasonably well be approximated by adopting a 2D equivalent model. For soft soil conditions, as present in the considered case project pile spacing has hardly any effect on pile efficiency if the side-side spacing exceeds 2.5D, and consequently the reduction factor for pile stiffness, pile top fixation and lateral loading should not be chosen higher than 2.5D.

7.1.5 Pushover analysis of jetty cross-section (3 rows of piles in loading direction)

This paragraph presents the results from pushover analysis on the jetty cross-section as was presented in paragraph 5.1. The outcomes of pushover analysis from 3D Plaxis is assumed to represent reality reasonably well, as was proved in section 7.1.2 where the modelling of a single pile response in Plaxis 3D has been proved to fit

reasonably well to test results from Jeanjean (2009). In this section the effects of grouping in a jetty transverse configuration are studied, and appropriateness of defining an equivalent 2D model is investigated.

Jetty global response in this section is again studied by comparing the lateral deck displacement and the fixation bending moment at the connection of the pile to the deck, which are typical representative variables for global response in performance based design. The results for these variables with increasing pushover loading are presented in figures Figure 7.15 and Figure 7.16. As shown in Figure 7.15 a reasonable equivalent 2D model can be found. As for the single piles a considerable reduction of structure stiffness and pushover loads however is required, even for pile groups with piles spaced in the loading direction. These required reductions make the approach is not suitable for performing seismic analysis of piles embedded in a soil deposit, since it would not be convenient to reduce bedrock loads. On the contrary when keeping the actual seismic loads, a lower pile stiffness would result unrealistic displacements and including the actual pile stiffness would overestimate pile stiffness compared to soil stiffness.

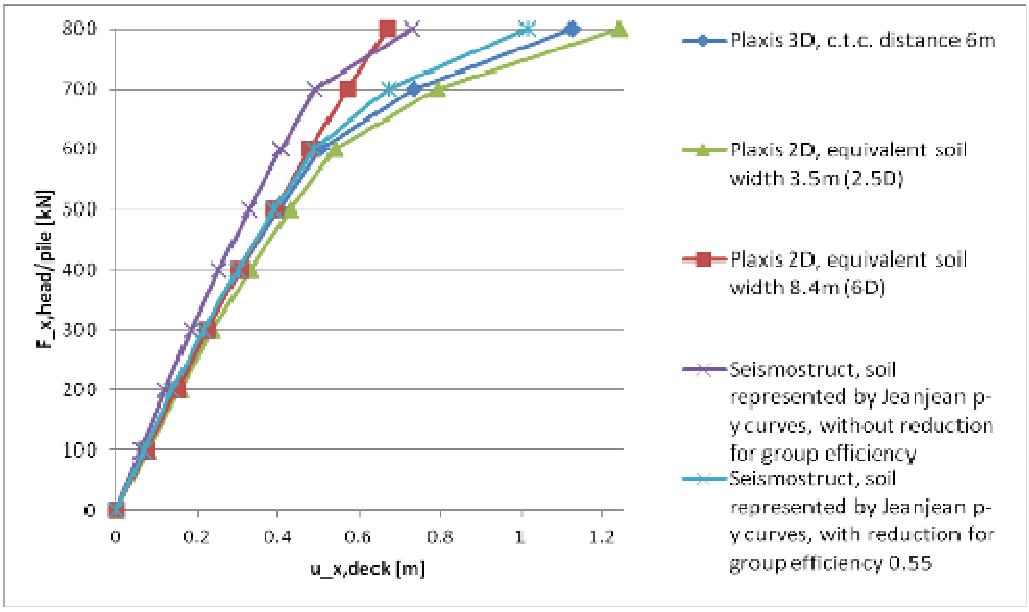

Figure 7.15: Pushover characteristics for jetty cross-section with piles spaced in loading direction, sensitivity to increased relative soil stiffness

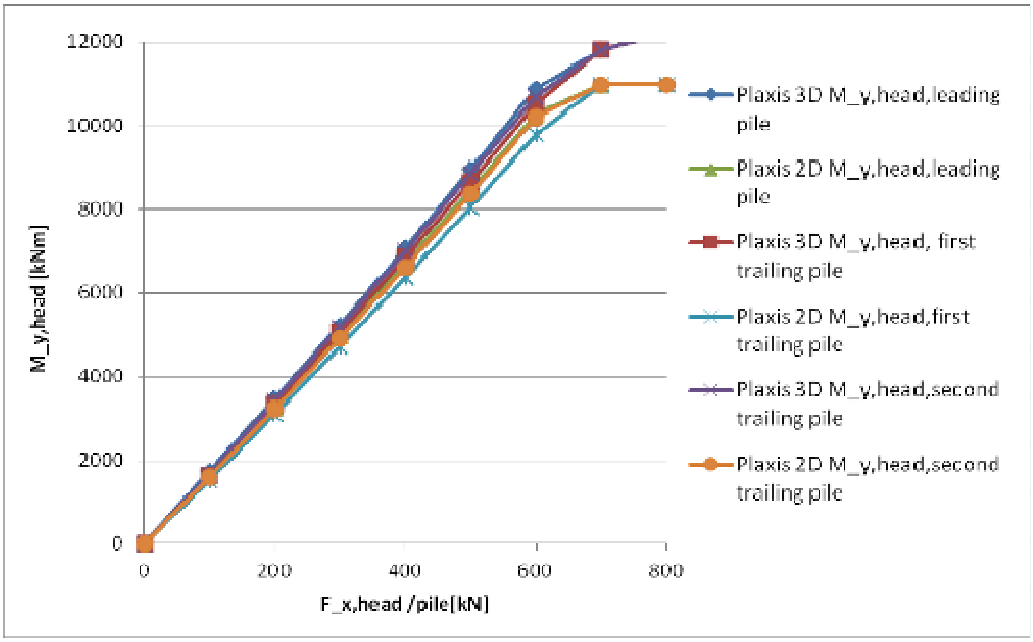

Figure 7.16: Pile head bending moment $M_{y,head}$ development for

Based on the analyses results, the following conclusion can be drawn:

- A significant efficiency reduction is obtained due to the pile interaction in the loading direction. According to Reese and van Ympe (2001) the efficiency factor is 1.00 for the leading piles and 0.79 for the trailing piles (see appendix III), which would result in an average efficiency of 0.86 for a jetty transverse pile row of 3 piles. The system lateral efficiency obtained from the Plaxis 3D analysis for the 3 in row jetty piles is ranging from 0.87 to 0.65 with increasing load level compared to single pile lateral stiffness. The lateral system response however is affected by both structure stiffness and soil stiffness. Consequently soil subgrade reaction efficiency for the grouped piles will be even lower than these efficiency factors. Actual soil efficiency was found by reducing the p-y expressions initial stiffness and ultimate capacity up to a level for which again a good fit is found with Plaxis 3D as there was for single pile response. The average efficiency was found to be approximately 0.55 for the leading and two trailing piles. Apparently the efficiency reduction is higher than provided by Reese and van Ympe and is more in accordance with the higher efficiency reductions as proposed by NCHRP report 461 (Transportation Research Board, 2001). The significant reduction of pile efficiency for the trailing piles is explained by the inability of the soil to mobilize lateral resistance as is indicated by Figure 7.17. (horizontal section at z = -23.5m+MSL) that shows relatively low soil strains in the zone between the pile implying a kind of rigid body movement of the local soil.

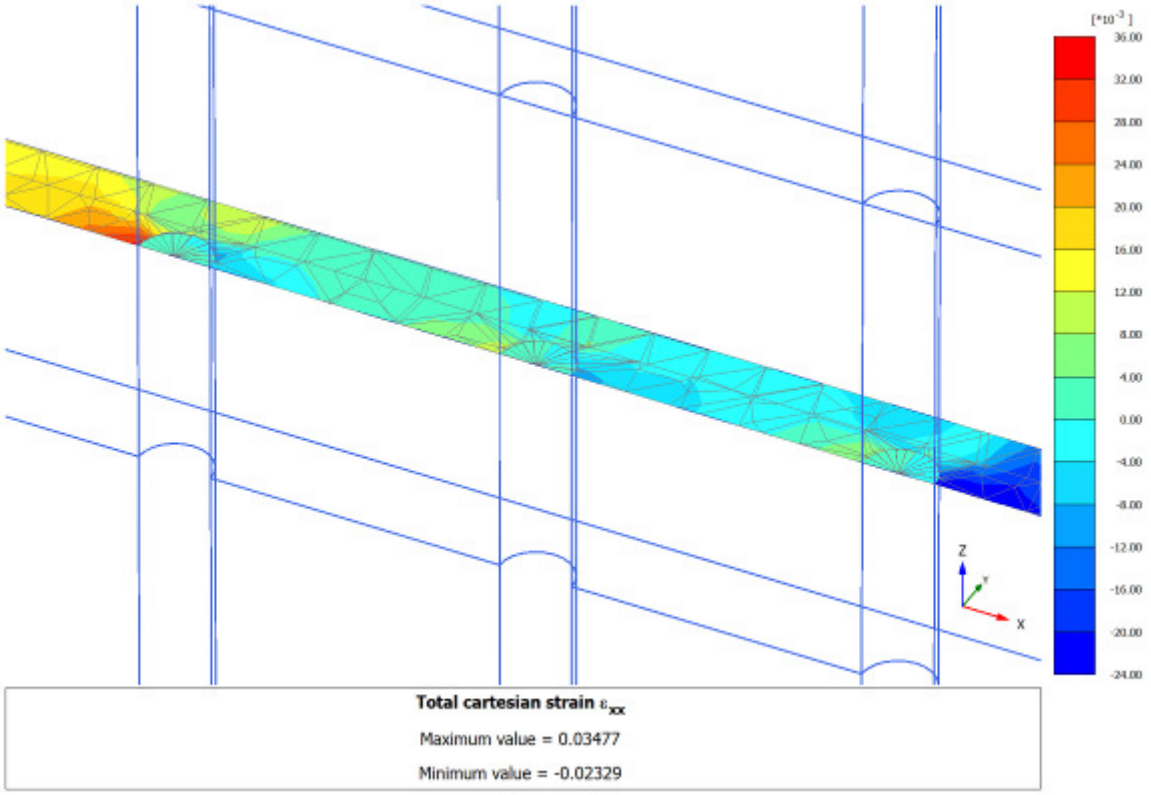

Figure 7.17: Relatively low Cartesian strains ε_{xx} in the soil between the piles for Plaxis 3D jetty modelling in soft soil

Zooming in at the local stress development in the soil in between the pile however reveals the load spreading effects in the soil in Plaxis 3D also for the trailing piles, as becomes clear from comparison of Figure 7.18 and Figure 7.19. For the 2D equivalent model soil stresses mobilized by the displacement of the trailing piles (walls) are perfectly passed through to the leading pile (wall), and real passive resistance is mobilized in front of the leading pile. For the 3D model however mobilized resistance is to some extend spread over a soil width exceeding the pile diameter, which results a decreasing stress with increasing distance from the pile towards it leading pile at the piles centre plane y = 0 m.

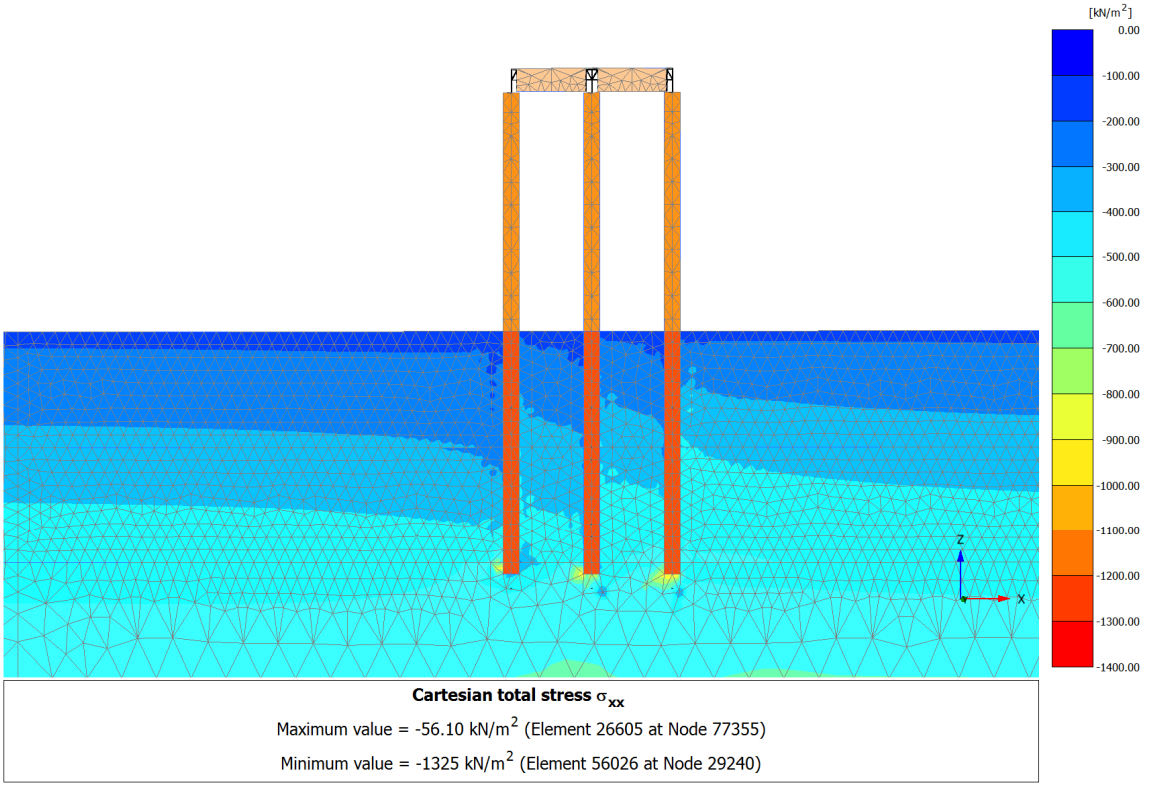

Figure 7.18: Cartesian total stress σ_{xx} for Plaxis 3D jetty modelling

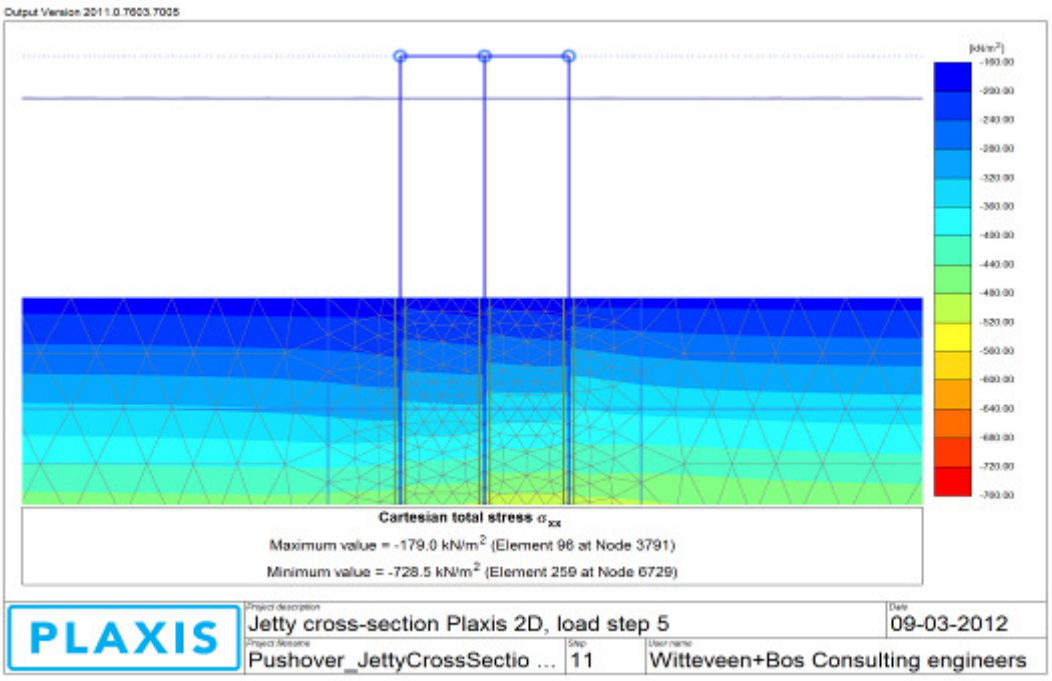

Figure 7.19: Cartesian total stress σ_{xx} for equivalent Plaxis 2D jetty modelling

It is concluded that an equivalent Plaxis 2D model may be defined for pushover analysis of a jetty structure. Since computationally effort of pushover analysis is limited this however would not be very useful. , where this equivalent 2D approach might be attractive to perform efficient dynamic analysis of piles + soil subjected to dynamic pile head loading, as for example dynamic analysis of piles under offshore wind turbines or for piles as

machine foundations. Hereby it is noted that one should make sure that the dynamic pile characteristics are included correct and an appropriate Winkler or Plaxis 3D continuum model conceptually would be preferable.

Aiming at the analysis of pile-soil interaction for jetties under seismic loading, the equivalent Plaxis 2D model is not suitable, since load is formed by a bedrock excitation which cannot be reduced inherently with pile stiffness since this would underestimate soil deposit response levels. Hence the dynamic jetty slice transverse response for earthquake signals preferably is to be analyzed with a dynamic structure on Winkler foundation model or by a coupled analysis in Plaxis 3D dynamics module, that show very similar pushover load-deformation characteristics as presented in Figure 7.20. and Figure 7.21.

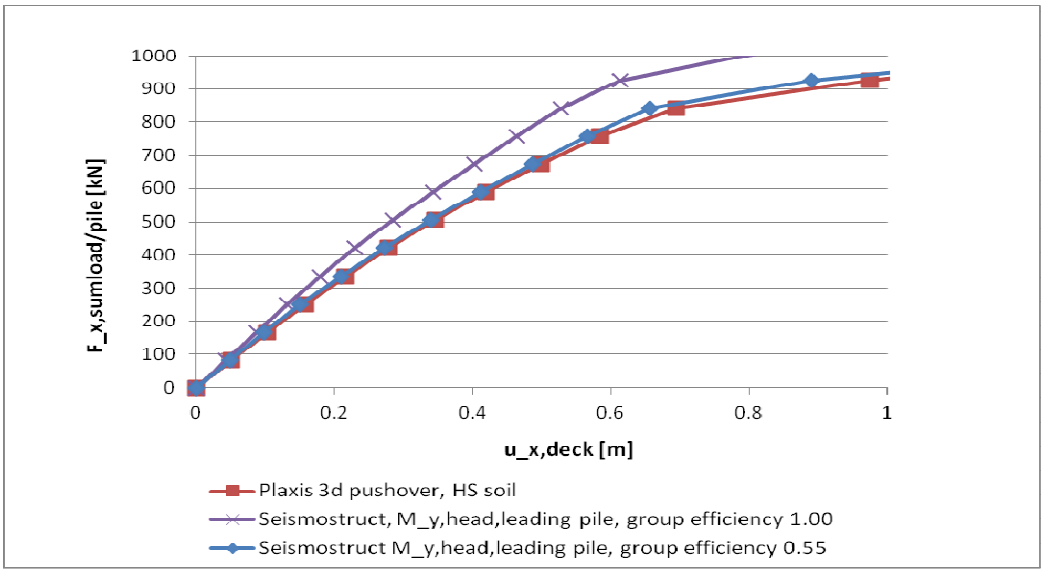

Figure 7.20: Pushover curve jetty loaded by force vector proportional to the fundamental mode vector

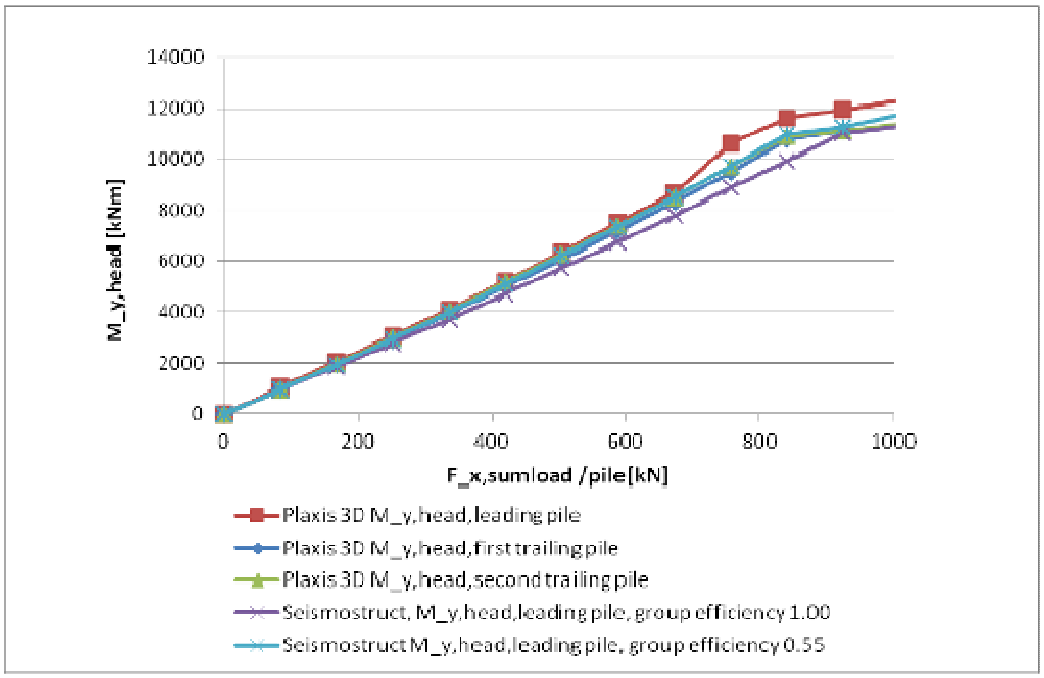

Figure 7.21: Pile head bending moment development for jetty pushover loaded by force vector proportional to the fundamental mode vector

For the case jetty configuration an average efficiency of the Winkler foundation was found to be 0.55ver for the row of three piles. For the Plaxis 3D model a width of 2.5*D was calibrated to be sufficient for the piles in soft-soil conditions.

Based the results obtained, one may conclude that by applying the simple Winkler foundation concept with p-y curves as prescribed in the preceding, the monotonic load-deformation characteristics found from advanced finite element analysis can be approximated quite well. For cyclic behaviour however one may expect the response from Winkler analysis to deviate somewhat from Plaxis finite element analysis, since soil deformations and soil state will not be completely restored in Plaxis when monotonically loaded up to a level beyond the onset of plasticity and subsequently unloading and reloading in opposite direction. These deviations were investigated and the result is shown in Figure 7.22.

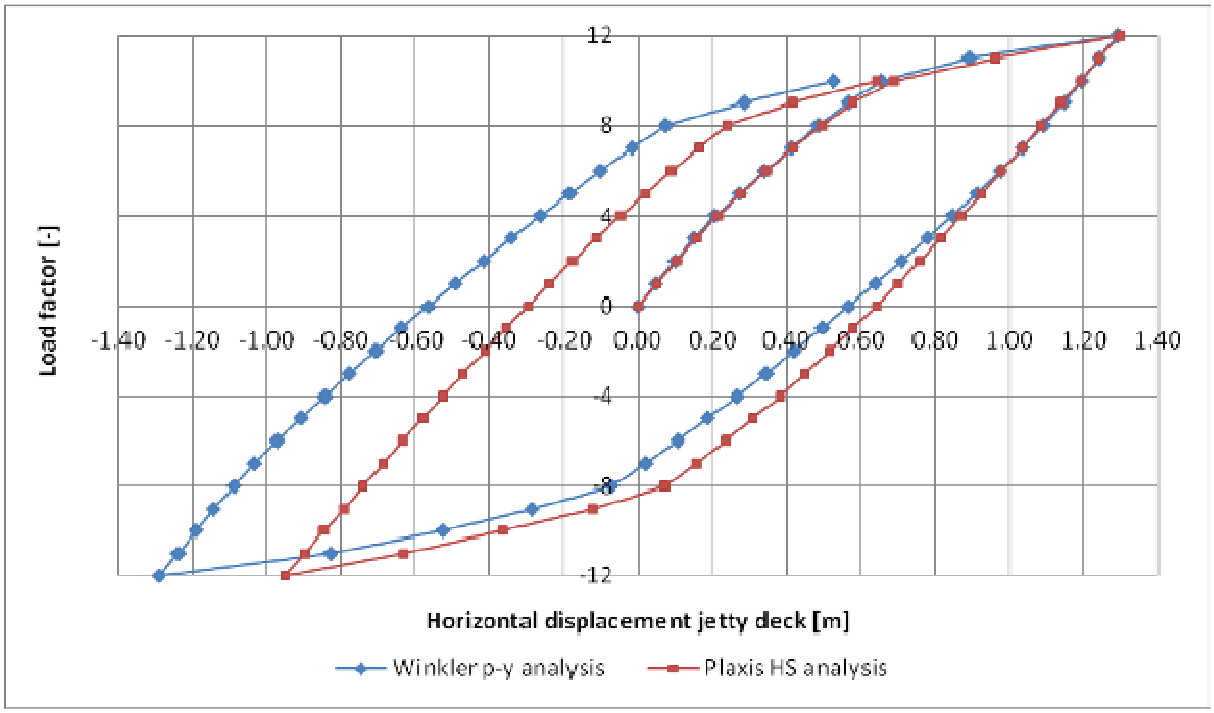

Figure 7.22: Cyclic pushover characteristics from Winkler p-y and Plaxis 3D HS analysis

Clearly a preference direction of the structure deformation response is developed in the Plaxis 3D HS analysis, where this effect is not present in Winkler p-y analysis but will be present in reality for loading considerably into the post-elastic range. Plaxis pile-soil interfaces however do not properly include gapping closure and hence the preference direction found from these analysis may be somewhat overestimate reality. It is noted that the development of a preference direction of displacements will be even more pronounced for pile-deck structures founded in slopes, for which the simplified Winkler p-y analysis hence will introduce significant errors when not accounted for.

7.2 Free field site response analysis

7.2.1 Calibration of the finite element model

7.2.1.1 Plaxis finite element mesh size

Initially the element size applied in the numerical analyses was based on references as noted in paragraph 6.4.4.1. For this mesh configuration analysis are performed for harmonic and random bedrock signals. The results show that a very good fit of the numerical finite element and frequency domain analysis responses is obtained. The very fine meshes however are not convenient with respect to computational requirements (especially towards 3D FE models) and therefore it was investigated how responses are affected by applying somewhat bigger elements. It is expected that resulting errors are bigger for high frequency components of the signal, since related wave lengths for these frequencies are smaller. However, since the high frequencies are expected to be of minor importance for resulting forces and deformations, some error of resulting response for this frequency range may be accepted.

The effects of increasing element sizes by approximately a factor 2 are presented below for both the 3 and 10 Hz harmonic signals and linear elastic material with 5% critical added Rayleigh viscous damping in Figure 7.23 and Figure 7.24.

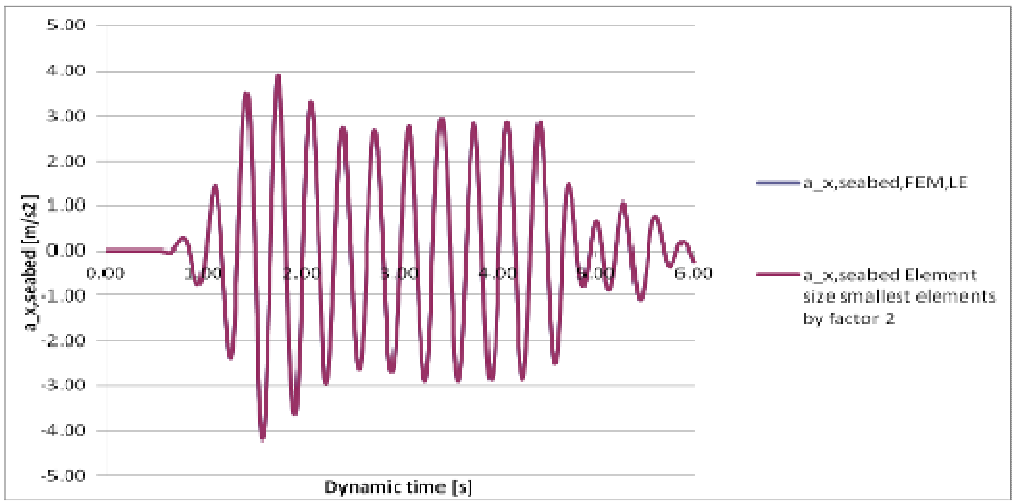

Figure 7.23: Sensitivity of acceleration response to element size for 3 Hz harmonic bedrock excitation

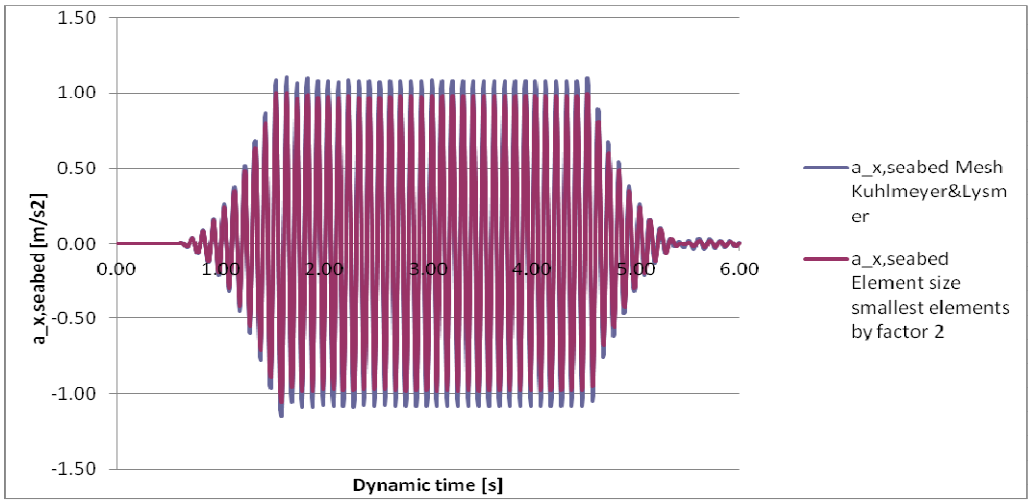

Figure 7.24: Sensitivity of acceleration response to element size for 10 Hz harmonic bedrock excitation

From the figures it can be concluded that the bigger mesh element does not affect the 3 Hz harmonic input signal response and for the 10 Hz harmonic input signal a reduction of peak accelerations of approximately 10% is obtained. Consequently the error resulting for natural seismic signals will be depending on the frequency content of the input signal. Actual signals have the highest energy content generally in the frequency range 1-10 Hz, which would imply that errors in accelerations due to a factor two increased element sizes can be estimated to be <5% non-conservative.

The figures above show the clear effects mesh coarsening can have. However, with respect to computational requirement lowering the number of elements has appeared to be critical. Hence, in this study it was decided to accept the slight deviations for the higher frequencies, by adopting the somewhat coarser mesh compared to the recommended maximum element sizes (Lysmer & Kuhlmeyer R.L., 1969). Sensitivity of results to further coarsening of the mesh is not included in this study but probably not to be recommended with respect to accuracy of the results.

7.2.1.2 Finite element model width

Based on bedrock excitations by both the random Duzce signal and the simple harmonic signals the model width was calibrated, focussing on the two criteria as noted in paragraph 6.4.4.2. The sufficient model width was found to be 300 m, with standard Plaxis viscous boundaries applied at the x_{min} and x_{max} boundaries. Results supporting this conclusion are presented below.

With respect to horizontal seabed accelerations (first criterion paragraph 6.4.4.2) it was found that the boundary effect reach approximately 50 to 100 m away from the boundary. At 100 m from the boundary sufficient convergence of horizontal accelerations is obtained. Considering the time accelerations history obtained one may conclude that model width variations seem to most affect the obtained horizontal accelerations in the latest stadium of the earthquake, but for the 200 m model also clear deviations of peak accelerations (up to 25% conservative and non-conservative) in the strong motion stage are obtained. Apparently wave reflections are becoming significant for the centre model response and 200 m model width is insufficient.

With respect to vertical accelerations at seabed level (second criterion paragraph 6.4.4.2), no real convergence is obtained towards the widest models, but clearly very low acceleration levels (up to approximately 0.1 m/s^2) are obtained at the model centre seabed for all three model widths. Away from the model centre, vertical accelerations grow rapidly, especially for the smaller models as is shown in Figure 7.25 for location (seabed,x=50m)

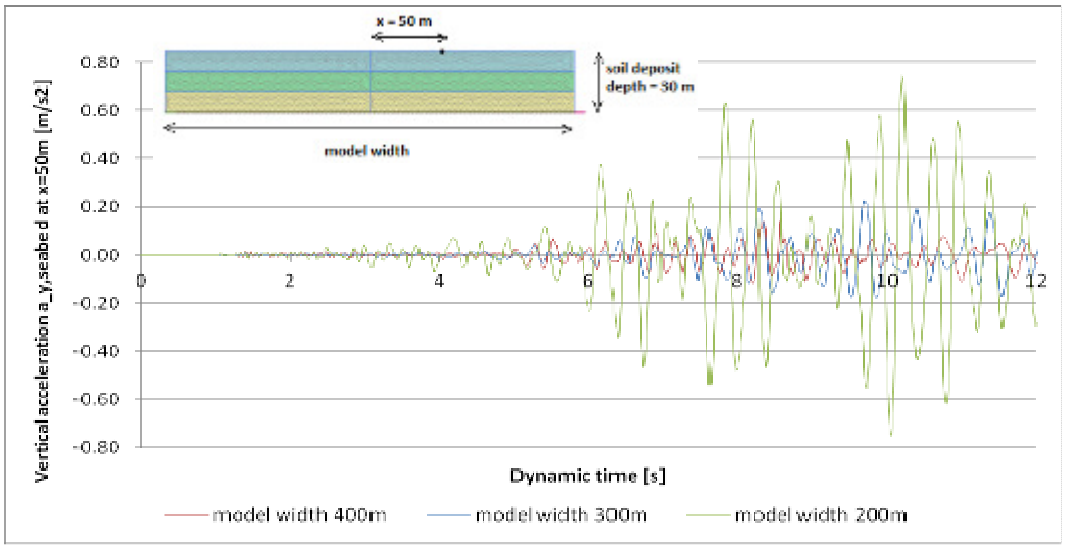

Figure 7.25: Vertical seabed accelerations at x=50m for model width 400, 300 and 200 m

When subjected to the 3 Hz harmonic input signal, peak vertical accelerations in the centre region are about 0.04 m/s^2, which is less than 1% of the horizontal peak accelerations. Towards the boundaries the peak vertical accelerations grow up to a maximum absolute value of about 0.4 m/s^2. For the 10 Hz harmonic bedrock signal

peak vertical accelerations are below 0.02 m/s^2 which is smaller than 2% of the obtained peak horizontal accelerations. For this signal the peak vertical acceleration found towards the lateral boundaries is about 0.3 m/s^2.

The vertical oscillations in the 2D Plaxis models are dominated by wave reflections at the boundaries generating surface waves. Analyses have shown that the effects are significant in the area near the lateral boundaries for both the random and harmonic bedrock motions. However, vertical accelerations are very limited in the centre of the model already for a critical damping percentage of only 5%, which is a lower bound approximation for actual soil damping levels. It may therefore be concluded that boundary effects are sufficiently damped out towards the model centre for the 300 m model and consequently this model width will be used in the next steps of this study. In the 1D frequency domain analysis vertical motions are not considered and the response for an infinitely extending soil column subjected to uniform bedrock excitation is determined, hence it cannot be used as a comparison in this sense.

7.2.2 Comparison of responses from the linear elastic finite element model and equivalent linear frequency domain analysis for layered soil profile

The finite element acceleration responses obtained show a proper fit with the linear frequency domain solution for both harmonic bedrock excitation and random seismic bedrock signals. The applied harmonic signal was smoothened to avoid high frequency noise resulting from numerical problems in Plaxis with respect to initial conditions. Plaxis has shown to be very sensitive for both initial conditions and phase-to-phase transitions in calculations, which is a problem recommended for future Plaxis improvement and in this study was solved by inclusion of a numerically damped time integration scheme. Figure 7.26 shows the almost perfect fit for the 3 Hz harmonic input signal in the time domain. A conservative soil material damping ratio of 0.05 was adopted in this analysis.

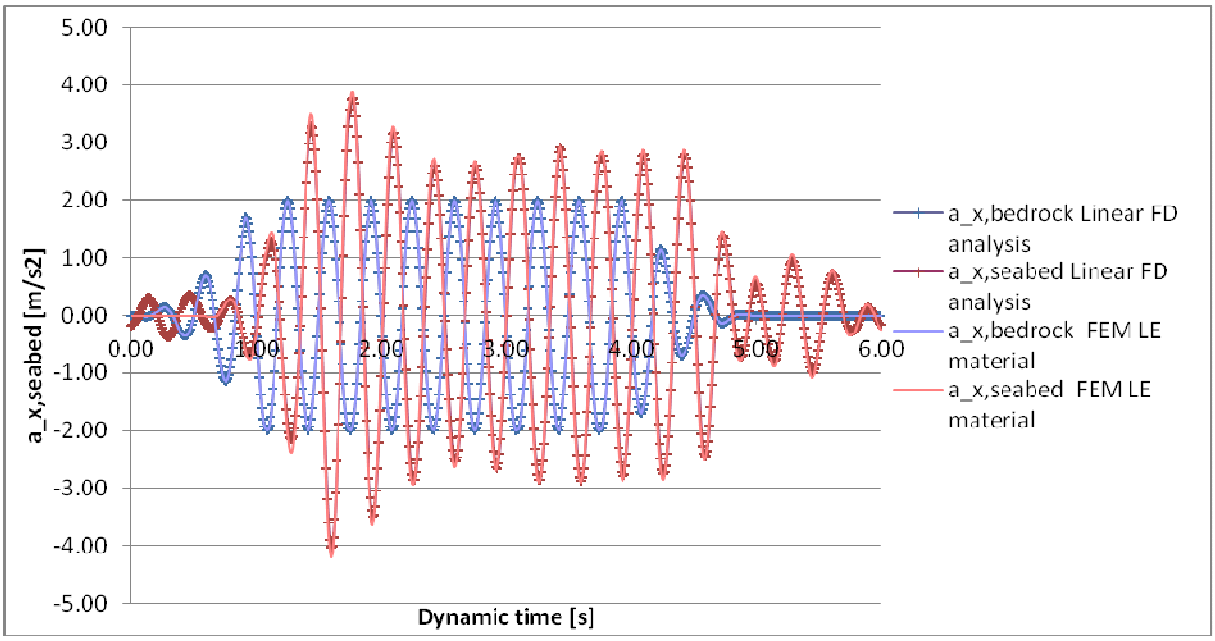

Figure 7.26: Excitation and response acceleration time histories for a 3 Hz harmonic signal

For the high level earthquakes commonly much higher damping levels are realistic, especially for soft soil conditions. This much higher material damping results from material internal hysteretic behaviour, even for load levels below failure. Linear elastic and Mohr-Coulomb soil models do not include this hysteretic damping in the elastic range, that on the contrary is captured in the HSsmall soil model. Consequently for LE and MC soils an equivalent damping has to be determine preliminary, for which in this study the equivalent linear frequency domain analysis was used for this because of computational convenience. The resulting effective soil parameters for a peak bedrock acceleration of 0.5g are as presented in Table 7.2.

Table 7.2: Effective soil dynamic parameters based on equivalent linear frequency domain analysis

Soil layer	Clay C1	Clay C2	Sand S3
γ_{eff} [-]	0.0026	0.0011	0.0006
G_{eff} [kPa]	4790	23790	126250
$V_{s,eff}$ [m/s^2]	53	116	248
ξ_{eff} [-]	0.179	0.093	0.063

Applying these parameters in linear elastic finite element analysis should essentially give results close to the results from frequency domain analysis. However, when adding Rayleigh damping to linear elastic material the target damping ratio cannot exactly be met over the entire frequency range. A best-fit Rayleigh damping was applied for the frequency range of interest, which for the Duzce signal combined with the soil profile is approximately 0.1 to 10 Hz.

Table 7.3: Rayleigh critical damping ratios estimated based on equivalent linear frequency domain analysis

Damping	Best estimate Rayleigh damping input frequencies			
Soil layer	f_1 [Hz]	ξ_1 [-]	f_2 [Hz]	ξ_2 [-]
C1 clay	2	0.20	7	0.20
C2 clay	2	0.10	7	0.10
S3 sand	2	0.07	7	0.07

The seabed horizontal acceleration response spectra of both equivalent linear frequency domain analysis and linear elastic and Mohr-Coulomb finite element analysis are presented in Figure 7.27.

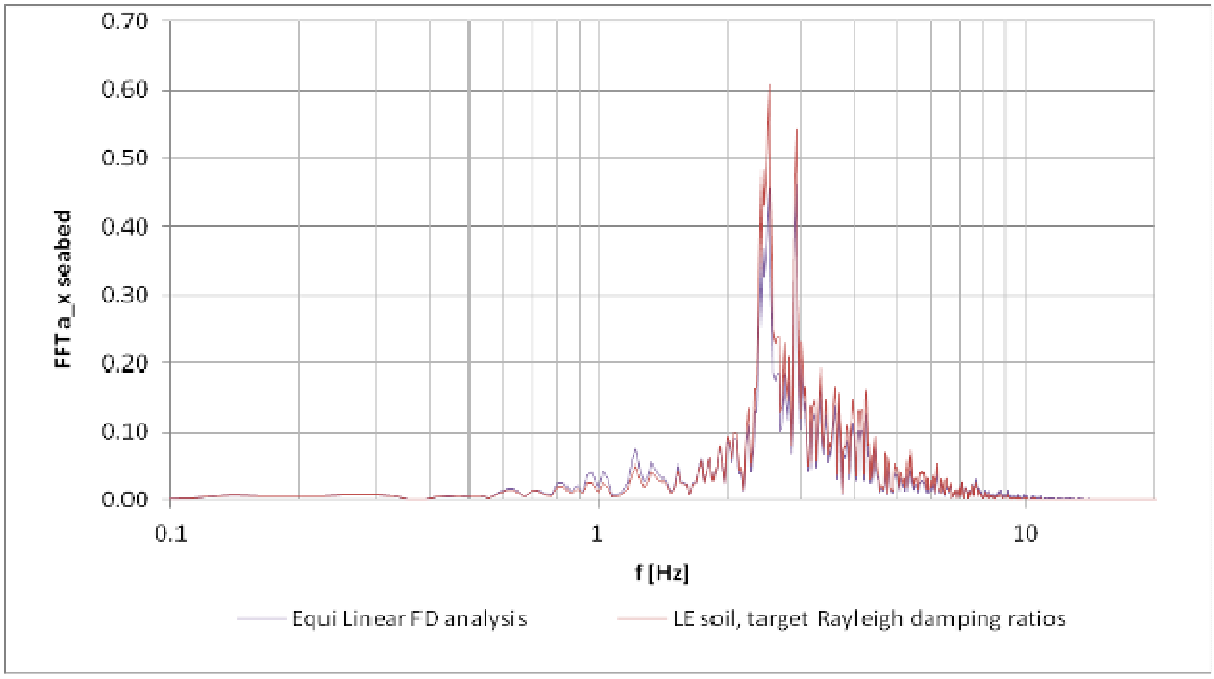

Figure 7.27: FFT amplitudes of seabed horizontal acceleration response due to Duzce bedrock signal

The figure shows the good fit of the Plaxis finite element model seabed response compared to the equivalent response by the equivalent linear frequency domain analysis. A somewhat higher spectral response of the finite element analysis is obtained in the frequency range around 3 Hz, which is related to the slightly lower Rayleigh damping level for these frequencies. Similar reasoning applies for the slightly lower frequency content of the finite element response around 1 Hz.

7.2.3 Site response for linear elastic, Mohr-Coulomb, HS and HSsmall soil constitutive models

7.2.3.1 Comparison of responses for linear elastic, Mohr-Coulomb and HSsmall soil constitutive models

In this paragraph the sensitivity of the site response to variation of the soil constitutive model is discussed. Four constitutive models are considered, being the linear elastic, Mohr-Coulomb, Hardening Soil and Hardening Soil with Small strain stiffness models (Plaxis Material Models Manual, 2011). Bedrock peak acceleration in this study was taken to be 0.5g, which is considered a common level representative for strong earthquakes. The linear elastic finite element analysis have shown to match the frequency domain solution very well. However, nonlinear physical phenomena like hardening/softening, plasticity, stress dependency of stiffness and stiffness dependency on loading history are not included in these analysis, where they are obtained for real soils. Consequently one may expect the Plaxis advanced soil models to result more accurate site responses, provided a good numerical performance.

The seabed horizontal acceleration Fourier response spectra for the LE, MC and HSsmall soil models are presented in Figure 7.28.

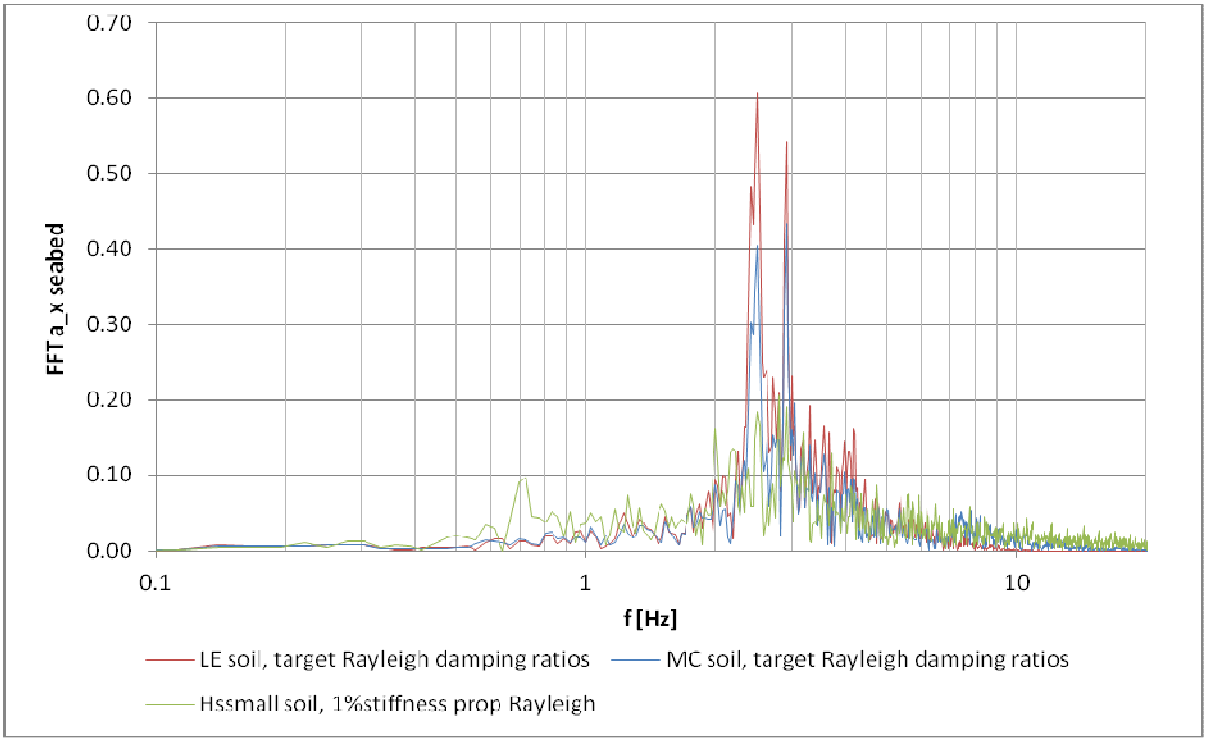

Figure 7.28: FFT amplitudes of seabed horizontal accelerations for the LE, MC and HSsmall soil models, subjected to Duzce bedrock signal

The figure shows the almost similar spectral response for the LE and MC soil models. The minor differences obtained are the somewhat lower spectral peaks for the MC model and the somewhat higher frequency content at the higher frequencies for the MC soil. The somewhat lower spectral peaks are explained by Figure 7.29 that shows the clear effects plasticity have on development of peak accelerations.

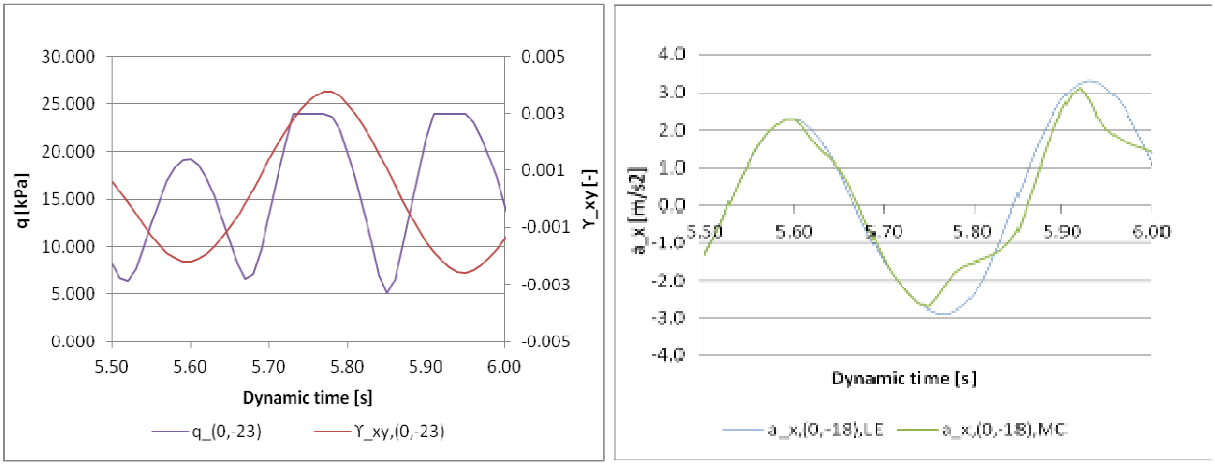

Figure 7.29: Mohr-Coulomb plasticity affecting free field accelerations, response subinterval 5-6 s for the Duzce signal

For the HSsmall however a significantly different response spectrum is obtained (Figure 7.28). Spectral peaks around the high frequency range of the input signal (~3 Hz) are much lower for the HSsmall model, where it has a much higher frequency content for the lower and higher frequency range. According to Brinkgreve, Bonnier and Kappert (2007) and oral communication with R.B.J. Brinkgreve, Nov 2011, 1-2% Rayleigh damping was added to the HSsmall material, in order to account for energy dissipation at very low strain levels as is observed in reality and not covered by the hysteretic damping included in the HSsmall model. This low Rayleigh damping percentage however is much lower than the Rayleigh damping added to the LE and MC soil models. Consequently much higher total damping is included in the LE and MC models for the lower and higher frequency range, which partly explains the higher frequency content of the HSsmall response for these frequency ranges. However, the total spectral response obtained for the HSsmall model is relatively far from the LE and MC response, for which reason it was decided to assess the HSsmall model response in more detail as presented in the next paragraph.

More insight regarding the response for different soil constitutive models is provided by analyzing the acceleration responses in the time domain. The acceleration time history for seabed level due to the Duzce random bedrock signal for time interval 0-10 sec is presented in Figure 7.30

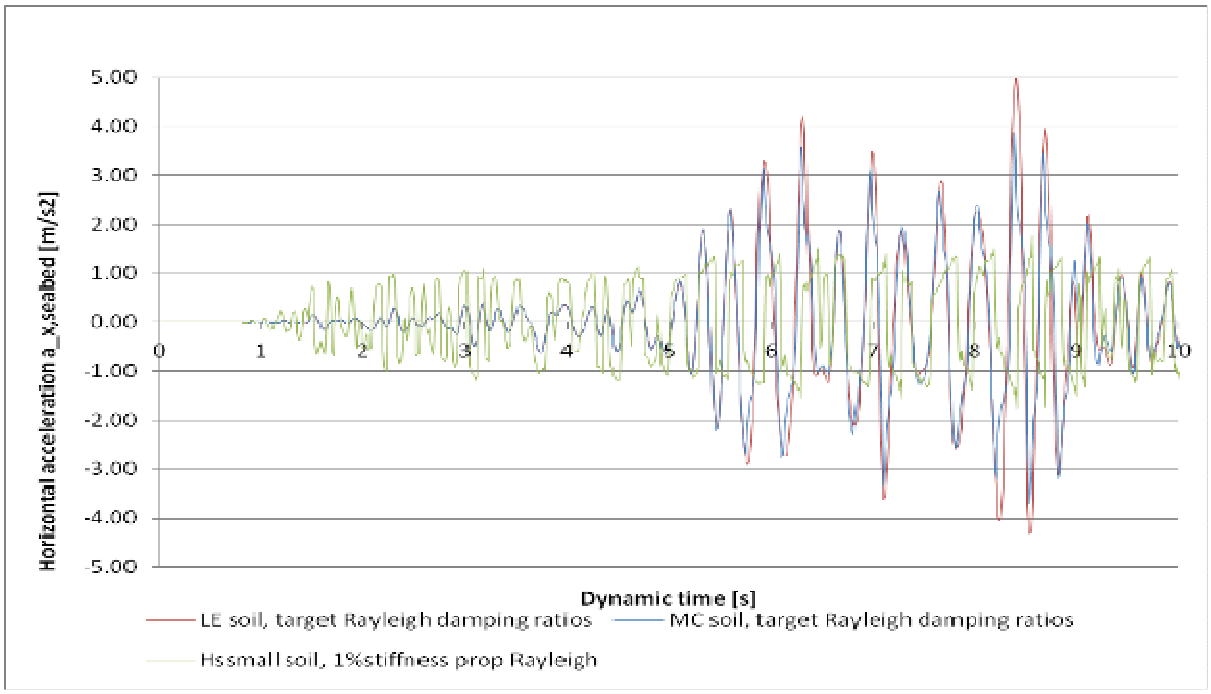

Figure 7.30: Horizontal acceleration response time histories (subinterval 0<t<10 s) at seabed level due to bedrock excitation for Duzce bedrock acceleration signal

For very low strain levels the HSsmall model underestimates soil damping levels (Brinkgreve, Bonnier and Kappert (2007), which may contribute to the higher response for the initial phase of the earthquake. The 1-2% Rayleigh damping for the frequency range of interest (0.5 – 8 Hz) was included in two different ways, mass-and-stiffness proportional and stiffness proportional only. The first option results very high effective damping levels for the very low frequency range, which for the Duzce signal and present soil turned out to be not very significant. However an appropriate definition of the additional Rayleigh damping should be made case dependent based on input signal frequency content and system fundamental frequency level.
The material viscous damping percentage in equivalent linear frequency domain analysis and linear elastic and Mohr-Coulomb finite element analysis is taken constant over the total time history. The damping level is determined as a function of the extreme shear stress level, which generally will overestimate realistic damping for low level response phases and underestimate damping for high level response phases. These effects become clear from Figure 7.30, showing the acceleration amplitudes developing over the time interval. A more realistic approximation of soil responses by linear elastic analysis may be obtained when sub-phases with varying damping levels are defined, which however doesn't fit in the Fourier frequency domain analysis and cannot be applied in dynamic Plaxis analysis method, since for each sub-phase start strong deviations of response will result. It may be clear from these conclusions that properly accounting for soil damping by adding of Rayleigh damping is difficult and so the HSsmall model feature of including hysteretic damping is very attractive from this perspective.

7.2.3.2 Performance of the HSsmall soil constitutive model in dynamics

For strong motion phases of the time signal, the HSsmall material site response shows a phase delay compared to the linear elastic and Mohr-Coulomb materials. This out of phase response is not obtained in the initial low intensity interval and also is restored when motion levels decrease. Since this effect is not present for Mohr-Coulomb materials it cannot be related to plasticity and it needs to be a result of the stress dependent stiffness development in the HSsmall model. Furthermore sudden acceleration jumps in response of HSsmall modelled clay layers is obtained, which seems not very realistic when the soil responses at bedrock, layer interfaces and seabed levels are presented for a shorter time interval as presented in Figure 7.31.

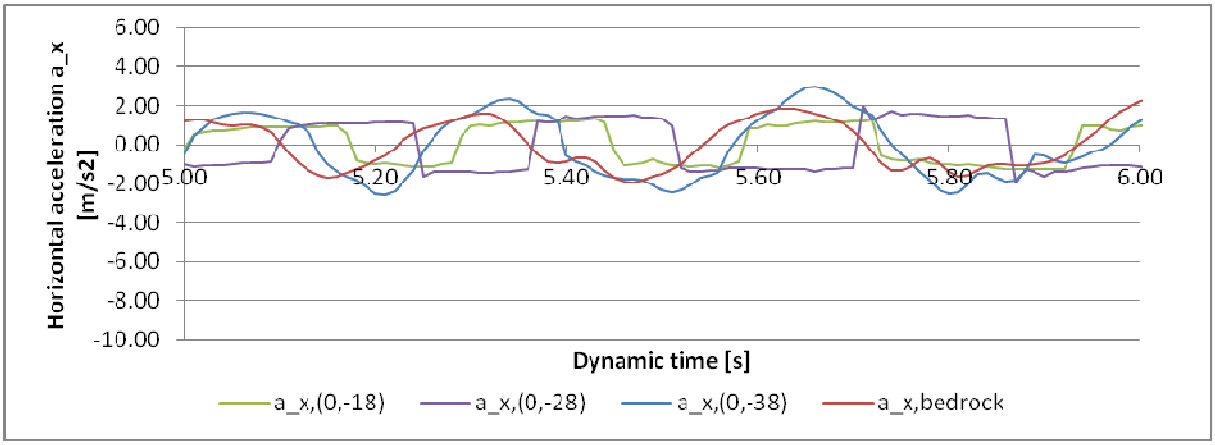

Figure 7.31: Horizontal soil accelerations at various depths

These sudden accelerations jumps are not obtained for the HS , Mohr-Coulomb and linear elastic constitutive soil models. The most sudden changes in accelerations are obtained at seabed level, but also the deeper C1-C2 layer interface shows a very unrealistic acceleration response. However, Figure 7.31 a more smooth and realistic response for the sand layer underneath. Hence it may be concluded that the HSsmall soil constitutive model is not resulting unrealistic responses in general when applied in dynamics. It seems that just a peculiar configuration of model layering, soil parameters and the HSsmall model operation in dynamics results the sudden jumps in acceleration level, which is considered in more detail.

The sudden changes in the soil accelerograms were found to be a consequence of the initial very high small strain stiffness when the small strain overlay model resets stiffness. Reference in this explanation can be made

to the free vibration equation of motion in dynamics (equation), where for simplicity damping related terms are neglected:

$$[M]\underline{\ddot{u}} + [K]\underline{u} = 0 \tag{7.2}$$

Reset of the small strain stiffness gives an abrupt change in stiffness matrix $[K]$, since $[M]$ is constant and $\underline{u}$ has to be continuous, accelerations will abruptly develop too, in order to obey the equation of motion.
The HSsmall model returns to the small strain stiffness when according to Benz (2006) the scalar valued shear strain:

$$\gamma_{hist} = \sqrt{3}\frac{\left\|\underline{\underline{H}}\Delta\underline{e}\right\|}{\left\|\Delta\underline{e}\right\|} \tag{7.3}$$

is reset to zero by the deviatoric strain history tensor $\underline{\underline{H}}$ that multiplies the deviatoric stain increment $\Delta\underline{e}$ in the numerator, which occurs when a deviatoric principal strain rate reversal is detected. Apparently the sudden changes in stiffness (high ratio G_0 / G_{ur} then for soft soils) strongly affects the accelerograms, resulting the sudden jumps in accelerations. The direct link between principal strain rate reversal and sudden change in acceleration level is demonstrated by Figure 7.32 and Figure 7.33 that show horizontal accelerations and principal strains for the locations (0,-23) and (0,-33) in the C1 and C2 clay layers for the Duzce seismic signal (5-6 sec).

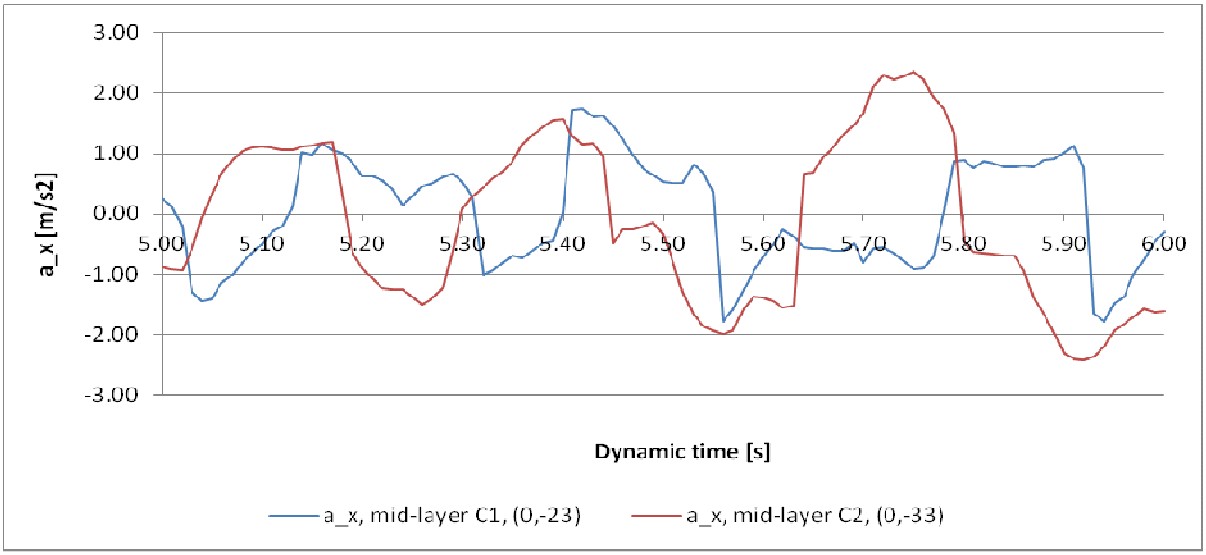

Figure 7.32: Horizontal accelerations for the C1 and C2 clay mid-layer levels

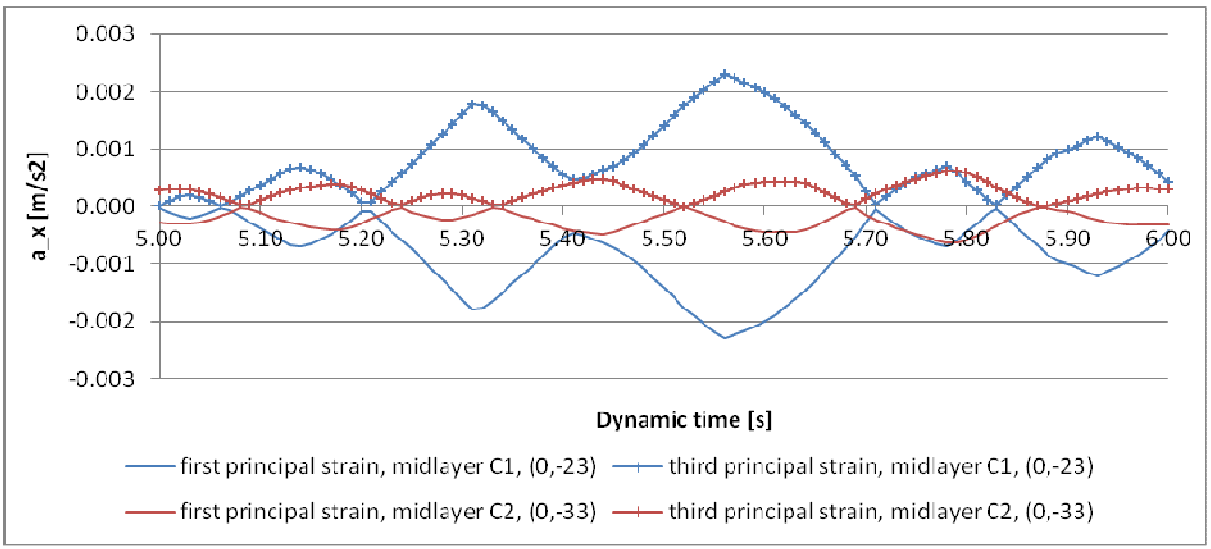

Figure 7.33: Principal strains for the C1 and C2 clay mid-layer levels

Sensitivity of the acceleration for the following analysis input parameters was considered:

- Number of dynamic sub steps
- Undrained/drained analysis of the clays
- Small strain overlay model parameters G_0 and $\gamma_{0.7}$
- Additional Rayleigh damping included in the HSsmall model
- Stress dependency included in HSsmall soil model

The number of dynamic sub steps as determined in 6.4.4.1 is significantly lower than the default number of dynamic sub steps provided by Plaxis. This is caused because Plaxis calculated the number based on the compression wave velocity that tends to infinity when undrained conditions are applied to soils. Since the problem studied is expected to be dominated by shear loading a lower number of dynamic sub steps was chosen for computational convenience. In order to exclude a relation of the unrealistic sudden jumps in acceleration obtained now with the lower number of sub steps an analysis was performed with a higher number of dynamic sub steps. Results of this analysis still show the sudden jumps in acceleration.

Initially undrained analysis type A was applied for the clay layers, as has proven to give good results and stable calculations in static analysis. However, the unrealistic acceleration response in dynamic analysis was obtained for the undrained clays and not for the drained sand. Hence analyses have been performed in which drained analysis was applied to the clays as well. It was found that the only a slight smoothening of the blocked shape accelerograms in the clay is obtained and no significantly different response is obtained as is reasonable for this problem dominated by shear loading. Besides, as was noted before, the MC acceleration responses show lower peaks than the LE, which was explained by the effects of plasticity. It is noted that in Undrained analysis type A higher deviatoric stress levels can be accepted for MC soils compared to HS soils, since pore pressures in the HS and HSsmall models result a decrease of effective isotropic stress and consequently a lower Mohr-Coulomb failure limit. If this feature explains the much lower acceleration response peaks for the HSsmall soil was analyzed by comparing the results of drained and undrained type A analysis for the clays. It was concluded that an almost similar response was obtained, so pore pressure generation cannot be considered governing in this sense.

According to various empirical relations (e.g. (Alpan, 1970) and others) the ratio G_0 / G_{ur} varies with soil type. In general a higher ratio is obtained for clay than for sand. In this study the selected ratios are 6.9, 6.9 and 1.8 for the C1 clay, C2 clay and S3 sand layer respectively. Values applied for $\gamma_{0.7}$ are based on empirical relationships (Benz, 2006; Stokoe et al, 2004) were it is considered a function of plasticity index and overconsolidation ratio for clays and a function of estimated relative density for sands. Since the clays typically have a higher G_0 / G_{ur} ratio and threshold shear strain $\gamma_{0.7}$ compared to sand, it was doubted whether these input parameter may be affecting the blocked shape of accelerograms as obtained for clays. A dependence of the blocked shape on these parameters was indeed found. Generally lower ratio G_0 / G_{ur} and a higher value $\gamma_{0.7}$ smoothen the blocked shape, which is a consequence of the less sudden changes of the system stiffness properties when the deviatoric stress rate tensor is changes sign. However in the complete range of reasonable (empirically derived) values for G_0 / G_{ur} and $\gamma_{0.7}$ the HSsmall model results the typical acceleration responses, from which is concluded that the response sensitivity to these parameters is limited and they are not the critical factor in the unrealistic responses obtained.

The HSsmall model as initially applied to the soils includes stress dependency of stiffness. In order judge the effect of the resulting very low soil stiffness near seabed, the stress dependency of stiffness was removed by setting stress dependency power m=0. Setting stress dependency power m=0 for the HSsmall and HS models relatively most affects the top clay layer, since the lower limit stress dependent soil stiffness ratio:

$$\frac{actual\ soil\ stiffness}{reference\ soil\ stiffness} = \frac{c\ \cos(\varphi)}{c\ \cos(\varphi) + p^{ref}\ \sin(\varphi)} \approx 0.05$$

is not longer present in the model for very shallow soil material.

A comparison of the HSsmall, basic HS and the Mohr-Coulomb models was made in order to judge the effects of the small strain overlay model combined with stress dependent stiffness development over depth. The results are shown in Figure 7.34 and Figure 7.35 for seabed level and the clays C1 and C2 layer interface for time history interval 5-6 sec of the Duzce random signal.

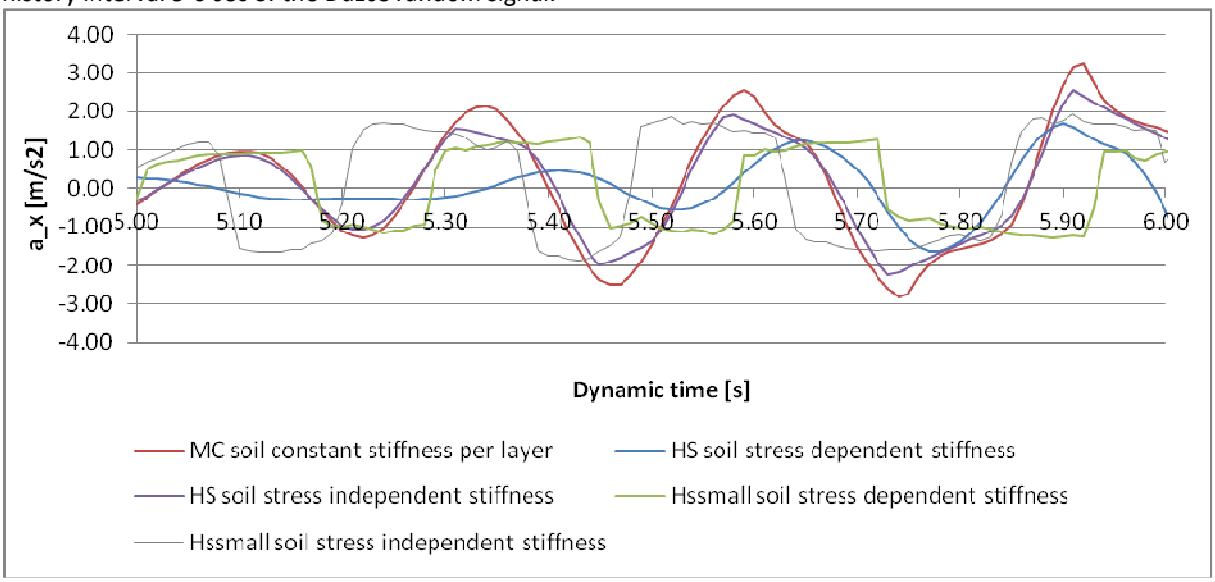

Figure 7.34: Horizontal accelerations at seabed level, relation with soil model and stress dependency

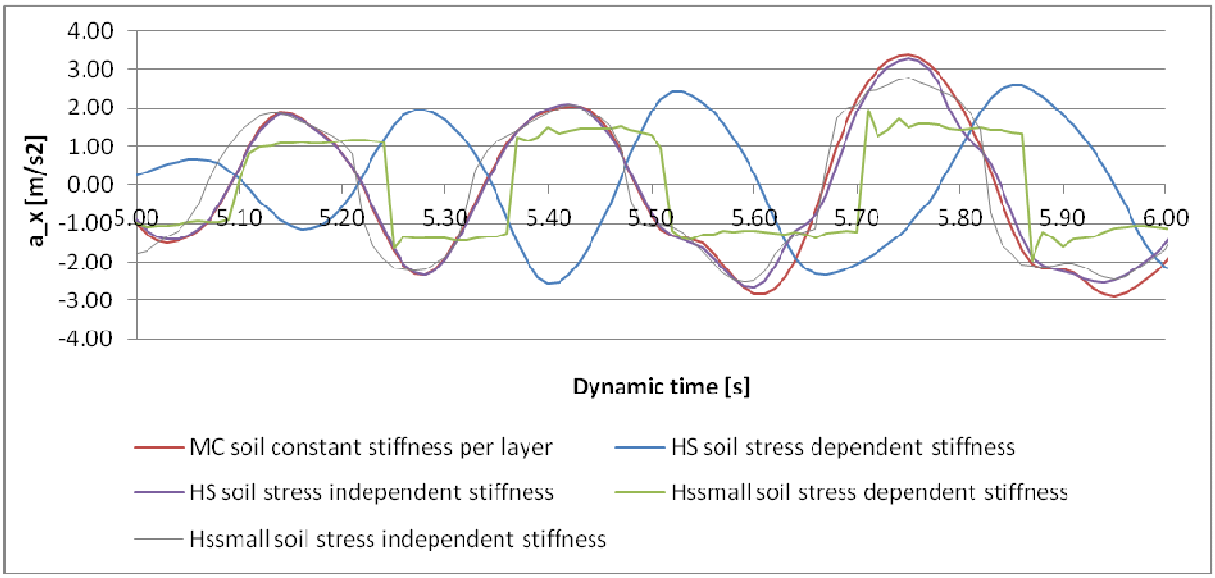

Figure 7.35: Horizontal accelerations at C1-C2 interface, relation with soil model and stress dependency

As shown, the typical blocked behaviour was not obtained for the HS and MC model, that match very well for overconsolidated soil, provided that E_{ur} is taken equal to elastic Young's modulus applied in MC model and the stress dependency of stiffness artificially removed from the constitutive model. When the stress dependency is included in the HS model, it gives accelerograms different from the accelerograms obtained for MC and LE modelled soils. A phase shift is obtained and lower acceleration amplitudes result, which are directly a result of the different stiffness. However, the sudden jumps in accelerations are not obtained. Figure 7.34 and Figure 7.35 also show the HSsmall soil response accelerograms where stress dependent stiffness is not included. Compared to the stress dependent HSsmall and HS and MC soil models one may conclude:

- The unrealistic sudden acceleration development is far less pronounced when the HSsmall model stiffness are made stress independent.
- At seabed level still some sudden changes in accelerations are obtained, but at the C1-C2 layer interface a perfectly smooth response is obtained.

- For the considered subinterval of the seismic event acceleration response amplitudes are converging for the HSsmall, HS and Mohr-Coulomb soil models when stress dependent stiffness is not included.

For the initial analysis with HSsmall soil including stress dependent stiffness, the sudden developing accelerations result almost 'blocked' accelerograms at seabed level, where at the C1-C2 layer interface this typically shaped responses seem to be somewhat smoothened. At the C2-S3 layer interface the effect was not observed at all, indicating the much stiffer sand layer to govern the local response at this depth. For the HSsmall soil analysis without stress dependent stiffness, sudden changes obtained in accelerograms are less extreme at seabed and not observed at all at the C1-C2 and C2-S3 layer interfaces.
These observations imply that the unrealistic shaped accelerograms are a result of the operation of HSsmall soil model for soft soils in dynamics, were it seems to give most unrealistic results for the very soft material near seabed. However the region where unrealistic responses are obtained seem to reach much deeper levels in the clay layers.

Based on observations presented in the preceding, it seems that the conceptually very attractive HSsmall constitutive model has its typical problems in dynamics, that are resulting from stress dependent very low stiffness for top soil layers combined with the stiffness reset of the small strain overlay model. This reset of stiffness may be realistic for static problems, but in dynamics stiffness development in reality needs a finite time interval, which is not included in the HSsmall model and consequently results the unrealistic development of accelerations. However, the HSsmall features of including hysteretic damping, damping developing over time as a function of strain amplitude, small strain stiffness and stress dependent stiffness, as obtained for real soils still make the HSsmall model very attractive for dynamic geotechnical problems and consequently a solution for the problem obtained is sought.
Considering possible solutions for the problem obtained and variations already studied, it is concluded that any reasonable variations in HSsmall soil parameters for soft soils do not overcome the problem obtained. An attempt was made to limit the problem by making only the top soil layer stiffness parameters stress independent and keep the attractive stress dependent properties for deeper soil layers. For the top layer then averaged stiffness parameters over depth are applied. The subinterval 0 – 12 sec. of the resulting acceleration response at the C1-C2 layer interface is presented in Figure 7.36.

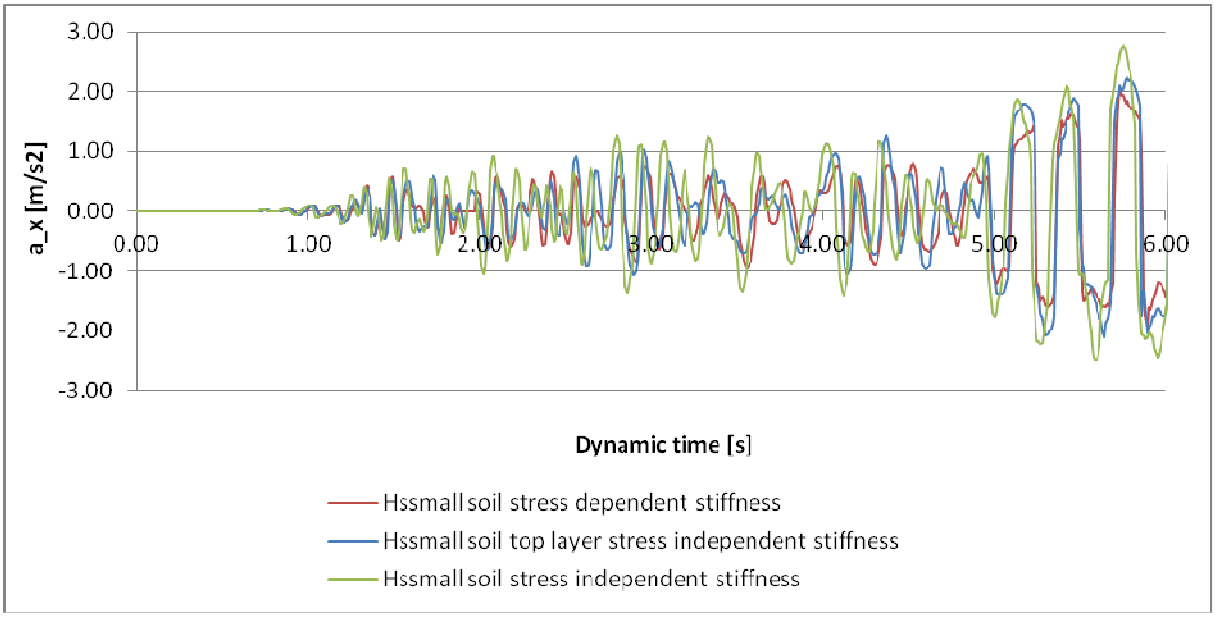

Figure 7.36: Horizontal accelerations at C1-C2 interface, HSsmall soil with only top layer stress independent stiffness

Although more realistic accelerograms are obtained compared to the models were all soil layers have stress dependent stiffness parameters, again the unrealistic sudden changes in acceleration level are found in the response for both clay layers. This observation implies that sudden changes obtained in accelerograms at greater depths are not dominated by propagating waves generated near seabed, but may also result from local unrealistic HSsmall model behaviour.

7.2.3.3 Conclusions regarding soil modelling in dynamic analysis

Unrealistic ("blocked") acceleration responses obtained by applying the HSsmall soil constitutive model were found to be the direct result of stiffness reset at principal strain rate reversals. The effects of this stiffness update seem to be a function of interaction of the small strain overlay model (with its input parameters) and the stress dependency of stiffness can cause unrealistic accelerograms. Improvement of the HSsmall method for dynamics is recommended, where implementation of a mobilisation time for stiffness reset probably is the solution closest representing reality.

Consequently it might for this moment be more convenient to remove the stress dependent stiffness feature from the HSsmall model for very weak soils. This can be done by artificially setting stress dependency power m=0. By this means the attractive features of the HSsmall model related to hysteretic damping and small strain stiffness development can be kept in the analyses. If required a soil profile may then be subdivided into more layers, in order to overcome errors resulting from an oversimplification of the soil profile when stress dependence of stiffness is not included anymore.

As an alternative linear elastic, Mohr-Coulomb or Hardening Soil constitutive models can be used for dynamic analysis. However it is noted that Rayleigh damping as is to be applied in these models must be carefully selected since it is by definition frequency dependent and the level is fixed for the total duration of the seismic signal, irrespective of the motion intensity. Generally the viscous damping will be most accurate for saturated permeable soils for which damping is governed by relative motions of pore water and soil particles. Damping resulting from this phenomena is related to relative velocities and therefore relatively well described by viscous damping. However, for dry or impermeable soils including viscous damping may be considered less appropriate.

Mohr-Coulomb and Hardening Soil models include plasticity effects and hence will conceptually represent actual soil behaviour more accurate compared to linear elasticity. However, their disadvantages are the much higher computational effort and no inclusion of hysteretic damping. Consequently in this study the dynamic jetty analysis will be performed for the soil deposit modelled by HSsmall soil (with stress dependency power m=0 for the top clay layer) and the simplified and computationally much more convenient linear elastic soil. To this end Rayleigh damping added to the HSsmall soil will be assumed at 1-2% critical (paragraph 4.6.4.4) and Rayleigh damping for the linear elastic soil will be estimated based on equivalent linear frequency domain analysis as was done for the free field dynamic analysis.

7.2.4 Operation Plaxis 3D dynamics module (Release 2011.01 February 2012)

The operation of the new Plaxis 3D dynamic module was verified initially for the 3 Hz harmonic signal for sake of simplicity and computational convenience, were linear elastic material behaviour with 5% critical added Rayleigh viscous damping was applied. A plane strain configuration for a slice of soil was modelled in Plaxis 3D by setting y_{min} and y_{max} boundaries to plane strain boundaries and x_{min} and x_{max} boundaries to default Plaxis viscous boundaries. Figure 7.37 presents the seabed level acceleration and displacement responses for the Plaxis 2D and 3D models, which give almost identical results. It can be concluded that no significant 3D effects disturb the free field response for bedrock motions applied in the x-direction of the x-z plane strain model configuration.

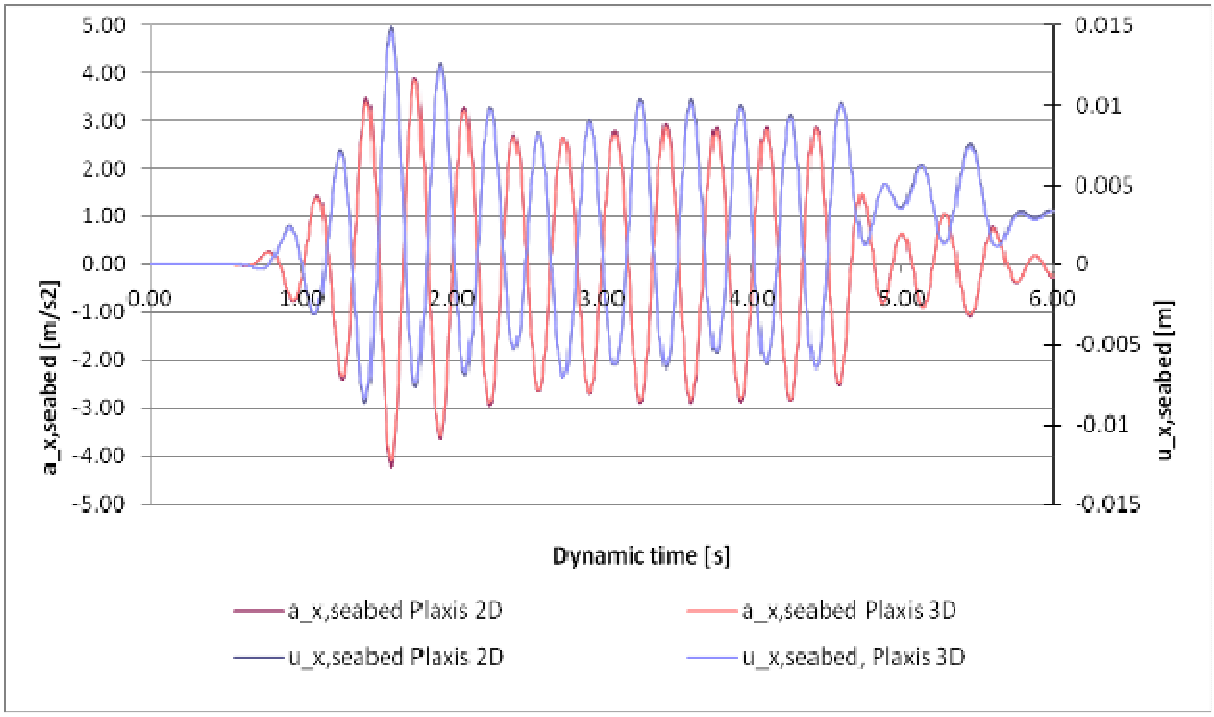

Figure 7.37: Plaxis 2D and Plaxis 3D site response for a 3 Hz harmonic bedrock excitation

Subsequently the free field responses due to the random Duzce bedrock signal obtained from the Plaxis 2D and 3D dynamic modules were compared. For computational convenience again linear elastic material was applied, with Rayleigh damping ratios according to Table 7.3. Again a perfect fit for the Plaxis 2D and 3D modules was found, providing confidence in proper operation of the very new Plaxis 3D dynamics module.

The good fit of the 2D and 3D dynamics modules provide good confidence in the performance of the new released 3D dynamics module and so allows to perform coupled soil deposit +jetty structure dynamic analysis with Plaxis 3D. It is however noted that free field analysis with the HSsmall soil constitutive model is not performed in Plaxis 3D because of time limitation, which however would be recommended for a future project.

7.3 Jetty simplified dynamic analysis according to Fajfar N2-response spectrum method

The peak horizontal bedrock accelerations that are used as a starting point in the N2- response spectrum procedure are 0.7g and 1.02g for the earthquake intensities related to 10% and 2% probability of exceedance in 50 years respectively. applied at bedrock.

The resulting Turkish/ISO regulations response spectrum for the 1.02g soil deposit peak acceleration is shown in Figure 7.38, where also the reduced response spectra for ductility levels 1.1, 1.5, 2.0, 3.0 and 5.0 are plotted as an indication. The response spectrum shown below is plotted in the common acceleration-displacement response spectrum (ADRS) -format, relating spectral accelerations to spectral pseudo-displacements by:

$$u(t) = Ue^{i\omega_0 t} \rightarrow \ddot{u}(t) = -\omega_0^2 Ue^{i\omega_0 t} \rightarrow \left|\frac{S_u}{S_{\ddot{u}}}\right| = \frac{1}{\omega_0^2} = \frac{T_0^2}{4\pi^2} \qquad (7.4)$$

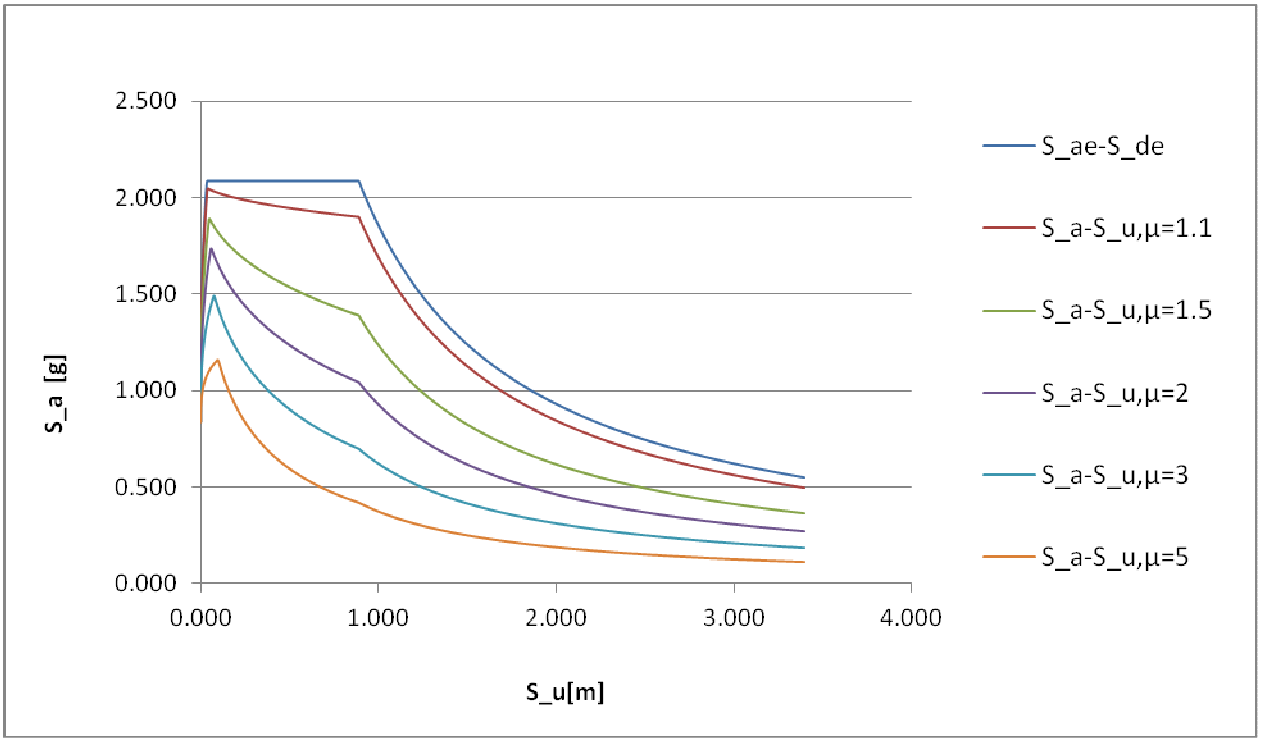

Figure 7.38: ISO normal response spectrum for bedrock acceleration 1.02g in ADRS format

It is noted that this ADRS representation is purely a tool in graphically representing the capacity and demand in the same format, where it is not really contributing to the analytical solving procedure.
The key item in the simplified dynamic analysis is the nonlinear pushover curve, from which the fundamental frequency for the linear range and consequently the load are estimated and the structure's ductility capacity is derived. The pushover curve is derived for lateral jetty analysis in Plaxis 3D subjected to an increasing lateral load vector proportional to $\underline{F} = \underline{m}\underline{\varphi}a_{ground}$, where $\underline{m}$ is the structures simplified mass vector and $\underline{\varphi}$ is the normalized fundamental mode shape vector. The single point representation of the global structure pushover characteristics is presented in Figure 7.39.

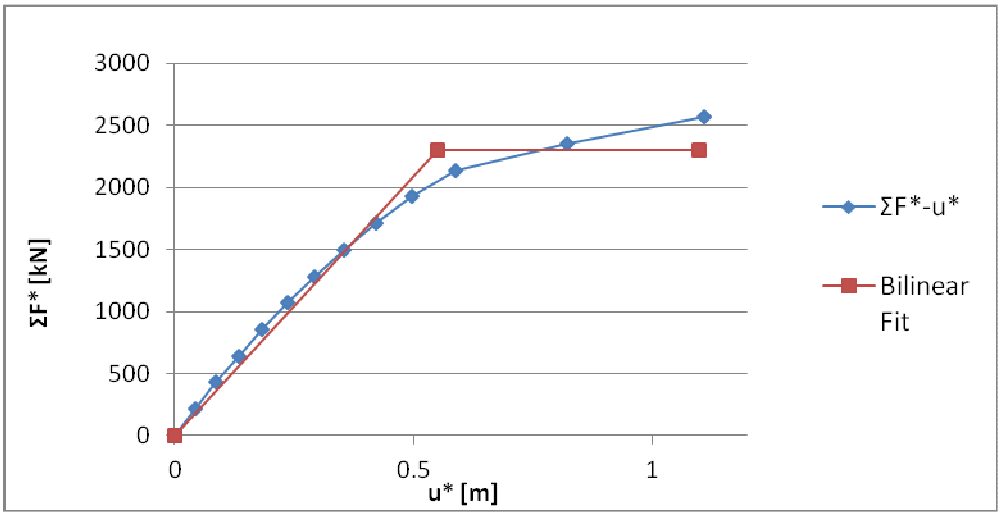

Figure 7.39: Single point representation of jetty global lateral load-deformation characteristic

A bilinear approximation of nonlinear global pushover characteristic is then made, from which initial stiffness and equivalent mass the natural period of the equivalent SDOF system can be estimated to be $T_0 = 1.26\,s$.
Subsequently a coupling of seismic demand, reduction of demand by ductility related required displacement demand is resulting the design global jetty displacement demand. This can be graphically represented in the

ADRS-format as shown in Figure 7.40 for the 1.02g earthquake with spectral shapes corresponding to deep foundations according to ISO 19901:2004 – p14. For convenience the graphical representation of other load levels and spectral configurations is not presented herein. The related results are summarized in Table 7.4 and details can be found in appendix VIII.

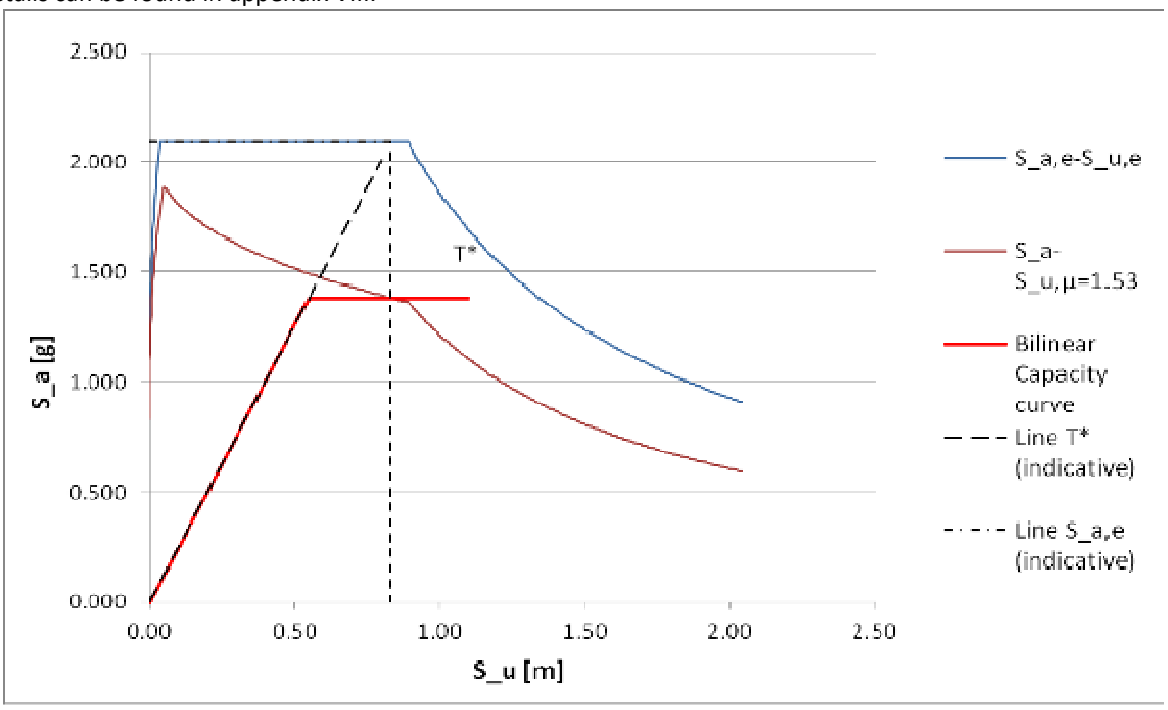

Figure 7.40: Graphical representation of N2-method solution for seismic displacement demand

Table 7.4: Summary of required ductility and displacement demands for the different seismic load configurations

$a_{peak\ bedrock}$	Response spectrum characteristics	Ductility demand μ	Jetty deck dynamic displacement demand
[g]		[-]	[m]
0.7	Soil class E, normal spectrum	0.96 (elastic range)	0.62
0.7	Soil class E, deep foundations spectrum	0.72 (elastic range)	0.47
1.02	Soil class E, normal spectrum	1.53	0.99
1.02	Soil class E, deep foundations spectrum	1.17	0.76

According to the pushover characteristics of the system now local response quantities can be determined, which results pile head bending moments of 10200 and 11500 kNm for the 0.7g and 1.02g earthquake signal respectively.

As noted before, single mode simplified dynamic approaches rely on the assumption that the structure response can be assumed to be on the single fundamental mode. Literature and seismic standards generally recommend to take into account the number of modes up to a cumulative effective modal participating mass percentage of 90%. For the jetty structure transverse cross-section the modal masses where identified based on eigenvalue analysis of the equivalent beam on Winkler foundation model in Seismostruct, with initial (linearized) stiffness. The results are shown in Table 7.5.

Table 7.5: Jetty transverse cross-section modes and effective participating modal mass

Mode number	f_n	Effective modal mass	Cumulative effective modal mass
[-]	[Hz]	[-]	[-]
1	0.84	0.556	0.556
2	4.14	0.167	0.724
3	5.78	0.051	0.775
4	8.62	0.130	0.905

The results show that considering the threshold value of 90%, the jetty structure response (see 4.5.3) may not be assumed to be well represented by the fundamental mode only. Consequently the single mode simplified dynamic analysis results might be somewhat non-conservative compared to results obtained from dynamic analysis, which however will be strongly related to the frequency content of the seismic input signals adopted in dynamic analysis. The sensitivity of obtained deformation demands to the included number of modes in simplified dynamic analysis of jetty structures is recommended for further research.

7.4 Uncoupled and coupled site and jetty nonlinear dynamic time domain analysis

The transverse jetty responses from dynamic analysis are presented in this chapter. The focus herein is on the jetty horizontal displacements at deck, seabed and pile tip level, the pile head bending moment development of the outer right pile (pile 1), relative horizontal displacements of deck and seabed level to pile tip level (dynamic drift/residual drift), relative displacements of pile at seabed and surrounding soil at seabed (pile-soil interaction) and the spectral representation of accelerations.
Both two different uncoupled dynamic analysis approaches and fully coupled dynamic analysis were performed:

- Uncoupled dynamic analysis of structure in Seismostruct, were Winkler support node input signals are determined from equivalent linear site response analysis
- Uncoupled dynamic analysis of structure in Seismostruct, were Winkler support node input signals are determined from nonlinear Plaxis 2D site response analysis
- Coupled nonlinear dynamic analysis of soil deposit slice + jetty cross-section in Plaxis 3D

The system responses were calculated for Duzce and Kocaeli2 input signals scaled to 0.7g and 1.02g peak bedrock accelerations.

Additionally a single coupled 3D analysis was performed for the Kocaeli2 0.7g signal with a linear elastic soil included. This analysis appeared to result responses almost identical to the uncoupled nonlinear structure + equivalent linear soil analysis except from drifts resulting in permanent p-y elements. Because of its large computational demand but limited added value it was not repeated for other signals and this approach is not further taken into consideration.

The Plaxis 3D coupled analyses were performed for a 1.75 m slice of soil including three half jetty piles so advantage is taken of symmetry to limit the finite element model size. A model width of 300 m was adopted which was sufficient with respect to boundary disturbances based on the free field model calibration. For more details regarding the model configuration one is referred to paragraph

Dynamic analysis results are included in appendix IX, where this paragraph does provide a summary and the important observed phenomena with explanatory figures.

7.4.1 Summary of acceleration, displacement and pile head bending moment response quantities

Table 7.6 shows the extreme relative deck – pile tip displacements and pile head bending moments observed from both uncoupled and coupled dynamic analysis during the earthquake.

Table 7.6: Dynamic peak displacements and pile head bending moments

Signal	Response quantity		Uncoupled analysis, equi. lin. soil	Uncoupled analysis, nonlinear soil	Coupled analysis, nonlinear soil
			Matlab + Seismostruct	Plaxis 2D + Seismostruct	Plaxis 3D
Duzce 0.7g	$a_{x,min,deck}$	[m/s^2]	-9.24	-7.52	-6.78
	$a_{x,max,deck}$	[m/s^2]	7.65	6.05	6.44
	$\Delta u_{min,\ deck\text{-}pile\ tip}$	[m]	-0.06	-0.17	-0.15
	$\Delta u_{max,\ deck\text{-}pile\ tip}$	[m]	0.06	0.08	0.05
	$M_{y,min,pile\ head}$	[kNm]	-3693	-3158	-2295
	$M_{y,max,pile\ head}$	[kNm]	3344	2775	2870
Duzce 1.02g	$a_{x,min,deck}$	[m/s^2]	-11.32	-8.39	8,71
	$a_{x,max,deck}$	[m/s^2]	9.35	6.85	7.96
	$\Delta u_{min,\ deck\text{-}pile\ tip}$	[m]	-0.08	-0.17	-0.23
	$\Delta u_{max,\ deck\text{-}pile\ tip}$	[m]	0.08	0.16	0.06
	$M_{y,min,pile\ head}$	[kNm]	-4536	-3966	-2996
	$M_{y,max,pile\ head}$	[kNm]	4078	2915	3662
Kocaeli2 0.7g	$a_{x,min,deck}$	[m/s^2]	-20.21	-9.05	-15.55
	$a_{x,max,deck}$	[m/s^2]	18.82	11.52	13.41
	$\Delta u_{min,\ deck\text{-}pile\ tip}$	[m]	-0.67	-0.64	-0.55
	$\Delta u_{max,\ deck\text{-}pile\ tip}$	[m]	0.63	0.90	0.59
	$M_{y,min,pile\ head}$	[kNm]	-11131	-9030	-6198
	$M_{y,max,pile\ head}$	[kNm]	11186	7440	6950
Kocaeli2 1.02g	$a_{x,min,deck}$	[m/s^2]	-27.04	-13.43	-11.95
	$a_{x,max,deck}$	[m/s^2]	22.29	13.45	11.67
	$\Delta u_{min,\ deck\text{-}pile\ tip}$	[m]	-0.89	-1.08	-0.95
	$\Delta u_{max,\ deck\text{-}pile\ tip}$	[m]	2.16	0.73	0.52
	$M_{y,min,pile\ head}$	[kNm]	-13094	-7601	-7112
	$M_{y,max,pile\ head}$	[kNm]	11484	10317	8304

Dynamic response sensitivity to input signal selection can based on Table 7.6 be considered very high, since the peak dynamic response quantities for the Kocaeli2 signal are by far exceeding the Duzce responses. The importance of considering a large number of seismic input signals is evident and seems to be a critical issue when dynamic analysis is used as a tool for design.

According to Table 7.6 one may conclude that with the uncoupled approach based on equivalent linear analysis of the soil results the most extreme horizontal deck acceleration levels and the highest pile head bending moments. These higher response quantities are a direct consequence of higher soil deposit acceleration levels for the equivalent linear soil in the highest intensity part of the seismic event. Figure 7.41 shows the much higher energy content near the jetty fundamental frequency (0.8 Hz) for the case of equivalent linear soil by presenting the FFT of seabed soil accelerations. The coupled and uncoupled nonlinear approach show to be very similar, but reaching much lower peak spectral values, where the uncoupled analysis shows lower spectral values in the high frequency range due to the stiffness proportional dashpot coefficients filtering out the higher frequency content. These conclusions comply to all analysis performed (see appendix IX)

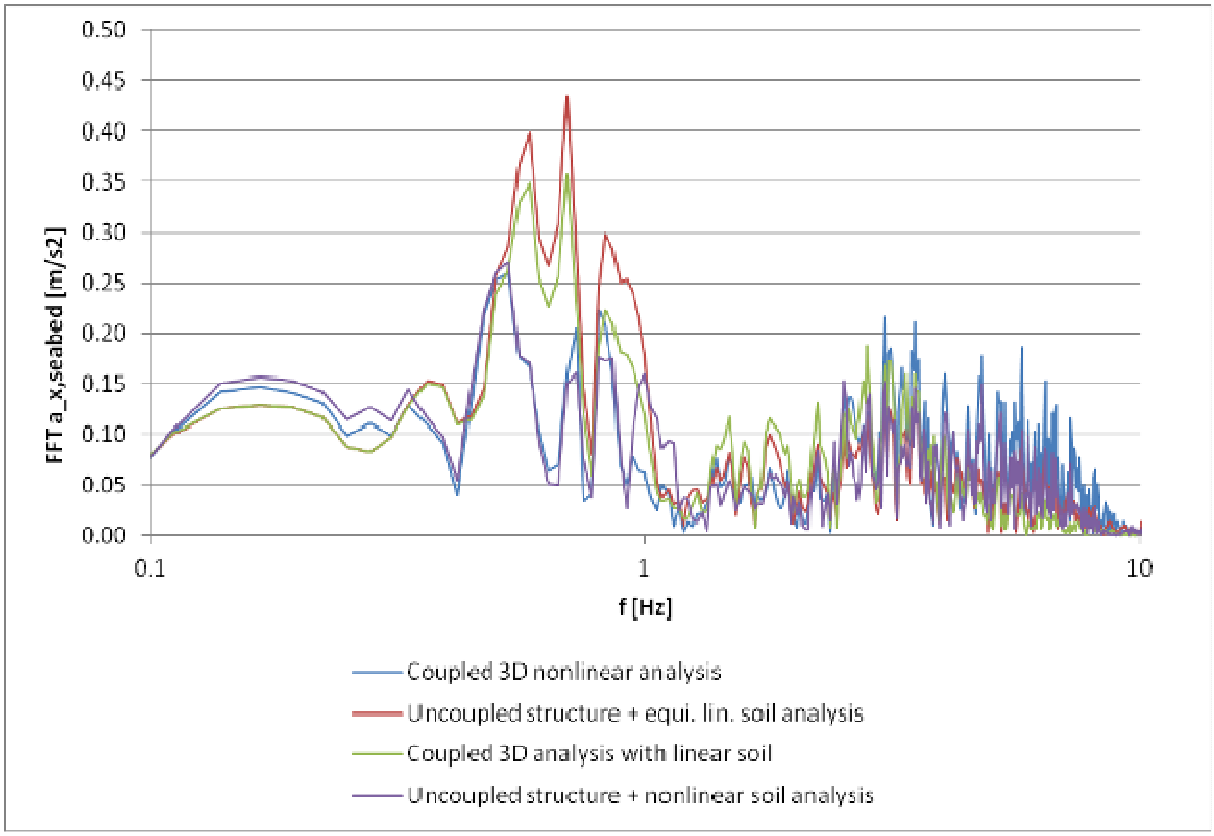

Figure 7.41: FFT jetty pile at seabed horizontal acceleration spectra for Kocaeli2 0.7g input signal

According to Table 7.6 differential horizontal jetty deck – pile tip displacement extremes obtained over the signal time history are not systematically higher when one follows the uncoupled approach with equivalent linear soil deposit analysis. However, as will be shown in the next paragraph dynamic displacement amplitudes obtained from uncoupled analysis with equivalent linear soil analysis are typically higher where this is not true for overall peak displacements, since no permanent deformations of the soil stratum are included when soil is assumed to respond equivalent linear.

According to performance based design principles, the residual response quantities after an earthquake event are also of importance, since they related to the post-earthquake serviceability performance of the structure. Table 7.7 shows the residual relative horizontal displacements jetty deck – pile tip obtained from the performed analysis.

Table 7.7: Residual displacements and pile head bending moments

Signal	Response quantity		Uncoupled analysis, equi. lin. soil	Uncoupled analysis, nonlinear soil	Coupled analysis, nonlinear soil
Duzce 0.7g	$\Delta u_{residual,\ deck\text{-}pile\ tip}$	[m]	0	-0.12	-0.11
	$M_{y,residual,pile\ head}$	[kNm]	-43	568	708
Duzce 1.02g	$\Delta u_{residual,\ deck\text{-}pile\ tip}$	[m]	0	-0.11	-0.18
	$M_{y,residual,pile\ head}$	[kNm]	-51	294	879
Kocaeli2 0.7g	$\Delta u_{residual,\ deck\text{-}pile\ tip}$	[m]	0.07	0.55	0.25
	$M_{y,residual,pile\ head}$	[kNm]	521	-3231	-1440
Kocaeli2 1.02g	$\Delta u_{residual,\ deck\text{-}pile\ tip}$	[m]	-0.26	0.39	0.21
	$M_{y,residual,pile\ head}$	[kNm]	1494	-2023	-1854

In relation to Table 7.7 it is noted that residual displacements of the system for the uncoupled approach based on equivalent linear site response analysis are resulting from residual p-y spring displacements and residual pile head moments/rotations only, where the other two approaches also allow permanent deformation of the soil stratum to affect significantly the post-earthquake state of the system.

A remarkable observation from Table 7.7 can be made regarding the residual drifts resulting from the Kocaeli2 signal for the 0.7g and 1.02g intensities. The higher intensity signal namely is resulting lower residual drift. An explanation was found from Figure 7.42 and Figure 7.43, that show the drift time histories for both intensities. Apparently the higher intensity signal results development of permanent soil deformations and consequently pile drifts fist in the negative direction and then in the positive direction, where the lower intensity signal mainly develops permanent drift in the positive direction. Consequently the lower intensity signal according to these analysis results a higher post-earthquake drift.

7.4.2 Displacement time histories and shifts of system equilibrium position

As was concluded in the previous paragraph, the conservatism of displacement level extremes cannot not directly be related to the analysis approach applied. This conclusion is supported by Figure 7.42 and Figure 7.43, that show the differential jetty deck – pile tip horizontal displacements time histories obtained.

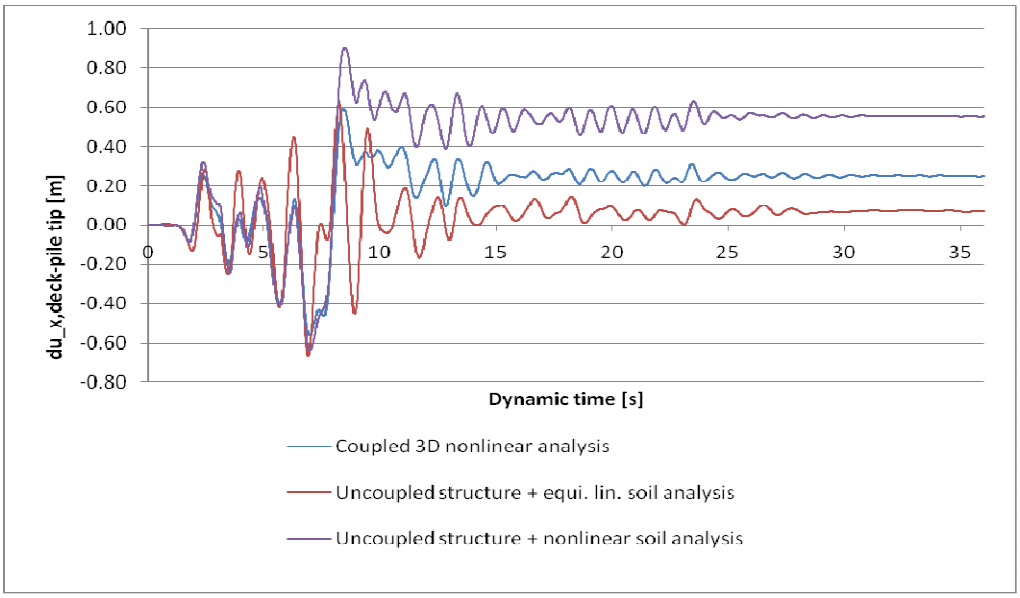

Figure 7.42: Relative horizontal displacement time history deck – pile tip, Kocaeli2 0.7g signal

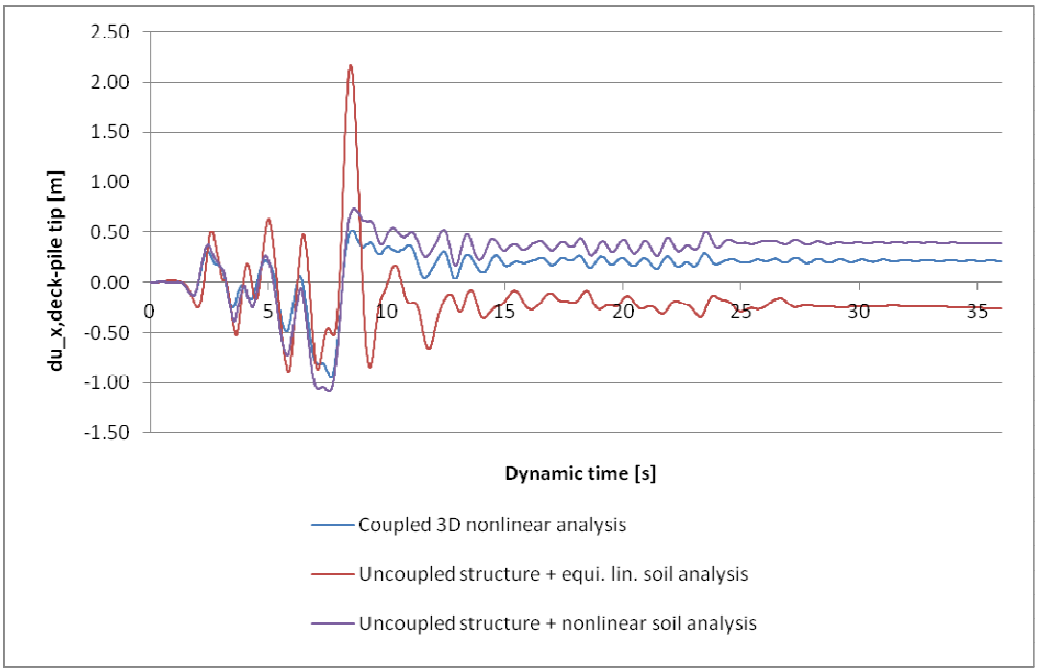

Figure 7.43: Relative horizontal displacement time history deck-pile tip, Kocaeli2 1.02g signal

The displacement responses obtained from coupled and uncoupled analysis based on nonlinear soil deposit analysis initially are corresponding very well. At the onset of very high shaking intensities a different in shift of equilibrium position due to different global soil failure is obtained for the coupled and uncoupled nonlinear analysis, which then becomes the new equilibrium position of the vibrating system. Then after development of the different drifts again almost synchronous development of displacements is observed. The typical good correspondence of coupled and uncoupled nonlinear analysis, expect from the sudden developments of different drifts was found for all analysis performed (see appendix IX). The synchronous development of jetty displacements for phases of less strong shaking provides a good confidence in the performance of the uncoupled Winkler approach with nonlinear soil analysis for lower shaking levels without significant global soil failure.
The observed different drifts resulting after onset of global soil failure is explained by the fact that the piles support the soil and hence reasonably a different permanent deformation will develop.

The figures clearly show how soil failure and related permanent soil stratum deformations may affect the jetty displacements along the coupled analysis and uncoupled structure +nonlinear soil deposit analysis. This effect was found to be strongly dependent on the input signal, and according to these figures even on the peak acceleration level to which the signal is scaled. Observations after past earthquakes confirm the residual drifts resulting from soil failure to occur and design guidelines like PIANC impose limit values to these residual displacements for designers. Consequently it can be concluded that simplified dynamic analysis procedures may be useful for preliminary design stages but are not sufficient for final design stages as they do not consider residual displacements and related effects of global soil failure which typically is of importance because of the deep foundation. The extreme sensitivity of the structure and soil deposit permanent deformations to the selected seismic signal and intensity found in this study however make clear that dynamic analyses need to be performed for a much larger number of input signals in order to be able to more reasonably estimate the expected permanent deformations. This conclusion is consistent with the generally larger required minimum number of 7 (ISO recommendations, Turkish Technical Seismic Recommendations) and 3 (Eurocode) earthquake time history records.

Figure 7.42 and Figure 7.43 also clearly show the uncoupled approach based on equivalent linear analysis to result a much different development of displacements in time, with the strongest differences around onset of global soil failure in the nonlinear models where this is not included for equivalent linear soil. Consequently significantly different dynamic drifts are observed, that are not believed to be very realistic since based on the nonlinear models the soil capacity mobilized to allow for these extreme motion levels is exceeds reasonable soil strength.

For the uncoupled nonlinear analysis the soil deposit global plastic deformations are imposed to the structure with Winkler foundation system. Then the structure responds to these imposed deformations, allowing for local soil-structure interaction by p-y springs, but not affecting the development of the global soil deformations. Here is the fundamental difference with the coupled analysis where global soil, local soil and structure response are interacting. This interaction of jetty and soil becomes apparent from Figure 7.44 that clearly shows how soil deposit displacements are affected by pile displacements.

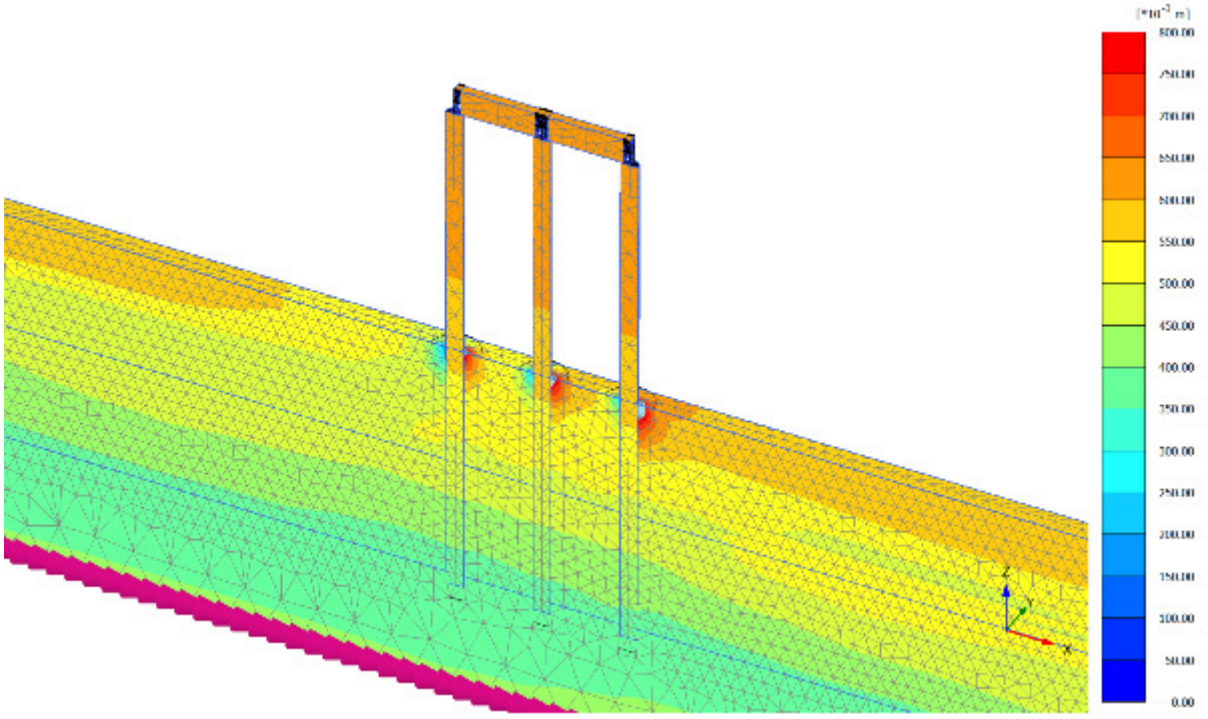

Figure 7.44: Horizontal displacement contours, influence zone interaction of pile and soil, Kocaeli 1.02g signal at 18.00 s

The differences obtained in permanent structure drift and permanent soil deformations from the coupled and uncoupled analysis probably are a consequence of this fundamental difference. However more future study regarding the pile, soil and interface displacement and acceleration developments in these strong motion phases is required in order to investigate the precise effects of coupled/uncoupled interaction and Plaxis 3D interface performance. The sensitivity of the jetty displacement response to variations in Winkler dashpot parameters of the uncoupled model was found to be low. The development of gapping in Plaxis needs special attention and its effect on the results is recommended for future study. The current Plaxis 3D interfaces are not accounting for gap closure, resulting accumulating soil deformations surrounding the piles as shown in Figure 7.45.

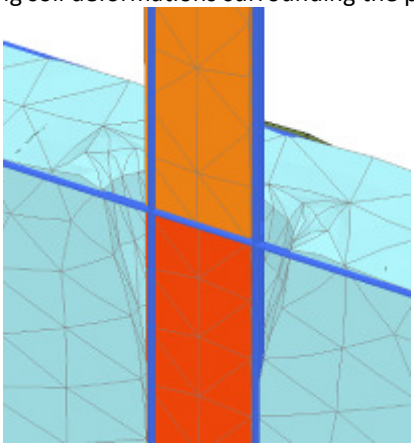

Figure 7.45: Gapping of pile soil interface in Plaxis 3D

7.4.3 Kinematic pile loading

When one considers the bending moments in piles due to single inertial loading, the resulting pile deformations and bending moments develop as for inertial loading pushover analysis. However, in dynamic analysis the kinematic pile loading contribution is included as well. Consequently bending moments and pile displacements will not be coupled by the fundamental mode shape as was assumed in simplified dynamic analysis. Figure 7.46 shows the deformed pile shapes for four points in time for both coupled and uncoupled nonlinear analysis. The results for both analyses show the same trend in pile deformation shapes, where for the uncoupled approach higher drifts are observed. For the 5.6 s and 8.47 s point in time the soil deposit permanent deformations have

not developed and the deformation shape of the jetty is close to the fundamental mode shape. Kinematic pile loading effects appear limited for these points in time since the first mode shape of the soft soil layers is not pronounced in the pile deformation shape. This may be explained by the very soft soil conditions and the relatively stiff pile. However for the 12.00 s and 36.00 s point in time the permanent soil deformations are clearly present in the pile deformations as well. Hence may be concluded that for the typical situation considered with stiff end-bearing piles in a soft soil deposit, kinematic pile loading by permanent soil deformations rather than dynamic soil deformations strongly affect the jetty displacement response. It is noted that based on literature the effects of dynamic kinematic pile loading will be more pronounced for layered soils with strongly varying soil stiffness along the pile shaft.

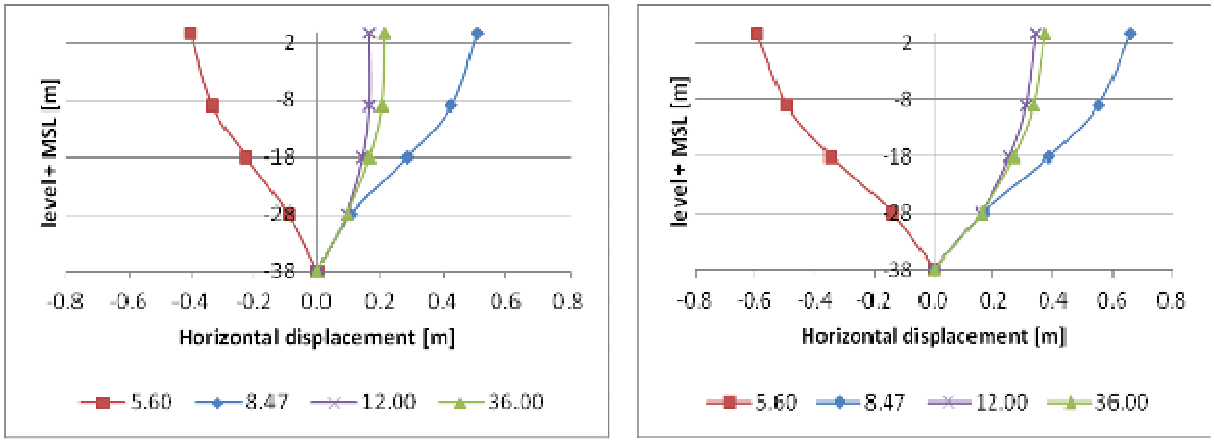

Figure 7.46: Pile deformation shapes for Kocaeli2 1.02g signal at dynamic time 5.60 s, 8.47 s, 12.00 s and 36.00 s, *left:* results coupled analysis, *right:* results uncoupled analysis with nonlinear soil deposit analysis

The significance of kinematic pile loading when global soil failure is observed would be interesting for further study. Especially the development of bending moments along the pile would be of interest,

7.4.4 Conclusions dynamic jetty analysis

Based on the preceding paragraphs it is concluded that:

- Coupled nonlinear analysis and uncoupled nonlinear analysis result reasonably synchronous responses with respect to both horizontal displacements and pile head bending moments, except from a difference in jetty drift obtained after global soil failure. Whether this systematic difference in drift is directly related to the coupled vs. uncoupled approach, or if other model parameters as for example Plaxis 3D interfaces might affect this behaviour is recommended for future study.
- From the analysis performed is becomes clear that global soil failure and related permanent structure drifts may have a significant effect on the performance of the structure during and after an earthquake. This conclusion is confirmed by observations done after past earthquakes. From this perspective both the coupled analysis and the uncoupled analysis with nonlinear soil included are attractive because a much better insight in effect of soil failure is obtained.
- Since the shifts in drift at global soil failure do not systematically result in higher deformation responses for either the coupled or the uncoupled dynamic analysis approach, not a single one can be selected which is the most conservative. Investigation of their performance for a higher number of input signals and different jetty structure and soil deposit configurations is recommended in order obtain a better insight.
- At this moment Plaxis is implementing embedded pile elements that result 2.5D approach when applied to 2D plane strain soil models. To the authors best knowledge the performance of these embedded piles for lateral pile loading however is still poor, which was the reason why they were not included in this study. However when a better performance for lateral loading can be achieved embedded pile elements probably may be very useful for practical dynamic soil-structure interaction problems.

7.5 Conclusions regarding jetty transverse seismic analysis

Table 7.8 and
Table 7.9 show the representative jetty response quantities for respectively the 0.7g and 1.02g level earthquake that were found for the different analysis approaches considered. The most conservative values obtained from dynamic analysis for the Duzce and Kocaeli2 signals are included in these tables. Corresponding minor damage and no-collapse performance requirements are also given as far as they are quantified in codes.

Table 7.8: Level 1 earthquake response

Design parameter	Units	Performance requirement	Simplified dynamic analysis results	Uncoupled dynamic analysis, equi. lin soil	Uncoupled dynamic analysis, non. lin soil	Coupled dynamic analysis, non. lin soil
			Plaxis 3D + response spectrum procedure	Matlab + Seismostruct	Plaxis 2D + Seismostruct	Plaxis 3D
Peak dynamic displacement demand	[m]	According to client or serviceability requirements of installations located at the jetty	0.62	0.67	0.90	0.59
Residual displacement	[m]	Pianc: res. tilt = 2° → $u_{x,residual}$ = 0.76m	-	0.07	0.55	0.25
Plastic hinge material strains	[-]	0.008	$M_{y,head}$=10200 kNm, ε=0.0012< ε_y	$M_{y,head}$=11186 kNm, ε=0.011	$M_{y,head}$=9030 kNm, ε=0.0011< ε_y	$M_{y,head}$=6950 kNm, ε=0.0008< ε_y

Table 7.9: Level 2 earthquake response

Design parameter	Units	Performance requirement	Simplified dynamic analysis results	Uncoupled dynamic analysis, equi. lin soil	Uncoupled dynamic analysis, non. lin soil	Coupled dynamic analysis, non. lin. soil
			Plaxis 3D + response spectrum procedure	Matlab + Seismostruct	Plaxis 2D + Seismostruct	Plaxis 3D
Peak dynamic displacement	[m]	No no-collapse requirement jetty and installations on top of it like safety of pipelines for which requirements differ with varying codes	0.99	2.16	1.08	0.95
Residual displacement	[m]	-	-	0.26	0.39	0.21
Plastic hinge material strains	[-]	0.025	$M_{y,head}$=11500 kNm, ε=0.026	$M_{y,head}$=13094 kNm, ε=0.10	$M_{y,head}$=10317 kNm, ε=0.0012< ε_y	$M_{y,head}$=8304 kNm, ε=0.0010< ε_y

Based on these results the following is noted:

- Responses obtained from simplified dynamic analysis are of the same order or magnitude as the responses from dynamic analysis and hence it seems reasonable to apply simplified dynamic analysis as a tool in preliminary stages of seismic jetty design. However, it is noted that insight in actual earth-

quake response and development of possible permanent deformations is not provided by this method.

- The displacement responses obtained from these coupled/uncoupled nonlinear dynamic analyses have shown to possibly exceed response levels obtained from simplified dynamic analysis, which therefore cannot strictly be considered a conservative approach for design of jetty structures. More advanced analysis seems to be required in final design stages.
- Including nonlinear soil in the dynamic soil-structure analysis limits pile head bending moments due to high inertia loading, however the penalty is in the form of development of residual drifts as is also observed after real earthquake events. Along modern performance based design principles this residual drifts are also to be considered in design since they may be critical for post-earthquake serviceability of the structure. From this perspective nonlinear dynamic analysis seems to be preferable, but problems are related to strong signal dependence which requires many signals to be taken into account.
- Coupled nonlinear analysis and uncoupled nonlinear analysis result reasonably synchronous responses with respect to both horizontal displacements and pile head bending moments, except from a varying difference in jetty drift obtained at global soil failure where after a new equilibrium position is found and responses again are very similar. The synchronous responses imply the relatively dominating effect of pile tip excitation by the stiffer material, where the different residual drifts seem to be dominated by the different soft soil deformations at failure for the coupled and uncoupled approach. The latter difference in drift level is recommended for future studies in order to gain more confidence or improve in the computationally very attractive uncoupled nonlinear dynamic analysis, which then would be a very attractive tool fitting well in the concept of performance based design.
- Peak transverse horizontal displacements of the jetty as considered in this study show to reach considerably high levels. When out of phase motions develop for different sections of the long jetty structure these relative horizontal displacements may even increase further, which may become critical with respect to jetty deck capacity and safety of pipelines on top of the jetty. Uncoupled nonlinear analysis that according to this study results reasonably accurate responses and is computationally very efficient, may very well be used to study these possible directional effects on safety of jetty and installations.
- Simplified dynamic analysis was performed based on an peak bedrock excitation levels from PSHA. When the same input acceleration levels were applied and equivalent linear site response analysis output was used as input for uncoupled dynamic analysis, significantly higher and lower responses in terms of drifts and pile head bending moments resulted for the Kocaeli2 and de Duzce signal respectively. This implies the strong signal dependence, but reveals that the response spectrum procedures according to the codes is not necessarily conservative in design. It is noted that the signals applied in this study are recorded very near-fault signals, where the Kocaeli2 signal also is characterized by relatively large bedrock displacements that then seems to strongly affect the deep pile foundation. The frequency content of the signals close to the jetty fundamental frequency is not extremely high. It seems therefore to be recommended for future projects to make sure that really the most unfavourable but realistic recorded accelerograms are accounted for in order to end up with a safe design. Proper probabilistic seismic hazard assessment and carefully considering recorded past earthquakes of the dominant fault(s) are of major importance herein.

8 Conclusions and Discussion

Performance based design and soil-structure interaction
Over the past decade the seismic design community has shown a clear trend switch towards performance based design. Deformation quantities rather than inertia forces have become of main interest in verifying earthquake resistance and related safety of structures. Besides, the effects of soil-foundation-structure interaction have become increasingly important issues in seismic design. Along these observations three different design approaches for pile-deck systems in highly seismic areas were based on literature found to satisfactory, being simplified dynamic analysis (pushover + response spectrum), uncoupled and coupled nonlinear dynamic analysis. The configuration of a jetty supported by large end-bearing piles in soft soil conditions subjected to vertically propagating shear waves is considered, where it is noted that the same soil-structure interaction design concepts with some modifications can be applied to other pile supported onshore/offshore structures in soft soil conditions.

Pushover analysis and p-y curves
A large series of pushover analysis was performed on single jetty piles and jetty pile groups, in order to compare the performance of conventional Winkler p-y analysis to advanced nonlinear finite element analysis with Plaxis 3D. Hardening soil parameter selection herein is found to be a critical issue, which has been addressed through an extensive literature study. Based on single pile pushover analyses it was concluded that ISO p-y expressions for soft clays are very conservative, and applying them will not result realistic designs. Alternative expressions were sought in literature and based on comparison to Plaxis 3D hardening soil analysis the p-y expressions recently proposed by Jeanjean (2009) appear to perform very well. Subsequently pile group analysis has shown pile efficiency reduction for side-side spaced piles with spacing less than 2.5*D and very significant efficiency reduction for shadowing piles depending on the spacing. Plaxis 3D pushover analysis was in this sense found to be a very valuable and practical tool for deriving efficiency factors for specific pile group configurations.

Free field site response analysis
Free field site response analysis is an important step towards soil structure interaction modelling for jetties, since the structure response is dominated by pile response and pile response is strongly affected by soil deposit dynamic and permanent deformations. Free field responses from equivalent linear frequency domain analysis and results from Plaxis 2D finite element analysis were compared. A good fit was found to linear elastic finite element models. However, it was concluded that equivalent linear solutions may result significantly different responses compared to nonlinear finite element analysis

Soil failure and permanent displacements
Post-earthquake investigations indicate that soil failure (plasticity) during seismic conditions causes permanent displacements, which is often a critical factor for seismic performance of port structures. Hence nonlinear finite element site response analysis is preferable since possible effects of soil failure can be better included in the analysis. The Plaxis HSsmall soil constitutive model including hysteretic damping in the unload/reload range and hardening plasticity is conceptually attractive from this perspective.

HSsmall performance
Verification of the model performance in dynamics in this study however has shown that the HSsmall model needs improvements in order to overcome unrealistic behaviour in soft soil dynamics. The HSsmall sudden reset of stiffness at deviatoric strain rate reversals directly causes unrealistic sudden changes in acceleration levels, where in reality stiffness mobilisation is believed to include a time factor smoothening the acceleration response. Despite unrealistic acceleration levels resulting from HSsmall soft soil dynamics, displacement time histories obtained appear reasonable, however they cannot be trusted and verification by analysis with different soil models is required for the time being. Improvement of HSsmall model performance in site response analysis was obtained when a constant stress independent stiffness of the top soil layer was assumed. However, a reformulation of the HSsmall model seems to be required to make it suitable for dynamic analysis of soft soils.

Simplified dynamic analysis
Based on comparison of responses obtained from simplified dynamic, coupled and uncoupled dynamic design approaches it was concluded that simplified dynamic analysis based on code provided spectra cannot be generally considered a conservative approach with respect to calculated displacement responses for jetty type structures. This is explained by the importance of kinematic pile loading by the soil that in addition to superstructure inertial loading may contribute significantly to the total response. Additionally it was found that response spectra relating to structures with deep foundations did result significantly lower design responses for the applied bedrock acceleration levels, which are by far exceeded by responses obtained from dynamic analysis.

Coupled and uncoupled dynamic soil-structure analysis
Coupled soil structure interaction finite element analysis results very high computational demands and consequently is not covering engineering design purposes. Alternatively uncoupled dynamic analysis of soil deposit and jetty structure can be performed, which based on this study was concluded to be a promising approach for engineering practice. This study has shown that very synchronous responses can be obtained from far less demanding uncoupled nonlinear analysis of site and structure, except from a different shift in jetty drift due to different permanent soil deformations developing at global soil failure. The performance and possible improvements of the uncoupled approach in this sense need more study.

Recommended design approach
Based on the present state of knowledge the following recommendations for practicing engineers that need to account for soil-structure interaction in jetty design are proposed:

- Plaxis 3D pushover analysis is an attractive tool to verify pushover characteristics of soil-foundation-structure systems. Effects that typical soil profiles and pile group effects may have can be found from Plaxis 3D pushover analysis and subsequently can be accounted for in equivalent Winkler model by defining specific pile efficiency multipliers. The resulting validated Winker models may subsequently be applied for dynamic analysis.
- Application of simplified dynamic analysis for preliminary design stages seems reasonable in order to find basic dimensions of the structure. Soil acceleration levels may in this preliminary design stage conservatively be estimated based on equivalent linear layered site response analysis for code specified bedrock acceleration levels.
- For final design stages uncoupled nonlinear analysis of soil deposit and structure seems to be the best available tool for engineers to assess possible effects soil structure interaction in design. Since its computational demand is limited it can be applied to find the dynamic response for a large number of selected signals based on PSHA and by this means provides much more insight in possible jetty response compared to simplified dynamic analysis. Additionally the low computational demand of the uncoupled dynamic approach allows for considering 3D effects as for example torsional effects for jetties and wharves constructed in slopes.

Finite element modelling
Finite element modelling has been an important part of this study, and some important conclusions regarding the use of finite element analysis for engineering purposes have to be made because they have appeared to be a critical factor in the design process. It is important to realize that as a designer you have the responsibility for the models you build and the results that you get from them. Experience with the pre-processing certainly is helps in this sense, but then still it was obtained that very extensive verification of all steps really is necessary in order to make sure that output is reasonable. This also was found to be necessary for assumptions that initially seem very obvious but may not be valid and introduce significant errors in the results. Additionally it has to be concluded that for the time being computational demand required for 3D coupled nonlinear soil structure dynamic analysis exceeds reasonable limits for design purposes. “The sky is the limit” certainly still does not hold for finite element software currently available to practising engineers, who consequently have to rely on somehow simplified design techniques.

9 Suggestions for further research

Based on the present study the performance of the HSsmall soil constitutive model needs to be improved to better describe soft soil dynamics. The introduction of a time factor in the reset of the HSsmall small strain stiffness is considered to be a possible improvement since in real soils stiffness development also needs a finite time interval which then will possibly smoothen the obtained response.

Based on the dynamic analysis output results the uncoupled dynamic analysis approach with nonlinear soil deposit analysis allowing for soil failure and permanent displacements included appears very promising for design purposes. However further validation of the obtained differences in jetty drift resulting from soil permanent deformations for the coupled and uncoupled analysis methods is recommended for future study. Verification of the Plaxis 3D interface performance in dynamics is considered an important related issue.

In this study a single-mode simplified dynamic analysis method was adopted. However for building structures multi-mode methods may increase accuracy of obtained results. Whether this may also be the case for jetty structures is recommended for further study.

The conventional engineering assumption representing seismic input as vertically polarized shear waves was adopted as a starting point in this study as these waves are often assumed to be critical. It is realized that this may be an oversimplification, where Rayleigh waves and vertical motions may also affect the structure seismic response. The effect Rayleigh waves and vertical soil motions may have on jetty structures hence are suggested for future research.

The present study focuses on the case of soft clays overlying dense sand, both of which have a low liquefaction potential. However when potentially liquefiable soils are present these definitely have to be accounted for in design, since past earthquakes have shown the extreme effects laterally spreading soil layers may have on structures with pile foundations embedded in these layers. Advance soil constitutive models allowing for pore pressure build-up and liquefaction are nowadays becoming available, and also p-y expression including these effects recently have been proposed (Bouckovalas, 2012) Validation of these continuum and Winkler models is recommended for future study before one of them reasonably can be applied for design purposes.

Appendices

Since most appendices consist of Excel worksheets, Plaxis projects and Matlab scripts that are generally poorly represented on A4 size hard-copy, it was decided to store them in digital format on the enclosed CD. A brief table of contents is shown below, where the subdirectories when necessary contain a guiding document.

Appendix	Contents
I	Summary seismic design guidelines
II	Soil parameter selection
III	Winkler p-y curve expressions, dashpot coefficients and group efficiency reductions
IV	Selected seismic bedrock signals
V	Pushover analysis
VI	Equivalent linear free field site response analysis
VII	Finite element free field site response analysis
VIII	Simplified dynamic jetty analysis
IX	Uncoupled and coupled dynamic jetty analysis

References

- Allotey, N. K. & El Naggar, M. H. (2005). *Cyclic Normal Force Displacement Model for Nonlinear Soil Structure Interaction Analysis: Seismostruct implementation* (Rep. No. GEOT 02-05). Geotechnical Research Centre, Department of Civil & Environmental Engineering, University of Western Ontario, London, Ontario, Canada.
- Alpan, I. (1970). Geotechnical Properties of Soils. *Earth-Science Reviews, 6,* 5-&.
- Aydinoglu, M. N. & Fahjan, Y. M. (2003). A unified formulation of the piecewise exact method for inelastic seismic demand analysis including the P-delta effect. *Earthquake Engineering & Structural Dynamics, 32,* 871-890.
- Barton, Y. O. (1982). *Laterally Loaded Model Piles in Sand: Centrifuge Tests and Finite Element Analyses.* PhD Thesis University of Cambridge.
- Benz, T. (2006). *Small-Strain Stiffness of Soils and its Numerical Consequences, PhD thesis.* Universität Stuttgart.
- Berger, B. S. (1977). Vibrations of An Infinite Orthotropic Layered Cylindrical Viscoelastic Shell in An Acoustic Medium. *Mechanical Engineering, 99,* 105.
- Bouckovalas, G. (2012). Kinematic interaction of piles into laterally spreading soil. *Proc.2nd International conference on Performance Based Design in Earthquake Geotechnical Engineering*.
- Boulanger, R. W., Curras, C. J., Kutter, B. L., Wilson, D. W., & Abghari, A. (1999). Seismic soil-pile-structure interaction experiments and analyses. *Journal of Geotechnical and Geoenvironmental Engineering, 125,* 750-759.
- Brinch Hansen J. (1961). The ultimate resistance of rigid piles against transversal forces. *Danish Geotechnical Institute, Copenhagen, Denmark, 98,* 5-11.
- Brinkgreve, R. B. J., Kappert, M. H., & Bonnier, P. G. (2007). Hysteretic damping in a small-strain stiffness model. *Proc.NUMOG X,* 737-742.
- Broms, B. B. (1964a). Lateral resistance of piles in cohesionless soils. *Journal Soil Mechanics and Foundations Division, ASCE.90(SM3),* 123-156.
- Broms, B. B. (1964b). Lateral resistance of piles in cohesive soils. *Journal Soil Mechanics and Foundations Division, ASCE.90(SM2),* 27-63.
- Chopra, A. K. (2001). *Dynamics of Structures, Theory and Applications to Earthquake Engineering, 2nd edition*. Prentice Hall, New Jersey.
- Chopra, A. K. & Chintanapakdee, C. (2001). Drift Spectrum vs modal analysis of structural response to near-fault ground motions. *Earthquake Spectra, 17,* 221-234.
- Chopra, A. K. & Goel, R. K. (2002). A modal pushover analysis procedure for estimating seismic demands for buildings. *Earthquake Engineering & Structural Dynamics, 31,* 561-582.
- Chopra, A. K. & Goel, R. K. (2004). A modal pushover analysis procedure to estimate seismic demands for unsymmetric-plan buildings. *Earthquake Engineering & Structural Dynamics, 33,* 903-927.
- Chopra, A. K., Goel, R. K., & Chintanapakdee, C. (2004). Evaluation of a modified MPA procedure assuming higher modes as elastic to estimate seismic demands. *Earthquake Spectra, 20,* 757-778.
- Clough & Penzien (1993). *Dynamics of Structures*.
- DNV OS-J101 (2012).
- Dunnavant, T. W. & O'Neill, M. W. (1985). Performance, analysis and interpretation of a lateral load test of a 72-inch-diameter bored pile in overconsolidated clay. *Report UHCE 85-4, 57 pp.*.
- El Naggar, M. H. & Bentley, K. J. (2000). Dynamic analysis for laterally loaded piles and dynamic p-y curves. *Canadian Geotechnical Journal, 37,* 1166-1183.
- El Naggar, M. H. a. N. M. (1996). Nonlinear analysis for dynamic lateral pile response. *Soil Dynamics and Earthquake Engineering, 15,* 233-244.
- Erdik, M. e. al. (2004). Earthquake Hazard in Marmara Region, Turkey. *Proc.13th World Conference of Earthquake Engineering, Vancouver, Canada*.
- Fajfar, P. (1999). Capacity spectrum method based on inelastic demand spectra. *Earthquake Engineering & Structural Dynamics, 28,* 979-993.
- Freeman, S. A. (1998). Development and Use of Capacity Spectrum Method. In.

- Freeman, S. A. (2000). The Capacity Spectrum Method as a Tool for Seismic Design. In.
- Gazetas, G. (2012). Nonlinear Soil-Foundation-Structure Interaction. *Proc.2nd International conference on Performance Based Design in Earthquake Geotechnical Engineering*.
- Gazetas, G. & Dobry, R. (1984a). Horizontal Response of Piles in Layered Soils. *Journal of Geotechnical Engineering-Asce, 110,* 20-40.
- Gazetas, G. & Dobry, R. (1984b). Simple Radiation Damping Model for Piles and Footings. *Journal of Engineering Mechanics-Asce, 110,* 937-956.
- Goel, R. K. (2010). *Simplified Procedures for Seismic Analysis and Design of Piers and Wharves in Marine Oil and LNG Terminals* (Rep. No. California State Lands Commission, Contract No. C2005-051 and Dep. of the Navy, Office and Naval Research Award No. N00014-08-1-1-1209). California Polytechnic State University, San Luis Obispo.
- Hanks, T. C. & Kanamori, H. (1979). Moment Magnitude Scale. *Journal of Geophysical Research, 84,* 2348-2350.
- Hardin, B. O. (1965). Dynamic Versus Static Shear Modulus for Dry Sand. *Materials Research and Standards, 5,* 232-&.
- Hardin, B. O. & Black, W. L. (1969). Closure to vibration modulus of normally consolidated clays. *Proc.ASCE: Journal of the Soil Mechanics and Foundations Division, 98(SM7),* 1531-1537.
- Hardin, B. O. & Drnevich, V. P. (1972). Shear Modulus and damping in soils. *Proc.ASCE: Journal of the Soil Mechanics and Foundations Division, 95(SM6), 1531-1537*.
- Hartsuijker, C. W. J. W. (2004). *Toegepaste Mechanica, Deel 3*.
- Hashash, Y. M. A. & Park, D. (2002). Viscous damping formulation and high frequency motion propagation in non-linear site response analysis. *Soil Dynamics and Earthquake Engineering, 22,* 611-624.
- Idriss and Sun (1992). *SHAKE91: a computer program for conducting equivalent linear seismic response analyses of horizontally layered soil deposits, User's Guide* University of California, Davis.
- Ishibashi, I. & Zhang, X. (1993). Unified Dynamic Shear Moduli and Damping Ratios of Sand and Clay. *Soils and Foudations, Japanese Society of Soil Mechanics and Foundation Engineering, 33,* 182-191.
- ISO 19901-2, I. (2004). *Petroleum and Natural Gas Industries, Specific requirements for offshore structures - Part 2: Seismic design procedures and criteria* International Organization for Standardization,Technical Committee ISO/TC 67,Subcommittee SC 7.
- ISO 19902 (2006). *Petroleum and Natural Gas Industries - Fixed Steel Offshore Structures* International Organization for Standardization,Technical Committee ISO/TC 67,Subcommittee SC 7.
- ISO 19902:2006 (2006). *Petroleum and Natural Gas Industries - Fixed Steel Offshore Structures* International Organization for Standardization,Technical Committee ISO/TC 67,Subcommittee SC 7.
- ISO 19903 (2006). *Petroleum and Natural Gas Industries, Fixed concrete offshore structures* International Organization of Standardization,Technical Committee ISO/TC67,Technical Committee CEN/TC 1.
- Jeanjean, P. (2009). Re-assessment of P-Y Curves for Soft Clays from Centrifuge Testing and Finite Element Modeling. *Proc.Offshore Technology Conference (20158)*.
- Juirnarongrit, T. & Ashford, S. A. (2001). *Effect of Pile Diameter on the Modulus of Sub-grade Reaction* (Rep. No. SSRP-2001/22). Department of Structural Engineering, University of California, San Diego.
- Kalkan, E. & Kunnath, S. K. (2006). Adaptive Modal Combination Procedure for Nonlinear Static Analysis of Building Structures. *Journal of Structural Engineering ASCE,* 1721-1731.
- Kanamori, H. (1983). Magnitude Scale and Quantification of Earthquakes. *Tectonophysics, 93,* 185-199.
- Kavvadas, M. & Gazetas, G. (1993). Kinematic Seismic Response and Bending of Free-Head Piles in Layered Soil. *Geotechnique, 43,* 207-222.
- Kramer, S. L. (1996). *Geotechnical Earthquake Engineering*.
- Kulhawy, F. H. & Mayne, P. W. (1990). *Manual on Estimating Soil Properties for Foundation Design*. Cornell University ,Ithaca, New York.
- Lengkeek, H. J. (2003). Estimation of sand stiffness parameters from cone resistance. *Plaxis Bulletin 13, Januari 2002,* 15-19.
- Lysmer, J. & Kuhlmeyer R.L. (1969). Finite Dynamic Model for Infinite Media. *Journal of Engineering and Mechnical Division,* 859-877.
- Makris, N. & Gazetas, G. (1992). Dynamic Pile Soil Pile Interaction .2. Lateral and Seismic Response. *Earthquake Engineering & Structural Dynamics, 21,* 145-162.

- Martin, C. M. & Randolph, M. F. (2006). Upper-bound analysis of lateral pile capacity in cohesive soil. *Geotechnique, 56,* 141-145.
- Matlock, H. (1970). Correlations for design of laterally loaded piles in soft clay. *Preprints Second Annual Offshore Technology Conference, 1,* 577-588.
- Matlock, H. (1979). Fugro Internal Memorandum. -.
- Meyerhof, G. G. (1995). Standard Penetration Tests and Pile Behavior Under Lateral Loads in Cohesionless Soils. *Canadian Geotechnical Journal, 32,* 913-916.
- Michaels, P. (1998). In situ determination of soil stiffness and damping. *Journal of Geotechnical and Geoenvironmental Engineering, 124,* 709-719.
- Michaels, P. (2006a). Comparison of Viscous Damping in Unsaturated Soils, Compression and Shear. *Unsaturated Soils, 2006, Vol.1, Proceedings of the Fourth International Conference on Unsaturated Soils, (GSP 147), ASCE, Reston, VA.565-576*.
- Michaels, P. (2006b). Relating damping to soil permeability. *Int.Journal of Geomechanics, Vol.6 (3), 158-165*.
- Michaels, P. (2008). Water, Inertial damping and the Complex shear modulus. *ASCE*.
- Miranda, E. & Bertero, V. V. (1994). Evaluation of Strength Reduction Factors for Earthquake-Resistant Design. *Earthquake Spectra, 10,* 357-379.
- MOTEMS (2010). *Marine Oil Terminal Engineering and Maintenance Standards, Chapter 31F of the 2010 California Building Code*. California Building Standards Commission.
- Muir Wood, D. (1990). *Soil Behaviour and Critical State Soil Mechanics*. Cambridge University Press.
- Murff, J. D. & Hamilton, J. M. (1993). P-Ultimate for Undrained Analysis of Laterally Loaded Piles. *Journal of Geotechnical Engineering-Asce, 119,* 91-107.
- Mylonakis, G. & Gazetas, G. (2000). Seismic soil-structure interaction: Beneficial or detrimental? *Journal of Earthquake Engineering, 4,* 277-301.
- Mylonakis, G., Nikolaou, A., & Gazetas, G. (1997). Soil-pile-bridge seismic interaction: Kinematic and inertial effects .1. Soft soil. *Earthquake Engineering & Structural Dynamics, 26,* 337-359.
- NEHRP Fema-450 (2012). *NEHRP FEMA450*.
- NEN-EN 1998 (2004). *Eurocode NEN-EN 1998;2004 Design of structures for earthquake resistance*. European Committee for Standardization.
- Nogami, T., Otani, J., Konagai, K., & Chen, H. L. (1992). Nonlinear Soil-Pile Interaction-Model for Dynamic Lateral Motion. *Journal of Geotechnical Engineering-Asce, 118,* 89-106.
- Novak, M. (1974). Dynamic stiffness and damping of piles. *Canadian Geotechnical Journal, 11,* 574-598.
- O'Neill, M. W. & Dunnavant, T. W. (1984). A study of the effects of scale, velocity and cyclic degradability on laterally loaded single piles in overconsolidated clay. *Report UHCE 84-7: 368 pp.*.
- O'Neill, M. W. & Murchison, J. M. (1983). An evaluation of p-y relationships in sands. *A report to the American Petroleum Institute, PRAC 82-41-1*.
- O'Neill, M. W., Reese, L. C., & Cox, W. R. (1990). Soil Behaviour for Piles Under Lateral Loading. *Proc.Offshore Technolgy Conference, Houston, Texas*.
- PIANC, P. I. N. A. (2001). *PIANC Design Guidelines for Port Structures*. A.A. Balkema, Rotterdam, Brookfield.
- Plaxis Material Models Manual (2011). *Plaxis Material Models Manual, 2011* Plaxis b.v, Delft, The Netherlands.
- Priestley, M. J. N., Calvi, G. M., & Kowalski, M. J. (2007). *Displacement-Based Seismic Design of Structures*. IUSS Press, Pavia, Italy.
- Priestley, M. J. N. & Park, R. (1987). Strength and Ductility of Concrete Bridge Columns Under Seismic Loading. *Aci Structural Journal, 84,* 61-76.
- Randolph, M. & Gouvernic, S. (2011). *Offshore Geotechnical Engineering*. Spon Press, Abingdon, Oxon.
- Randolph, M. F. & Houlsby, G. T. (1984). The limiting pressure on a circular pile loaded laterally in cohesive soil. *Geotechnique, 34(4),* 613-623.
- Reese, L. C. & an Ympe, W. F. (2001). *Single Piles and Pile Groups under Lateral Loading*. A.A. Balkema, Rotterdam, Brookfield.
- Reese, L. C., Cox, W. R., & Koop, F. D. (1974). Analysis of laterally loaded piles in sand. *Proceedings Fifth Annual Offshore Technology Conference, Houston TX*.
- Reese, L. C. a. W. R. C. (1975). Lateral loading of deep foundations in stiff clay. *Journal Geotechnical Engineering Division, American Society of Civil Engineering, 101,* 633-649.

- Roesset (1970). Fundamentals of Soil Amplification. *Seismic Design for Nuclear Power Plants,* 183-244.
- Santos, J. A. & Correia, A. G. (2001). Reference threshold shear strain of soil, its application to obtain unique strain-dependent shear modulus curve for soil. *Proc.15th International Conference on Soil Mechanics and Geotechnical Engineering, Istanbul, Turkey, 1,* 267-270.
- Schanz, T., Vermeer, P. A., & Bonnier, P. G. (1999). The Hardening-soil model: Formulation and verification. *Beyond 2000 in Computational Geotechnics,* 281-290.
- Schnabel, P., Seed, H. B., & Lysmer, J. (1972). Modification of Seismograph Records for Effects of Local Soil Conditions. *Bulletin of the Seismological Society of America, 62,* 1649-1664.
- Schonfield, A. N. & Wroth, P. (1968). *Critical state soil mechanics*. McGraw-Hill.
- Sigaran Loria, C. & Jaspers-Focks D.J (2011). HSS model adequacy in performance-based design approach, Filyos New Port, Turkey. *Proc.15th European Conference on Soil Mechanics and Geotechnical Engineering, Istanbul, Turkey,* 1579-1586.
- Sluys, L. J. & Borst de, R. (2010). *Computational Methods in Nonlinear Solid Mechanics, Lecture Notes CT5142*. Delft University of Technology, The Netherlands.
- Stokoe et al, K. H. (2004). Development of a new family of normalized modulus reduction and material damping curves. *International Workshop on Uncertainties in Nonlinear Soil Properties and their Impact on Modeling Dynamic Soil Response, UC Berkeley, CA*.
- Stoll, R. (1985). Computer-aided studies of complex soil moduli. *Proc., Measurement and Use of Shear Wave Velocity for Evaluating Dynamic Soil Properties, ASCE, New York,* 18-33.
- Transportation Research Board, N. R. C. (2001). *NCHRP Report 461, Static and Dynamic Lateral Loading of Pile Groups*.
- Turkish Technical Seismic Regulations (2008). *Turkish Technical Seismic Regulation on Construction of Coastal and Harbour Structures, Railway and Airports*. Turkish Ministry of Transportation.
- Verruijt, A. (2005). *Soil Dynamics*.
- Vesic (1961). Beam on elastic subgrade and the Winkler hypothesis. *Proc.International Conference Soil Mechanics and Foundation Engineering, Paris, 1,* 845-850.
- Vucetic, M. & Dobry, R. (1991). Effect of Soil Plasticity on Cyclic Response. *Journal of Geotechnical Engineering-Asce, 117,* 89-107.
- Wilson, J. F. (2003). *Dynamics of Offshore Structures*. John Wiley & Sons, Inc, Hoboken, New Jersey.
- Wolf, J. P. & Deeks, A. J. (2004). *Foundation Vibration Analysis: A Strength-of-Materials Approach*. Elsevier, Oxford, U.K.